



DISSERTATION

In Partial Fulfillment of the Requirements
for the Degree of Doctor of Philosophy
from TELECOM ParisTech

Specialization: Communication and Electronics

Erhan Yılmaz

Coding Strategies for Relay Based Networks

Defense scheduled on the 2nd of July 2010 before a committee composed of:

Reporters	Prof. Erdal Arıkan, Bilkent University Prof. Luc Vandendorpe, UC Louvain
Examiners	Prof. Luc Deneire, University of Nice-Sophia Antipolis Assist. Prof. Michèle A. Wigger, TELECOM ParisTech
Thesis supervisors	Prof. Raymond Knopp, EURECOM Prof. David Gesbert, EURECOM



THESE

présentée pour obtenir le grade de

Docteur de TELECOM ParisTech

Spécialité: Communication et Electronique

Erhan Yilmaz

Stratégies de Codage pour les Réseaux à base de Relais

Thèse prévue le 2 juillet 2010 devant le jury composé de :

Rapporteurs	Prof. Erdal Arıkan, Université de Bilkent Prof. Luc Vandendorpe, Université catholique de Louvain
Examineurs	Maître de Conférence HDR Luc Deneire, Université de Nice-Sophia Antipolis Maître de Conférence Michèle A. Wigger, TELECOM ParisTech
Directeur de thèse	Prof. Raymond Knopp, EURECOM Prof. David Gesbert, EURECOM

Abstract

For future wireless communication networks one of the major concerns for service providers is to provide seamless connectivity to the end-users with quality of service (QoS) as high as possible. However, to achieve the determined QoSs for all users in the network is a challenging issue due to the time-varying characteristics of communication channels, caused by multi-path fading, path-loss and shadowing, and interference as a result of sharing the same time-frequency system resources with the other communicating terminals. Recently, base station (BS) cooperation and relay station (RS) deployment have been proposed as promising technologies to notably improve the performance of next-generation wireless systems in terms of fairness, coverage, energy/cost and spectral efficiency.

In this thesis, we gravitate our attention towards the use of relay stations in different wireless communication systems such as cellular telephony, Ad-hoc and satellite networks with *reliability* and *achievable rates* being our main figures of merit. In particular, we project the insights gained from information theoretic analysis of various relaying strategies into the real world settings, and assess the effectiveness and potentials of relaying in various wireless applications.

We first focus on parallel relay networks (PRNs), which might find applications in cellular uplink (UL) communications, in long-range sensor networks, and in rapidly deployable infrastructure networks for military or civil applications. As the processing capabilities of RSs have prominent effects on system performance, we investigate whether it is possible to have good performance by using *simple* and *cheap* RSs for PRNs with limited backhaul connections to the destination. In particular, we propose a *simple* and *practical* quantization technique at the RSs which relies on symbol-by-symbol uniform scalar quantization (uSQ). For the same network model, we also characterize the random coding error exponents (EEs) corresponding to different relaying strategies used by the RSs. We show that in certain regimes the EEs achieved by simple relaying strategies, such as quantize-and-forward (QF) relaying wherein finite-alphabet modulation, simple symbol-by-symbol uSQ are used at the sources and RSs, respectively, are better than the EEs of more complex relaying strategies, such as decode-and-forward (DF) and compress-and-forward (CF) relaying wherein Gaussian codebooks, vector quantization (VQ) and maximum-likelihood (ML) decoding are used at the sources, RSs and destination, respectively.

Next, inspired by the PRN setup we consider a cellular network assisted

by fixed RSs, which are used by mobile stations (MSs) to access a BS. We analyze the achievable sum-of-rates for UL communications assuming that MS and RS signals are emitted on orthogonal frequency bands. Due to high link budget requirements in next generation cellular systems, power constraints at MSs will be a bottleneck for UL communications especially for the MSs close to cell boundaries, where multi-hopping might be a feasible and efficient solution to this problem. Regarding this, the influences of RS deployment in cellular systems on the achievable sum-rates are thoroughly assessed by considering several parameters used in the system such as the number of RSs deployed in each cell, their locations and powers they use.

In relay-assisted cellular systems, the main factors that limit the achievable gains are the quality of the link between RSs and BS, the multiplexing loss due to multi-hopping, the effect of the interference which increases with the number of deployed RSs, and the feedback overhead especially in centralized solutions where an estimate of the channel state information (CSI) is required at the BS side. Taking these into account we propose a two-step *distributed* scheduling algorithm for relay-assisted cellular networks for downlink (DL) communications where a given MS can be served by either the BS or one of the deployed RSs, in an opportunistic way. Such a distributed approach allows a reduced *feedback* signaling with respect to the centralized case, especially when a simple scalar feedback is not sufficient for estimating the channel quality. As a result of the reduced feedback signaling requirements the system becomes more *scalable*, as new RSs can be deployed where required without need of a careful network planning.

In the thesis, we also consider a RS deployment scenario where MSs communicate with each other through the aid of a common RS since no mutual direct communication links between the MSs. This channel model is called two-way relaying channel (TWRC). We propose various coding strategies for this network model and in particular show that lattice-based partial decoding strategies achieve near optimal performance. However, since this coding scheme is highly sensitive to channel impairments, it might not find applications in real scenarios. To this end, we show that the use of binning-type relaying strategies might be a more practical approach since phase coherence of the signals at the RS is not required.

Finally, we extend the single-pair TWRC model to a multi-pair case where in each pair the single-antenna MSs seek to communicate via a common multiple antenna RS. In the multi-pair TWRC, the main bottleneck on system performance is the interference seen by each MS due to the other communicating MS pairs. We try to tackle this problem in the *spatial domain* by using multiple antennas at the RS.

Acknowledgements

Any thanks must begin with my advisers, Prof. Raymond Knopp and Prof. David Gesbert, who made it easy for me to reach the end. In the beginning, I was a bit worried about how to work and synchronize with two advisers since each of them is an endless source of ideas and enthusiasm. But, thanks to them, with their patience and everlasting support everything has been smoothed out. Also having worked with them, who have different research interests, gave me the opportunity to gain knowledge on various subjects and to become a better researcher. I would also like to thank Dr. Federico Boccardi, who helped show me the role of engineering research in industry.

I would also like to thank my thesis jury members, Prof. Erdal Arıkan, Prof. Luc Vandendorpe, Prof. Luc Deneire, and Prof. Michèle A. Wigger, for their valuable comments, especially the ones regarding implementation aspects of the ideas present in the thesis.

Now the most important, and also hardest, part of the acknowledgements: Friends! Without them I can't imagine it would have been possible for me to finalize this tough and long journey. During the last four years, I have had lots of good memories all together with my friends. Many thanks to Ikbal Msaada, Daniel Camara, Konstantinos Papakonstantinou, Agisilaos Papadogiannis with whom I shared the same office, EC-02, for the first two years; and to Randa Zakhour, Antony Schutz, Mustapha Amara with whom I shared the same office, ES-202, for the last two years of my PhD. I feel so lucky for having shared in the same office with them since, in both offices, we managed to create the best ambiances in Eurecom with friendship and sympathy. I would also like to thank to Turgut Oktem, Najam Ul Islam, Umer Salim, Ka Ming Ho, Sara Akbarzadeh, Carina Schmidt-Knorreck, Rizwan Ghaffar and Bassem Zayen. Again, I am so grateful to Ikbal Msaada and Randa Zakhour for their everlasting help and precious companion, and Daniel Camara for his valuable advices and guidance. Finally, many thanks to Melek Onen who has been always there for helping us, I and my wife, whenever we needed.

Special mention goes to my wife, Kubra, who has been at my side throughout all of the stressful and exhilarating moments of the past four years. Even though she had hard times to adapt to live in France, she has still supported me in so many ways and helped keep me going through this intense time. Also, I would like to thank her in advance since she is going to give birth to our sister Melike. Finally, I would like to thank my family and family-in-law for their everlasting

support and love.

Contents

Abstract	i
Acknowledgements	iii
Contents	v
List of Figures	ix
Acronyms	xiii
Notations	xv
1 Introduction	1
1.1 Motivation	1
1.1.1 Potential scenarios for Relay deployment	2
1.1.2 Main challenges to design multi-hop networks	2
1.2 Background	4
1.2.1 The one-way Relay Channel	4
1.2.2 The two-way Relay Channel	6
1.3 Contributions and Outline of this Dissertation	7
2 Multi-Source Parallel Relay Networks: Coding Strategies	11
2.1 Introduction	11
2.1.1 Motivation	12
2.1.2 Prior work	12
2.1.3 Contributions	13
2.2 Channel Model	15
2.2.1 Shared MAC between the RSs and the Destination	16
2.2.2 Orthogonal limited-capacity links between the RSs and the Destination	16
2.2.3 Preliminaries	16
2.3 PRN with Gaussian Signaling at the Sources and the RSs	19
2.3.1 Shared MAC between the RSs and the Destination	19
2.3.2 Orthogonal limited-capacity links between the RSs and the Destination	26
2.4 Quantization for PRN with Non-Gaussian Signaling Sets	29
2.4.1 Coded Modulation at the Source(s)	30
2.4.2 Uniform Scalar Quantizer (uSQ)	30
2.4.3 Coded Modulation with Uniform Scalar Quantization at the RSs	31

2.4.4	Coded Modulation with Gaussian Mapping at the RSs . . .	35
2.5	Numerical Results	38
2.6	Conclusions	44
2.A	Outer bound	45
2.B	The achievable rate region for BQRB relaying strategy	46
3	Multi-Source Parallel Relay Networks: Error Exponent Analysis	57
3.1	Introduction	57
3.1.1	Channel Model	58
3.2	Error Exponent Analysis for Single-Source and Two-source PRNs	58
3.2.1	Random Coding Error Exponent	58
3.2.2	Error Exponent Analysis for Single Source Case	59
3.2.3	Error Exponent analysis for Two Sources Case	67
3.3	Numerical Results	73
3.3.1	Single Source Case	73
3.3.2	Two Sources Case	74
3.4	Conclusions and Future Directions	74
3.A	The pdf of difference of exponentially distributed Random variables	78
3.B	The exact expression and an upper bound on the $\Pr\{\beta_2 > \beta_1\}$.	79
4	Relay Deployment in Cellular Uplink Communications	81
4.1	Introduction	81
4.1.1	Motivation	82
4.1.2	Prior Work	82
4.1.3	Contributions	82
4.1.4	Outline of the chapter	83
4.2	The Generalized Orthogonal Relay Channel	83
4.2.1	Model	84
4.2.2	Outer Region	86
4.2.3	Achievable Rates	87
4.3	Cellular Networks with Relay Deployment: System Model	90
4.3.1	Channel Model	91
4.3.2	Signal Model	92
4.4	Amplify-and-Forward Relaying	94
4.5	Decode-and-Forward Relaying	96
4.6	Compress-and-Forward Relaying	96
4.7	Quantize-and-Forward Relaying	99
4.8	Conventional Cellular Systems	100
4.8.1	Co-Located Antenna Cellular System	100
4.8.2	Ideal Distributed Antenna System (DAS)	100
4.9	Simulation Setup	101
4.9.1	User Loading	101
4.9.2	Parameters	102
4.10	Numerical Results	103
4.10.1	Relays with Sectoral Antennas	104

4.10.2	Relays with Omnidirectional Antennas	104
4.11	Conclusions	105
5	Relay Deployment in Cellular Downlink Communications	109
5.1	Introduction	109
5.1.1	Related Work	110
5.1.2	Motivation for Relaying in Cellular Systems	110
5.1.3	Our Contributions	112
5.1.4	Outline of the chapter	112
5.2	System Model	112
5.3	Centralized Scheduling Algorithm	113
5.4	Decentralized Scheduling Algorithm	115
5.4.1	Feedback Reduction with Decentralized Scheduling Algorithm	117
5.5	Numerical Results	117
5.5.1	Simulation Setup	119
5.5.2	Simulation Methodology	119
5.5.3	Results	119
5.6	Conclusion and Outlook	120
6	Coding Strategies for Two-way Relay Channels	123
6.1	Introduction	123
6.1.1	Related Work on Two-Way Relaying	123
6.1.2	Application Scenarios	124
6.2	The channel model	125
6.3	Outer Bound on Achievable Rates	126
6.3.1	Information-Theoretic System Model	126
6.3.2	Outer Bound	127
6.4	Coding Strategies for Additive Channels using Group Codes	128
6.4.1	Binary Adder Channel	128
6.4.2	AWGN Channel	129
6.5	Decode-, Hash- and Compress-and-Forward Schemes at the Relay	132
6.5.1	Degraded BC with successive refinement	132
6.5.2	Decode-and-Forward Relaying	133
6.5.3	Hash-and-Forward Relaying	136
6.5.4	Compress-and-Forward Relaying	138
6.5.5	AWGN Channel	138
6.5.6	Amplify-and-Forward Relaying	139
6.6	Numerical Examples	141
6.7	Conclusions	141
6.A	Outer Bound	143
6.B	Achievable rates with CF relaying strategy	144

7	Multi-pair Two-way Relay Channel with Multiple Antenna Relay Station	149
7.1	Introduction	149
7.2	System Model	150
7.3	Amplify-and-forward (AF) Relaying Schemes	152
7.3.1	General structure of the linear processing matrix \mathbf{A}_R	152
7.3.2	Receive and Transmit Zero-Forcing at the Relay	153
7.3.3	Block-Diagonalization (BD) for the TWRC	154
7.4	Quantize-and-Forward (QF) Relaying	156
7.5	Simulation Results	158
7.6	Conclusion	159
7.A	Optimizing over \mathbf{d}_k	160
7.B	Solving Problem (7.33)	161
8	Conclusions	165
8.1	Future Work Directions	167
9	Appendix: Summary of the thesis in French	169
9.1	Abstract en français	169
9.2	Introduction	170
9.2.1	Motivation	170
9.2.2	Background	174
9.2.3	Contributions et cadre de cette thèse	178
9.3	Résumé du Chapitre 2	180
9.4	Modèle du canal	184
9.5	Résumé du Chapitre 3	187
9.5.1	Directions Futures	188
9.6	Résumé du Chapitre 4	188
9.6.1	Conclusions	190
9.7	Résumé du Chapitre 5	191
9.7.1	Modèle de système	192
9.7.2	Conclusion et Perspectives	192
9.8	Résumé du Chapitre 6	192
9.8.1	Le modèle de canal	193
9.9	Résumé du Chapitre 7	194
9.10	Conclusions	195
9.10.1	Futures travaux	198

List of Figures

1.1	An illustration of possible relaying scenarios.	3
2.1	A general M -source, K -relay and single destination PRN setup with phase fading.	17
2.2	A general M -source, K -relay and single destination PRN setup with orthogonal error-free finite-capacity backhaul links between the RSs and the destination, where C_i in [bits/channel use] is the link capacity between the i -th RS and the destination, for $i = 1, 2, \dots, K$	17
2.3	Achievable rates for phase fading PRN with symmetric channel gains, where $ h_i = g_i = 1$, for $i = 1, 2$, and $P_s/\sigma^2 = 10$ dB.	39
2.4	Achievable rates for phase fading PRN with asymmetric channel gains, where $ h_1 = g_2 = 0.5$ and $ h_2 = g_1 = 1$, and $P_s/\sigma^2 = 10$ dB.	40
2.5	1 Source, 2 Relays complex Gaussian PRN: Achievable rates versus $SNR = \frac{P_s}{\sigma^2}$ with $C = C_1 = C_2 = 4$ [bits/transmission] and $\mathbf{h}^T = [1 + j \ 1 + j]$	40
2.6	Achievable rates region for phase fading PRN with asymmetric channel gains, where $ \mathbf{H}[ij] = \mathbf{g}[i] = 1$, $\forall i, j = 1, 2$, and $P_s/\sigma^2 = 0$ dB, $P_r/\sigma^2 = 10$ dB. We used 500 channel realizations to average over phase fading.	41
2.7	2 Source, 2 Relays complex Gaussian PRN: Achievable rates versus $SNR = \frac{P_s}{\sigma^2}$ for 4-QAM with $C = C_1 = C_2 = 2$ [bits/transmission] and sample channel matrix (2.59).	42
2.8	2 Source, 2 Relays complex Gaussian PRN: Achievable rates versus $SNR = \frac{P_s}{\sigma^2}$ for 4-QAM with $C = C_1 = C_2 = 4$ [bits/transmission] and sample channel matrix (2.59).	42
2.9	2 Source, 2 Relays complex Gaussian PRN: Achievable rates versus $SNR = \frac{P_s}{\sigma^2}$ for 4-QAM with $C = C_1 = C_2 = 6$ [bits/transmission] and sample channel matrix (2.59).	43
2.10	2 Source, 2 Relays complex Gaussian PRN: Achievable rates versus $SNR = \frac{P_s}{\sigma^2}$ for 16-QAM with $C = C_1 = C_2 = 4$ [bits/transmission] and sample channel matrix (2.59).	43

3.1	An illustration for ML decoding at the RSs where the k -th RS sends the detected signal $\hat{\mathbf{x}}_{ML,k}$ and the reliability information $\beta_k \in \mathbb{R}^+$ to the destination, for $k = 1, 2$	61
3.2	Random coding EEs for 1-Source, 2-Relay PRN with $\Gamma = \frac{P_s h^2}{\sigma^2} = 0$ [dB] and $C = C_1 = C_2 = 4$ [bits/transmission].	76
3.3	Random coding EEs for 1-Source, 2-Relay PRN with $\Gamma = \frac{P_s h^2}{\sigma^2} = 10$ [dB] and $C = C_1 = C_2 = 4$ [bits/transmission].	76
3.4	Random coding EEs for 2-Source, 2-Relay PRN with $\frac{P_s}{\sigma^2} = \frac{P_1}{\sigma^2} = \frac{P_2}{\sigma^2} = 0$ [dB] and $C = C_1 = C_2 = 4$ [bits/transmission].	77
3.5	Random coding EEs for 2-Source, 2-Relay PRN with $\frac{P_s}{\sigma^2} = \frac{P_1}{\sigma^2} = \frac{P_2}{\sigma^2} = 10$ [dB] and $C = C_1 = C_2 = 4$ [bits/transmission].	77
4.1	A d.m. GORC with M sources, K RSs where the channel from the sources to the RSs and destination (channel 1) is orthogonal to the channels from the RSs to the destination (channel 2). . .	84
4.2	The bandwidth allocation in the first and second hop.	91
4.3	A RS deployment scenario in $B = 19$ cells network. The BSs have $N = 6$ sectoral antennas each directed to a unique RS. Each RS consists of 3 RF elements each serving a unique cell.	101
4.4	A RS deployment scenario in $B = 19$ cells network. The BSs have $N = 6$ sectoral antennas each directed to a unique RS. Each RS is equipped with a single omnidirectional antenna.	102
4.5	Antenna gain pattern for $A_{max} = 20$ dB and $\theta_{3dB} = 30$ as a function of the horizontal angle.	103
4.6	The average sum-of-rates [bits/sec] versus $F = W_2/W_1$ for fixed $P_s = \{-5, 0\}$ [dBW] and $P_r = 10$ [dBW]. The RSs are located at the cell-edges.	106
4.7	The average sum-of-rates with respect to P_r for fixed $P_s = 0$ [dBW] and $F = W_2/W_1 = 0.3$ where the RSs are located at the cell-edges.	107
4.8	The average sum-of-rates [bits/sec] versus bandwidth ratio, F for $P_s = -5$ [dBW] and $P_r = 10$ [dBW]. The RS-to-BS distance is $d_{RS \rightarrow BS} = 1.2$ km	107
4.9	The average sum-of-rates [bits/sec] versus the RS-to-BS distance $d_{RS \rightarrow BS}$ for fixed $P_s = -5$ [dBW], $P_r = 10$ [dBW] and $F = W_2/W_1 = 0.3$	108
4.10	The average sum-of-rates with respect to P_r for fixed $P_s = -5$ [dBW] and $F = W_2/W_1 = 0.2$ where the RS-to-BS distance is $d_{RS \rightarrow BS} = 1.2$ km.	108
5.1	Multi-cell hexagonal layout, $R = 2$ km, $d_{BS \rightarrow RS} = 1$ km with $N = 6$ RSs and uniformly distributed $K = 30$ mobile stations. . .	118
5.2	Total Average throughput versus BS transmit power, P_{bs} , for total packet arrival rate $\mu_{TOT} = \{4, 8\}$ [bps/Hz], $R = 2$ km, $d_{BS \rightarrow RS} = 1$ km, $P_{rs} = 35$ [dBm] with $N = 6$ RSs and $K = 30$ mobile stations.	121

5.3	Total Average throughput versus total packet arrival rate μ_{TOT} for BS transmit powers $P_{bs} = \{40, 50\}$ [dBm], $R = 2$ km, $d_{BS \rightarrow RS} = 1$ km, $P_{rs} = 35$ [dBm] with $N = 6$ RSs and $K = 30$ mobile stations.	122
5.4	Sorted average user rates for $R = 2$ km, $d_{BS \rightarrow RS} = 1$ km, $P_{bs} = \{40, 50\}$ [dBm], $P_{rs} = 35$ [dBm], $\mu_{TOT} = \{4, 8\}$ [bps/Hz], with $N = 6$ RSs.	122
6.1	Two-way relay network	126
6.2	Two-user two-way relay network	127
6.3	Binary Adder Channel Codebook Time-Sharing	129
6.4	Rate regions for TWR channel.	141
6.5	Sum-rates for TWR channel.	142
7.1	K -pair ($N = 2K$ MSs) TWRC with an M antenna RS.	151
7.2	Average sum-rate vs. SNR_{RS} for $K = 4$ pair TWRC with $M = 8$ antenna RS and single antenna MSs with $SNR_{MS} = SNR_{RS}$.	158
7.3	Average sum-rate vs. SNR_{MS} for $K = 4$ pair TWRC with $M = 8$ antenna RS and single antenna MSs with $SNR_{RS} = 10$ [dB].	159
9.1	Une illustration de scénarios possibles relais.	173
9.2	Un PRN général avec M -sources, k -relais et une seule destination avec atténuation de phase.	186
9.3	Un PRN général avec M -sources, k -relais et une seule destination avec des liens orthogonaux sans erreur à capacité limitée entre les RSs et la destination, où C_i in [bits/usage du canal] est la capacité du lien entre la i -ème RS et la destination, pour $i = 1, 2, \dots, K$.	187
9.4	L'allocation de la bande passante pour les première et deuxième étapes.	190
9.5	Réseau de relais à double sens	194
9.6	K -paire ($N = 2K$ MSs) TWRC avec M antennes RS.	196

Acronyms

Here are the main acronyms used in this document. The meaning of an acronym is usually indicated once, when it first occurs in the text. The English acronyms are also used for the French summary.

3GPP	Third Generation Partnership Project
AF	Amplify-and-Forward
AWGN	Additive White Gaussian Noise
BS	Base Station
BD	Block Diagonalization
BQRB	Block-quantization and random binning
bps	bit per second
CDMA	Code Division Multiple Access
CF	Compress-and-Forward
CM	Coded Modulation
CRC	Cyclic Redundancy Check
CSI	Channel State Information
CSIR	Channel State Information at Receiver
CSIT	Channel State Information at Transmitter
DAS	Distributed Antenna System
DF	Decode-and-Forward
DMT	Diversity-gain-to-Multiplexing-gain Tradeoff
EE	Error Exponent
FDD	Frequency Division Duplex
FDMA	Frequency Division Multiple Access
LHS	Left Hand Side
GORC	Generalized orthogonal relay channel
LTE	Long Term Evolution
LOS	Line of Sight
MAC	Multiple Access Channel
ML	Maximum Likelihood
MS	Mobile Station
MSE	Mean Square Error
MIMO	Multi-Input Multi-Output
MISO	Multi-Input Single-Output
NC	Network Coding

QAM	Quadrature Amplitude Modulation
QF	Quantize-and-Forward
OFDM	Orthogonal Frequency Division Multiplexing
QPSK	Quadrature Phase-Shift Keying
pdf	probability density function
PRN	Parallel Relay Network
RCU	Remote Central Unit
RHS	Right Hand Side
RS	Relay Station
SDMA	Space Division Multiple Access
SQ	Scalar Quantization
SIC	Successive Interference Cancellation
SIMO	Single-Input Multi-Output
SINR	Signal-to-Interference-Noise Ratio
SISO	Single-Input Single-Output
STBC	Space-Time Block Coding/Code
TDD	Time Division Duplex
TWRC	Two-Way Relay Channel
uSQ	Uniform Scalar Quantization
ZF	Zero Forcing
VQ	Vector Quantization
WLAN	Wireless Local Area Network

Notations

Throughout the dissertation, we use the following notations. We use capital letters, e.g., X , for random variables (RVs), lower case letters, e.g., x , for the realization of these RVs, and calligraphic letters, e.g., \mathcal{X} , for their alphabets. A calligraphic letter denotes a set, e.g., $\mathcal{S} = \{1, 2, \dots, T\}$. A complement (denoted by the superscript c) of some subset \mathcal{S} of a set \mathcal{T} refers to the subset \mathcal{S}^c which fulfills: $\mathcal{S} \cup \mathcal{S}^c = \mathcal{T}$ and $\mathcal{S} \cap \mathcal{S}^c = \emptyset$. Bold uppercase letters, e.g., \mathbf{H} , refers to matrix while bold lowercase letters, e.g., \mathbf{h} , refer to column vector of appropriate dimensions. For the information theoretic expressions we follow the notations used in [1]. Other notational conventions are summarized as follows:

\mathbb{R}, \mathbb{C}	Sets of real and complex numbers, respectively
\mathbb{R}^+	Set of positive real numbers
$ x $	The absolute value of a scalar
$\angle x$	The phase of a complex scalar (in radians)
$\ \mathbf{x}\ $	The Euclidian (ℓ^2) norm of a vector
$ \mathcal{X} $	The cardinality of the set \mathcal{X} , i.e. the number of elements in the set \mathcal{X}
X^n	(X_1, X_2, \dots, X_n)
X_i	The i th element of the vector X^n
X_k^m	The vector (X_k, \dots, X_m)
$X_{(\mathcal{S})}$	$\{X_i\}_{i \in \mathcal{S}}$
$\text{CN}(\mu, \sigma^2)$	The circularly symmetric complex Gaussian distribution with mean μ and variance σ^2
$\mathbb{E}_X[\cdot]$	The expectation operator over the RV X
\mathbf{X}^*	The conjugate operation on \mathbf{X}
\mathbf{X}^H	The complex conjugate (Hermitian) operation on \mathbf{X}
\mathbf{X}^T	The transpose operation on \mathbf{X}
$\text{Tr}(\mathbf{X})$	The trace of \mathbf{X}
$\det(\mathbf{X})$	The determinant of \mathbf{X}
\mathbf{X}^{-1}	The inverse of \mathbf{X}
\mathbf{X}^\dagger	The Moore-Penrose pseudoinverse of \mathbf{X}
$\vec{\mathbf{X}}$	The vector obtained by stacking the columns of \mathbf{X}
\mathbf{I}_m	$m \times m$ identity matrix
$\mathbf{0}$	All zeros matrix of appropriate dimensions
$A_\epsilon^{(n)}$	The set of weakly jointly typical sequences for any intended set of RVs
\oplus	The XOR operation

Thesis specific Notations

We summarize here the symbols and notations that are commonly used in this dissertation. We have tried to keep consistent notations throughout the document, but some symbols have different definitions depending on where they occur in the text.

$\text{Exp}(\lambda_f)$	An exponentially distribution with mean λ_f
P_s	Source/Mobile transmit power
P_r	Relay station transmit power
$C(x)$	$\log_2(1 + x)$

Chapter 1

Introduction

1.1 Motivation

In next generation cellular systems, such as WiMAX and 3GPP LTE/LTE-A, one of the major concerns for service providers is to provide seamless connectivity to the end users with enhanced quality of service (QoS) in terms of reliability, data rate and robustness, which are not feasible with the conventional cellular architectures. The increasing number of applications, ranging from wireless access to the Internet and emergency/disaster recovery services, require a smarter and more complex network architecture design integrating various air interfaces, such as wireless LANs (WLAN) and Ad-hoc/mesh networks, to form a large network. Although integrating recently developed advanced transmission techniques (such as MIMO, OFDM, interference cancellation, etc.) into the system provides better throughput, reliability and coverage performance, these techniques alone cannot meet future demands of wireless systems without further deployment of infrastructure devices. Hence, the integration of multi-hopping (or relaying) into conventional wireless networks has been considered as a promising solution [2–7].

In wireless networks, multi-hopping provides several benefits such as cost reduction, power saving, coverage extension, increased data rates and diversity gain, as detailed below.

Firstly, thanks to the resulting shorter wireless links and cooperative diversity gain, significant power savings can be achieved with multi-hop relaying. Due to high link budget requirements in next generation cellular systems, power constraints at the mobile stations (MSs) will constitute a bottleneck for uplink (UL) communications especially for the mobiles close to the cell boundary. Moreover, if the MSs did have higher power levels, then the system would operate in an

interference limited regime and the mobiles at the cell-edges would still suffer. Also, the processing capability and size constraint at the MSs may prevent them from performing fancy MIMO precoding (or beamforming) techniques.

If, on the other hand, one is interested in achieving higher data rates, a naive solution in conventional cellular systems might be to increase base station (BS) density (so called cell-splitting approach). This, however, results in prohibitive deployment costs since each BS requires new backhaul links and cell-site leasing. Compared to cell splitting, infrastructure costs for relay station (RS) deployment are far less since there is no need for wired infrastructure links and availability of flexible site acquisition. If a MS in a cell is significantly closer to one of the RSs in the cell than to the BS, then the path-loss from the BS to the MS is larger than from the nearby RS to the MS. This in turn offers higher data rates on the link between the RS and the MS; hence potentially solving the *coverage* problem for high data rates in larger cells [2].

Also, by exploiting the *spatial reuse* potential of multi-hop relaying cellular system, where both BS and RSs simultaneously transmit to different MSs over the same system resources, higher data rates can be achieved.

1.1.1 Potential scenarios for Relay deployment

Given the benefits of multi-hopping, we now shortly overview several RS deployment scenarios provisioned for IEEE 802.16j [7]. All possible relaying schemes are illustrated in Figure 9.1.

Fixed infrastructure RSs are one of the possible RS deployment scenarios where they are intended to increase both coverage and throughput. In most cases, the link between a BS and each fixed RS is engineered to have line-of-sight (LOS) component. The RSs might have omni- or directional antennas directed to the BS. The latter needs more effort since depending on the traffic pattern it might be necessary to relocate the RSs, and hence to steer antennas' beams accordingly.

Communicating outdoor to indoor (or vice versa) with high QoS is challenging as building penetration loss faced by electromagnetic waves results in severe degradation of received signal strength. By installing a RS this problem could be solved easily. This type of RS also can be deployed near tunnels or subways to provide coverage extension.

RSs can be deployed in emergency situations (like earthquake, flooding, etc.) where some BSs are damaged. This type of RS is called temporal RS (or nomadic RS). Another form of relaying can be used to provide wireless connection to the end users located in trains or buses.

1.1.2 Main challenges to design multi-hop networks

As discussed earlier, multi-hop relaying has the potential to increase system performance in terms of throughput, fairness and coverage. However, introducing multi-hop relaying also comes with some specific challenges related to physical

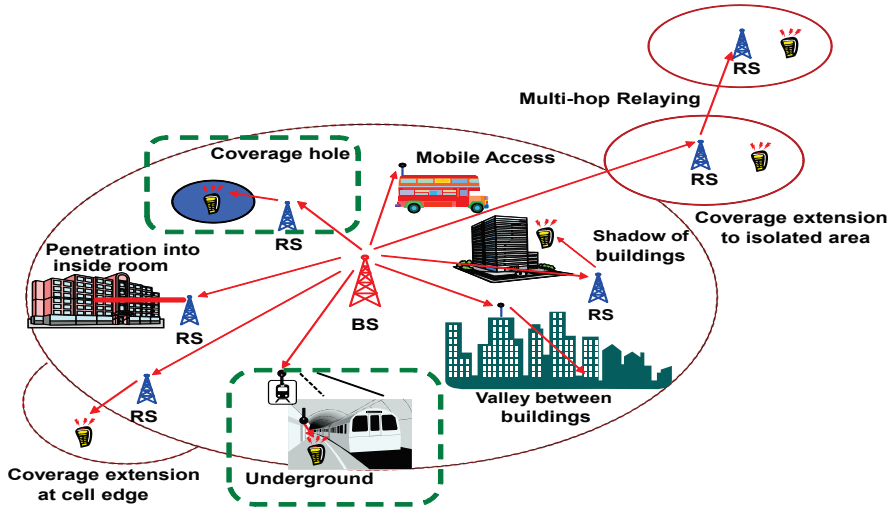


Figure 1.1: An illustration of possible relaying scenarios.

and MAC layer design [2, 4, 8]. The main factors that limit the achievable gains can be categorized as

- the multiplexing loss due to multi-hopping
- the quality of the link between RSs and BS
- the effect of the interference which increases with the number of deployed RSs, and
- the feedback overhead, especially in centralized solutions where an estimate of the channel state information (CSI) is required at the BS side.

To overcome the multiplexing loss, and hence target certain QoS constraints such as reliability, fairness and latency, smart resource allocation plays a crucial role in multi-hop cellular networks. As a result, one needs to pay special attention to scheduling and routing algorithms. Depending on the complexity and the level of intelligence at the relay stations (RSs), resource allocation might be performed either in *centralized* or in *distributed* fashion. In the centralized case, the base station makes all decisions, the system is fully coordinated and all advantages of multi-hopping can be exploited. However, since centralized resource allocation highly relies on global perfect CSI at the base station, thereby significantly increasing the feedback overhead in the system, such an approach may become intractable if there is fast fading and terminals are equipped with multiple antennas, thus also limiting system performance and scalability.

On the other hand, in the distributed resource allocation case the RSs are allowed to do scheduling, resource allocation and interference management. The

RSs perform resource allocation across users in their locality, with no influence from the BS. In Chapter 5, we address this problem and propose a distributed scheduling algorithm which requires less feedback at the BS while offering enhanced throughput.

With increasing user load, the RS might need to convey multiple user data to the BS which necessitates the system designer to engineer near line-of-sight (LOS) links between the BS and RSs at deployment time. RS sectorization, through which the interference in the cellular system might also be controlled, is an important degrees of freedom that would enable higher capacity gains from more aggressive spatial reuse schemes. In Chapter 4, we address, for uplink (UL) communications, the issues related to resource allocation on the access links from MSs to the BS and RSs, and the backhaul links from the RSs to the BS; the effects of antenna patterns used at the RS side are also considered.

Furthermore, introducing RSs in cellular systems allows spatial reuse of resources which is an important factor to increase system throughput. However, unless carefully treated, adding RSs could increase intra- and inter-cell interference. In Chapter 4, we also address this problem.

Apart from the above mentioned, there are still other practical issues that need to be addressed while deploying relay networks such as synchronization of spatially separated antennas and distributed CSI acquisition. Though these are fundamental issues in wireless Ad-hoc networks, in this thesis we make simplifications and assume these issues are solved.

1.2 Background

Relaying between radio nodes has been shown to reduce the aggregate path-loss and improve performance in wireless channels. This concept exploits the inherent *broadcast* nature of a wireless channel and is popularly referred to as multi-hopping. The relay channel formulation and protocols have been studied in various works in which the gains achievable with cooperation are observed to be promising. In the following subsections we will briefly introduce the evolution process of conventional relaying (one-way) protocols and continue with the recently introduced two-way relaying protocols and related concepts.

1.2.1 The one-way Relay Channel

The classical three terminal relay network which is central for cooperative networking was first developed by Van der Muelen in [9]: one node acts as a source with the RS assisting it without its own information to transmit. Cover and El Gamal made further progress by developing upper and lower bounds on its capacity, which is still an open problem, and proposed three relaying strategies: cooperation, facilitation and estimation [10]. Carleial has examined user cooperation in multiple-access channel via generalized (different channel outputs) feedback from the final destination to the transmitters [11]. Recently, user cooperation diversity received great attention as it provides spatial diversity gain

in a distributed fashion. Put simply, the source cooperates with a partner to transmit its information to the destination. This scheme forms a virtual transmit antenna array which provides more reliable transmission to destination than transmission from the source alone [12–14]. Cooperative diversity is also attractive in the fashion of no extra bandwidth requirement as in spatial (or antenna) diversity case. To increase channel capacity several cooperative modes at RS have been proposed [12, 15, 16].

Up to now, different protocols and relaying strategies have been proposed and widely studied in the literature in order to improve spectral efficiency and reliability of wireless systems [12, 15, 17, 18]. Depending on the knowledge and complexity of the RSs, these may process the received signals in different ways where amplify-and-forward (AF), decode-and-forward (DF) and compress-and-forward (CF) relaying strategies are the fundamental ones. In AF, the RSs simply amplify the received signal according to a power constraint and forward the amplified version of the signal to the destination node. In DF, the RSs decode the received signals, re-encode them and transmit to the destination node. Note that, the performance of DF strategy is limited by the source-to-relay links due to decoding process. In CF, the RSs compress (or estimate/quantize) the received signals with a certain fidelity and forward to the destination node.

Distributed space-time code design and information-theoretic performance limits for single antenna fading relay channels (with a finite number of nodes) have been studied in [12, 15, 18, 19]. Achievable rate results for MIMO relay channels with a finite number of relays can be found in [20–22].

In [23], Schein introduced a parallel relay network (PRN) where a source node communicates with a destination node through two parallel RSs, and also studied lower and upper bounds on capacity. This channel might be a model for multi-hop relaying networks where MSs that are in coverage hole can see only RSs. In the literature, there are several works where different aspects of PRN are studied [24–31]. Gastpar showed that the multiple-parallel relay channel capacity scales as the logarithm of the number of relays in [24] for Rayleigh fading channels. A variant of the PRN, where RSs are independently connected to the destination via lossless links of limited capacity, is considered by Sanderovich *et. al.* in [28, 29] where the authors assessed achievable rates with compress-and-forward relaying using distributed Wyner-Ziv [32] compression at the relays. It has also been shown by Sanderovich *et. al.* [28] that for a nomadic transmitter setting in which a source node communicates with a destination node via two intermediate RSs, each having limited lossless 1 [bit/transmission] capacity link to the destination, the rate achieved by using BPSK signaling at the source node along with 2-level hard-detectors (symbol-wise) at each RS outperforms the rate achieved by using Gaussian signaling at the source node and Gaussian mapping at the RSs. Motivated by these observations, in Chapter 2 we study different relaying strategies under simplified and realistic settings.

In the last decade, there has been a great deal of research on relay-assisted infrastructure based networks due to the potential improvements, discussed in the previous section, offered by relaying [2–4, 33–36].

References [4], [33] and [35] tackle some of the issues listed above. In [4], a

centralized downlink scheduling scheme is proposed, that guarantees the stability of the user queues for the largest set of arrival rates and achieves a significant gain with respect to the case of a system without RSs. It has been shown that with increasing number of RSs and multi-hops, the achievable gain also increases because of increasing reuse efficiency in the system which is achieved by simultaneous multiple transmissions. However, with more RSs the interference will be much more, thus limiting system performance. Hence, one should be aware of the interference associated with adding extra RSs into the system. In [33] the capacity benefits of in-band backhaul relaying for cellular uplink communications is studied under the assumption of a common maximum rate achievable by all the users in the network and of orthogonal separation of resources between BS-to-RS and BS/RS-to-MS links. They proposed a relaying scheme to exploit full spatial-reuse in the system where the spatial-reuse gain increases with increasing number of half-duplex RSs, wherein DF relaying strategy is used. Simulation results show the benefit of the proposal with respect to the base line without relays. Similarly, in [34] different communication modes are proposed in order to increase spatial reuse (i.e., increasing spectral efficiency) in a cellular system for the cases of one and two RSs in each cell sector with one- or two-hop transmission. Also, the optimal assignment of the proposed modes to the mobile users is presented. In [35], the power saving collaborative relaying schemes are proposed for cellular DL communications systems with half-duplex low-power RSs: the authors point out that coordinated transmission should be a promising solution to tackle the interference effect which is a big obstacle to power saving.

As explained above, RSs are used in wireless networks to extend coverage or enhance channel quality. Since RS deployment is a cost-effective solution for many applications, several standardization committees, including IEEE 802.16j [7, 37], work on adding the relaying functionality to their current standard. For instance, IEEE 802.16j adopts a two-hop network connection without a direct link between the source and the destination [7].

1.2.2 The two-way Relay Channel

Due to complexity issues, considering RSs operating in half-duplex (HD) mode (where they cannot transmit and receive during the same time) is more practical than full-duplex (FD) RSs. However, the HD constraint at RSs imposes a pre-log factor of $1/2$ on the overall system throughput and therefore limits the achievable spectral efficiency. To circumvent the spectral loss in the one-way relay channel, recently the concept of two-way (bi-directional) relay channel (TWRC) has been introduced where two mobiles exchange information via an intermediate RS [38–45]. Briefly, the communicating mobiles first send their messages to the RS and then in the second phase the RS processes the received signals according to a given relaying strategy and broadcasts to the mobiles. TWR provides interference-free reception at each mobile by canceling the self-interference before decoding the unknown message. The capacity region for general TWRC remains open.

The simplest transmission scheme for TWRC consists of four phases where the two nodes transmit their messages to the RS successively and then the RS decodes and forwards each mobile's message in the following two time slots. However, using ideas from network coding (NC) [46], a two-way relaying scheme that requires three time slots is considered in [47] where in the first two time slots the mobiles send their messages to the RS in orthogonal time slots, the RS decodes both messages and then combines them by means of the bit-wise XOR operation and retransmits it to the mobiles. There the mobiles are assumed to use the bit-wise XOR operation on the decoded message and the own transmitted message to obtain the message sent from the other mobile. Requiring three time slots, this bit-wise XOR based TWR scheme provides a pre-log factor of $2/3$ with respect to the sum-rate.

The number of required time slots for the communication between the two nodes can be reduced even further to two time slots by allowing them to simultaneously access the RS [41, 44, 48–53]. In [41, 48, 49, 54] AF, DF and CF based relaying schemes consisting only of two time slots are proposed for TWRC. In [44] an analog network coding (ANC) scheme, where the RS amplifies and forwards mixed received signals, is proposed and compared to the traditional and the digital network coding (bit-wise XOR at the RS) schemes in terms of network throughput. In [41, 49], denoise-and-forward (DNF) relaying is proposed for TWRC where the RS removes the noise from the combined mobiles' messages (on the multiple-access channel) before broadcasting and compared to AF, DF based TWR schemes as well as to the traditional four phase scheme.

1.3 Contributions and Outline of this Dissertation

The goal of this dissertation is to propose simple and flexible relaying architectures for various wireless networks with achievable rates and reliability being our main figures of merit. Specifically, we will try to project the insights gained from information theoretic analysis of various relaying strategies into the real world and see the effectiveness and potentials of relaying in various wireless application. In particular, we analyze parallel relay networks (PRNs), which might model several wireless communication scenarios such as uplink with backhaul constraint base stations, multi-hop relaying in cellular uplink and downlink communications, and two-way relaying networks, which might model several wireless communication setups such as satellite communications.

In Chapter 2, we study outer bounds and achievable rates for various relaying strategies, such as AF, DF, block quantization and random binning (BQRB) and QF, for the AWGN PRN with phase fading under two different access channel models from the RSs to the destination. We also show the possibility of achieving relatively good performance with simplified processing assumptions at the source and RSs. The results were published in

- Erhan Yılmaz, David Gesbert and Raymond Knopp, "Parallel Relay

Networks with Phase Fading", in the proceedings of *IEEE Global Communications Conference (GLOBECOM)*, New Orleans, USA, 2008.

and will be submitted as one part of

- Erhan Yilmaz, Raymond Knopp and David Gesbert, "**Coding strategies and Error exponents for multi-source Parallel Relay Networks**", under preparation.

In Chapter 3, we focus our attention on the random coding error exponents corresponding to the DF, BQRB and QF relaying strategies for the single- and two-source PRN setups, consisting of two RSs which are connected to the destination via an error-free finite capacity backhaul, in order to have thorough characterization of system performance. We show that using a finite constellation modulation, e.g., M-QAM, at the source nodes along with simple processing at the RSs, uniform scalar quantization to be specific, can provide better error exponents than more complex and non-practical relaying strategies thanks to the structure inherent in the considered modulation scheme. A part of this work was published in

- Erhan Yilmaz, Raymond Knopp and David Gesbert, "**Error Exponents for Backhaul-Constrained Parallel Relay Networks**", in the proceedings of *IEEE International Symposium Personal, Indoor and Mobile Radio Communications (PIMRC)*, September 2010, Istanbul, Turkey.

and will be submitted as one part of

- Erhan Yilmaz, Raymond Knopp and David Gesbert, "**Coding strategies and Error exponents for multi-source Parallel Relay Networks**", under preparation.

In Chapter 4, we consider relay-aided cellular UL communications under intercell interference. Assuming orthogonal frequencies for the mobile-to-relay and relay-to-base links, the achievable average sum-rates are analyzed for the AF, DF, CF and QF relaying strategies and compared with two well-known cellular systems, namely the conventional cellular system and the ideal distributed antenna system (DAS). The effects of positioning and antenna pattern selection of RSs are examined. The results were published in

- Erhan Yilmaz, Raymond Knopp and David Gesbert, "**Some System Aspects Regarding Compressive Relaying with Wireless Infrastructure Links**", in the proceedings of *IEEE Global Communications Conference (GLOBECOM)*, New Orleans, USA, 2008.
- Erhan Yilmaz, Raymond Knopp and David Gesbert, "**Relaying with Wireless Infrastructure Links in Cellular Networks**", in the proceedings of the *IEEE Winter School on Information Theory*, Loen, Norway, March 29 – April 3, 2009.

- Erhan Yılmaz, Raymond Knopp and David Gesbert, "**On the gains of fixed relays in cellular networks with intercell interference**", in *the proceedings of IEEE International Workshop on Signal Processing Advances in Wireless Communications (SPAWC)*, Perugia, Italy, June 21–24, 2009.

and will be submitted as

- Erhan Yılmaz, Raymond Knopp and David Gesbert, "**On the gains of fixed relays in cellular uplink communications with intercell interference**", under preparation.

In Chapter 5, we propose a distributed scheduling algorithm for DL transmissions in relay deployed cellular systems, where a given mobile user can be either served by the base station or by a relay, in an opportunistic way. We show that such a distributed approach allows *reduced* feedback with respect to the centralized case, especially when a simple scalar feedback is not sufficient for estimating the channel quality. As a result of the reduced feedback requirements the system becomes more *scalable*, as new relays can be deployed where needed without need of a careful network planning. The results were published in

- Erhan Yılmaz, Federico Boccardi and Angeliki Alexiou, "**Distributed and Centralized Architectures for Relay-Aided Cellular Systems**", in *the proceedings of IEEE Vehicular Technology Conference (VTC Spring)*, 2009, Barcelona, Spain (*invited paper*).

In Chapter 6, we analyze different coding strategies for two-way relay channels. In particular, lattice-based partial decoding and compression-based strategies are studied. We show that the CF relaying strategy, based on binning at the RS, can nearly achieve optimal performance when the relay transmit power increases. The results were published in

- Erhan Yılmaz and Raymond Knopp, "**Coding Strategies for Two-Way Relay Channels**", under preparation.

In Chapter 7, we consider a multi-pair two-way relay channel (TWRC) where the single-antenna MSs on each pair seek to communicate via a common multiple antenna RS. In the multi-pair TWRC, the main bottleneck on system performance is the interference seen by each mobile due to the other communicating mobile pairs. We propose different transmit/receive beamforming schemes at the RS, assuming AF and QF relaying strategies, in order to tackle this problem in the *spatial* domain by using multiple antennas at the RS. This work was done in collaboration with fellow PhD student, Randa Zakhour, and the results were published in

- Erhan Yılmaz, Randa Zakhour, David Gesbert and Raymond Knopp, "**Multi-pair Two-way Relay Channel with Multiple Antenna Relay Station**", in *the proceedings of IEEE International Conference on Communications (ICC)*, June 2010, Cape Town, South Africa.

Chapter 2

Multi-Source Parallel Relay Networks: Coding Strategies

2.1 Introduction

In this chapter, we examine a general version of the Gaussian parallel relay networks (PRNs), primarily proposed and studied in [23,55], with phase fading. The general PRN with phase fading consists of multiple source and relay nodes, and a single destination node where source nodes want to communicate with the destination node by the assistance of intermediate relay nodes (RSs). There is no direct link from the sources to the destination. For the links between the RSs and the destination node we consider two particular channel models:

- a regular multiple-access channel (MAC) with constant channel gains and random phase shifts (i.e., shared wireless MAC)
- orthogonal error-free limited-capacity backhaul (e.g., microwave links or fiber-optic cable) links between the RSs and the destination (orthogonal MAC).

We note that, if feasible, each rate-tuple for the error-free orthogonal backhaul links from the RSs to the destination (orthogonal MAC case) might correspond to an operating point in shared wireless MAC capacity region. Hence, we might have the same performance as for the shared wireless medium access case by selecting different rate-tuples for orthogonal MAC case.

2.1.1 Motivation

The PRN studied in this chapter, wherein an error-free finite capacity backhaul connection and a regular MAC connection between the RSs and the destination are assumed, can find *applications* in cellular networks for UL communications.

For future cellular systems, the use of MCP is a promising tool for increasing system spectral efficiency and reliability both by alleviating inter-cell interference effect via joint processing of BSs' received signals at a remote central unit (RCU) for UL communications, which would be one of the cooperating BSs, and by providing spatial diversity (and/or shadowing diversity) [29, 56, 57]. Moreover, allowing joint processing would lead to reduction in required transmit power at MSs. In most of the evaluations done so far for MCP, it is assumed that the BSs are connected to a RCU via a reliable and infinite capacity backhaul link, which however is an unrealistic assumption especially when system load is high. Hence, in this chapter, we consider a more realistic system model where the BSs (in our setup RSs) are connected to the final destination via a lossless limited-capacity links.

The considered PRN model can also find applications in long-range sensor networks where RSs could be satellites with deep-space link to earth stations. Moreover, rapidly deployable infrastructure networks (military or civil applications) would also be target application of the PRN studied in this chapter. In rapidly deployable infrastructure networks, some nomadic RSs, which are placed in different geographic locations, are connected to a RCU via reliable but finite-capacity links, and provide coverage for MSs (depending on the application this would be users terminals willing access core cellular network or sensor nodes emitting some environmental data toward a central collector) on the geography.

As mentioned earlier, multi-antenna reception can be mimicked by assuming infinite backhaul capacity links between RSs and a destination node. This assumption also constitutes an outer bound on the achievable rates. However, since this assumption is not practical, we study a more realistic and simpler PRN setup where limited-capacity backhaul links are considered. Note that system performance is highly dependent on the processing capabilities of RSs. In this chapter, we investigate whether it is possible to reach multi-user MIMO performance by using simple and cheap RSs with limited backhaul connection.

2.1.2 Prior work

The PRN consisting of a single source, two relays and a single destination is first introduced by Schein and Gallager in [23, 55] where outer bounds on capacity, which is still an open problem, are derived and several coding strategies are proposed assuming Gaussian and discrete memoryless channels models. For the scalar Gaussian case, they propose Amplify-and-Forward (AF), Decode-and-Forward (DF) and also another relaying strategy based on the time sharing of these strategies. For the discrete case, where links between relays and the destination are assumed to be finite-rate lossless orthogonal links, they propose a novel relaying strategy based on compression strategy of Wyner-Ziv [32] followed

by random binning strategy of Slepian-Wolf [58]. They name this strategy as *block-quantization and random binning* (BQRB) relaying. For Gaussian channel, they conjecture that compression based relaying scheme can not give better achievable rate than the AF due to *coherent combining* effect of the Gaussian channel. In [25, 59], it is shown that for a Gaussian PRN operating in the wide-band regime, there is no benefit from employing the AF strategy, since a part of relay power is wasted in amplifying the receiver noise which results in reduced AF gain. In [24, 60], it is shown that with uncoded transmission at the source, two-hop AF relaying strategy achieves capacity as the number of relays increases. Recently, in [26] a Rematch-and-Forward (RF) relaying strategy, based on the use of analog modulo-lattice modulation, is proposed for a type of PRN where there is a bandwidth mismatch between the source-relays and relays-destination channels. A similar model with half-duplex relays is studied in [30]. Using the deterministic approach, see [61], the authors of [62] show that their new achievable rate for general scalar Gaussian relay networks is within a constant number of bits from the cut-set upper bound on the capacity. A new achievable rate for the original Schein's network is derived using a combined AF-DF scheme in [27]. Recently, the vector Gaussian PRN model, involving multi-antenna source and destination node is considered in [31] where several interesting results are derived.

2.1.3 Contributions

The contributions of this chapter are

- Different outer bounds and achievable rates are examined by Schein in [23, 55] for a simple Gaussian PRN consisting of a single source and two relay nodes. Here, we derive a new outer bound which is a multi-source generalization of Schein's scheme and compare this outer bound to the cut-set bound consisting only of broadcast and multi-access cuts. Then, we examine how far the achievable rates corresponding to AF, DF, BQRB and QF relaying strategies are from the outer bound.
- Schein in his thesis [23] shows that when broadcast channel (BC) quality is inferior to that of multiple-access channel (MAC), then DF relaying is suboptimal, i.e., the corresponding achievable rate falls short of the network capacity; however, AF relaying achieves network capacity in the limit of infinite power consumption in the MAC components due to the *coherent combining* effect at the destination node. For this scenario, using the well-known source coding tools (reproducing the RS observation with some fidelity) can not yield better performance [23]. In [23], for discrete PRNs where relays are connected to the destination via noiseless orthogonal finite-capacity backhaul links, it is shown that if the backhaul links have enough capacity in order to be able to reproduce the RS observations at the destination node, then the use of BQRB technique can achieve the network capacity. We note however that for *phase fading* Gaussian PRNs,

coherent combining effect does not hold anymore, and *independent* signal transmission is the optimal way of communication in phase-fading MACs [17,18]. Hence, we can apply the quantization and random binning tools [32,58] to RS observations and get higher achievable rates than those proposed in [23]. Notice that, although the RS observations are dependent random variables (RVs), and their quantized versions as well, the use of random binning (independent of the transmitted source signal) will result in independent relay bin indexes. This is exactly the feature that enables us to have improved network achievable rates compared to the AF and DF relaying strategies.

- With lower channel quality at the BC part than the MAC part, the achievable rate region performance of BQRB is shown to outperform that of AF and DF relaying schemes and to tend to the rate region achievable by a MAC with multi-antenna destination for multi-source case.
- In most of the papers dealing with CF (or QF) relaying strategy, Gaussian codebooks at the sources and Gaussian mapping at the RSs are assumed, without claiming optimality, in order to make the analysis of the relaying scheme easier [17,18]. Lately, in [28, Section VI-B] it is shown that for a nomadic transmitter setting where a source communicates with a destination via two intermediate RSs each having limited lossless 1 [bit/transmission] capacity link to the destination, the rate achieved by using BPSK signaling at the source along with 2-level hard-detectors (symbol-wise) at each RS outperforms the rate achieved by using Gaussian signaling at the source and Gaussian mapping at the RSs. Parallel conclusions are also remarked in [63,64] for the Gaussian relay channel setup with coded modulation (CM) at the source and orthogonal relay-to-destination link where an estimate-and-forward (EF) relaying scheme with different RS mappings is studied. They concluded that for the CM scenario at *low* source-relay SNR EF with Gaussian mapping at the RS is the best, at *high* source-relay SNR DF is superior and at *intermediate* SNR region EF with *hard-decision per symbol* at the RS is better than the above two methods. Motivated by these observations, we studied the BQRB and QF relaying schemes assuming finite constellation codebooks (i.e., M-ary Quadratic Amplitude Modulation (M-QAM)) at sources and non-Gaussian mapping (e.g., simple uniform scalar quantization (uSQ)) at RSs.
- The processing capabilities of RSs highly affect system performance. Thus, in this chapter, we investigate whether it is possible to have good performance by using simple and cheap RSs with limited backhaul connections to the destination. In particular, we look at a *simpler* and more *practical* quantization technique at the RSs which relies on symbol-by-symbol uSQ since in the high resolution regime the performance loss compared to vector quantization (VQ) becomes negligible [65–67].
- At *low* source-to-relay SNR regime, where the CF or QF relaying gives the best gain [18], it is possible to approach the limits of the system by using

CM at the sources. Moreover, with CM at the sources it is possible to exploit the *structure* of source codewords by using non-Gaussian mapping at the RSs. Through numerical simulations we observe that from low to medium SNR regime, with sufficient backhaul capacities in order to be able to convey decoded bits reliably to the destination, the achievable sum-rate by using QF relaying with CM at the sources and uSQ at the RSs outperforms that of DF relaying with Gaussian signaling at the sources. Moreover, we observe that this achievable sum-rate is directly proportional to the modulation alphabet size.

2.2 Channel Model

We study the general PRN model shown in Figure 9.2 where a set of $\mathcal{J} = \{1, 2, \dots, T\}$ sources want to communicate with a destination with the assistance of a set $\mathcal{K} = \{1, 2, \dots, K\}$ of RSs. We assume neither direct link between the sources and the destination nor among the RSs. All the channels are modeled as time-invariant, memoryless additive white Gaussian noise (AWGN) channels with constant gain (which may correspond to path-loss between each transmitter and receiver) and ergodic phase fading. The RSs operate in *full-duplex* (FD) mode. Each source encodes its message $W_t \in \mathcal{W}_t$, where $\mathcal{W}_t = \{1, 2, \dots, 2^{nR_t}\}$ and R_t is the transmission rate of the t -th source, into the codeword $X_t^n(W_t)$. All source channel inputs are independent of each other.

The received signal at the k -th RS after the i -th channel use, for $i \in [1, n]$, is

$$Y_{R_k,i} = \sum_{t=1}^T h_{kt} e^{j\Phi_{kt,i}} X_{t,i} + Z_{k,i}, \quad \forall k \in \mathcal{K}, \quad (2.1)$$

where $h_{kt} \in \mathbb{R}^+$ for all $k \in \mathcal{K}$ and $t \in \mathcal{J}$, is the fixed channel gain from the t -th source to the k -th RS, $Z_{k,i} \sim \mathcal{CN}(0, \sigma^2)$ is circularly symmetric complex AWGN at the k -th RS. The $\Phi_{kt,i}, \forall \{k, t\}$ denote the set of random phases induced by the channels from the t -th source to the k -th RS. We assume an average power constraint for each codeword $X_t^n(W_t)$ transmitted by the sources, which in the limit $n \rightarrow \infty$ can be expressed as follows

$$\frac{1}{n} \sum_{i=1}^n |X_{t,i}(W_t)|^2 \leq P_s \quad (2.2)$$

for all $t \in \mathcal{J}$ and $W_t \in \mathcal{W}_t$.

The k -th RS transmits X_{R_k} based on the previously received signals (causal encoding) [10]

$$X_{R_k,i} = f_{R_k,i}(Y_{R_k,1}, Y_{R_k,2}, \dots, Y_{R_k,i-1}) \quad (2.3)$$

where $i \in [1, n]$ is the time index.

For the access channel from the RSs to the destination, we consider 2 different channel models: 1) a regular AWGN MAC with constant channel gain and random phase fading, and 2) lossless orthogonal links with finite capacity between each RS and the destination.

2.2.1 Shared MAC between the RSs and the Destination

In this case, we consider an AWGN MAC from the RSs to the destination consisting of constant channel gain and random uniform phase fading, as shown in Figure 9.2. We assume an average power constraint for each RS, which in the limit $n \rightarrow \infty$ can be expressed as follows

$$\frac{1}{n} \sum_{i=1}^n |X_{R_k,i}|^2 \leq P_r, \quad \forall k \in \mathcal{K}. \quad (2.4)$$

With this model the received signal at the destination after the i -th channel use, for $i \in [1, n]$, is given by

$$Y_i = \sum_{k=1}^K g_k e^{j\Phi_{Dk,i}} X_{R_k,i} + Z_i \quad (2.5)$$

where $g_k \in \mathbb{R}^+$, $\forall k \in \mathcal{K}$, is the fixed channel gain from the k -th RS to the destination, and $Z_i \sim \mathcal{CN}(0, \sigma^2)$ is circularly symmetric complex AWGN at the destination. The $\Phi_{Dk,i}$, $\forall k \in \mathcal{K}$ denote the set of random phases induced by the channel from the k -th RS to the destination at the i -th channel use.

Note that we assume ergodic phase fading where each of $\Phi_{kt,i}$ and $\Phi_{Dk,i}$ is a random variable distributed uniformly over $[-\pi; \pi]$. Random phases are perfectly known to the relevant receivers and unknown to the transmitters.

2.2.2 Orthogonal limited-capacity links between the RSs and the Destination

Considering cellular telephony systems it is possible that some of the BSs connect to a central control unit either via fiber-optic links or via microwave links. In order to add these application scenarios in the scope of the chapter, we also consider the channel model between the RSs and the destination as an orthogonal error-free finite-capacity backhaul links where we let the link capacity from RS i to the destination be C_i in [bits/channel use]. This scheme is depicted in Figure 9.3.

2.2.3 Preliminaries

Before proceeding with the derivation of an outer bound and some achievable rate regions for the AWGN PRN, we first give some information theoretic definitions for this system model illustrated in Figure 9.2:

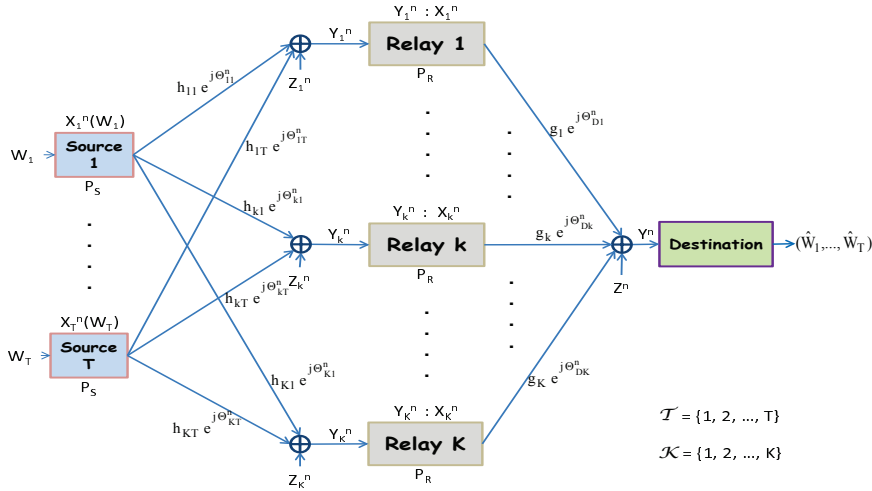


Figure 2.1: A general M -source, K -relay and single destination PRN setup with phase fading.

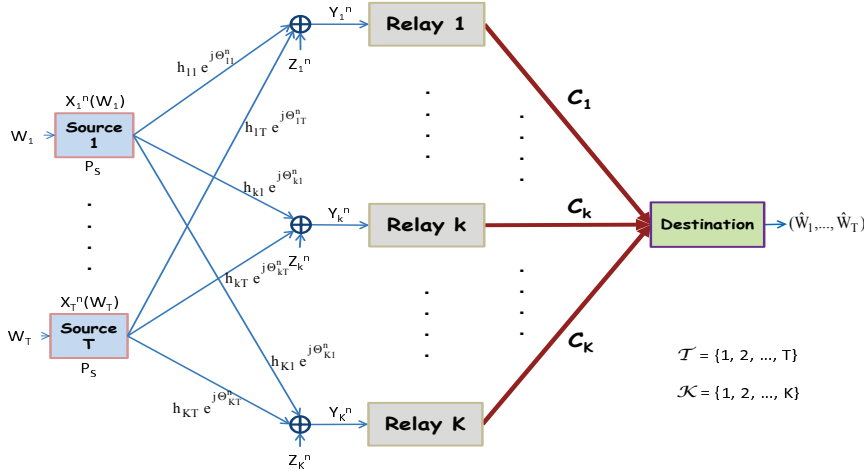


Figure 2.2: A general M -source, K -relay and single destination PRN setup with orthogonal error-free finite-capacity backhaul links between the RSs and the destination, where C_i in [bits/channel use] is the link capacity between the i -th RS and the destination, for $i = 1, 2, \dots, K$.

Definition 1. A time invariant and memoryless AWGN PRN is defined by

$$\{(\{\mathcal{X}_t\}_{t=1}^T, \{\mathcal{X}_{R_k}\}_{k=1}^K), f(\{y_{R_k}\}_{k=1}^K | \{x_t\}_{t=1}^T) f(y | \{x_{R_k}\}_{k=1}^K), (\{\mathcal{Y}_{R_k}\}_{k=1}^K, \mathcal{Y})\}, \quad (2.6)$$

where $\{\mathcal{X}_t\}_{t=1}^T$ and $\{\mathcal{X}_{R_k}\}_{k=1}^K$ are the input alphabets, \mathcal{Y} and $\{\mathcal{Y}_{R_k}\}_{k=1}^K$ are the output alphabets and $f(\cdot|\cdot)$ is the channel transition probability matrix. The time invariant and memoryless channel is represented by

$$\begin{aligned} f(\mathbf{y}, \mathbf{y}_{R_1}, \dots, \mathbf{y}_{R_K} | \mathbf{x}_1, \dots, \mathbf{x}_T, \mathbf{x}_{R_1}, \dots, \mathbf{x}_{R_K}) \\ &= \prod_{i=1}^n f(y_i, y_{R_1 i}, \dots, y_{R_K i} | x_{1i}, \dots, x_{Ti}, x_{R_1 i}, \dots, x_{R_K i}) \\ &= \prod_{i=1}^n f(y_{R_1 i}, \dots, y_{R_K i} | x_{1i}, \dots, x_{Ti}) f(y_i | x_{R_1 i}, \dots, x_{R_K i}) \end{aligned} \quad (2.7)$$

where $x_{ti}, x_{R_k i}, y_i, y_{R_k i}, \forall t \in \mathcal{T}$ and $\forall k \in \mathcal{K}$, are the inputs and outputs of the channel at time i , respectively.

At the beginning of each block of n channel uses, the message sources produce random integers W_t from the sets $\mathcal{W}_t, \forall t \in \mathcal{T}$. The message tuple $\{W_t\}_{t=1}^T$ is drawn according to a uniform distribution over $\{\mathcal{W}_t\}_{t=1}^T$ and occurs with probability $1/2^{n \sum_{t=1}^T R_t}$.

Definition 2. A $(2^{nR_1}, 2^{nR_2}, \dots, 2^{nR_T}, n)$ code for the AWGN PRN model shown in Figure 9.2, where a set of $\mathcal{T} = \{1, 2, \dots, T\}$ sources want to communicate with a destination with the help of a set $\mathcal{K} = \{1, 2, \dots, K\}$ of RSs, consists of the following:

- T index sets $\mathcal{W}_t = \{1, 2, \dots, 2^{nR_t}\}$ and signal spaces $\mathcal{X}_t, \forall t \in \mathcal{T}$,
- T source encoding functions

$$f_t : \mathcal{W}_t \rightarrow \mathcal{X}_t^n, \quad \forall t \in \mathcal{T}, \quad (2.8)$$

that map each source message $W_t \in \mathcal{W}_t$ into a codeword $X_t^n(W_t)$, satisfying the average power constraint P_s , i.e., for every codeword $W_t \in \mathcal{W}_t$,

$$\frac{1}{n} \sum_{i=1}^n |X_{t,i}(W_t)|^2 \leq P_s, \quad \forall t \in \mathcal{T}, \quad (2.9)$$

- For each RS, a set of relay encoding (causal) functions $\{f_{R_k,i}\}_{i=1}^n, \forall k \in \mathcal{K}$, such that

$$x_{R_k,i} = f_{R_k,i}(Y_{R_k,1}, Y_{R_k,2}, \dots, Y_{R_k,i-1}), \quad 1 \leq i \leq n, \quad (2.10)$$

- and a decoding function at the destination

$$g_d : \mathcal{Y}^n \rightarrow \mathcal{W}_1 \times \mathcal{W}_2 \times \dots \times \mathcal{W}_T. \quad (2.11)$$

After defining $g_d(\mathcal{Y}^n) = (\hat{W}_1, \hat{W}_2, \dots, \hat{W}_T)$, the average probability of error is given by

$$P_e^{(n)} = \frac{1}{2^{n \sum_{i=1}^T R_i}} \sum_{(W_1, \dots, W_T) \in \mathcal{W}_1 \times \dots \times \mathcal{W}_T} \Pr[g_d(\mathcal{Y}^n) \neq (W_1, W_2, \dots, W_T)]. \quad (2.12)$$

Definition 3. A rate tuple (R_1, \dots, R_T) is said to be achievable for the AWGN PRN with respective power constraints P_s and P_r at the sources and RSs if there exists a sequence of $(2^{nR_1}, \dots, 2^{nR_T}, n)$ codes with average probability of error $P_e^{(n)} \rightarrow 0$ as $n \rightarrow \infty$. The capacity region is the closure of the set of all achievable rate tuples (R_1, R_2, \dots, R_T) .

2.3 PRN with Gaussian Signaling at the Sources and the RSs

In this section, we examine different relaying strategies for the AWGN PRN with phase fading under the assumptions of Gaussian signaling at the sources and Gaussian mapping¹ at the RSs. Though with these assumptions it is easier to analyze system performance for various relaying strategies, it is not obvious whether these assumptions are the best one can make. Hence, in the following section, we will also look at non-Gaussian settings and investigate the performances of different relaying strategies.

2.3.1 Shared MAC between the RSs and the Destination

We derive an outer bound and some inner bounds corresponding to the AWGN PRN with phase fading setup depicted in Figure 9.2, which consists of T sources, K RSs and a single destination. In particular, assuming *Gaussian signaling* at both the sources and the RSs, we derive some inner bounds corresponding to different relaying strategies used at the RSs, namely AF, DF, BQRB and QF relaying. We assume that signals transmitted by the sources are independent of each other. In the following, for brevity of exposition, we consider $T = 2$ sources that are willing to communicate with the destination via $K = 2$ RSs. Moreover, for the sake of simplicity, we drop the time index variable. Note that a similar setup with a single source is analyzed in [23] and [24] for AWGN channels without phase-fading.

Outer Bound (Converse Analysis)

Using the well-known cut-set bound theory and the data processing inequalities [1], we come up with the following bound on the achievable rates:

¹By "Gaussian mapping" we mean that "Gaussian Quantization" is used at the RSs, as in [63, 64]. Also, by "Gaussian signalling" it is meant that "Gaussian codebooks" are used at the relevant terminals.

Theorem 4. *An outer bound for the T -source K -relay AWGN PRN with phase fading is given by*

$$\sum_{i \in \mathcal{M}} R_i \leq \max_{p(\mathbf{x}, \mathbf{x}_R)} \min_{\mathcal{R} \subseteq \mathcal{K}} \left\{ I(X_{(\mathcal{M})}; Y_{R_{(\mathcal{R})}} | X_{(\mathcal{M}^c)}) + I(X_{R_{(\mathcal{R}^c)}}; Y | X_{R_{(\mathcal{R})}}) \right\} \quad (2.13)$$

for $\mathcal{M} \subseteq \mathcal{T}$ and the channel transition probability distribution

$$f(\mathbf{x}_{(\mathcal{T})}, \mathbf{x}_{R_{(\mathcal{K})}}, \mathbf{y}_{R_{(\mathcal{K})}}, \mathbf{y}) = f(\mathbf{x}_{(\mathcal{T})}) f(\mathbf{y}_{R_{(\mathcal{K})}} | \mathbf{x}_{(\mathcal{T})}) f(\mathbf{x}_{R_{(\mathcal{K})}} | \mathbf{y}_{R_{(\mathcal{K})}}) f(\mathbf{y} | \mathbf{x}_{R_{(\mathcal{K})}}).$$

Proof. See Appendix-2.A for the proof. \square

For the $T = 2$ sources $K = 2$ relays AWGN PRN with phase fading, we have the following outer-bound:

$$\begin{aligned} R_1 &= \min \left\{ \log_2 (1 + (h_{11}^2 + h_{21}^2) \gamma_r), \log_2 (1 + h_{21}^2 \gamma_r) + \log_2 (1 + g_1^2 \gamma_d), \right. \\ &\quad \left. \log_2 (1 + h_{11}^2 \gamma_r) + \log_2 (1 + g_2^2 \gamma_d), \log_2 (1 + (g_1^2 + g_2^2) \gamma_d) \right\} \\ R_2 &= \min \left\{ \log_2 (1 + (h_{12}^2 + h_{22}^2) \gamma_r), \log_2 (1 + h_{22}^2 \gamma_r) + \log_2 (1 + g_1^2 \gamma_d), \right. \\ &\quad \left. \log_2 (1 + h_{12}^2 \gamma_r) + \log_2 (1 + g_2^2 \gamma_d), \log_2 (1 + (g_1^2 + g_2^2) \gamma_d) \right\} \\ R_1 + R_2 &= \min \left\{ \mathbb{E}_{\{\Phi_{kt}\}} \left[\log_2 \det (\mathbf{I}_2 + \gamma_r \mathbf{H} \mathbf{H}^H) \right], \log_2 (1 + (h_{21}^2 + h_{22}^2) \gamma_r) + \log_2 (1 + g_1^2 \gamma_d), \right. \\ &\quad \left. \log_2 (1 + (h_{11}^2 + h_{12}^2) \gamma_r) + \log_2 (1 + g_2^2 \gamma_d), \log_2 (1 + (g_1^2 + g_2^2) \gamma_d) \right\} \end{aligned}$$

where $\gamma_r = P_s / \sigma^2$, $\gamma_d = P_r / \sigma^2$, and

$$\mathbf{H} = \begin{bmatrix} h_{11} e^{j\Phi_{11}} & h_{12} e^{j\Phi_{12}} \\ h_{21} e^{j\Phi_{21}} & h_{22} e^{j\Phi_{22}} \end{bmatrix} = \begin{bmatrix} \mathbf{h}_1^T \\ \mathbf{h}_2^T \end{bmatrix} \in \mathbb{C}^{2 \times 2} \quad (2.14)$$

is the channel matrix between the sources and the RSs. Note that in deriving the mutual information expressions, we use the fact that the mutual information maximizing input distribution at the sources and the RSs is jointly independent Gaussian distribution.

AF Relaying Strategy

In this relaying strategy each RS scales its received signal to satisfy the power constraint P_r and retransmits it. The scaling factor α_k at the k -th RS is given by

$$\alpha_k = \sqrt{\frac{P_r}{\sum_{t=1}^T h_{kt}^2 P_s + \sigma^2}}, \quad \forall k \in \mathcal{K} \quad (2.15)$$

The k -th RS transmits $X_{k,i} = \alpha_k Y_{k,i}$, $i \in [1, n]$, to the destination. Then, the received signal at the destination, given by (9.5), can be re-written as follows

$$\begin{aligned}
Y_i &= \sum_{k=1}^K g_k e^{j\Phi_{Dk,i}} X_{Rk,i} + Z_i = \sum_{k=1}^K \alpha_k g_k e^{j\Phi_{Dk,i}} Y_{Rk,i} + Z_i \\
&= \sum_{k=1}^K \alpha_k g_k e^{j\Phi_{Dk,i}} \left(\sum_{t=1}^T h_{kt} e^{j\Phi_{kt,i}} X_{t,i} + Z_{k,i} \right) + Z_i \\
&= \sum_{t=1}^T \left(\sum_{k=1}^K \alpha_k g_k h_{kt} e^{j(\Phi_{Dk,i} + \Phi_{kt,i})} \right) X_{t,i} + \sum_{k=1}^K \alpha_k g_k e^{j\Phi_{Dk,i}} Z_{k,i} + Z_i. \quad (2.16)
\end{aligned}$$

Considering the received signal model for $T = 2$ sources and $K = 2$ RSs, we have the following achievable rate region for the AF relaying strategy

$$R_1 \leq \mathbb{E}_{\Phi_1} \log_2 \left(1 + \frac{\Gamma_1 \gamma_{1,1} + \Gamma_2 \gamma_{2,1} + 2\sqrt{\Gamma_1 \Gamma_2 \gamma_{1,1} \gamma_{2,1}} \cos(\Phi_1)}{1 + \Gamma_1 + \Gamma_2} \right) \quad (2.17a)$$

$$R_2 \leq \mathbb{E}_{\Phi_2} \log_2 \left(1 + \frac{\Gamma_1 \gamma_{1,2} + \Gamma_2 \gamma_{2,2} + 2\sqrt{\Gamma_1 \Gamma_2 \gamma_{1,2} \gamma_{2,2}} \cos(\Phi_2)}{1 + \Gamma_1 + \Gamma_2} \right) \quad (2.17b)$$

$$R_1 + R_2 \leq \mathbb{E} \log_2 \left(1 + \frac{\sum_{i=1}^2 \Gamma_i (\gamma_{i,1} + \gamma_{i,2}) + 2\sqrt{\Gamma_1 \Gamma_2 \gamma_{1,i} \gamma_{2,i}} \cos(\Phi_i)}{1 + \Gamma_1 + \Gamma_2} \right) \quad (2.17c)$$

where $\Gamma_k = \frac{\gamma_{D,k}}{\gamma_{k,1} + \gamma_{k,2} + 1}$, $\Phi_k = \Phi_{D1} - \Phi_{D2} + \Phi_{1k} - \Phi_{2k}$, and $\gamma_{k,t} = \frac{h_{kt}^2 P_s}{\sigma^2}$ and $\gamma_{D,k} = \frac{g_k^2 P_r}{\sigma^2}$, $\forall t \in \mathcal{T}$ and $\forall k \in \mathcal{K}$.

Remark 5. Note that for single user and no phase fading setup, it is shown in [23] that the AF relaying strategy achieves the network capacity when RS-to-destination SNR goes to infinity; this is because the amplified signals combine coherently at the destination. Hence, it was pointed out that there is no need to resort to more advanced and complex coding techniques at the RSs. However, for the phase fading case the same conclusions do not hold as the random phase shifts do not allow for coherent combining of the amplified signals at the destination. Therefore, one needs to look for more subtle ways of relaying which take into account phase fading.

Remark 6. Note that AF relaying strategy is not applicable to the orthogonal MAC case.

DF Relaying Strategy

In this section, we give an achievable rate region for DF relaying where each RS tries to decode all source messages and forwards them to the destination. Due to full decoding assumption at the RSs, the first hop corresponds to a T -source

and K -destination multi-cast channel. To be able to send each source message to all RSs, one needs to select the transmission rates as follows

$$\mathcal{R}_{MAC} = \{(R_1, R_2, \dots, R_T) \mid (R_1, R_2, \dots, R_T) \in \mathcal{C}_1 \cap \mathcal{C}_2 \dots \cap \mathcal{C}_K\} \quad (2.18)$$

where, for $k = 1, 2, \dots, K$,

$$\mathcal{C}_k = \left\{ (R_1, \dots, R_T) \mid \sum_{t \in \mathcal{M}} R_t \leq I(X_{(\mathcal{M})}; Y_{R_k} \mid X_{(\mathcal{M}^c)}), \mathcal{M} \subseteq \mathcal{T} \right\} \quad (2.19)$$

is the capacity region from all sources to the k -th RS. Assuming the transmission rates $(R_1, R_2, \dots, R_T) \in \mathcal{R}_{MAC}$, then all RSs can decode the sources' messages with small probability of error [1]. In the second hop, we have a communication channel consisting of K transmitters (here the RSs), having the same messages, and a destination. In the second hop, assuming independent codebooks at the RSs the following sum-rate is achievable

$$\sum_{t=1}^T R_t \leq I(X_{R_1}, X_{R_2}, \dots, X_{R_K}; Y). \quad (2.20)$$

Now putting all inequalities together, we have the following achievable rate for the DF relaying strategy where each RS decodes all the source messages and forwards to the destination

$$\begin{aligned} \mathcal{R}_{DF} &= \left\{ (R_1, \dots, R_T) \mid (R_1, \dots, R_T) \in \mathcal{R}_{MAC} \cap \left\{ \sum_{t=1}^T R_t \leq I(X_{R_1}, \dots, X_{R_K}; Y) \right\} \right\} \\ &= \left\{ (R_1, \dots, R_T) \mid \begin{array}{l} \sum_{t \in \mathcal{M}} R_t \leq \min_{k=1, \dots, K} \{I(X_{(\mathcal{M})}; Y_{R_k} \mid X_{(\mathcal{M}^c)})\}, \mathcal{M} \subseteq \mathcal{T} \\ \sum_{t=1}^T R_t \leq I(X_{R_1}, \dots, X_{R_K}; Y). \end{array} \right\} \end{aligned} \quad (2.21)$$

Remark 7. Note that in order to achieve the rate expression corresponding to communicating the same message from all RSs to destination, RSs encode $W_r = (W_1, \dots, W_T) \in [1, 2^{n(\sum_{t=1}^T R_t)}]$ to independent codebooks and the destination tries to decode W_r .

Remark 8. The achievable rate region of $T = K = 2$ AWGN PRN with i.i.d. phase shifts corresponding to the full DF relaying strategy is given by

$$\mathcal{R}_{DF} = \left\{ \begin{array}{l} (R_1, R_2) : R_1 > 0, R_2 > 0, \\ R_1 \leq \min \{ \log_2(1 + \gamma_{1,1}), \log_2(1 + \gamma_{2,1}) \} \\ R_2 \leq \min \{ \log_2(1 + \gamma_{1,2}), \log_2(1 + \gamma_{2,2}) \} \\ R_1 + R_2 \leq \min \{ \log_2(1 + \gamma_{1,1} + \gamma_{1,2}), \log_2(1 + \gamma_{2,1} + \gamma_{2,2}), \\ \log_2(1 + \gamma_{d,1} + \gamma_{d,2}) \}. \end{array} \right.$$

where we used the fact that the rate maximizing input distributions are shown to be uncorrelated Gaussian distribution, e.g., $\mathbb{E}[X_1 X_2^*] = \mathbb{E}[X_{R_1} X_{R_2}^*] = 0$ for the MAC with phase shifts [17, 18].

Block Quantization and Random Binning (BQRB) Relaying Strategy

It was shown by Schein [23] that without phase fading using the AF relaying strategy achieves the network capacity due to the *coherent combining* effect when the MAC part is strong enough. However, for the phase fading AWGN PRN it is shown in Section-2.3.1 that the AF relaying strategy can not achieve the network capacity even for high SNR values in the MAC part. Motivated by this observation, we investigate an achievable scheme that mimics multiple-antenna reception performance in the sense that the destination jointly processes the representations of the received signals at the RSs. Throughout this chapter, we assume perfect CSI only at the receiver nodes, i.e., each RS has its corresponding CSI between the source and itself, and the destination has full network CSI.

The scheme we consider here is the continuous counterpart of the scheme considered by Schein in [23]. In addition, we use some fundamental results by Oohama [68] based on joint (weak) typicality among sequences having Markov chain relation.

We generate 2^{nR_t} input codewords according to the input density $f(x_t)$, $\forall t \in \mathcal{J}$. Upon receiving Y_{R_k} , the k -th RS looks for any quantization codeword jointly typical with Y_{R_k} , $\forall k \in \mathcal{K}$. Note that the rate-distortion theory [1] tells us that such a quantization codeword (jointly typical with Y_{R_k}) exists with high probability if we generate more than $2^{nI(Y_{R_k};V_k)}$ quantization codewords where V_k is the quantized codeword at the k -th RS. Hence, we generate approximately $2^{nI(Y_{R_k};V_k)}$ quantization codewords according to the marginal density $f(v_k) = \int_{y_{R_k}} f(y_{R_k})f(v_k|y_{R_k}) dy_{R_k}$, and randomly assign these quantization codewords to $2^{nR_{Q_k}}$ bins. Then, we generate $2^{nR_{Q_k}}$ channel input codewords for RS k using the input density $f(x_{R_k})$.

Before continuing, we should indicate that at the destination there are two decoding steps: 1) a channel decoder for the RS bin indexes corresponding to the representations of the RS observations, and 2) a channel decoder for the sources' messages. Note that if there is an error in the first decoding step, the destination declares an error for the sources' messages. Hence, we need to be careful whilst choosing the rate tuple $(R_{Q_1}, R_{Q_2}, \dots, R_{Q_K})$ for communication between the RSs and the destination. We follow the same procedure as in [23] and generalize the BQRB relaying scheme to the multi-source case.

In this section, we look at the achievable rates for the scheme depicted in Figure 9.2 by performing BQRB at the RSs. We have the following theorem for the phase fading Gaussian PRN for $T = K = 2$ case.

Theorem 9. *For the AWGN PRN with phase fading memoryless channels $f(y_{R_1}, y_{R_2}|x_1, x_2)$ and $f(y|x_{R_1}, x_{R_2})$, choose any probability density function, i.e., $f(x_1, x_2) = f(x_1)f(x_2)$, and any pair of conditional densities $f(v_1|y_{R_1})$ and $f(v_2|y_{R_2})$. Then, we can reliably achieve the rates R_1 and R_2 satisfying*

$$R_1 \leq I(X_1; V_1, V_2 | X_2) \quad (2.22a)$$

$$R_2 \leq I(X_2; V_1, V_2 | X_1) \quad (2.22b)$$

$$R_1 + R_2 \leq I(X_1, X_2; V_1, V_2) \quad (2.22c)$$

provided

$$I(Y_{R_1}; V_1) - I(V_1; V_2) \leq I(X_{R_1}; Y | X_{R_2}) \quad (2.23a)$$

$$I(Y_{R_2}; V_2) - I(V_1; V_2) \leq I(X_{R_2}; Y | X_{R_1}) \quad (2.23b)$$

$$I(Y_{R_1}; V_1) + I(Y_{R_2}; V_2) - I(V_1; V_2) \leq I(X_{R_1}, X_{R_2}; Y). \quad (2.23c)$$

These values are computed with respect to the density

$$\begin{aligned} f(x_1, x_2, y_{R_1}, y_{R_2}, v_1, v_2, x_{R_1}, x_{R_2}, y) &= f(x_1)f(x_2)f(y_{R_1}, y_{R_2} | x_1, x_2) \\ & f(v_1 | y_{R_1})f(v_2 | y_{R_2})f(x_{R_1} | v_1)f(x_{R_2} | v_2)f(y | x_{R_1}, x_{R_2}). \end{aligned} \quad (2.24)$$

Proof. See Appendix-2.B for the proof. \square

Remark 10. By using the same coding and decoding procedures, one can easily generalize the above 2-source 2-relay achievable compression scheme to the case where the network consists of $T \geq 2$ sources and $K \geq 2$ RSs.

Theorem 11. For the T -source K -relay Gaussian PRN with phase fading memoryless channels $f(y_{R_1}, \dots, y_{R_K} | x_1, \dots, x_T)$ and $f(y | x_{R_1}, \dots, x_{R_K})$, choose any p.d.f. $f(x_1, \dots, x_T) = \prod_{t=1}^T f(x_t)$ and any pair of conditional densities $f(v_k | y_{R_k})$, $\forall k \in \mathcal{K}$. We can reliably achieve the rates R_t , $\forall t \in \mathcal{T}$, satisfying

$$\sum_{t \in \mathcal{M}} R_t \leq I(X_{(\mathcal{M})}; V_1, V_2, \dots, V_K | X_{(\mathcal{M}^c)}), \quad \mathcal{M} \subseteq \mathcal{T} \quad (2.25)$$

provided that

$$\begin{aligned} I(Y_{R_{(\mathcal{S})}}; V_{(\mathcal{S})} | V_{(\mathcal{S}^c)}) &= I(V_{(\mathcal{S})}; Y_{R_{(\mathcal{S})}}, V_{(\mathcal{S}^c)}) - I(V_{(\mathcal{S})}; V_{(\mathcal{S}^c)}) \\ &= I(V_{(\mathcal{S})}; Y_{R_{(\mathcal{S})}}) - I(V_{(\mathcal{S})}; V_{(\mathcal{S}^c)}) \\ &\leq I(X_{R_{(\mathcal{S})}}; Y | X_{R_{(\mathcal{S}^c)}}) \end{aligned} \quad (2.26)$$

for all $\mathcal{S} \subseteq \mathcal{K}$ with respect to the joint p.d.f.

$$\begin{aligned} f(x_1, \dots, x_T, y_{R_1}, \dots, y_{R_K}, v_1, \dots, v_K, x_{R_1}, \dots, x_{R_K}, y) &= \\ \prod_{t=1}^T f(x_t) \left(\prod_{k=1}^K f(y_{R_k} | x_1, \dots, x_T) f(v_k | y_{R_k}) f(x_{R_k} | v_k) \right) & f(y | x_{R_1}, \dots, x_{R_K}). \end{aligned} \quad (2.27)$$

Proof. The proof follows immediately from the proof of Theorem-9. \square

To evaluate the mutual information terms given in (2.22) for $T = 2$ sources and $K = 2$ RSs, we (possibly suboptimally) choose Gaussian quantization on the received signals Y_{R_k} at each RS (see (9.1)) and generate the quantization codewords V_k according to the distribution $f(v_k|y_{R_k}) \sim \mathcal{CN}(y_{R_k}, D_k)$, i.e.,

$$V_k = Y_{R_k} + Z_{q,k} = h_{k1} e^{j\Phi_{k1}} X_1 + h_{k2} e^{j\Phi_{k2}} X_2 + Z_k + Z_{q,k} \quad (2.28)$$

where $Z_k \sim \mathcal{CN}(0, \sigma^2)$ and $Z_{q,k} \sim \mathcal{CN}(0, D_k)$ for $k = 1, 2$. With these settings we have

$$R_1 \leq \mathbb{E}_{\{\Phi_{kt}\}} \log_2 \left(1 + \frac{h_{11}^2 P_s}{\sigma^2 + D_1} + \frac{h_{21}^2 P_s}{\sigma^2 + D_2} \right) \quad (2.29a)$$

$$R_2 \leq \mathbb{E}_{\{\Phi_{kt}\}} \log_2 \left(1 + \frac{h_{12}^2 P_s}{\sigma^2 + D_1} + \frac{h_{22}^2 P_s}{\sigma^2 + D_2} \right) \quad (2.29b)$$

$$R_1 + R_2 \leq \mathbb{E}_{\{\Phi_{kt}\}} \log_2 \det \left(\mathbf{I}_2 + P_s \mathbf{H} \mathbf{H}^H \mathbf{Z}^{-1} \right) \quad (2.29c)$$

provided that

$$\begin{aligned} \log_2 \left(\frac{\sigma_{v_1}^2}{D_1} (1 - \zeta^2) \right) &\leq \log_2 (1 + \gamma_{d,1}) \\ \log_2 \left(\frac{\sigma_{v_2}^2}{D_2} (1 - \zeta^2) \right) &\leq \log_2 (1 + \gamma_{d,2}) \\ \log_2 \left(\frac{\sigma_{v_1}^2 \sigma_{v_2}^2}{D_1 D_2} (1 - \zeta^2) \right) &\leq \log_2 (1 + \gamma_{d,1} + \gamma_{d,2}) \end{aligned}$$

where \mathbf{H} is defined in (2.14), $\mathbf{Z} = \text{diag}\{\sigma^2 + D_1, \sigma^2 + D_2\}$, $\sigma_{v_k}^2 = (h_{k1}^2 + h_{k2}^2)P_s + \sigma^2 + D_k$, $k = 1, 2$, and $\zeta \in [-1, 1]$ is the correlation factor between V_1 and V_2 :

$$\begin{aligned} \zeta &= \frac{\mathbb{E}[V_1 V_2^H]}{\sqrt{\mathbb{E}[|V_1|^2] \mathbb{E}[|V_2|^2]}} \\ &= \frac{P_s \mathbf{h}_1^T \mathbf{h}_2^*}{\sqrt{\sigma_{v_1}^2 \sigma_{v_2}^2}} \end{aligned} \quad (2.30)$$

where $\mathbf{h}_1^T = [h_{11} e^{j\Phi_{11}}, h_{12} e^{j\Phi_{12}}]$ and $\mathbf{h}_2^T = [h_{21} e^{j\Phi_{21}}, h_{22} e^{j\Phi_{22}}]$. Note that here we have lower bounds depending on the variances and correlation coefficient between quantization outputs, V_1 and V_2 , respectively.

For the symmetric channel case where $\mathbf{h} = \mathbf{h}_1 = \mathbf{h}_2$ (hence $\sigma_{v_1}^2 = \sigma_{v_2}^2 = \sigma_v^2$ and $\zeta = P_s \|\mathbf{h}\|^2 / \sigma_v^2$) and $g = g_1 = g_2$, we choose $D_k = D$ for $k = 1, 2$. After some algebra, we can find a lower bound on D as follows:

$$\begin{aligned} D &\geq \frac{P_s \|\mathbf{h}\|^2 + \sigma^2 + \sqrt{(P_s \|\mathbf{h}\|^2 + \sigma^2)^2 + \frac{2g^2 P_r}{\sigma^2} (2P_s \|\mathbf{h}\|^2 + \sigma^2) \sigma^2}}{\frac{2g^2 P_r}{\sigma^2}} \\ &= \frac{\sigma^2 \left(\gamma_r \|\mathbf{h}\|^2 + 1 + \sqrt{(\gamma_r \|\mathbf{h}\|^2 + 1)^2 + 2g^2 \gamma_d (2\gamma_r \|\mathbf{h}\|^2 + 1)} \right)}{2g^2 \gamma_d}. \end{aligned} \quad (2.31)$$

Then one can insert the minimum distortion value D into the achievable rate expressions in order to get corresponding achievable rates.

Remark 12. *We note that in general the distortion values, $D_k, k = 1, 2$, depend on random channel phases as can be seen from (2.30).*

Quantize-and-Forward (QF) Relaying Strategy

In wireless communication systems it is desirable to use low complexity algorithms at wireless terminals in order to reduce deployment cost. Hence, in this section we consider a low-complexity relaying strategy, called QF relaying, where each RS just quantizes its received signal and forwards the quantized signal to the destination, i.e., no binning (distributed source coding) is performed as opposed to the BQRB relaying strategy. There is no need for full CSI at each RS in the QF relaying, hence providing less complex relaying strategy at the cost of lower spectral efficiency.

Compared to the achievable rate region for the BQRB relaying, the only difference for the QF case is on the rate constraints given in (2.26). Regarding these, for the QF relaying we have the same achievable rate expressions as in BQRB relaying with the following constraints

$$\sum_{k \in \mathcal{S}} I(V_k; Y_{R_k}) \leq I(X_{R(\mathcal{S})}; Y | X_{R(\mathcal{S}^c)}), \quad \mathcal{S} \subseteq \mathcal{K}. \quad (2.32)$$

2.3.2 Orthogonal limited-capacity links between the RSs and the Destination

In this section, we concentrate on phase fading PRNs with limited-capacity (error-free) orthogonal backhaul links connecting the RSs to the destination. Let C_i [bits/transmission] be the link capacity from the k -th RS to the destination. We note that, if feasible, each capacity tuple $\{C_k\}_{k=1}^K$ for the error-free orthogonal backhaul links might correspond to an operating point in the capacity region corresponding to the wireless MAC case between the RSs and the destination. Hence, by selecting different tuples $\{C_k\}_{k=1}^K$, we can have the same performance as in the previous section, where the channels between the RSs and the destination are random (due to wireless medium assumption).

We first briefly give the outer bound and achievable rates corresponding to the limited-capacity backhaul assumption. Then, we look at some practical relaying strategies and find corresponding achievable rate regions.

For lossless orthogonal limited-capacity backhaul links between the RSs and the destination, we have the following outer bound:

Corollary 13. *We have the following outer bound for the T -source K -relay PRN where each RS has lossless links to the destination with a capacity constraint C_k , for $k = 1, 2, \dots, K$, as depicted in Figure 9.3*

$$\sum_{i \in \mathcal{M}} R_i \leq \max_{p(\mathbf{x})} \min_{\mathcal{R} \subseteq \mathcal{K}} \left\{ I(X_{(\mathcal{M})}; Y_{R(\mathcal{R})} | X_{(\mathcal{M}^c)}) + \sum_{k \in \mathcal{R}^c} C_k \right\}, \quad \mathcal{M} \subseteq \mathcal{T}. \quad (2.33)$$

Remark 14. Note that for a single source assumption, similar outer bounds are derived in [28]. Using their notation, the outer bound given in (2.33) is equivalent to the outer bound given in [28, Corollary 2] for $U_t = Y_{R_t}$.

Corollary 15. For the $T = 2$ sources, $K = 2$ RSs AWGN PRN with phase fading, the outer bounds given in (2.33) becomes:

$$\begin{aligned} R_1 &= \min\{\log_2(1 + (h_{11}^2 + h_{21}^2)\gamma_r), \log_2(1 + h_{21}^2\gamma_r) + C_1, \\ &\quad \log_2(1 + h_{11}^2\gamma_r) + C_2, C_1 + C_2\} \\ R_2 &= \min\{\log_2(1 + (h_{12}^2 + h_{22}^2)\gamma_r), \log_2(1 + h_{22}^2\gamma_r) + C_1, \\ &\quad \log_2(1 + h_{12}^2\gamma_r) + C_2, C_1 + C_2\} \\ R_1 + R_2 &= \min\{\mathbb{E}_{\{\Phi_{kt}\}} \left[\log_2 \det(\mathbf{I}_2 + \gamma_r \mathbf{H} \mathbf{H}^H) \right], \log_2(1 + (h_{21}^2 + h_{22}^2)\gamma_r) + C_1, \\ &\quad \log_2(1 + (h_{11}^2 + h_{12}^2)\gamma_r) + C_2, C_1 + C_2\} \end{aligned}$$

where $\gamma_r = P_s/\sigma^2$, $\gamma_d = P_r/\sigma^2$, and $\mathbf{H} \in \mathbb{C}^{2 \times 2}$ is the channel matrix given by (2.14). Again we note that in deriving the mutual information expressions we use the fact that the mutual information maximizing input distribution at the source and RSs is jointly independent Gaussian distribution.

Now consider the DF relaying for the orthogonal lossless backhaul case where each RS tries to decode all source messages and forwards them to the destination. Due to the full decoding assumption at the RSs, the first hop corresponds to a T -source and K -destination multi-cast channel. In the second hop, each RS sends different portions of the decoded signals to the destination via orthogonal backhaul links with the corresponding individual capacity constraints. We have the following achievable rate for the DF relaying where each RS decodes all the sources' messages and forwards different portions to the destination

$$\begin{aligned} \mathcal{R}_{DF} &= \left\{ (R_1, \dots, R_T) \mid (R_1, \dots, R_T) \in \mathcal{R}_{MAC} \cap \left\{ \sum_{t=1}^T R_t \leq \sum_{t=1}^T C_t \right\} \right\} \\ &= \left\{ (R_1, \dots, R_T) \mid \begin{array}{l} \sum_{t \in \mathcal{M}} R_t \leq \min_{k=1, \dots, K} \{I(X_{(\mathcal{M})}; Y_{R_k} | X_{(\mathcal{M}^c)})\}, \mathcal{M} \subseteq \mathcal{T} \\ \sum_{t=1}^T R_t \leq \sum_{t=1}^T C_t. \end{array} \right. \end{aligned} \quad (2.34)$$

Remark 16. The achievable rate region of $T = K = 2$ AWGN PRN with i.i.d. phase shifts corresponding to the full DF relaying strategy is given by

$$\mathcal{R}_{DF} = \left\{ \begin{array}{l} (R_1, R_2) : R_1 > 0, R_2 > 0, \\ R_1 \leq \min\{\log_2(1 + \gamma_{1,1}), \log_2(1 + \gamma_{2,1})\} \\ R_2 \leq \min\{\log_2(1 + \gamma_{1,2}), \log_2(1 + \gamma_{2,2})\} \\ R_1 + R_2 \leq \min\{\log_2(1 + \gamma_{1,1} + \gamma_{1,2}), \log_2(1 + \gamma_{2,1} + \gamma_{2,2}), C_1 + C_2\}. \end{array} \right. \quad (2.35)$$

where we used the fact that the rate maximizing input distributions are shown to be uncorrelated Gaussian distribution, e.g., $\mathbb{E}[X_1 X_2^*] = 0$ for the MAC with phase shifts [17, 18].

The following theorem corresponds to the BQRB relaying for the phase fading PRNs with capacity-constraint backhaul links from the RSs to the destination, see Figure 9.3.

Theorem 17. *For the T -source K -relay Gaussian PRN with phase fading memoryless channel $f(y_{R_1}, \dots, y_{R_K} | x_1, \dots, x_T)$ and backhaul link capacity constraint C_k between the k -th RS and the destination, choose any p.d.f. $f(x_1, \dots, x_T) = \prod_{t=1}^T f(x_t)$ and any pair of conditional densities $f(v_k | y_{R_k})$, $\forall k \in \mathcal{K}$. We can reliably achieve the rates R_t , $\forall t \in \mathcal{J}$, satisfying*

$$\sum_{t \in \mathcal{M}} R_t \leq I(X_{(\mathcal{M})}; V_1, V_2, \dots, V_K | X_{(\mathcal{M}^c)}), \mathcal{M} \subseteq \mathcal{J} = \{1, \dots, T\} \quad (2.36)$$

provided that

$$\begin{aligned} I(Y_{R_{(\mathcal{S})}}; V_{(\mathcal{S})} | V_{(\mathcal{S}^c)}) &= I(V_{(\mathcal{S})}; Y_{R_{(\mathcal{S})}}, V_{(\mathcal{S}^c)}) - I(V_{(\mathcal{S})}; V_{(\mathcal{S}^c)}) \\ &= I(V_{(\mathcal{S})}; Y_{R_{(\mathcal{S})}}) - I(V_{(\mathcal{S})}; V_{(\mathcal{S}^c)}) \\ &\leq \sum_{k \in \mathcal{S}} C_k, \end{aligned} \quad (2.37)$$

for all $\mathcal{S} \subseteq \mathcal{K}$ with respect to the joint p.d.f.

$$\begin{aligned} f(x_1, \dots, x_T, y_{R_1}, \dots, y_{R_K}, v_1, \dots, v_K) &= \\ &= \prod_{t=1}^T f(x_t) \prod_{k=1}^K f(y_{R_k} | x_1, \dots, x_T) f(v_k | y_{R_k}). \end{aligned}$$

Proof. The proof follows immediately from the proof of Theorem-9. \square

For the symmetric case where $\mathbf{h} = \mathbf{h}_1 = \mathbf{h}_2$ (hence $\sigma_{v_1}^2 = \sigma_{v_2}^2 = \sigma_v^2$ and $\zeta = P_s \|\mathbf{h}\|^2 / \sigma_v^2$) and $C = C_1 = C_2$, we will have $D_k = D$ for $k = 1, 2$. After some algebra, as in the previous section we can find a lower bound on D as follows:

$$\begin{aligned} D &\geq \frac{P_s \|\mathbf{h}\|^2 + \sigma^2 + \sqrt{(P_s \|\mathbf{h}\|^2 + \sigma^2)^2 + (2^{2C} - 1)(2P_s \|\mathbf{h}\|^2 + \sigma^2)\sigma^2}}{2^{2C} - 1} \\ &= \frac{\sigma^2 \left(\gamma_r \|\mathbf{h}\|^2 + 1 + \sqrt{(\gamma_r \|\mathbf{h}\|^2 + 1)^2 + (2^{2C} - 1)(2\gamma_r \|\mathbf{h}\|^2 + 1)} \right)}{2^{2C} - 1}. \end{aligned}$$

Compared to the achievable rate region for the BQRB relaying, the only difference for the QF relaying is on the rate constraints given in (2.37). Regarding

these, for the QF relaying we have the same achievable rate expressions as in BQRB relaying with the following constraints

$$I(V_k; Y_{R_k}) \leq C_k, \quad \forall k \in \mathcal{K}. \quad (2.38)$$

Up to this point, we considered different relaying strategies assuming Gaussian signaling at the source nodes and Gaussian mapping at the RSs. However, it is not obvious whether these assumptions are optimal for the underlying PRN. Following the remarks in [63], in the following sections we consider finite-alphabet signaling and non-Gaussian mapping (e.g., scalar quantization) at the RSs. We believe that with these practical assumptions one might have some intuitions on how to have better spectral efficiency and to come close to the limits of the network by using simple and practical schemes.

2.4 Quantization for PRN with Non-Gaussian Signaling Sets

It is known that vector quantizers (VQ) may require lower rates (even for independent source outputs) than scalar quantizers (SQ) to achieve the same target fidelity criteria; however note that the difference between scalar and vector quantization rates falls below 0.255 bit as the allowed distortion decreases (at high resolution/rate regime) [66]. Moreover, VQ is generally more *complex* and consumes more *processing time*. Hence, together with the high link rate assumption between the RSs and the destination, where we fall in the *high resolution* quantization regime, we concentrate on SQs in the following.

QF relaying gives the best gain at *low* source-to-relay SNR [18] where it is possible to approach capacity by using coded modulation at the source node(s). Moreover, it is predicted that using non-Gaussian mapping at the relay nodes make sense due to the ability to exploit the *structure* of source codewords.

For the BQRB (or CF) relaying scheme studied in the previous section, the RSs perform the compression operation over received signal vectors of size n , i.e. the VQ, which relies on long block length assumption $n \rightarrow \infty$. However, since RSs are preferred to be as simple as possible, the BQRB relaying strategy presented above is unfavorable. Hence, here we look at a *simpler* and more *practical* quantization technique at the RSs which relies on symbol-by-symbol quantization (i.e., SQ). As specified above, even though there is performance degradation with the SQ, at the high resolution regime (e.g., high C_k , $\forall k \in \mathcal{K}$) the performance loss compared to the VQ becomes negligible [65–67].

Moreover, most of the literature dealing with BQRB relaying strategy assumes Gaussian codebooks at the sources, without claiming optimality, in order to make the analysis easier [17, 18]. Lately, in [28, Section VI-B] it is shown that for the nomadic transmitter setting, where a source communicates with a destination node via intermediate agents (RSs in our set-up) each having limited lossless capacity links ($C_1 = C_2 = 1$ [bit/transmission]) to the destination,

using binary phase shift keying (BPSK) signaling at the source with demodulation of every received channel output at the RSs into 1 bit outperforms Gaussian signaling at the source and Gaussian mapping at the RSs. Similar conclusions are pointed out in [63, 64] for the Gaussian relay channel setup with coded modulation (CM) at the source and orthogonal relay-to-destination link where an estimate-and-forward (EF) relaying strategy with different RS mappings is studied. They conclude that for the CM scenario at *low* source-relay SNR EF with Gaussian mapping at the RS is the best, at *high* source-relay SNR DF is superior and at *intermediate* SNR region EF with *hard-decision per symbol* at the RS is better than the above two methods. Motivated by these observations, in the following we consider CM (e.g., M-ary Quadratic Amplitude Modulation (M-QAM)) at the source(s) and non-Gaussian mapping at the RSs.

2.4.1 Coded Modulation at the Source(s)

For complex AWGN channels, we consider square M-ary Quadratic Amplitude Modulation (M-QAM) at the source(s). For the M-QAM case, again we assume equally probable constellation points of the form $x_m = x_m^I + jx_m^Q$ where $p(x_m^I, x_k^Q) = p(x_m^I)p(x_k^Q) = \frac{1}{\sqrt{M}}\frac{1}{\sqrt{M}} = \frac{1}{M}, \forall \{m, k\} \in \{1, 2, \dots, \sqrt{M}\}$, i.e. the in-phase and quadrature components of each signal constellation are independent. The in-phase and quadrature components follow the same structure as the \sqrt{M} -PAM modulation where $x_m^R \in \Omega$ and $x_m^I \in \Omega$, for all $m \in \{1, 2, \dots, \sqrt{M}\}$ with $\Omega = \{(2m-1-M)d, m = 1, 2, \dots, \sqrt{M}\}$ being the set for the constellation points with $d = \sqrt{\frac{3P_s}{2(M-1)}}$. We note that $E[|x^I|^2] = E[|x^Q|^2] = P_s/2$.

2.4.2 Uniform Scalar Quantizer (uSQ)

In this section, we briefly describe the structure of uniform scalar quantizers (uSQs). The uSQ maps the received signal (continuous source) y , into one of a finite set of rational numbers v_1, v_2, \dots, v_L . Let $u_j, j = 2, \dots, L$ denote the transition levels with u_1 and u_{L+1} the greatest lower bound and the least upper bound of the received signal y . With these settings, the quantizer mapping is given by

$$\hat{y} = Q(y) = v_l \quad \text{if} \quad y \in \mathcal{S}_l = (u_l, u_{l+1}], \quad l = 1, 2, \dots, L \quad (2.39)$$

for $u_1 = -\infty, u_{L+1} = \infty$. Assuming the source nodes having symmetric probability densities and L even, for optimum SQ ($\frac{L}{2} - 1$) parameters need to be determined while for the optimum uSQ only one parameter needs to be found/optimized. Hence, using uSQ reduces the complexity by a factor of $(\frac{L}{2} - 1)$ while having a negligible penalty on performance for the high fidelity region.

The uSQ has uniform distance between the transition levels with the quantization interval r , and requires that the quantization values be the midpoints

of the intervals. For a symmetric probability density $p_Y(y)$ and L even, we have

$$v_l = \left(l - \frac{L+1}{2} \right) r, \quad l = 1, 2, \dots, L \quad (2.40)$$

$$u_k = \left(k - 1 - \frac{L}{2} \right) r, \quad k = 2, 3, \dots, L \quad (2.41)$$

with u_1 and u_{L+1} defined above.

The entropy of the quantizer output V can be computed as

$$H(V) = - \sum_{l=1}^L p(v_l) \log_2(p(v_l)) \quad [\text{bits/sample}] \quad (2.42)$$

where

$$p(v_l) = \Pr[\hat{y} = v_l] = \Pr[u_l \leq y < u_{l+1}] = \int_{u_l}^{u_{l+1}} p_Y(y) dy. \quad (2.43)$$

Remark 18. Note that $H(V) \leq \log_2(L)$ where L is the cardinality of the quantizer output V .

2.4.3 Coded Modulation with Uniform Scalar Quantization at the RSs

Considering complex Gaussian PRN model with T sources and K RSs, here we give the uSQ structure used at the RSs where each has a noiseless link to the destination with finite capacity $C_k, \forall k \in \mathcal{K}$, [bits/transmission]. We note that since we use M-QAM at the sources, the received signals at the RSs are not Gaussian, but Gaussian-mixtures.

The received signal at the k -th RS is given by²

$$y_{R_k} = \sum_{t=1}^T h_{kt} e^{j\Phi_{kt}} x_t + z_k = \tilde{\mathbf{h}}_k^T \mathbf{x} + z_k, \quad \forall k \in \mathcal{K} \quad (2.44)$$

where $\tilde{\mathbf{h}}_k^T = [h_{k1} e^{j\Phi_{k1}}, \dots, h_{kT} e^{j\Phi_{kT}}]$ and $\mathbf{x} = [x_1, \dots, x_T]^T$. The input-output model can be decomposed into real and imaginary parts as follows

$$\begin{aligned} \underline{y}_{R_k} &= \begin{bmatrix} y_{R_k}^R \\ y_{R_k}^I \end{bmatrix} = \begin{bmatrix} \text{Re}\{y_{R_k}\} \\ \text{Im}\{y_{R_k}\} \end{bmatrix} \\ &= \begin{bmatrix} \text{Re}\{\tilde{\mathbf{h}}_k^T\} & -\text{Im}\{\tilde{\mathbf{h}}_k^T\} \\ \text{Im}\{\tilde{\mathbf{h}}_k^T\} & \text{Re}\{\tilde{\mathbf{h}}_k^T\} \end{bmatrix} \begin{bmatrix} \text{Re}\{\mathbf{x}\} \\ \text{Im}\{\mathbf{x}\} \end{bmatrix} + \begin{bmatrix} \text{Re}\{z_k\} \\ \text{Im}\{z_k\} \end{bmatrix} \\ &= \begin{bmatrix} \tilde{\mathbf{h}}_{k,1}^T \\ \tilde{\mathbf{h}}_{k,2}^T \end{bmatrix} \begin{bmatrix} \mathbf{x}^R \\ \mathbf{x}^I \end{bmatrix} + \begin{bmatrix} z_k^R \\ z_k^I \end{bmatrix} = \begin{bmatrix} \tilde{\mathbf{h}}_{k,1}^T \\ \tilde{\mathbf{h}}_{k,2}^T \end{bmatrix} \underline{\mathbf{x}} + \underline{z}_k \quad (2.45) \end{aligned}$$

²The time index n is dropped without loss of generality.

where $\tilde{\mathbf{h}}_{k,i}^T \in \mathbb{C}^{1 \times 2T}$ for $i = 1, 2$, and $\mathbf{x}^R = \text{Re}\{\mathbf{x}\} = [x_1^R \ x_2^R \ \dots \ x_T^R]^T$ and $\mathbf{x}^I = \text{Im}\{\mathbf{x}\} = [x_1^I \ x_2^I \ \dots \ x_T^I]^T$ are the real and imaginary parts of the source signal vector, respectively, and $\underline{\mathbf{x}} = [\mathbf{x}^R \ \mathbf{x}^I]^T \in \Omega^{2T \times 1}$ is the concatenation of the real and imaginary parts of the source signal vector, where $\mathbb{E}[\underline{\mathbf{x}}\underline{\mathbf{x}}^T] = \frac{P_s}{2} \mathbf{I}_{2T}$ (note that $\mathbb{E}[\mathbf{x}^R \mathbf{x}^{I^T}] = \mathbf{0}_T$). The noise components have zero mean and covariance matrix $\mathbb{E}[\underline{\mathbf{z}}_k \underline{\mathbf{z}}_k^T] = \frac{\sigma^2}{2} \mathbf{I}_2$. We also note that the cross-correlation between $y_{R_k}^R$ and $y_{R_k}^I$ is zero, i.e., $\mathbb{E}[y_{R_k}^R y_{R_k}^I] = 0$. This property ensures *no bandwidth consumption* due to the correlation between the signal components in the use of uSQ wherein the real and imaginary parts of the received signal at each RS are compressed separately. Note that were the signal components correlated at each RS, then this information would be utilized as side information, similar to [32], while quantizing the real and imaginary components of the received signal at the RS. However, this may incur additional complexity at the RSs.

At the k -th RS, the quantizer maps each received signal component $y_{R_k}^a$ into one of a finite set of rational numbers $v_{k,1}^a, v_{k,2}^a, \dots, v_{k,L_k^a}^a$, for $a = \{R, I\}$. Let $u_{k,l^a}^a, l^a = 2, 3, \dots, L_k^a$ denote the transition levels with $u_{k,1}^a$ and $u_{k,L_k^a+1}^a$ being the greatest lower bound and the least upper bound of the received signal $y_{R_k}^a$. Assuming SQ, the quantizer mapping is given by

$$v_{k,l^a}^a = Q_k^a(y_{R_k}^a) \text{ if } y_{R_k}^a \in \mathcal{S}_{k,l^a}^a = (u_{k,l^a}^a, u_{k,l^a+1}^a] \quad l^a = 1, \dots, L_k^a. \quad (2.46)$$

Conditional probabilities of the Quantizer Outputs

At each RS we assume two independent uSQs each quantizing the in-phase and quadrature parts of the received signal into L_k^R and L_k^I transition levels, respectively. Given the transmitted signals at the sources, the probability of the quantizer outputs can be calculated as follows.

For a given source input signal vector $\underline{\mathbf{x}} \in \Omega^{2T \times 1}$, the probability that the quantizer output is in the $\underline{l} = (l^R, l^I)$ -th quantizing interval, i.e., $\underline{V}_k =$

$(V_k^R, V_k^I) = \underline{v}_{k,\underline{l}} = (v_{k,l^R}^R, v_{k,l^I}^I)$, $\forall k \in \mathcal{K}$, is given by

$$\begin{aligned}
\Pr \left[\underline{V}_k = \underline{v}_{k,\underline{l}} \mid \underline{\mathbf{x}} \right] &= \Pr \left[(V_k^R, V_k^I) = (v_{k,l^R}^R, v_{k,l^I}^I) \mid \underline{\mathbf{x}} \right] \\
&\stackrel{(a)}{=} \Pr \left[V_k^R = v_{k,l^R}^R \mid \underline{\mathbf{x}} \right] \Pr \left[V_k^I = v_{k,l^I}^I \mid \underline{\mathbf{x}} \right] \\
&= \Pr \left[y_{R_k}^R \in \mathcal{S}_{k,l^R}^R \mid \underline{\mathbf{x}} \right] \Pr \left[y_{R_k}^I \in \mathcal{S}_{k,l^I}^I \mid \underline{\mathbf{x}} \right] \\
&= \left(\int_{u_{k,l^R}^R}^{u_{k,l^R+1}^R} G_{y_{R_k}^R} \left(\tilde{\mathbf{h}}_{k,1}^T \underline{\mathbf{x}}, \frac{\sigma^2}{2} \right) dy_{R_k}^R \right) \left(\int_{u_{k,l^I}^I}^{u_{k,l^I+1}^I} G_{y_{R_k}^I} \left(\tilde{\mathbf{h}}_{k,2}^T \underline{\mathbf{x}}, \frac{\sigma^2}{2} \right) dy_{R_k}^I \right) \\
&= \left(\int_{u_{k,l^R}^R}^{u_{k,l^R+1}^R} \frac{1}{\sqrt{\pi\sigma^2}} e^{-\frac{(y_{R_k}^R - \tilde{\mathbf{h}}_{k,1}^T \underline{\mathbf{x}})^2}{\sigma^2}} dy_{R_k}^R \right) \left(\int_{u_{k,l^I}^I}^{u_{k,l^I+1}^I} \frac{1}{\sqrt{\pi\sigma^2}} e^{-\frac{(y_{R_k}^I - \tilde{\mathbf{h}}_{k,2}^T \underline{\mathbf{x}})^2}{\sigma^2}} dy_{R_k}^I \right) \\
&= \left[Q \left(\frac{u_{k,l^R}^R - \tilde{\mathbf{h}}_{k,1}^T \underline{\mathbf{x}}}{\sigma/\sqrt{2}} \right) - Q \left(\frac{u_{k,l^R+1}^R - \tilde{\mathbf{h}}_{k,1}^T \underline{\mathbf{x}}}{\sigma/\sqrt{2}} \right) \right] \times \\
&\quad \left[Q \left(\frac{u_{k,l^I}^I - \tilde{\mathbf{h}}_{k,2}^T \underline{\mathbf{x}}}{\sigma/\sqrt{2}} \right) - Q \left(\frac{u_{k,l^I+1}^I - \tilde{\mathbf{h}}_{k,2}^T \underline{\mathbf{x}}}{\sigma/\sqrt{2}} \right) \right] \quad (2.47)
\end{aligned}$$

for $\underline{l} = [1, 2, \dots, L_k^R] \times [1, 2, \dots, L_k^I]$, $\forall k \in \mathcal{K}$, and where

$$\begin{aligned}
G_x(a, b^2) &= \frac{1}{\sqrt{2\pi b^2}} e^{-\frac{(x-a)^2}{2b^2}} \quad \text{and} \\
Q(x) &= \int_x^\infty \frac{1}{\sqrt{2\pi}} e^{-\frac{t^2}{2}} dt
\end{aligned}$$

are the p.d.f. of a Gaussian RV with mean a and variance b^2 , and the standard tail function for Gaussian RVs, respectively. We note that equation (a) in (2.47) follows due to the independence between the the real and imaginary parts of the received signal at each RS conditioned on the transmitted signals.

Then, the probability of the quantizer outcome being equal to $\underline{V}_k = (V_k^R, V_k^I) = \underline{v}_{k,\underline{l}} = (v_{k,l^R}^R, v_{k,l^I}^I)$, $\forall k \in \mathcal{K}$ and for $\underline{l} = (l^R, l^I) = 1, 2, \dots, L_k$, with $L_k = L_k^R L_k^I$, is given by

$$\begin{aligned}
\Pr \left[\underline{V}_k = \underline{v}_{k,\underline{l}} \right] &= \sum_{\underline{\mathbf{x}} \in \Omega^{2T \times 1}} p(\underline{\mathbf{x}}) \Pr \left[\underline{V}_k = \underline{v}_{k,\underline{l}} \mid \underline{\mathbf{x}} \right] \\
&= \frac{1}{M^T} \sum_{\underline{\mathbf{x}} \in \Omega^{2T \times 1}} \left\{ \left[Q \left(\frac{u_{k,l^R}^R - \tilde{\mathbf{h}}_{k,1}^T \underline{\mathbf{x}}}{\sigma/\sqrt{2}} \right) - Q \left(\frac{u_{k,l^R+1}^R - \tilde{\mathbf{h}}_{k,1}^T \underline{\mathbf{x}}}{\sigma/\sqrt{2}} \right) \right] \times \right. \\
&\quad \left. \left[Q \left(\frac{u_{k,l^I}^I - \tilde{\mathbf{h}}_{k,2}^T \underline{\mathbf{x}}}{\sigma/\sqrt{2}} \right) - Q \left(\frac{u_{k,l^I+1}^I - \tilde{\mathbf{h}}_{k,2}^T \underline{\mathbf{x}}}{\sigma/\sqrt{2}} \right) \right] \right\}. \quad (2.48)
\end{aligned}$$

Achievable Rates

The achievable rate region of the proposed QF relaying (using the uSQ at the RSs) with T sources and K RSs is given by

$$\sum_{i \in \mathcal{S}} R_i \leq I(X_{(\mathcal{S})}; \mathbf{Y} | X_{(\mathcal{S}^c)}), \quad \mathcal{S} \subseteq \{1, 2, \dots, T\} \quad (2.49)$$

subject to

$$I(\underline{V}_k; Y_{R_k}) \leq C_k, \quad \forall k \in \mathcal{K} \quad (2.50)$$

where $\mathbf{V} = (\underline{V}_1, \underline{V}_2, \dots, \underline{V}_K)$ with $\underline{V}_k = (V_k^R, V_k^I) \in [1, 2, \dots, L_k^R] \times [1, 2, \dots, L_k^I]$. We can re-write the mutual information term as follows

$$\begin{aligned} \sum_{i \in \mathcal{S}} R_i &= I(X_{(\mathcal{S})}; \mathbf{Y} | X_{(\mathcal{S}^c)}) \\ &= \sum_{x_{(\mathcal{T})}} \sum_{\mathbf{y}} p(x_{(\mathcal{S}^c)}) p(x_{(\mathcal{S})}, \mathbf{y} | x_{(\mathcal{S}^c)}) \log_2 \left[\frac{p(x_{(\mathcal{S})}, \mathbf{y} | x_{(\mathcal{S}^c)})}{p(x_{(\mathcal{S})} | x_{(\mathcal{S}^c)}) p(\mathbf{y} | x_{(\mathcal{S}^c)})} \right] \\ &= \sum_{x_{(\mathcal{T})}} \sum_{\mathbf{y}} p(x_{(\mathcal{S}^c)}) p(x_{(\mathcal{S})} | x_{(\mathcal{S}^c)}) p(\mathbf{y} | x_{(\mathcal{T})}) \log_2 \left[\frac{p(x_{(\mathcal{S})} | x_{(\mathcal{S}^c)}) p(\mathbf{y} | x_{(\mathcal{T})})}{p(x_{(\mathcal{S})} | x_{(\mathcal{S}^c)}) p(\mathbf{y} | x_{(\mathcal{S}^c)})} \right] \\ &= \sum_{x_{(\mathcal{T})}} \left(\prod_{m=1}^T p(x_m) \right) \sum_{\mathbf{y}} p(\mathbf{y} | x_{(\mathcal{T})}) \log_2 \left[\frac{p(\mathbf{y} | x_{(\mathcal{T})})}{p(\mathbf{y} | x_{(\mathcal{S}^c)})} \right] \\ &= \sum_{x_{(\mathcal{T})}} \left(\prod_{m=1}^T p(x_m) \right) \sum_{\mathbf{y}} p(\mathbf{y} | x_{(\mathcal{T})}) \log_2 \left[\frac{p(\mathbf{y} | x_{(\mathcal{T})})}{\sum_{x'_{(\mathcal{S})}} p(x'_{(\mathcal{S})}) p(\mathbf{y} | x'_{(\mathcal{S})}, x_{(\mathcal{S}^c)})} \right] \\ &= \log_2 \left(\prod_{i \in \mathcal{S}} M_i \right) - \frac{1}{\prod_{j=1}^T M_j} \sum_{x_{(\mathcal{T})}} \sum_{\mathbf{y}} p(\mathbf{y} | x_{(\mathcal{T})}) \log_2 \left[\frac{\sum_{x'_{(\mathcal{S})}} p(\mathbf{y} | x'_{(\mathcal{S})}, x_{(\mathcal{S}^c)})}{p(\mathbf{y} | x_{(\mathcal{T})})} \right] \\ &= \sum_{i \in \mathcal{S}} \log_2(M_i) - \frac{1}{\prod_{j=1}^T M_j} \sum_{x_{(\mathcal{T})}} \sum_{\mathbf{y}} \left(\prod_{k=1}^K p(\underline{v}_k | x_{(\mathcal{T})}) \right) \log_2 \left[\frac{\sum_{x'_{(\mathcal{S})}} \prod_{k=1}^K p(\underline{v}_k | x'_{(\mathcal{S})}, x_{(\mathcal{S}^c)})}{\prod_{k=1}^K p(\underline{v}_k | x_{(\mathcal{T})})} \right] \\ &= \sum_{i \in \mathcal{S}} \log_2(M_i) - \left(\prod_{j=1}^T \frac{1}{M_j} \right) \sum_{x_{(\mathcal{T})}} \sum_{\mathbf{v}=(\mathbf{v}^R, \mathbf{v}^I)} \left(\prod_{k=1}^K p(v_k^R | x_{(\mathcal{T})}) p(v_k^I | x_{(\mathcal{T})}) \right) \times \\ &\quad \log_2 \left[\frac{\sum_{x'_{(\mathcal{S})}} \prod_{k=1}^K p(v_k^R | x'_{(\mathcal{S})}, x_{(\mathcal{S}^c)}) p(v_k^I | x'_{(\mathcal{S})}, x_{(\mathcal{S}^c)})}{\prod_{k=1}^K p(v_k^R | x_{(\mathcal{T})}) p(v_k^I | x_{(\mathcal{T})})} \right] \end{aligned} \quad (2.51)$$

where the conditional probabilities are given in (2.47) and $\mathcal{S} = \{\mathcal{S} \subseteq \mathcal{T} \mid \mathcal{S} \cap \mathcal{S}^c = \emptyset \text{ and } \mathcal{S} \cup \mathcal{S}^c = \mathcal{T}\}$. From the quantization rate constraint in (2.50) we have

$$\begin{aligned} I(Y_{R_k}; \underline{V}_k) &= H(\underline{V}_k) - \underbrace{H(\underline{V}_k | Y_{R_k})}_{=0} \\ &= H(\underline{V}_k) = H(V_k^R, V_k^I) \leq \log_2(L_k) \\ &\leq C_k. \end{aligned} \tag{2.52}$$

We assume equal number of bits allocation for the real and imaginary parts of quantization, i.e. $\sqrt{L_k} = L_k^R = L_k^I, \forall k \in \mathcal{K}$. Hence, with C_k [bits/transmission] link capacity from the k -th RS to the destination if we select $L_k^R = L_k^I = 2^{\frac{C_k}{2}}$ transition levels we will not violate the quantization rate constraints given in (2.50).

2.4.4 Coded Modulation with Gaussian Mapping at the RSs

In [64], different RS mapping techniques are investigated for the conventional relay channel with finite capacity link between the RS and destination. It is shown that for *low* source-relay SNR region using a Gaussian mapping (for compression) at the RS gives the best result compared to non-Gaussian mapping (three-level quantization) and the DF relaying strategy where coded modulation at the source is used. For simplicity, we also look at the Gaussian mapping case for PRNs.

With Gaussian mapping at the RSs, the QF relaying scheme achieves the rate region given in (2.49) with the constraints (2.50). The input-output relation at the k -th RS is given by, assuming Gaussian mapping,

$$V_k = Y_k + Z_{Q,k} \tag{2.53}$$

where $Z_{Q,k} \sim \mathcal{NC}(0, \sigma_{k,D}^2), \forall k \in \mathcal{K}$, is the quantization noise. We can re-write

the mutual information term in (2.49) as follows

$$\begin{aligned}
 \sum_{i \in \mathcal{S}} R_i &= I(X_{(\mathcal{S})}; \mathbf{V} | X_{(\mathcal{S}^c)}) \\
 &= H(X_{(\mathcal{S})} | X_{(\mathcal{S}^c)}) - H(X_{(\mathcal{S})} | \mathbf{V}, X_{(\mathcal{S}^c)}) \\
 &= H(X_{(\mathcal{S})}) - H(X_{(\mathcal{S})} | \mathbf{V}, X_{(\mathcal{S}^c)}) \\
 &= \log_2 \left(\prod_{i \in \mathcal{S}} M_i \right) - \left(\prod_{j=1}^T \frac{1}{M_j} \right) \times \\
 &\quad \sum_{x_{(\mathcal{T})}} \int_{\mathbf{v}} f(\mathbf{v} | x_{(\mathcal{T})}) \log_2 \left[\frac{\sum_{x'_{(\mathcal{S})}} f(\mathbf{v} | x'_{(\mathcal{S})}, x_{(\mathcal{S}^c)})}{f(\mathbf{v} | x_{(\mathcal{T})})} \right] d\mathbf{v} \\
 &= \log_2 \left(\prod_{i \in \mathcal{S}} M_i \right) - \frac{1}{N_z} \left(\prod_{j=1}^T \frac{1}{M_j} \right) \times \\
 &\quad \sum_{n=1}^{N_z} \sum_{x_{(\mathcal{T})}} \log_2 \left[\frac{\sum_{x'_{(\mathcal{S})}} \exp\{-(\mathbf{v} - \mathbf{H}\mathbf{x}')^H \Lambda^{-1} (\mathbf{v} - \mathbf{H}\mathbf{x}')\}}{\exp\{-(\mathbf{v} - \mathbf{H}\mathbf{x})^H \Lambda^{-1} (\mathbf{v} - \mathbf{H}\mathbf{x})\}} \right] \quad (2.54)
 \end{aligned}$$

for $\mathcal{S} \subseteq \mathcal{T}$, where $\mathbf{V} = (V_1, V_2, \dots, V_K)$, $\mathbf{x} = [x_1, x_2, \dots, x_T]^T$, $\mathbf{x}' = [x'_{(\mathcal{S})}, x_{(\mathcal{S}^c)}]^T$ and $\Lambda \in \mathbb{C}^{K \times K}$ is diagonal matrix with j -th diagonal $\Lambda_{j,j} = \sigma_j^2 + \sigma_{j,D}^2$. For the last equation we used the Monte-Carlo method over the noise samples, with N_z being the number of samples.

The quantization rate constraints for the QF relaying with Gaussian mapping become³

$$\begin{aligned}
 I(Y_k; V_k) &= h(V_k) - h(V_k | Y_k) \\
 &= h(V_k) - \log_2(\pi e D_k) \leq C_k, \quad \forall k \in \mathcal{K} \quad (2.55)
 \end{aligned}$$

³here $h(\cdot)$ stands for differential entropy.

where $h(V_k)$ is given by⁴

$$\begin{aligned}
h(V_k) &= - \int_{v_k} f(v_k) \log_2(f(v_k)) dv_k \\
&= - \int_{v_k} \sum_{x_{(\mathcal{T})}} f(x_{(\mathcal{T})}, v_k) \log_2 \left(\sum_{x'_{(\mathcal{T})}} f(x'_{(\mathcal{T})}, v_k) \right) dv_k \\
&= - \frac{1}{\prod_{i=1}^T M_i} \int_{v_k} \sum_{x_{(\mathcal{T})}} f(v_k | x_{(\mathcal{T})}) \log_2 \left(\frac{1}{\prod_{j=1}^T M_j} \sum_{x'_{(\mathcal{T})}} f(v_k | x'_{(\mathcal{T})}) \right) dv_k \\
&= \sum_{j=1}^T \log_2(M_j) - \frac{1}{\prod_{i=1}^T M_i} \sum_{x_{(\mathcal{T})}} \int_{v_k} f(v_k | x_{(\mathcal{T})}) \log_2 \left(\sum_{x'_{(\mathcal{T})}} f(v_k | x'_{(\mathcal{T})}) \right) dv_k \\
&= \sum_{j=1}^T \log_2(M_j) - \frac{1}{\prod_{i=1}^T M_i} \frac{1}{N_z} \times \\
&\quad \sum_{n=1}^{N_z} \sum_{x_{(\mathcal{T})}} \log_2 \left[\sum_{x'_{(\mathcal{T})}} \frac{1}{\pi(\sigma^2 + D_k)} \exp \left\{ -\frac{|v_k - \mathbf{h}_k^T x'_{(\mathcal{T})}|^2}{\sigma^2 + D_k} \right\} \right]. \quad (2.56)
\end{aligned}$$

For the case of BQRB relaying with Gaussian mapping, the constraints on the quantization rates become [28]

$$\begin{aligned}
I(Y_{(\mathcal{S})}; V_{(\mathcal{S})} | V_{(\mathcal{S}^c)}) &= h(V_{(\mathcal{S})} | V_{(\mathcal{S}^c)}) - h(V_{(\mathcal{S})} | V_{(\mathcal{S}^c)}, Y_{(\mathcal{S})}) \\
&= h(V_{(\mathcal{S})}, V_{(\mathcal{S}^c)}) - h(V_{(\mathcal{S}^c)}) - h(Z_{(\mathcal{S})}) \\
&= h(V_{(\mathcal{K})}) - h(V_{(\mathcal{S}^c)}) - \sum_{j \in \mathcal{S}} \log_2(\pi e D_j) \\
&\leq \sum_{i \in \mathcal{S}} C_i, \quad \forall \mathcal{S} \subseteq \mathcal{K} \quad (2.57)
\end{aligned}$$

where $h(V_{(\mathcal{S})})$ can be calculated as follow, similar to (2.56),

$$\begin{aligned}
h(V_{(\mathcal{S})}) &= - \int_{v_{(\mathcal{S})}} f(v_{(\mathcal{S})}) \log_2(f(v_{(\mathcal{S})})) \mathbf{d}v_{(\mathcal{S})} \\
&= \sum_{j=1}^T \log_2(M_j) - \frac{1}{\prod_{i=1}^T M_i} \frac{1}{N_z} \times \\
&\quad \sum_{n=1}^{N_z} \sum_{x_{(\mathcal{T})}} \log_2 \left[\frac{\sum_{x'_{(\mathcal{T})}} \exp \left\{ -(\mathbf{v}_{(\mathcal{S})} - \mathbf{H}_{(\mathcal{S})} \mathbf{x}'_{(\mathcal{T})})^H \Lambda_{(\mathcal{S})} (\mathbf{v}_{(\mathcal{S})} - \mathbf{H}_{(\mathcal{S})} \mathbf{x}'_{(\mathcal{T})}) \right\}}{\det(\pi \Lambda_{(\mathcal{S})})} \right] \quad (2.58)
\end{aligned}$$

⁴The distribution of complex Gaussian random vector $\mathbf{x} \sim \mathcal{CN}(\underline{\mu}, \Lambda)$ is $f(\mathbf{x}) = \det(\pi \Lambda)^{-1} \exp\{-\mathbf{x} - \underline{\mu}\}^H \Lambda^{-1} (\mathbf{x} - \underline{\mu})\}$.

where $\mathbf{H}_{(s)} \in \mathbb{C}^{|\mathcal{S}| \times M}$, $\mathbf{v}_{(s)} \in \mathbb{C}^{|\mathcal{S}| \times 1}$ and $\Lambda_{(s)} \in \mathbb{C}^{|\mathcal{S}| \times |\mathcal{S}|}$ are the channel matrix from all sources, the quantized signal vector and the diagonal matrix holding additive and quantization noise variances corresponding to the RSs in the set $\mathcal{S} \subseteq \mathcal{K}$.

2.5 Numerical Results

In this section, we compare the achievable rate performances of the relaying strategies studied above for the symmetric PRN model where all the sources have the same power P_s and all the RSs have the same power P_r . Moreover, the channel gains from all the sources to each RS are assumed to be the same; and for case of orthogonal relay-to-destination backhaul links, the link capacities assumed to be the same, $C = C_1 = C_2 = \dots, C_K$. In the following, we evaluate the performances of AF, DF, BQRB and QF relaying strategies through numerical simulations.

Single Source Case

First, we consider complex AWGN PRN with *single source* and $K = 2$ RSs. We examine the achievable rate performance of each relaying strategy for both non-orthogonal and orthogonal MAC links between the RSs and the destination.

Assuming non-orthogonal (shared) wireless MAC case, we examine the corresponding outer bounds and achievable rates which are given by (2.13), (2.17), (2.22a) and (2.29). To see the performance of these relaying strategies, we fix the transmit SNR as $\gamma_s = P_s/\sigma^2 = 10$ dB, and give average achievable rates for different $\gamma_r = P_r/\sigma^2$ SNR values. We also select symmetric and asymmetric channel gains in order to show the tightness of the outer bound considering cross cut-sets. The results are depicted in Figure 2.3 and Figure 2.4 for symmetric channel gains, where $|h_i| = |g_i| = 1$ for $i = 1, 2$, and asymmetric channel gains, where $|h_1| = |g_2| = 0.5$ and $|h_2| = |g_1| = 1$, respectively. In Figure 2.3 representing the symmetric case, it can be seen that the DF relaying achieves the network capacity for low γ_r up to $\gamma_r = 7$ dB, exceeding this value the DF performance is bounded by BC link. In contrast to the AWGN PRN studied in [23], with phase fading PRN, the AF relaying does not even converge to the DF performance due to the non-coherent reception at the destination. On the other hand, the proposed BQRB relaying converges to the outer bound, and always outperforms the AF and DF in the strong relay regime. Moreover, we note that the outer bounds coincide for the symmetric case. In Figure 2.4 we consider the case of asymmetric channel gains. From this figure it can be seen that the outer bound with cross-cuts is tighter, and the AF relaying can achieve the same rate as the DF at high γ_r regime.

Assuming orthogonal lossless links between the RSs and the destination, we examine the corresponding outer bound and achievable rates which are given by (2.33), (2.34), (2.22), (2.54) and (2.51). In Figure 2.5 we plot the outer bound (given by (2.33)) and the achievable rates corresponding to DF (given by (2.34)),

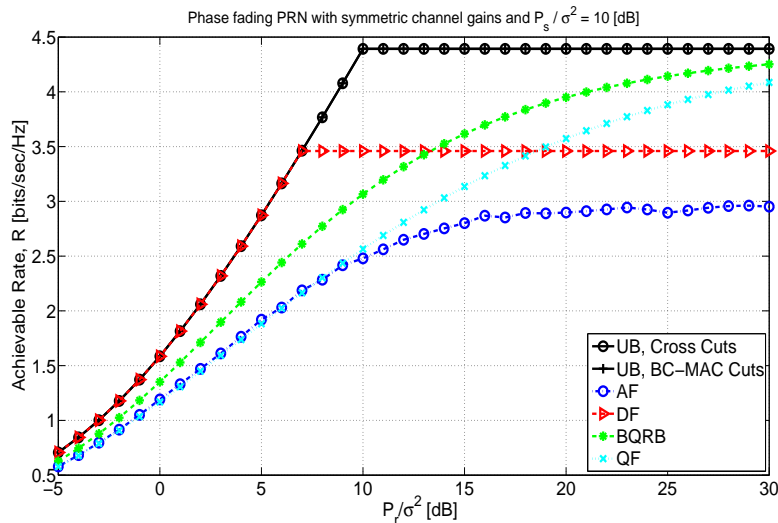


Figure 2.3: Achievable rates for phase fading PRN with symmetric channel gains, where $|h_i| = |g_i| = 1$, for $i = 1, 2$, and $P_s/\sigma^2 = 10$ dB.

CF-GSGM (CF relaying with Gaussian signaling and Gaussian mapping) (given by (2.22)), QF-GSGM, CF-CMGM (QF relaying with CM and Gaussian mapping) and QF-CMSQ (QF relaying with CM and uSQ) relaying strategies with respect to varying SNR $\gamma_s = \frac{P_s}{\sigma_s^2}$ values. We select 4-QAM at the source for non-Gaussian alphabets and uSQ for the non-Gaussian mapping at the RSs. It is seen that with increasing γ_s , for fixed C , the DF outperforms the others. However, in the low SNR regime, $\gamma_s \leq 0$ [dB], we see that by using a practical and less complex relaying strategy (namely QF-CMSQ relaying) one can beat the DF achievable rate performance by selecting a proper modulation alphabet size. Note also that, at low SNR regime, using CM with a proper alphabet size, Shannon theoretical limit can be achieved.

Two Sources Case

In Figure 2.6 we plot the achievable rate regions corresponding to $T = 2$ source, $K = 2$ RS phase fading AWGN PRN with non-orthogonal relay-to-destination links for $\gamma_s \leq 0$ dB, $\gamma_r \leq 10$ dB and symmetric channel gains $|\mathbf{H}[i, j]| = |\mathbf{g}[i]| = 1$, $\forall i, j = 1, 2$. We averaged the results over 500 realizations of phase shifts.

Next, we consider $T = 2$ sources, $K = 2$ RSs phase fading AWGN PRN with orthogonal relay-to-destination links with limited capacity $C = C_1 = C_2$. We take a sample channel matrix from sources to RSs as

$$\mathbf{H} = \frac{1}{\sqrt{2}} \begin{bmatrix} 1 & \exp\{-j\pi/3\} \\ \exp\{-j2\pi/3\} & 1 \end{bmatrix} \quad (2.59)$$

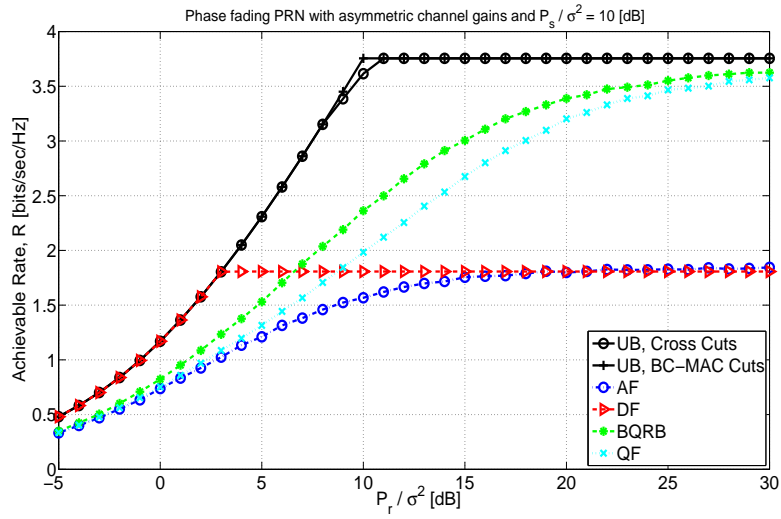


Figure 2.4: Achievable rates for phase fading PRN with asymmetric channel gains, where $|h_1| = |g_2| = 0.5$ and $|h_2| = |g_1| = 1$, and $P_s / \sigma^2 = 10$ dB.

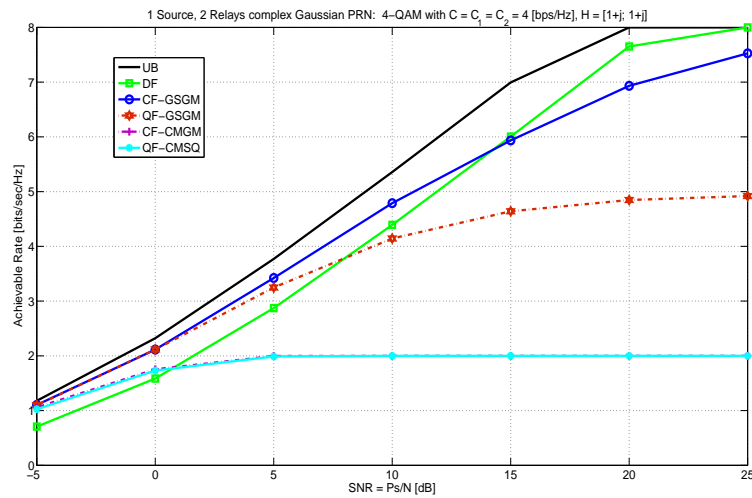


Figure 2.5: 1 Source, 2 Relays complex Gaussian PRN: Achievable rates versus $SNR = \frac{P_s}{\sigma^2}$ with $C = C_1 = C_2 = 4$ [bits/transmission] and $\mathbf{h}^T = [1 + j \ 1 + j]$.

We plot outer bound and achievable sum-rates with respect to $SNR = P_s/\sigma^2$.

In Figure 2.7, 2.8 and 2.9, we examine the outer bound on the sum-rate and the achievable sum-rates corresponding to DF, CF-GSGM, and QF-GSGM for respective backhaul rates $C = \{2, 4, 6\}$ [bits/transmission], and compare these classical relaying strategies (Gaussian codebooks at the sources and Gaussian mapping at the RSs) to CF-CMGM and QF-CMSQ wherein 4-QAM is used at the sources. For $C = 2$ [bps/Hz], at high SNR all the studied strategies achieve the network capacity. Note that a total backhaul capacity of 4 [bps/Hz] is enough for sending two sources' messages using 4-QAM via QF-CMSQ relaying; hence at high SNR its sum-rate performance approaches the outer limit. For higher backhaul rates, e.g., $C = \{4, 6\}$ [bps/Hz], even though there are enough backhaul resources since the use of finite alphabet of cardinality 4 (4-QAM) the achievable sum-rate with QF-CMSQ relaying is upper bounded by 4 [bps/Hz]. However, a more interesting behavior is in the low SNR regime, $SNR \leq 10$ dB, where the DF sum-rate performance is worse than that of QF-CMSQ relaying.

Similarly, in Figure 2.10 we compare the achievable sum-rates for the CF-CMGM and QF-CMSQ relaying strategies, wherein 16-QAM is used at the sources, with the ideal relaying strategies for $C = 4$ [bits/transmission].

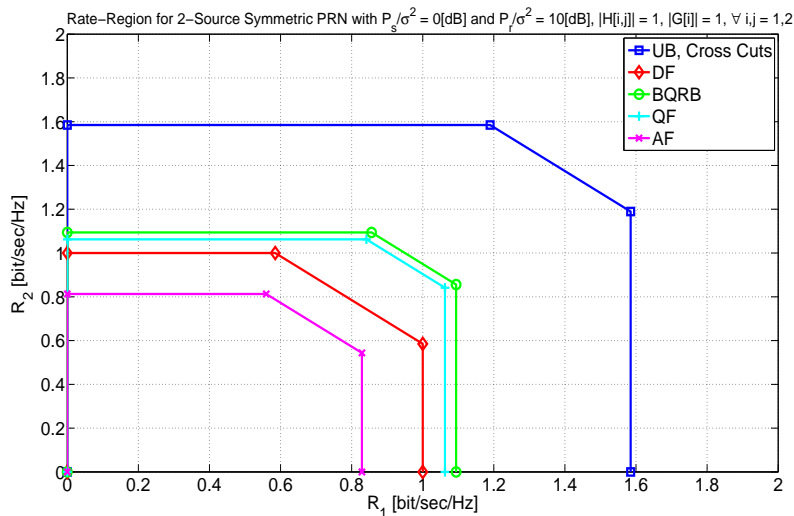


Figure 2.6: Achievable rates region for phase fading PRN with asymmetric channel gains, where $|\mathbf{H}[i,j]| = |\mathbf{g}[i]| = 1$, $\forall i, j = 1, 2$, and $P_s/\sigma^2 = 0$ dB, $P_r/\sigma^2 = 10$ dB. We used 500 channel realizations to average over phase fading.

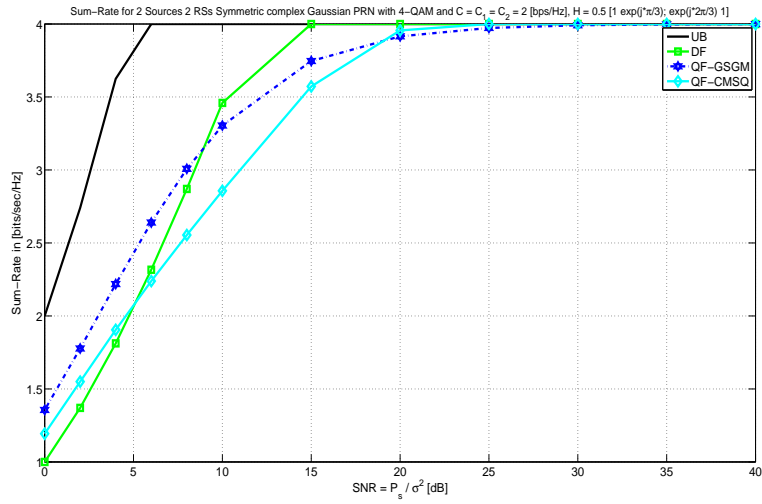


Figure 2.7: 2 Source, 2 Relays complex Gaussian PRN: Achievable rates versus $SNR = \frac{P_s}{\sigma^2}$ for 4-QAM with $C = C_1 = C_2 = 2$ [bits/transmission] and sample channel matrix (2.59).

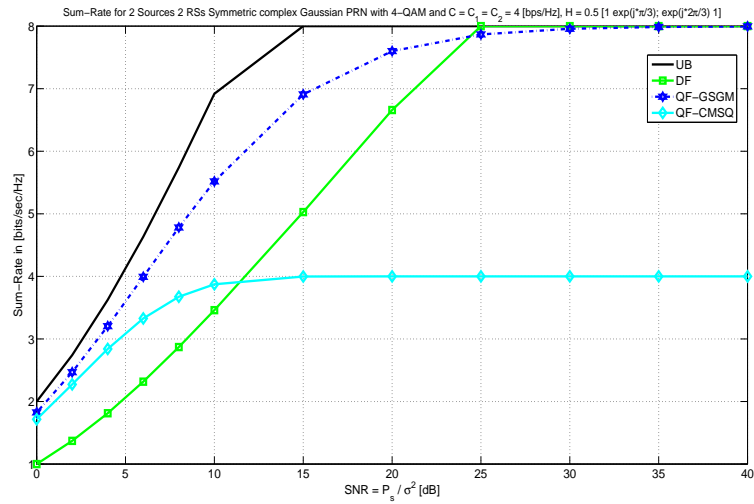


Figure 2.8: 2 Source, 2 Relays complex Gaussian PRN: Achievable rates versus $SNR = \frac{P_s}{\sigma^2}$ for 4-QAM with $C = C_1 = C_2 = 4$ [bits/transmission] and sample channel matrix (2.59).

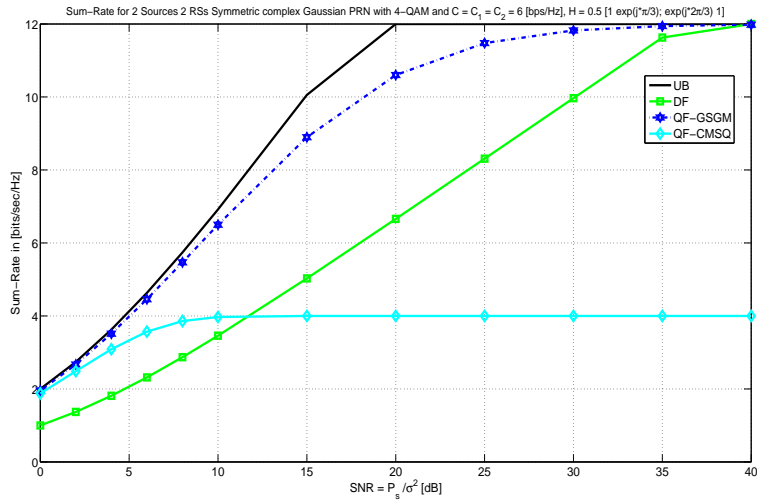


Figure 2.9: 2 Source, 2 Relays complex Gaussian PRN: Achievable rates versus $SNR = \frac{P_s}{\sigma^2}$ for 4-QAM with $C = C_1 = C_2 = 6$ [bits/transmission] and sample channel matrix (2.59).

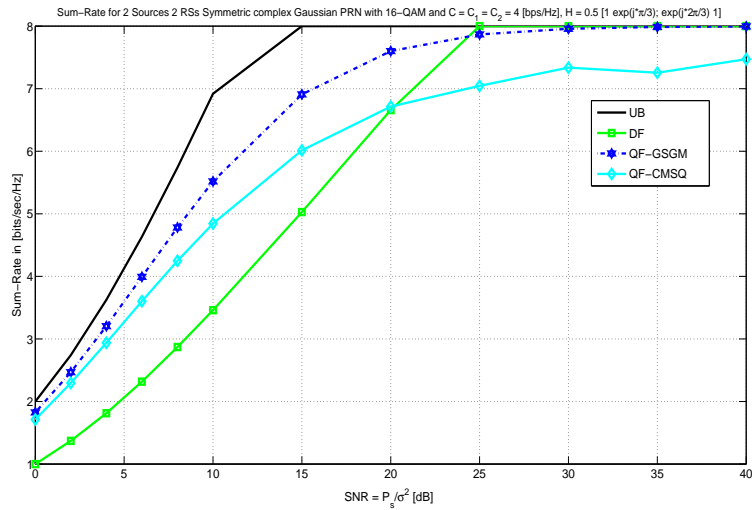


Figure 2.10: 2 Source, 2 Relays complex Gaussian PRN: Achievable rates versus $SNR = \frac{P_s}{\sigma^2}$ for 16-QAM with $C = C_1 = C_2 = 4$ [bits/transmission] and sample channel matrix (2.59).

2.6 Conclusions

In this chapter, we study outer bounds and achievable rates for various relaying strategies, such as AF, DF, BQRB and QF, for the AWGN PRN with phase fading, where T sources want to communicate with a destination with the assistance of K intermediate RSs. Two different channel models for the RSs to destination links are considered: 1) a regular AWGN MAC with constant channel gain and random phase shifts, and 2) lossless orthogonal links with finite capacity between each RS and the destination.

We also show that it is possible to achieve relatively good performance with simplified assumptions at the sources and at the RSs, i.e., coded modulation at the sources and uniform scalar quantization at the RSs. Through simulations it is shown, for low-to-medium SNR regime and sufficient backhaul capacity assumption, that the sum-rate achieved by using QF relaying with finite alphabet codebooks at the sources and uniform scalar quantizers at the RSs outperforms that of DF relaying with Gaussian signaling at the sources. Moreover, we observe that this achievable sum-rate is directly proportional to the size of the modulation alphabet.

2.A Outer bound

Only the receivers are assumed to have phase knowledge. The sources' input messages are chosen uniformly over the sets $W_t \in \{1, 2, \dots, 2^{nR_i}\}$, $\forall t \in \mathcal{T}$. We define $\underline{\Phi}^n = \{\{\Phi_{kt}^n \mid \forall k \in \mathcal{K} \text{ and } \forall t \in \mathcal{T}\}, \{\Phi_{Dk}^n \mid \forall k \in \mathcal{K}\}\}$ and define $\tilde{Y}^n = (Y^n, \underline{\Phi}^n)$, $\tilde{Y}_{R_k}^n = (Y_{R_k}^n, \{\Phi_{kt}^n \mid \forall t \in \mathcal{T}\})$, $\forall k \in \mathcal{K}$, for notational convenience. Due to Fano's inequality, with $P_e^{(n)} \rightarrow 0$ as $n \rightarrow \infty$, we have

$$\mathrm{H}(W_{(\mathcal{T})} | \tilde{Y}^n) \leq n\epsilon_n \quad (2.60)$$

where $\epsilon_n \rightarrow 0$ as $n \rightarrow \infty$, which implies that

$$\mathrm{H}(W_{(\mathcal{M})} | W_{(\mathcal{M}^c)}, \tilde{Y}^n) \leq n\epsilon_n, \quad \forall \mathcal{M} \subseteq \mathcal{T} \quad (2.61)$$

$$\mathrm{H}(W_{(\mathcal{M})} | W_{(\mathcal{M}^c)}, X_{R_{(\mathcal{R})}}^n, \tilde{Y}^n) \leq n\epsilon_n, \quad \forall \mathcal{M} \subseteq \mathcal{T}, \forall \mathcal{R} \subseteq \mathcal{K} \quad (2.62)$$

and we also have the following bound

$$\begin{aligned} \mathrm{H}(W_{(\mathcal{M})} | W_{(\mathcal{M}^c)}, X_{R_{(\mathcal{R})}}^n) &\stackrel{(a)}{=} \mathrm{H}(W_{(\mathcal{M})} | W_{(\mathcal{M}^c)}, \tilde{Y}^n, X_{R_{(\mathcal{R})}}^n) \\ &\stackrel{(b)}{\leq} \mathrm{H}(W_{(\mathcal{M})} | W_{(\mathcal{M}^c)}, \tilde{Y}^n) \\ &\leq n\epsilon_n. \end{aligned} \quad (2.63)$$

where (a) is due to the Markov chain $W_{(\mathcal{M})} - \{X_{R_{(\mathcal{R})}}^n\} - \tilde{Y}^n$, $\forall \mathcal{M} \subseteq \mathcal{T}$, and (b) follows since conditioning reduces entropy. Now assuming $\mathcal{R} \subseteq \mathcal{K}$ is the sub-set of relay nodes involved in the communication between a subset $\mathcal{M} \subseteq \mathcal{T}$ of the source nodes and the destination node, we can bound the sum-rate $\sum_{i \in \mathcal{M}} R_i$ as

follows:

$$\begin{aligned}
 \sum_{i \in \mathcal{M}} nR_i &= \mathbb{I}(W_{(\mathcal{M})}; X_{R(\mathcal{R})}^n, \tilde{Y}^n | W_{(\mathcal{M}^c)}) + \mathbb{H}(W_{(\mathcal{M})} | W_{(\mathcal{M}^c)}, X_{R(\mathcal{R})}^n, \tilde{Y}^n) \\
 &\leq \mathbb{I}(W_{(\mathcal{M})}; X_{R(\mathcal{R})}^n, \tilde{Y}^n | W_{(\mathcal{M}^c)}) + n\epsilon_n \quad [\text{Fano's Inequality}] \\
 &= \sum_{i=1}^n \mathbb{H}(X_{R(\mathcal{R}),i}, \tilde{Y}_i | X_{R(\mathcal{R})}^{i-1}, \tilde{Y}^{i-1}, W_{(\mathcal{M}^c)}) - \mathbb{H}(X_{R(\mathcal{R}),i}, \tilde{Y}_i | X_{R(\mathcal{R})}^{i-1}, \tilde{Y}^{i-1}, W_{(\mathcal{T})}) + n\epsilon_n \\
 &= \sum_{i=1}^n \mathbb{H}(X_{R(\mathcal{R}),i} | X_{R(\mathcal{R})}^{i-1}, \tilde{Y}^{i-1}, W_{(\mathcal{M}^c)}) + \mathbb{H}(\tilde{Y}_i | \tilde{Y}^{i-1}, X_{R(\mathcal{R})}^i, W_{(\mathcal{M}^c)}) \\
 &\quad - \mathbb{H}(X_{R(\mathcal{R}),i} | \tilde{Y}^{i-1}, X_{R(\mathcal{R})}^{i-1}, W_{(\mathcal{T})}) - \mathbb{H}(\tilde{Y}_i | \tilde{Y}^{i-1}, X_{R(\mathcal{R})}^i, W_{(\mathcal{T})}) + n\epsilon_n \\
 &= \sum_{i=1}^n \mathbb{H}(X_{R(\mathcal{R}),i} | X_{R(\mathcal{R})}^{i-1}, \tilde{Y}^{i-1}, X_{(\mathcal{M}^c),i}, W_{(\mathcal{M}^c)}) + \mathbb{H}(\tilde{Y}_i | \tilde{Y}^{i-1}, X_{R(\mathcal{R})}^i, X_{(\mathcal{M}^c),i}, W_{(\mathcal{M}^c)}) \\
 &\quad - \mathbb{H}(X_{R(\mathcal{R}),i} | \tilde{Y}^{i-1}, X_{R(\mathcal{R})}^{i-1}, X_{(\mathcal{T}),i}, W_{(\mathcal{T})}) - \mathbb{H}(\tilde{Y}_i | \tilde{Y}^{i-1}, X_{R(\mathcal{R})}^i, X_{(\mathcal{T}),i}, W_{(\mathcal{T})}) + n\epsilon_n \\
 &\stackrel{(a)}{\leq} \sum_{i=1}^n \mathbb{H}(X_{R(\mathcal{R}),i} | X_{R(\mathcal{R})}^{i-1}, \tilde{Y}^{i-1}, X_{(\mathcal{M}^c),i}, W_{(\mathcal{M}^c)}) + \mathbb{H}(\tilde{Y}_i | \tilde{Y}^{i-1}, X_{R(\mathcal{R}),i}, X_{(\mathcal{M}^c),i}, W_{(\mathcal{M}^c)}) \\
 &\quad - \mathbb{H}(X_{R(\mathcal{R}),i} | \tilde{Y}^{i-1}, X_{R(\mathcal{R})}^{i-1}, X_{(\mathcal{T}),i}, W_{(\mathcal{T})}) - \mathbb{H}(\tilde{Y}_i | \tilde{Y}^{i-1}, X_{R(\mathcal{R}),i}, X_{(\mathcal{T}),i}, W_{(\mathcal{T})}) + n\epsilon_n \\
 &\stackrel{(b)}{\leq} \sum_{i=1}^n \mathbb{H}(X_{R(\mathcal{R}),i} | X_{(\mathcal{M}^c),i}) + \mathbb{H}(\tilde{Y}_i | X_{R(\mathcal{R}),i}) - \mathbb{H}(X_{R(\mathcal{R}),i} | X_{(\mathcal{T}),i}) - \mathbb{H}(\tilde{Y}_i | X_{R(\mathcal{R}),i}) + n\epsilon_n \\
 &= \sum_{i=1}^n \mathbb{I}(X_{(\mathcal{M}),i}; X_{R(\mathcal{R}),i} | X_{(\mathcal{M}^c),i}) + \sum_{i=1}^n \mathbb{I}(X_{R(\mathcal{R}^c),i}; \tilde{Y}_i | X_{R(\mathcal{R}),i}) + n\epsilon_n \\
 &\stackrel{(c)}{\leq} \sum_{i=1}^n \mathbb{I}(X_{(\mathcal{M}),i}; Y_{R(\mathcal{R}),i} | X_{(\mathcal{M}^c),i}) + \sum_{i=1}^n \mathbb{I}(X_{R(\mathcal{R}^c),i}; \tilde{Y}_i | X_{R(\mathcal{R}),i}) + n\epsilon_n. \tag{2.64}
 \end{aligned}$$

where (a) follows since conditioning reduces entropy; (b) follows since

$$(\tilde{Y}^{i-1}, W_{(\mathcal{M})}, X_{(\mathcal{M}),i}) - (X_{R(\mathcal{R}),i}) - \tilde{Y}_i$$

forms a Markov chain and because of the memoryless channel assumption, and (c) holds due to the data processing inequality.

We have the outer bound for the rate $\sum_{i \in \mathcal{M}} R_i$ given a subset \mathcal{R} of relay nodes are used. We can search over all the cuts to have the minimum one.

2.B The achievable rate region for BQRB relaying strategy

For now, we choose the decoder's typicality measure, ϵ , and the integer block length, n , arbitrarily. We will later set ϵ sufficiently small and n sufficiently large to make the probability of message error as small as possible.

Randomly generate 2^{nR_t} input codewords of block length n for $t = 1, 2, \dots, T$. Generate each symbol of each codeword independently according to $f_{X_t}(x_t)$. Denote these input codewords by $X_t^n(w_t)$, $w_t = 1, 2, \dots, 2^{nR_t}$, and denote the randomly chosen input codebook by $\mathcal{C}_t = \{\cup_{w_t=1}^{2^{nR_t}} X_t^n(w_t)\}$. For a particular

codebook choice, denote the input codewords by $x_t^n(w_t)$, $w_t = 1, 2, \dots, 2^{nR_t}$, and denote the input codebook by $c_t = \{\cup_{w_t=1}^{2^{nR_t}} x_t^n(w_t)\}$.

Set $\delta > 0$ as arbitrary parameter. Assume K relay nodes are present. Then for the k -th relay station RS_k , $k = 1, 2, \dots, K$, randomly generate $2^{n(I(Y_{R_k}; V_k) + \delta)}$ quantization codewords of block length n . Generate each symbol of each codeword independently according to $f_{V_k}(v_k) = \int_{y_{R_k}} f(y_{R_k}) f(v_k | y_{R_k}) dy_{R_k}$. Denote these RS_k quantization codewords by $V_k^n(j)$, $j = 1, \dots, 2^{n(I(Y_{R_k}; V_k) + \delta)}$. For a particular quantization codebook choice, denote the quantization codebook by $c_{q,k} = \{\cup_j v_k^n(j)\}$. Next, having randomly generated the RS_k quantization codebook, randomly and uniformly assign each RS_k quantization codeword, v_k^n , to one of $B_k \in \{1, \dots, 2^{nR_k^{MAC}}\}$ bins. Denote the randomly chosen bin assignments by the function $B_k = \varphi_k(v_k^n(j))$. Generate $2^{nR_k^{MAC}}$ independent codewords $X_{R_k}^n(B_k)$ of length n , $B_k \in \{1, \dots, 2^{nR_k^{MAC}}\}$, generating each element i.i.d. $\sim \prod_{i=1}^n f_{X_{R_k}}(x_{R_k,i})$. The other relays proceed similarly. Reveal all the codebooks (the sources' codebooks and the quantization codebooks) and the bin assignments to the destination node.

Encoding: The t -th source node transmits the codeword $x_t^n(w_t)$ corresponding to message w_t , $t = 1, 2, \dots, T$. The RS_k , after receiving $Y_{R_k}^n$, searches for any quantization codeword $v_k^n(j_k) \in c_{q,k}$ such that $(Y_{R_k}^n, v_k^n(j_k)) \in \mathcal{A}_\epsilon^{(n)}(Y_{R_k}, V_k)$. If one or more such quantization codewords exist, the RS_k chooses one of them randomly (uniformly amongst the candidates) and sends $X_{R_k}^n(B_k)$ where $B_k = \varphi_k(v_k^n(j_k))$. Otherwise, it declares an error (e.g., sends $B_k \equiv 0$). In this case, for notational convenience, we define the quantization codeword $v_k^n = \emptyset$.

Decoding: The destination node first tries to decode the bin indexes sent by the relay nodes. If it is able to decode the bin indexes correctly, then it moves into the following decoding step wherein it tries to decode the sources' messages. After receiving Y^n , the destination chooses the pair $(\hat{B}_1, \dots, \hat{B}_K)$ such that $(x_{R_1}^n(\hat{B}_1), \dots, x_{R_K}^n(\hat{B}_K), y^n) \in \mathcal{A}_\epsilon^{(n)}(X_{R_1}, \dots, X_{R_K}, Y)$ if such a pair $(\hat{B}_1, \hat{B}_2, \dots, \hat{B}_K)$ exists and is unique; otherwise, an error is declared.

Suppose in the first decoding step we correctly decoded the bin indexes sent by the relay nodes, $(\hat{B}_1, \dots, \hat{B}_K) = (B_1, \dots, B_K)$. Then, if any of these bin numbers equals the relay error message 0, the decoder declares an error. This indicates that at least one of the relay nodes failed the quantization step. Otherwise, the destination node declares that message vector (w_1, \dots, w_T) was sent if it is the unique message vector with quantization codewords, (v_1^n, \dots, v_K^n) , such that $\varphi_k(v_k^n) = \hat{B}_k$, $\forall k \in \{1, \dots, K\}$ and $(x_1^n(w_1), \dots, x_T^n(w_T), v_1^n, \dots, v_K^n) \in \mathcal{A}_\epsilon^{(n)}(X_1, \dots, X_T, V_1, \dots, V_K)$. If no message or if more than one message satisfy this criterion, the decoder declares an error.

Remark 19. For the signal model we consider, we have the following Markov chain:

$$(V_1, \dots, V_K) \leftrightarrow (Y_{R_1}, \dots, Y_{R_K}) \leftrightarrow (X_1, \dots, X_T) \leftrightarrow Y_{R_i} \leftrightarrow V_i, \quad i = 1, \dots, K.$$

A generalized Markov lemma that is proved by Oohama in [68] states that the

Markov chain implies,

$$\lim_{n \rightarrow \infty} \Pr \left((X_1^n, \dots, X_T^n, Y_{R_1}^n, \dots, Y_{R_K}^n, V_1^n, \dots, V_K^n) \in \mathcal{A}_\epsilon^{(n)} \right) = 1. \quad (2.65)$$

From the definition of jointly typical sequences [1, Theorem 15.2.1] if we have an ordered set of jointly distributed random variables being jointly typical, then any subset of this set also implies jointly typicality. Hence (2.65) implies

$$\lim_{n \rightarrow \infty} \Pr \left((X_1^n, \dots, X_T^n, V_1^n, \dots, V_K^n) \in \mathcal{A}_\epsilon^{(n)} \right) = 1. \quad (2.66)$$

We will use this generalized Markov property in the following for probability of error calculations.

Average Probability of Decoding Error: We compute the average probability of message error by averaging over the choice of input codewords, the choice of relay quantization codebooks, the quantization codeword bin assignments, and the broadcast channel outcomes. We denote the average probability of error by $P_e^{(n)} = \Pr[(W_1, \dots, W_T) \neq (\hat{W}_1, \dots, \hat{W}_T)]$.

Before averaging over the input codebook ensemble, the input codeword corresponding to the first message is denoted $X_t^n(1)$, $\forall t$. During operation, the relays receive the pair of observations $(Y_{R_1}^n, \dots, Y_{R_K}^n)$. When computing the average probability of message error, we will consider the input codebook without the first codeword. Define $\mathcal{C}_{t,-1} = \{\cup_{w_t=2}^{2^{nR_t}} X_t^n(w_t)\}$. Finally, we adopt the conventional set notation $\mathcal{C}_{q,k} \setminus V_k^n = \mathcal{C}_{q,k} - V_k^n$, $\forall k$.

We define following events:

E_{mac} : Event of error in MAC, i.e., $(\hat{B}_1, \dots, \hat{B}_K) \neq (B_1, \dots, B_K)$,

E_s : Event of error in decoding the source message, i.e., $(\hat{W}_1, \dots, \hat{W}_T) \neq (W_1, \dots, W_T)$.

Using these definitions, we can write the average overall probability of message error as

$$\begin{aligned} P_e^{(n)} &= \Pr(E_{mac}) \Pr(E_s | E_{mac}) + \Pr(E_{mac}^c) \Pr(E_s | E_{mac}^c) \\ &\leq \Pr(E_{mac}) + \Pr(E_s | E_{mac}^c) \Pr(E_{mac}^c) \\ &\leq \Pr(E_{mac}) + \Pr(E_s | E_{mac}^c) (1 - \Pr(E_{mac})) \\ &\leq \Pr(E_{mac}) + \Pr(E_s | E_{mac}^c). \end{aligned} \quad (2.67)$$

First, consider the communication between the relay nodes and the destination node. We want to reliably estimate the transmitted bin indexes at the destination node in order to proceed to decode the sources' messages. Due to random assignment of bin indexes at the relay nodes, the relay signals are uncorrelated, e.g. $\mathbb{E}[X_{R_i} X_{R_j}^*] = 0$, $\forall i \neq j$. Note that from [1, Theorem 15.3.1], with the upper bounds in the theorem satisfied, $\Pr(E_{mac}) \rightarrow 0$ with $n \rightarrow \infty$.

Assuming bin indexes, B_k , $\forall k$, sent by the relay nodes are correctly decoded at the destination node, then we need to decode the message pair $(W_1, \dots, W_T) = (1, \dots, 1)$ sent by the source nodes. We follow the MAC typical set decoding structure with K -antenna receiver. In the following we define R_k^{MAC} as the

achievable rates in the second hop from RS_k to the destination node, respectively.

In the following steps of the proof we will assume $T = 2$ and $K = 2$ in order to simplify the exposition of the proof which can easily be generalized to any number of source and relay nodes.

Assuming we perfectly decoded the relay bin indexes, then we can group all error events into the union of six events for $\Pr(E_s|E_{mac}^c)$ which are:

$$E_{0t} = \left\{ \frac{1}{n} \sum_{i=1}^n X_{t,i}^2(1) > P_s \right\} \quad \text{for } t = 1, 2;$$

is the event that the source power constraints are violated.

$$E_1 = \left\{ (X_1^n(1), X_2^n(1), V_1^n, V_2^n) \notin \mathcal{A}_\epsilon^{(n)}(X_1, X_2, V_1, V_2) \right\}$$

is the event that the input codewords and the actual relay quantization codewords are not jointly typical.

We define the following event

$$E_{i,j} = \left\{ (X_1^n(i), X_2^n(j), V_1^n, V_2^n) \in \mathcal{A}_\epsilon^{(n)}(X_1, X_2, V_1, V_2) \right\}$$

Assuming $(i, j) = (1, 1)$ is the message pair sent by the source nodes, we define the following event

$$E_2 = (\cup_{i \neq 1} E_{i1}) \cup (\cup_{j \neq 1} E_{1j}) \cup \left(\cup_{\substack{i \neq 1 \\ j \neq 1}} E_{ij} \right)$$

is the event that there are some incorrect codewords which are jointly typical with the relay quantization codewords.

For E_3 we have

$$E_{31} = \left\{ \begin{array}{l} (X_1^n(1), X_2^n(1), V_1^n, V_2^n) \in \mathcal{A}_\epsilon^{(n)}(X_1, X_2, V_1, V_2), \exists x_1'^n \in \mathcal{C}_{-1}^1 \\ \text{and } v_1'^n \in \mathcal{C}_{q,1} \setminus V_1^n \\ \text{s.t. } \varphi_1(v_1'^n) = \varphi_1(V_1^n) \text{ and } (x_1'^n, X_2^n(1), v_1'^n, V_2^n) \in \mathcal{A}_\epsilon^{(n)}(X_1, X_2, V_1, V_2) \end{array} \right\}$$

$$E_{32} = \left\{ \begin{array}{l} (X_1^n(1), X_2^n(1), V_1^n, V_2^n) \in \mathcal{A}_\epsilon^{(n)}(X_1, X_2, V_1, V_2), \exists x_2'^n \in \mathcal{C}_{-1}^2 \text{ and } v_1'^n \in \mathcal{C}_{q,1} \setminus V_1^n \\ \text{s.t. } \varphi_1(v_1'^n) = \varphi_1(V_1^n) \text{ and } (X_1^n(1), x_2'^n, v_1'^n, V_2^n) \in \mathcal{A}_\epsilon^{(n)}(X_1, X_2, V_1, V_2) \end{array} \right\}$$

$$E_{33} = \left\{ \begin{array}{l} (X_1^n(1), X_2^n(1), V_1^n, V_2^n) \in \mathcal{A}_\epsilon^{(n)}(X_1, X_2, V_1, V_2), \exists x_1'^n \in \mathcal{C}_{-1}^1, \exists s_2'^n \in \mathcal{C}_{-1}^2 \\ \text{and } v_1'^n \in \mathcal{C}_{q,1} \setminus V_1^n \text{ s.t. } \varphi_1(v_1'^n) = \varphi_1(V_1^n) \\ \text{and } (x_1'^n, x_2'^n, v_1'^n, V_2^n) \in \mathcal{A}_\epsilon^{(n)}(X_1, X_2, V_1, V_2) \end{array} \right\}$$

and

$$E_3 = \cup_{i=1}^3 E_{3i} = E_{31} \cup E_{32} \cup E_{33}.$$

is the event that $(X_1^n(1), X_2^n(1), V_1^n, V_2^n)$ is jointly typical, and there are incorrect input codewords, $x_1'^n, x_2'^n$, and a different RS_1 quantization codeword, $v_1'^n$,

assigned to the same bin as the chosen RS_1 quantization codeword, such that the quadruple $(x'_1, x'_2, v'_1, V_2^n)$ is jointly typical.

We have the similar expressions for E_4 where there is a wrong bin assignment at the RS_2 .

For E_5 we have

$$\begin{aligned}
 E_{51} &= \left\{ \begin{array}{l} (X_1^n(1), X_2^n(1), V_1^n, V_2^n) \in \mathcal{A}_\epsilon^{(n)}(X_1, X_2, V_1, V_2), \exists x'_1 \in \mathcal{C}_{-1}^1 \\ \text{and } v'_1 \in \mathcal{C}_{q,1} \setminus V_1^n, v'_2 \in \mathcal{C}_{q,2} \setminus V_2^n \text{ s.t. } \varphi_1(v'_1) = \varphi_1(V_1^n), \varphi_2(v'_2) = \varphi_2(V_2^n) \\ \text{and } (x'_1, X_2^n(1), v'_1, v'_2) \in \mathcal{A}_\epsilon^{(n)}(X_1, X_2, V_1, V_2) \end{array} \right\} \\
 E_{52} &= \left\{ \begin{array}{l} (X_1^n(1), X_2^n(1), V_1^n, V_2^n) \in \mathcal{A}_\epsilon^{(n)}(X_1, X_2, V_1, V_2), \exists x'_2 \in \mathcal{C}_{-1}^2 \\ \text{and } v'_1 \in \mathcal{C}_{q,1} \setminus V_1^n, v'_2 \in \mathcal{C}_{q,2} \setminus V_2^n \text{ s.t. } \varphi_1(v'_1) = \varphi_1(V_1^n), \varphi_2(v'_2) = \varphi_2(V_2^n) \\ \text{and } (X_1^n(1), x'_2, v'_1, v'_2) \in \mathcal{A}_\epsilon^{(n)}(X_1, X_2, V_1, V_2) \end{array} \right\} \\
 E_{53} &= \left\{ \begin{array}{l} (X_1^n(1), X_2^n(1), V_1^n, V_2^n) \in \mathcal{A}_\epsilon^{(n)}(X_1, X_2, V_1, V_2), \exists x'_1 \in \mathcal{C}_{-1}^1, \exists x'_2 \in \mathcal{C}_{-1}^2 \\ \text{and } v'_1 \in \mathcal{C}_{q,1} \setminus V_1^n, v'_2 \in \mathcal{C}_{q,2} \setminus V_2^n \text{ s.t. } \varphi_1(v'_1) = \varphi_1(V_1^n), \varphi_2(v'_2) = \varphi_2(V_2^n) \\ \text{and } (x'_1, x'_2, v'_1, v'_2) \in \mathcal{A}_\epsilon^{(n)}(X_1, X_2, V_1, V_2) \end{array} \right\}
 \end{aligned}$$

and

$$E_5 = \bigcup_{i=1}^3 E_{5i} = E_{51} \cup E_{52} \cup E_{53}.$$

is the event that $(X_1^n(1), X_2^n(1), V_1^n, V_2^n)$ is jointly typical, and there are incorrect input codewords, x'_1, x'_2 , and two different relay quantization codewords, v'_1 and v'_2 , each assigned to the same bin as the chosen relay quantization codewords, such that the quadruple (x'_1, x'_2, v'_1, v'_2) is jointly typical.

Using the basic set theory and the union bound,

$$\Pr(E_s | E_{mac}^c) = \Pr(\bigcup_{i=0}^5 E_i) \leq \sum_{i=0}^5 \Pr(E_i). \quad (2.68)$$

Error probabilities:

We need to show that each of these six probabilities can be made arbitrarily small as $n \rightarrow \infty$.

By the law of large numbers $\Pr(E_{0t}) \rightarrow 0$ as $n \rightarrow \infty$ for $t = 1, 2$.

To bound $\Pr(E_1)$ we need to show joint typicality between X_1, X_2 and V_1, V_2 . Using the generalized Markov lemma, as indicated in Remark-19, we ensure that the joint typicality between the inputs and outputs holds. As a consequence, $\Pr(E_1) \rightarrow 0$ as $\epsilon \rightarrow 0$ and $n \rightarrow \infty$ [1].

Consider event E_2 . By the union bound and the typicality in (2.66), we have

$$\Pr(E_2) \leq \sum_{i \neq 1} \Pr(E_{2,i1}) + \sum_{j \neq 1} \Pr(E_{2,1j}) + \sum_{\substack{i \neq 1 \\ j \neq 1}} \Pr(E_{2,ij})$$

and

$$\begin{aligned}
\Pr(E_{2,i1}) &\leq \Pr \left\{ (X_1^n(i), X_2^n(1), V_1^n, V_2^n) \in \mathcal{A}_\epsilon^{(n)} \right\} \\
&\leq \int_{(x_1^n, x_2^n, v_1^n, v_2^n) \in \mathcal{A}_\epsilon^{(n)}} f(x_1^n) f(x_2^n, v_1^n, v_2^n) dx_1^n dx_2^n dv_1^n dv_2^n \\
&\leq \text{Vol}\{\mathcal{A}_\epsilon^{(n)}\} \cdot 2^{-n(h(X_1)-\epsilon)} \cdot 2^{-n(h(X_2, V_1, V_2)-\epsilon)} \\
&\leq 2^{n(h(X_1, X_2, V_1, V_2)-\epsilon)} \cdot 2^{-n(h(X_1)-\epsilon)} \cdot 2^{-n(h(X_2, V_1, V_2)-\epsilon)} \\
&= 2^{-n(h(X_1)+h(X_2, V_1, V_2)-h(X_1, X_2, V_1, V_2)-\epsilon)} \\
&= 2^{-n(h(X_2, V_1, V_2)-h(X_2, V_1, V_2|X_1)-\epsilon)} \\
&= 2^{-n(I(X_1; X_2, V_1, V_2)-\epsilon)} \\
&= 2^{-n(I(X_1; X_2)+I(X_1; V_1, V_2|X_2)-\epsilon)} \\
&\stackrel{(a)}{=} 2^{-n(I(X_1; V_1, V_2|X_2)-\epsilon)}.
\end{aligned}$$

where (a) holds since X_1 and X_2 are independent. Following the same steps we have

$$\begin{aligned}
\Pr(E_{2,1j}) &\leq 2^{-n(I(X_2; V_1, V_2|X_1)-\epsilon)} \\
\Pr(E_{2,ij}) &\leq 2^{-n(I(X_1, X_2; V_1, V_2)-\epsilon)}
\end{aligned}$$

Then using the union bound we have the following upper-bound for $\Pr(E_2)$,

$$\begin{aligned}
\Pr(E_2) &\leq \sum_{i \neq 1} 2^{-n(I(X_1; V_1, V_2|X_2)-\epsilon)} + \sum_{i \neq 1} 2^{-n(I(X_2; V_1, V_2|X_1)-\epsilon)} + \sum_{\substack{i \neq 1 \\ j \neq 1}} 2^{-n(I(X_1, X_2; V_1, V_2)-\epsilon)} \\
&\leq 2^{-n(I(X_1; V_1, V_2|X_2)-R_1-\epsilon)} + 2^{-n(I(X_2; V_1, V_2|X_1)-R_2-\epsilon)} + 2^{-n(I(X_1, X_2; V_1, V_2)-R_1-R_2-\epsilon)}.
\end{aligned}$$

Note that $\Pr(E_2) \rightarrow 0$ if $n \rightarrow \infty$ and

$$\begin{aligned}
R_1 &\leq I(X_1; V_1, V_2|X_2) \\
R_2 &\leq I(X_2; V_1, V_2|X_1) \\
R_1 + R_2 &\leq I(X_1, X_2; V_1, V_2)
\end{aligned}$$

with $\epsilon \rightarrow 0$. Note that these rates are the achievable rates over the network from the source nodes to the destination node.

For the event E_3 we have

$$\Pr(E_3) \leq \sum_{i=1}^3 \Pr(E_{3i})$$

and

$$\begin{aligned}
 \Pr(E_{31}) &\leq \sum_{w_1=2}^{2^{nR_1}} \sum_{k=2}^{2^{n(I(Y_{R_1};V_1)+\delta)}} \int_{\substack{x'_1, v'_1 \\ (x'_1, x_2, v'_1, v_2^n) \in \mathcal{A}_\epsilon^{(n)}}} f(x'_1)f(v'_1) \Pr\{\varphi_1(v'_1) = \varphi_1(v_1^n)\} dx'_1 dv'_1 \\
 &\leq 2^{nR_1} \cdot 2^{n(I(Y_{R_1};V_1)+\delta)} \cdot 2^{n(h(X_1, V_1|X_2, V_2)-2\epsilon)} \cdot 2^{-n(h(X_1)-\epsilon)} \cdot 2^{-n(h(V_1)-\epsilon)} \cdot 2^{-nR_1^{MAC}} \\
 &= 2^{-n(h(X_1)+h(V_1)-h(X_1, V_1|X_2, V_2)+R_1^{MAC}-R_1-I(Y_{R_1};V_1)-\delta-4\epsilon)} \\
 &= 2^{-n(I(X_1;V_1, V_2|X_2)-R_1+R_1^{MAC}-(I(Y_{R_1};V_1)-I(V_1;V_2, X_2))-\delta-4\epsilon)}
 \end{aligned}$$

where we have

$$\begin{aligned}
 h(X_1) + h(V_1) - h(X_1, V_1|X_2, V_2) &= h(X_1) + h(V_1) - h(V_1|X_2, V_2) - h(X_1|X_2, V_1, V_2) \\
 &= h(V_1) - h(V_1|X_2, V_2) + h(X_1) - h(X_1|X_2, V_1, V_2) \\
 &= I(V_1; V_2, X_2) + I(X_1; X_2, V_1, V_2) \\
 &= I(V_1; V_2, X_2) + \underbrace{I(X_1; X_2)}_{=0} + I(X_1; V_1, V_2|X_2) \\
 &= I(V_1; V_2, X_2) + I(X_1; V_1, V_2|X_2).
 \end{aligned}$$

and similarly

$$\begin{aligned}
 \Pr(E_{32}) &\leq \sum_{w_2=2}^{2^{nR_2}} \sum_{k=2}^{2^{n(I(Y_{R_1};V_1)+\delta)}} \int_{\substack{x'_2, v'_1 \\ (x_1, x'_2, v'_1, v_2^n) \in \mathcal{A}_\epsilon^{(n)}}} f(x'_2)f(v'_1) \times \\
 &\quad \Pr\{\varphi_1(v'_1) = \varphi_1(v_1^n)\} dx'_2 dv'_1 \\
 &\leq 2^{nR_2} \cdot 2^{n(I(Y_{R_1};V_1)+\delta)} \cdot 2^{n(h(X_2, V_1|X_1, V_2)-2\epsilon)} \times \\
 &\quad 2^{-n(h(X_2)-\epsilon)} \cdot 2^{-n(h(V_1)-\epsilon)} \cdot 2^{-nR_1^{MAC}} \\
 &= 2^{-n(h(X_2)+h(V_1)-h(X_2, V_1|X_1, V_2)+R_1^{MAC}-R_2-I(Y_{R_1};V_1)-\delta-4\epsilon)} \\
 &= 2^{-n(I(X_2;V_1, V_2|X_1)-R_2+R_1^{MAC}-(I(Y_{R_1};V_1)-I(V_1;V_2, S_1))-\delta-4\epsilon)}
 \end{aligned}$$

and

$$\begin{aligned}
 \Pr(E_{33}) &\leq \sum_{w_1=2}^{2^{nR_1}} \sum_{w_2=2}^{2^{nR_2}} \sum_{k=2}^{2^{n(I(Y_{R_1};V_1)+\delta)}} \int_{\substack{x'_1, x'_2, v'_1 \\ (x'_1, x'_2, v'_1, v_2^n) \in \mathcal{A}_\epsilon^{(n)}}} f(x'_1)f(x'_2)f(v'_1) \times \\
 &\quad \Pr\{\varphi_1(v'_1) = \varphi_1(v_1^n)\} dx'_1 dx'_2 dv'_1 \\
 &\leq 2^{nR_1+R_2} \cdot 2^{n(I(Y_{R_1};V_1)+\delta)} \cdot 2^{n(h(X_1, X_2, V_1|V_2)-2\epsilon)} \times \\
 &\quad 2^{-n(h(X_1)+h(X_2)+h(V_1)-3\epsilon)} \cdot 2^{-nR_1^{MAC}} \\
 &= 2^{-n(h(X_1)+h(X_2)+h(V_1)-h(X_1, X_2, V_1|V_2)+R_1^{MAC}-(R_1+R_2)-I(Y_{R_1};V_1)-\delta-4\epsilon)} \\
 &= 2^{-n(I(X_1, X_2;V_1, V_2)-(R_1+R_2)+R_1^{MAC}-(I(Y_{R_1};V_1)-I(V_1;V_2))-\delta-4\epsilon)}
 \end{aligned}$$

where

$$\begin{aligned}
& h(X_1) + h(X_2) + h(V_1) - h(X_1, X_2, V_1|V_2) \\
&= h(X_1, X_2) + h(V_1) - h(X_1, X_2, V_1|V_2) \\
&= h(X_1, X_2) + h(V_1) - h(V_1|V_2) - h(X_1, X_2|V_1, V_2) \\
&= I(V_1; V_2) + I(X_1, X_2; V_1, V_2).
\end{aligned}$$

Then, for some $\epsilon > 0$, where $\epsilon \rightarrow 0$ as $n \rightarrow \infty$. Note that $\Pr(E_3) \rightarrow 0$ if $n \rightarrow \infty$ and

$$\begin{aligned}
R_1 &\leq I(X_1; V_1, V_2|X_2) \\
R_2 &\leq I(X_2; V_1, V_2|X_1) \\
R_1 + R_2 &\leq I(X_1, X_2; V_1, V_2) \\
R_1^{MAC} &\geq I(Y_{R_1}; V_1) - \min\{I(V_1; V_2), I(V_1; V_2, X_1), I(V_1; V_2, X_2)\} \\
&= I(Y_{R_1}; V_1) - I(V_1; V_2)
\end{aligned}$$

with $\epsilon \rightarrow 0$.

For $\Pr(E_4)$ following the same procedures we did above, we get $\Pr(E_4) \rightarrow 0$ if $n \rightarrow \infty$ and

$$\begin{aligned}
R_1 &\leq I(X_1; V_1, V_2|X_2) \\
R_2 &\leq I(X_2; V_1, V_2|X_1) \\
R_1 + R_2 &\leq I(X_1, X_2; V_1, V_2) \\
R_2^{MAC} &\geq I(Y_{R_2}; V_2) - I(V_1; V_2)
\end{aligned}$$

with $\epsilon \rightarrow 0$.

For the event E_5 we have

$$\Pr(E_5) \leq \sum_{i=1}^3 \Pr(E_{5i})$$

and

$$\begin{aligned}
\Pr(E_{51}) &\leq \sum_{w_1=2}^{2^{nR_1}} \sum_{k_1=2}^{2^{n(I(Y_{R_1}; V_1)+\delta)}} \sum_{k_2=2}^{2^{n(I(Y_{R_2}; V_2)+\delta)}} \int_{(x'_1, x_2, v'_1, v'_2) \in \mathcal{A}_\epsilon^{(n)}} f(x'_1) f(v'_1) f(v'_2) \times \\
&\quad \Pr\{\varphi_1(v'_1) = \varphi_1(v_1^n)\} \Pr\{\varphi_1(v'_2) = \varphi_1(v_2^n)\} dx'_1 dv'_1 dv'_2 \\
&\leq 2^{nR_1} \cdot 2^{n(I(Y_{R_1}; V_1)+I(Y_{R_2}; V_2)+2\delta)} \cdot 2^{n(h(X_1, V_1, V_2|X_2)-2\epsilon)} \times \\
&\quad 2^{-n(h(X_1)+h(V_1)+h(V_2)-3\epsilon)} \cdot 2^{-n(R_1^{MAC}+R_2^{MAC})} \\
&= 2^{-n(h(X_1)+h(V_1)+h(V_2)-h(X_1, V_1, V_2|X_2)+R_1^{MAC}+R_2^{MAC}-R_1-I(Y_{R_1}; V_1)-I(Y_{R_2}; V_2)-2\delta-4\epsilon)} \\
&= 2^{-n(I(X_1, X_2; V_1, V_2)-R_1+R_1^{MAC}+R_2^{MAC}-(I(Y_{R_1}; V_1)+I(Y_{R_2}; V_2)-I(V_1; V_2))-2\delta-4\epsilon)}
\end{aligned}$$

where we have

$$\begin{aligned}
& h(X_1) + h(V_1) + h(V_2) - h(X_1, V_1, V_2|X_2) \\
&= h(X_1) + h(V_1) + h(V_2) - h(X_1|X_2) - h(V_1, V_2|X_1, X_2) \\
&= h(X_1) + h(V_1) + h(V_2) - \underbrace{h(X_1|X_2)}_{=h(X_1)} - h(V_1, V_2|X_1, X_2) \\
&= h(V_1) + h(V_2) - h(V_1, V_2|X_1, X_2) \\
&= I(V_1; V_2) + h(V_1, V_2) - h(V_1, V_2|X_1, X_2) \\
&= I(V_1; V_2) + I(X_1, X_2; V_1, V_2),
\end{aligned}$$

and, similarly

$$\begin{aligned}
\Pr(E_{52}) &\leq \sum_{w_2=2}^{2^{nR_2}} \sum_{k_1=2}^{2^{n(I(Y_{R_1}; V_1)+\delta)}} \sum_{k_2=2}^{2^{n(I(Y_{R_2}; V_2)+\delta)}} \int_{(x_1, x_2', v_1', v_2') \in \mathcal{A}_\epsilon^{(n)}} f(x_2') f(v_1') f(v_2') \times \\
&\quad \Pr\{\varphi_1(v_1') = \varphi_1(v_1^n)\} \Pr\{\varphi_1(v_2') = \varphi_1(v_2^n)\} dx_2' dv_1' dv_2' \\
&\leq 2^{nR_2} \cdot 2^{n(I(Y_{R_1}; V_1)+I(Y_{R_2}; V_2)+2\delta)} \cdot 2^{n(h(X_2, V_1, V_2|X_1)-2\epsilon)} \times \\
&\quad 2^{-n(h(X_2)+h(V_1)+h(V_2)-3\epsilon)} \cdot 2^{-n(R_1^{MAC}+R_2^{MAC})} \\
&= 2^{-n(h(X_2)+h(V_1)+h(V_2)-h(X_2, V_1, V_2|X_1)+R_1^{MAC}+R_2^{MAC}-R_2-I(Y_{R_1}; V_1)-I(Y_{R_2}; V_2)-2\delta-4\epsilon)} \\
&= 2^{-n(I(X_1, X_2; V_1, V_2)-R_2+R_1^{MAC}+R_2^{MAC}-(I(Y_{R_1}; V_1)+I(Y_{R_2}; V_2)-I(V_1; V_2))-2\delta-4\epsilon)}
\end{aligned}$$

and

$$\begin{aligned}
\Pr(E_{53}) &\leq \sum_{w_1=2}^{2^{nR_1}} \sum_{w_2=2}^{2^{nR_2}} \sum_{k_1=2}^{2^{n(I(Y_{R_1}; V_1)+\delta)}} \sum_{k_2=2}^{2^{n(I(Y_{R_2}; V_2)+\delta)}} \int_{(x_1', x_2', v_1', v_2') \in \mathcal{A}_\epsilon^{(n)}} f(x_1') f(x_2') \times \\
&\quad f(v_1') f(v_2') \Pr\{\varphi_1(v_1') = \varphi_1(v_1^n)\} \Pr\{\varphi_1(v_2') = \varphi_1(v_2^n)\} dx_1' dx_2' dv_1' dv_2' \\
&\leq 2^{n(R_1+R_2)} \cdot 2^{n(I(Y_{R_1}; V_1)+I(Y_{R_2}; V_2)+2\delta)} \cdot 2^{n(h(X_1, X_2, V_1, V_2)-2\epsilon)} \times \\
&\quad 2^{-n(h(X_1)+h(X_2)+h(V_1)+h(V_2)-3\epsilon)} \cdot 2^{-n(R_1^{MAC}+R_2^{MAC})} \\
&= 2^{-n(I(X_1, X_2; V_1, V_2)-(R_1+R_2)+R_1^{MAC}+R_2^{MAC}-(I(Y_{R_1}; V_1)+I(Y_{R_2}; V_2)-I(V_1; V_2))-2\delta-4\epsilon)}.
\end{aligned}$$

Then, for some $\epsilon > 0$, where $\epsilon \rightarrow 0$ as $n \rightarrow \infty$. Note that $\Pr(E_5) \rightarrow 0$ if $n \rightarrow \infty$ and

$$\begin{aligned}
R_1 + R_2 &\leq I(X_1, X_2; V_1, V_2) \\
I(Y_{R_1}; V_1) + I(Y_{R_2}; V_2) - I(V_1; V_2) &\leq R_1^{MAC} + R_2^{MAC}
\end{aligned}$$

with $\epsilon \rightarrow 0$.

Finally considering all the error probability events together with rate conditions on MAC, then we can make the average probability of message errors

sufficiently small, $P_e^{(n)} = \Pr(E_{mac}) + \Pr(E_s|E_{mac}^c) \rightarrow 0$ if $n \rightarrow \infty$ and

$$R_1 \leq I(X_1; V_1, V_2 | X_2) \quad (2.69)$$

$$R_2 \leq I(X_2; V_1, V_2 | X_1) \quad (2.70)$$

$$R_1 + R_2 \leq I(X_1, X_2; V_1, V_2) \quad (2.71)$$

$$I(Y_{R_1}; V_1) - I(V_1; V_2) \leq I(X_{R_1}; Y | X_{R_2})$$

$$I(Y_{R_2}; V_2) - I(V_1; V_2) \leq I(X_{R_2}; Y | X_{R_1})$$

$$I(Y_{R_1}; V_1) + I(Y_{R_2}; V_2) - I(V_1; V_2) \leq I(X_{R_1}, X_{R_2}; Y). \quad (2.72)$$

This concludes the proof.

Chapter 3

Multi-Source Parallel Relay Networks: Error Exponent Analysis

3.1 Introduction

In order to have thorough characterization of a system's performance, knowing only the capacity of a system is not sufficient enough. Hence, in this chapter, our performance measure is the random coding error exponents (EEs) [69], also defined as channel reliability function which represents a decaying rate in the decoding error probability as a function of codeword length. In particular, we assess the random coding EEs corresponding to DF, CF and QF relaying strategies for single- and two-source PRN setups. Specifically, for the DF we assume Gaussian codebooks at the sources and maximum-likelihood (ML) decoding at the relays where each passes its own decision and a corresponding *reliability function* to the destination which makes the ultimate decision without requiring any CSI. For the BQRB (or CF) case, we assume Gaussian codebooks at the sources, VQ at the relays and ML decoding at the destination. For the QF, we assume coded modulation (M-QAM) at the sources and uSQ at the relays.

We show, through numerical analysis, that using a finite alphabet constellation (i.e., M-QAM) at the sources along with simple processing at the RSs (i.e., symbol-by-symbol uSQ) can provide better EEs compared to more complex strategies (such as DF and CF relaying strategies where Gaussian signalling at the sources and Gaussian mappings at the RS are used) when the system is in the low SNR regime and the backhaul capacity is sufficient. This is due to

the structure inherent in the considered modulation alphabets, which Gaussian signaling lacks.

3.1.1 Channel Model

In this chapter, we adopt the orthogonal MAC channel model defined in the previous chapter where the RSs are connected to the destination via orthogonal error-free limited-capacity backhaul links, see Section-9.4. We let, the same as previous chapter, the link capacity from the i -th RS to the destination be C_i in [bits/channel use]. See Figure 9.3 for an illustration. We assume that all other parameters are the same as in the previous chapter.

3.2 Error Exponent Analysis for Single-Source and Two-source PRNs

3.2.1 Random Coding Error Exponent

In order to have thorough characterization of a system's performance, the capacity of the system alone is not sufficient. The random coding EE [69], which is also defined as channel reliability function and represents a decaying rate in the decoding error probability as a function of codeword length, gives insights about how to achieve a certain level of reliability in communication at a rate below the channel capacity.

Definition 20. *The error exponent of a communication system is defined by [69]*

$$E(R) \triangleq \limsup_{n \rightarrow \infty} \frac{-\log_2 P_e(n, R)}{n} \quad (3.1)$$

where $P_e(R, n)$ is the average block error probability for the optimum block code of length n and rate R [bits/transmission].

For any rate below capacity, the average probability of decoding error $P_e(R, n)$ for codes of block length n can be bounded between the limits

$$2^{-n[E_{sp}(R)+O(n)]} \leq P_e(n, R) \leq 2^{-nE_r(R)} \quad (3.2)$$

where $E_{sp}(R)$, known as *sphere packing* EE, and $E_r(R)$, known as *random coding* EE, are lower and upper bounds on the reliability function $E(R)$, respectively, and $O(n)$ is a function going to 0 with increasing n .

For a given code \mathcal{C} of length n and alphabet size 2^{nR} , Gallager's random coding EE, which relies on ML decoding, is given by

$$E_r(R) = \max_{0 \leq \rho \leq 1} \max_{p(\mathbf{x})} [E_0(\rho, p(\mathbf{x})) - \rho R] \quad (3.3)$$

where $E_0(\rho, p(\mathbf{x}))$ is defined as

$$E_0(\rho, p(\mathbf{x})) = -\log_2 \left[\sum_{\mathbf{y}} \left(\sum_{\mathbf{x}} p(\mathbf{x}) p(\mathbf{y}|\mathbf{x})^{\frac{1}{1+\rho}} \right)^{1+\rho} \right] \quad (3.4)$$

for discrete channels where $p(\mathbf{x})$ is the input distribution and $p(\mathbf{y}|\mathbf{x})$ are the channel output distributions conditioned on the input, and

$$E_0(\rho, f(\mathbf{x})) = -\log_2 \left[\int_{-\infty}^{\infty} \left(\int_{-\infty}^{\infty} f(\mathbf{x}) f(\mathbf{y}|\mathbf{x})^{\frac{1}{1+\rho}} d\mathbf{x} \right)^{1+\rho} d\mathbf{y} \right] \quad (3.5)$$

for AWGN channels where $f(\mathbf{x})$ is the continuous input distribution and $f(\mathbf{y}|\mathbf{x})$ the channel output distributions conditioned on the input.

Consider the following AWGN MIMO channel model

$$\mathbf{y} = \mathbf{H}\mathbf{x} + \mathbf{z} \quad (3.6)$$

with input distribution $\mathbf{x} \sim \mathcal{CN}(\mathbf{0}, \mathbf{Q})$ and noise $\mathbf{z} \sim \mathcal{CN}(\mathbf{0}, \mathbf{W})$. Then, the random coding EE for the channel (3.6) corresponding to inputs with Gaussian distribution¹ is given by [70]

$$E_r(R) = \max_{0 \leq \rho \leq 1} [E_0(\rho, f(\mathbf{x})) - \rho R] \quad (3.7)$$

where $E_0(\rho, f(\mathbf{x}))$ is defined as

$$E_0(\rho, f(\mathbf{x})) = \rho \log_2 \mathbb{E}_{\mathbf{H}} \left| \mathbf{I} + \frac{1}{1+\rho} \mathbf{W}^{-1} \mathbf{H} \mathbf{Q} \mathbf{H}^H \right|, \quad (3.8)$$

where $|\mathbf{A}|$ represents the determinant of matrix \mathbf{A} .

3.2.2 Error Exponent Analysis for Single Source Case

In this section, we obtain expressions for the EEs corresponding to DF, CF and QF relaying strategies for single source, two-relay and a single destination PRN setup. For the DF relaying, we assume a Gaussian codebook at the source and ML decoding at the RSs where each passes its own decision and a corresponding *reliability information* to the destination. For the CF relaying, we use a Gaussian codebook at the source and VQ at the RSs and ML decoding at the destination. For the QF relaying, M-QAM at the source and uSQ at the RSs are considered.

For the single source PRN case, since each RS can perform *phase compensation* on their received signals, the received signal at the k -th RS, given in (9.1), is equivalent to

$$\tilde{y}_{R_k} = h_{k1} x_1 + \tilde{z}_k, \quad k = 1, 2, \quad (3.9)$$

where $h_{k1} \in \mathbb{R}^+$ is the fixed channel gain from the source to the k -th RS, $\tilde{z}_k \sim \mathcal{CN}(0, \sigma^2)$ is noise term at the k -th RS.

¹Choosing the input distribution $f(\mathbf{x})$ as Gaussian is *not* optimal and a distribution concentrated on a *thin spherical shell* will give better results [69], nonetheless Gaussian input distribution is a convenient lower bound on $E_0(\rho, f(\mathbf{x}))$ and thus provides an upper bound to the probability of error.

DF relaying with Gaussian Inputs

Assume each RS applies ML detection and sends the message corresponding to the detected signal along with a *reliability information* (which is a scalar variable equal to the logarithm of the Euclidean distance between the received signal and the detected signal) to the destination on orthogonal error- and cost-free limited capacity backhaul links. Here it is assumed that the reliability information is received at the destination freely². Moreover, we assume that the backhaul link capacities are at least equal to the source transmission rate, R . Hence, the backhaul links do not create a bottleneck for system performance.

Upon receiving the detected signals and the reliability information, the destination makes its decision by comparing the reliability information: it decides on the codeword which has the *minimum* reliability information (Euclidean distance), see Figure 3.1 for an illustration of ML decoding at the relay nodes. Hence, if the codeword detected at one of the RS is wrong and its corresponding reliability information is smaller, then the ultimate detection will be wrong even if the other RS has made a correct detection (but with greater reliability information).

Assume the w -th message, $w \in \mathcal{W}$, is encoded into the codeword $\mathbf{x}_1(w) \in \mathbb{C}^{n \times 1}$ of length n and let $\tilde{\mathbf{y}}_{R_k} \in \mathbb{C}^{n \times 1}$ denote the received signal vector of size n at the k -th RS for $k = 1, 2$. Then, the ML detection at the k -th RS is given by

$$\begin{aligned}
 \hat{\mathbf{x}}_{ML,k} &= \arg \max_{\mathbf{x}_1} p(\tilde{\mathbf{y}}_{R_k} | \mathbf{x}_1(w), h_{k1}) \\
 &= \arg \max_{\mathbf{x}_1} \ln(p(\tilde{\mathbf{y}}_{R_k} | \mathbf{x}_1(w), h_{k1})) \\
 &= \arg \max_{\mathbf{x}_1} -\frac{1}{\sigma^2} \|\tilde{\mathbf{y}}_{R_k} - h_{k1} \mathbf{x}_1\|^2 - n \ln(\pi \sigma^2) \\
 &= \arg \max_{\mathbf{x}_1} -\|\tilde{\mathbf{y}}_{R_k} - h_{k1} \mathbf{x}_1\| \\
 &= \arg \min_{\mathbf{x}_1} \|\tilde{\mathbf{y}}_{R_k} - h_{k1} \mathbf{x}_1\| \\
 &= \arg \min_{\mathbf{x}_1} \beta_k, \quad k = 1, 2,
 \end{aligned} \tag{3.10}$$

where we define β_k as the *reliability information*, i.e.,

$$\beta_k = \|\tilde{\mathbf{y}}_{R_k} - h_{k1} \mathbf{x}_1\|, \quad k = 1, 2. \tag{3.11}$$

Upon receiving the detected signal and the reliability information of each RS, the destination node makes the following final detection:

$$\hat{\mathbf{x}}_{ML} = \arg \min_{\hat{\mathbf{x}}_{ML,1}, \hat{\mathbf{x}}_{ML,2}} \beta_k, \quad k = 1, 2. \tag{3.12}$$

With this detection rule we have the following average probability of error

²In a practical system the reliability information, which is a scalar value, should be quantized with respect to a given rate constraint on the backhaul.

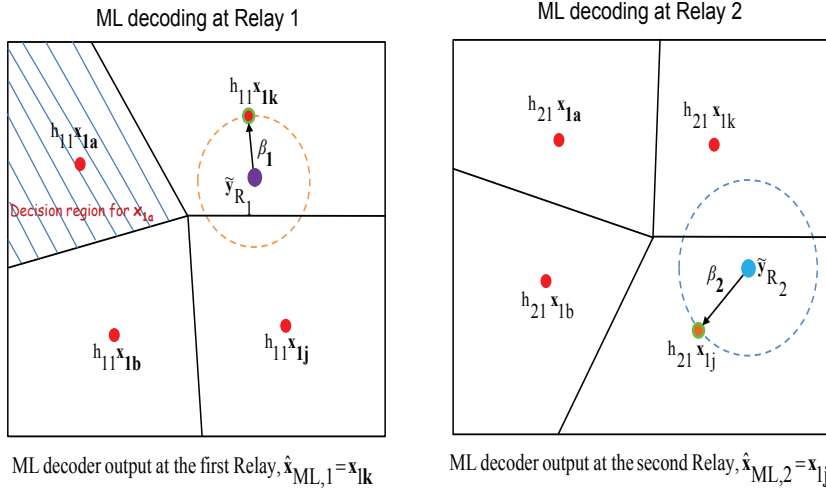


Figure 3.1: An illustration for ML decoding at the RSs where the k -th RS sends the detected signal $\hat{\mathbf{x}}_{ML,k}$ and the reliability information $\beta_k \in \mathbb{R}^+$ to the destination, for $k = 1, 2$.

(conditioned on $\mathbf{x}_1(w)$ was sent)

$$\begin{aligned}
 P_e &\leq P_{ML,1}P_{ML,2} + P_{ML,1}(1 - P_{ML,2}) \Pr\{\beta_2 > \beta_1 \mid \hat{\mathbf{x}}_{ML,1} \neq \mathbf{x}_1(w), \hat{\mathbf{x}}_{ML,2} = \mathbf{x}_1(w)\} \\
 &\quad + P_{ML,2}(1 - P_{ML,1}) \Pr\{\beta_1 > \beta_2 \mid \hat{\mathbf{x}}_{ML,2} \neq \mathbf{x}_1(w), \hat{\mathbf{x}}_{ML,1} = \mathbf{x}_1(w)\} \\
 &\leq P_{ML,1}P_{ML,2} + P_{ML,1} \Pr\{\beta_2 > \beta_1\} + P_{ML,2} \Pr\{\beta_1 > \beta_2\} \quad (3.13)
 \end{aligned}$$

where $P_{ML,k}$, for $k = 1, 2$, is the standard ML error probability at the k -th RS, and we use the notation $\Pr\{\beta_a > \beta_b\}$ to stand for $\Pr\{\beta_a > \beta_b \mid \hat{\mathbf{x}}_{ML,b} \neq \mathbf{x}_1(w), \hat{\mathbf{x}}_{ML,a} = \mathbf{x}_1(w)\}$ for $a, b = 1, 2, a \neq b$.

Assuming *symmetric* channels from the source to the RSs, i.e., $h = h_1 = h_2$, and hence $P_{ML} = P_{ML,k}$ and $\Pr\{\beta_1 > \beta_2\} = \Pr\{\beta_2 > \beta_1\}$, the probability of error will have the following simplified expression:

$$P_e \leq P_{ML}^2 + 2P_{ML} \Pr\{\beta_2 > \beta_1\}. \quad (3.14)$$

Now we need to find the expression for $\Pr\{\beta_2 > \beta_1\}$. This can be evaluated

as follows

$$\begin{aligned}
 \Pr\{\beta_2 > \beta_1\} &= \Pr\{\beta_2 > \beta_1 \mid \hat{\mathbf{x}}_{ML,1} \neq \mathbf{x}_1(w), \hat{\mathbf{x}}_{ML,2} = \mathbf{x}_1(w)\} \\
 &= \Pr\{\|\tilde{\mathbf{y}}_{R_1} - h_{11}\hat{\mathbf{x}}_{ML,1}\|^2 \leq \|\tilde{\mathbf{y}}_{R_2} - h_{21}\hat{\mathbf{x}}_{ML,2}\|^2\} \\
 &= \Pr\{\|\tilde{\mathbf{y}}_{R_1} - h_{11}\hat{\mathbf{x}}_{ML,1}\|^2 \leq \|\tilde{\mathbf{y}}_{R_2} - h_{21}\mathbf{x}_1\|^2\} \\
 &= \Pr\{\|h_{11}(\mathbf{x}_1 - \hat{\mathbf{x}}_{ML,1}) + \tilde{\mathbf{z}}_1\|^2 \leq \|\tilde{\mathbf{z}}_2\|^2\} \\
 &= \Pr\{\|\hat{\mathbf{z}}_1\|^2 - \|\tilde{\mathbf{z}}_2\|^2 \leq 0\} \\
 &= \Pr\{F - Y \leq 0\} \\
 &= \Pr\{Z \leq 0\}
 \end{aligned} \tag{3.15}$$

where $\hat{\mathbf{z}}_1 \triangleq h_{11}(\mathbf{x}_1 - \hat{\mathbf{x}}_{ML,1}) + \tilde{\mathbf{z}}_1 \sim \mathcal{CN}(\mathbf{0}, (2h_{11}^2 P_s + \sigma^2)\mathbf{I}_n)$, we note that Gaussian codebook is assumed at the transmitter with $P_s = \mathbb{E}[|x_1|^2]$ being the average source signal power, and $\tilde{\mathbf{z}}_2 \sim \mathcal{CN}(\mathbf{0}, \sigma^2\mathbf{I}_n)$. Furthermore, we define the RVs $F \triangleq \|\hat{\mathbf{z}}_1\|^2$, $Y \triangleq \|\tilde{\mathbf{z}}_2\|^2$ and $Z \triangleq F - Y$.

The RV Z can be re-written in the following form

$$\begin{aligned}
 Z &= F - Y = \|\hat{\mathbf{z}}_1\|^2 - \|\tilde{\mathbf{z}}_2\|^2 \\
 &= \sum_{i=1}^n (|\hat{z}_{1,i}|^2 - |\tilde{z}_{2,i}|^2) = \sum_{i=1}^n (F_i - Y_i) = \sum_{i=1}^n Z_i
 \end{aligned} \tag{3.16}$$

where³ $F_i \triangleq |\hat{z}_{1,i}|^2 \sim \text{Exp}(\lambda_f)$ with $\lambda_f = 1/(2h_{11}^2 P_s + \sigma^2)$, $Y_i \triangleq |\tilde{z}_{2,i}|^2 \sim \text{Exp}(\lambda_y)$ with $\lambda_y = 1/\sigma^2$, and $Z_i = F_i - Y_i$, $i = 1, \dots, n$. With these definitions the p.d.f. of Z_i , $f_{Z_i}(z_i)$, is given by (see Appendix-3.A for the derivations of the p.d.f.)

$$f_{Z_i}(z_i) = \begin{cases} \frac{\lambda_f \lambda_y}{\lambda_f + \lambda_y} e^{-\lambda_f z_i} & , z_i \geq 0 \\ \frac{\lambda_f \lambda_y}{\lambda_f + \lambda_y} e^{\lambda_y z_i} & , z_i < 0 \end{cases} \tag{3.17}$$

with mean $\mu_Z = \mathbb{E}[Z_i]$ and variance $\sigma_Z^2 = \text{VAR}[Z_i]$, for $i = 1, 2, \dots, n$, see Appendix-3.A for derivations,

$$\begin{aligned}
 \mu_Z &= \frac{1}{\lambda_f} - \frac{1}{\lambda_y} \\
 \sigma_Z^2 &= \frac{1}{(\lambda_f + \lambda_y)^2} \left[\frac{\lambda_y^2}{\lambda_f^2} + \frac{\lambda_f^2}{\lambda_y^2} \right].
 \end{aligned} \tag{3.18}$$

³The notation $F \sim \text{Exp}(\lambda_f)$ means that F is an exponentially distributed RV with mean λ_f , i.e., $p_F(f) = \lambda_f \exp\{-\lambda_f f\}$, $f \geq 0$.

Finally, we can upper bound $\Pr\{\beta_2 > \beta_1\}$ as follows, for sufficiently large n ,

$$\begin{aligned}
 \Pr\{\beta_2 > \beta_1\} &= \Pr\{\beta_2 > \beta_1 | \hat{\mathbf{x}}_{ML,1} \neq \mathbf{x}_1(w), \hat{\mathbf{x}}_{ML,2} = \mathbf{x}_1(w)\} \\
 &= \Pr\{Z \leq 0\} = \Pr\left\{\sum_{i=1}^n Z_i \leq 0\right\} \\
 &\stackrel{(a)}{\leq} Q\left(\frac{n\mu_Z}{\sqrt{n\sigma_Z^2}}\right) \stackrel{(b)}{\leq} \exp\left\{-n\frac{\mu_Z^2}{2\sigma_Z^2}\right\} \\
 &= \exp\left\{-n\left(\frac{1}{2} - \frac{\lambda_f^2\lambda_y^2}{\lambda_f^4 + \lambda_y^4}\right)\right\} \\
 &\stackrel{(c)}{\leq} 2^{-n\left(\frac{\log_2(e)}{2} - \frac{\log_2(e)(1+2\Gamma)^2}{1+(1+2\Gamma)^4}\right)} \tag{3.19}
 \end{aligned}$$

where $\Gamma = \frac{h^2 P_s}{\sigma^2}$ with $h = h_{11} = h_{21}$, (a) follows from the central limit theorem [1], (b) follows by upper-bounding the standard tail function $Q(\cdot)$ and (c) holds by inserting $\lambda_f = 1/(2h_{11}^2 P_s + \sigma^2)$ and $\lambda_y = 1/\sigma^2$. See Appendix-3.B for the derivations and the exact probability expression, as well.

Hence, the overall average probability of error can be approximated as

$$\begin{aligned}
 P_e &\leq P_{ML}^2 + 2P_{ML} \Pr\{\beta_2 > \beta_1\} \\
 &\leq P_{ML}^2 + 2P_{ML} 2^{-n\left(\frac{\log_2(e)}{2} - \frac{\log_2(e)(1+2\Gamma)^2}{1+(1+2\Gamma)^4}\right)} \\
 &\leq 2^{-n(2E_r(R))} + 2^{-n\left(E_r(R) + \frac{\log_2(e)}{2} - \frac{\log_2(e)(1+2\Gamma)^2}{1+(1+2\Gamma)^4} - \frac{1}{n}\right)} \\
 &\leq 2^{-n \min\left\{2E_r(R), E_r(R) + \frac{\log_2(e)}{2} - \frac{\log_2(e)(1+2\Gamma)^2}{1+(1+2\Gamma)^4} - \frac{1}{n}\right\}} \\
 &\leq 2^{-n \min\left\{2E_r(R), E_r(R) + \frac{\log_2(e)}{2} - \frac{\log_2(e)(1+2\Gamma)^2}{1+(1+2\Gamma)^4} - \frac{2}{n}\right\}} \tag{3.20}
 \end{aligned}$$

where we use $P_{ML} = \exp\{-nE_r(R)\}$ as the standard ML error probability at each RS. From the definition (3.1), as $n \rightarrow \infty$, the corresponding EE is given by

$$\begin{aligned}
 E_{DF}(R) &= \min\left\{2E_r(R), E_r(R) + \frac{\log_2(e)}{2} - \frac{\log_2(e)(1+2\Gamma)^2}{1+(1+2\Gamma)^4}\right\} \\
 &= \begin{cases} 2E_r(R) & , \text{if } E_r(R) < T(\Gamma) \\ E_r(R) + \frac{\log_2(e)}{2} - \frac{\log_2(e)(1+2\Gamma)^2}{1+(1+2\Gamma)^4} & , \text{if } E_r(R) \geq T(\Gamma) \end{cases} \tag{3.21}
 \end{aligned}$$

where $T(\Gamma) = \frac{\log_2(e)}{2} - \frac{\log_2(e)(1+2\Gamma)^2}{1+(1+2\Gamma)^4}$.

Remark 21. From (3.21) it can be seen that the proposed DF relaying strategy, where multiple RSs (here two) participate in communications between the source and destination, always provides diversity gains (against noise) at all SNR ranges.

BQRB relaying with Gaussian Signaling

Here we consider the BQRB relaying with the source transmit signal and relay mappings being taken as Gaussian. After phase compensation at each of the RSs, the quantizer outputs, in vector form, are given by

$$\mathbf{v} = \tilde{\mathbf{y}}_R + \mathbf{z}_q = \begin{bmatrix} h_{11} \\ h_{21} \end{bmatrix} x_1 + \tilde{\mathbf{z}} + \mathbf{z}_q = \mathbf{h}_1 x_1 + \tilde{\mathbf{z}} + \mathbf{z}_q$$

where $\tilde{\mathbf{z}}, \mathbf{z}_q \in \mathbb{C}^{2 \times 1}$ and $\tilde{z}_k \sim \mathcal{CN}(0, \sigma^2)$ and $z_{q,k} \sim \mathcal{CN}(0, D_k)$ for $k = 1, 2$. Define the 2×2 matrix $\mathbf{W} = \text{diag}\{\sigma^2 + D_1, \sigma^2 + D_2\}$. Then, $E_0(\rho, P_s)$ becomes

$$\begin{aligned} E_0(\rho, P_s) &= \rho \log_2 \left| \mathbf{I} + \frac{P_s}{1 + \rho} \mathbf{W}^{-1} \mathbf{h}_1 \mathbf{h}_1^H \right| = \rho \log_2 \left(1 + \frac{P_s}{1 + \rho} \mathbf{h}_1^H \mathbf{W}^{-1} \mathbf{h}_1 \right) \\ &= \rho \log_2 \left(1 + \frac{P_s}{1 + \rho} \left[\frac{h_{11}^2}{\sigma^2 + D_1} + \frac{h_{21}^2}{\sigma^2 + D_2} \right] \right). \end{aligned} \quad (3.22)$$

As in the process of achievable rate calculation, we have the compression rate constraints as follows:

$$\begin{aligned} \log_2 \left(\frac{\sigma_{v_1}^2}{D_1} (1 - \zeta^2) \right) &\leq C_1 \\ \log_2 \left(\frac{\sigma_{v_2}^2}{D_2} (1 - \zeta^2) \right) &\leq C_2 \\ \log_2 \left(\frac{\sigma_{v_1}^2}{D_1} \frac{\sigma_{v_2}^2}{D_2} (1 - \zeta^2) \right) &\leq C_1 + C_2 \end{aligned} \quad (3.23)$$

where $\sigma_{v_k}^2 = h_{k1}^2 P_s + \sigma^2 + D_k$, $k = 1, 2$, and $\zeta \in [-1, 1]$ is the correlation factor between v_1 and v_2 .

Then, the random coding error exponent corresponding to the CF is given by

$$E_{r,CF}(R_1) = \max_{0 \leq \rho \leq 1} [E_0(\rho, P_s) - \rho R_1] \quad (3.24)$$

subject to the rate constraints specified above. We note that $E_{r,CF}(R_1)$ is a decreasing function of both D_1 and D_2 , hence the minimum possible distortion values will result in optimum EE.

QF relaying with Non-Gaussian Signaling

In this section, we want to examine the EE for the PRNs where the source transmits (n, R_1) block-code where each letter of each codeword is independently

selected with probability assignment $p(x_1)$ and M-QAM constellation is used where 2^{nR_1} messages (alphabet size) are encoded over a block of n symbols. The received signals at the RSs are simply quantized by using uSQ, where correlation information is discarded. We assume that each symbol $x_1 = (x_1^R, x_1^I) = x_1^R + jx_1^I$ on the M-QAM constellation has equal probability $p(x_1) = 1/M$, and $p(x_1^R) = 1/\sqrt{M}$, $p(x_1^I) = 1/\sqrt{M}$.

The channel output at each RS, after phase compensation, can be expressed as in (3.9). The input-output model can be decomposed into real and imaginary parts as follows, as done in (2.45),

$$\underline{\tilde{y}}_{R_k} = \begin{bmatrix} \tilde{y}_{R_k}^R \\ \tilde{y}_{R_k}^I \end{bmatrix} = \begin{bmatrix} \text{Re}\{\tilde{y}_{R_k}\} \\ \text{Im}\{\tilde{y}_{R_k}\} \end{bmatrix} = \begin{bmatrix} h_k x_1^R + \tilde{z}_k^R \\ h_k x_1^I + \tilde{z}_k^I \end{bmatrix}, \quad k = 1, 2, \quad (3.25)$$

where $x_1^R = \text{Re}\{x_1\}$ and $x_1^I = \text{Im}\{x_1\}$ are the real and imaginary parts of the signal transmitted from the source, respectively, and $\mathbb{E}[(X_1^R)^2] = \mathbb{E}[(X_1^I)^2] = \frac{P_s}{2}$ (note that $\mathbb{E}[X_1^R X_1^I] = 0$). Noise components have zero mean and covariance matrix $\mathbb{E}[(\tilde{Z}_k^R)^2] = \mathbb{E}[(\tilde{Z}_k^I)^2] = \frac{\sigma^2}{2}$. We also note that the cross-correlation between $\tilde{Y}_{R_k}^R$ and $\tilde{Y}_{R_k}^I$ is zero, i.e., $\mathbb{E}[\tilde{Y}_{R_k}^R \tilde{Y}_{R_k}^I] = 0$.

The quantization process at each RS follows the same steps as in Section-2.4.3. Then, for a given source input signal x_1 , the probability that the quantizer output is in the $\underline{l} = (l^R, l^I)$ -th quantizing interval, i.e., $\underline{V}_k = (V_k^R, V_k^I) = \underline{v}_{k,\underline{l}} = (v_{k,l^R}^R, v_{k,l^I}^I)$, $k = 1, 2$, is given by

$$\begin{aligned} \Pr[\underline{V}_k = \underline{v}_{k,\underline{l}} \mid x_1] &= \Pr[(V_k^R, V_k^I) = (v_{k,l^R}^R, v_{k,l^I}^I) \mid x_1] \\ &= \Pr[V_k^R = v_{k,l^R}^R \mid x_1^R] \Pr[V_k^I = v_{k,l^I}^I \mid x_1^I] \\ &= \Pr[\tilde{y}_{R_k}^R \in \mathcal{S}_{k,l^R}^R \mid x_1^R] \Pr[\tilde{y}_{R_k}^I \in \mathcal{S}_{k,l^I}^I \mid x_1^I] \\ &= \left(\int_{u_{k,l^R}^R}^{u_{k,l^R+1}^R} G_{\tilde{y}_{R_k}^R} \left(h_k x_1^R, \frac{\sigma^2}{2} \right) d\tilde{y}_{R_k}^R \right) \left(\int_{u_{k,l^I}^I}^{u_{k,l^I+1}^I} G_{\tilde{y}_{R_k}^I} \left(h_k x_1^I, \frac{\sigma^2}{2} \right) d\tilde{y}_{R_k}^I \right) \\ &= \left(\int_{u_{k,l^R}^R}^{u_{k,l^R+1}^R} \frac{1}{\sqrt{\pi\sigma^2}} e^{-\frac{(\tilde{y}_{R_k}^R - h_k x_1^R)^2}{\sigma^2}} d\tilde{y}_{R_k}^R \right) \left(\int_{u_{k,l^I}^I}^{u_{k,l^I+1}^I} \frac{1}{\sqrt{\pi\sigma^2}} e^{-\frac{(\tilde{y}_{R_k}^I - h_k x_1^I)^2}{\sigma^2}} d\tilde{y}_{R_k}^I \right) \\ &= \left[Q \left(\frac{u_{k,l^R}^R - h_k x_1^R}{\sigma/\sqrt{2}} \right) - Q \left(\frac{u_{k,l^R+1}^R - h_k x_1^R}{\sigma/\sqrt{2}} \right) \right] \times \\ &\quad \left[Q \left(\frac{u_{k,l^I}^I - h_k x_1^I}{\sigma/\sqrt{2}} \right) - Q \left(\frac{u_{k,l^I+1}^I - h_k x_1^I}{\sigma/\sqrt{2}} \right) \right] \quad (3.26) \end{aligned}$$

for $\underline{l} = [1, 2, \dots, L_k^R] \times [1, 2, \dots, L_k^I]$, $k = 1, 2$.

We note that for symmetric channel gains $h = h_1 = h_2$ and $\sqrt{L_k} = L_k^R = L_k^I = 2^{\frac{C_k}{2}}$, the quantization steps for both real and imaginary parts become symmetric, then the representation points and the transition levels become the same, i.e., $v_{k,l}^R = v_{k,l}^I = \hat{v}_{k,l}$ and $u_{k,l}^R = u_{k,l}^I = \hat{u}_{k,l}$ for $l = 1, \dots, L_k$. Then, for a given source input signal $x_1 = (x_1^R, x_1^I)$, the probability that the quantizer

output is in the $\underline{l} = (l^R, l^I)$ -th quantizing interval, given in (3.26) in general form, becomes

$$\Pr [V_k = \hat{v}_{k,\underline{l}} | x_1] = \Pr [V_k^R = \hat{v}_{k,l^R} | x_1^R] \Pr [V_k^I = \hat{v}_{k,l^I} | x_1^I] \quad (3.27)$$

where

$$\begin{aligned} \Pr [V_k^R = \hat{v}_{k,l^R} | x_1^R] &= Q\left(\frac{\hat{u}_{k,l^R} - hx_1^R}{\sigma/\sqrt{2}}\right) - Q\left(\frac{\hat{u}_{k,l^R+1} - hx_1^R}{\sigma/\sqrt{2}}\right) \\ &\leq \exp\left\{-\frac{(\hat{u}_{k,l^R} - hx_1^R)^2}{\sigma^2}\right\} - \exp\left\{-\frac{(\hat{u}_{k,l^R+1} - hx_1^R)^2}{\sigma^2}\right\} \end{aligned} \quad (3.28)$$

and

$$\begin{aligned} \Pr [V_k^I = \hat{v}_{k,l^I} | x_1^I] &= Q\left(\frac{\hat{u}_{k,l^I} - hx_1^I}{\sigma/\sqrt{2}}\right) - Q\left(\frac{\hat{u}_{k,l^I+1} - hx_1^I}{\sigma/\sqrt{2}}\right) \\ &\leq \exp\left\{-\frac{(\hat{u}_{k,l^I} - hx_1^I)^2}{\sigma^2}\right\} - \exp\left\{-\frac{(\hat{u}_{k,l^I+1} - hx_1^I)^2}{\sigma^2}\right\}. \end{aligned} \quad (3.29)$$

The destination performs ML decoding on the observations v_1, v_2 , which are the representation points corresponding to the received signals at each RS. Then, we have the following EE for the QF relaying with M-QAM at the source and uSQ at the RSs

$$E_{r,QF}(R_1) = \max_{0 \leq \rho \leq 1} [E_0(\rho, p(x) = 1/M) - \rho R_1], \quad (3.30)$$

where $E_0(\rho, p(x) = 1/M) = E_0(\rho)$ is defined as

$$\begin{aligned}
 E_0(\rho) &= -\ln \left[\sum_{v_1, v_2} \left[\sum_{x_1} \frac{1}{M} p(v_1, v_2 | x_1)^{\frac{1}{1+\rho}} \right]^{1+\rho} \right] \\
 &= -\ln \left[\sum_{v_1, v_2} \left[\sum_{x_1} \frac{1}{M} p(v_1 | x_1)^{\frac{1}{1+\rho}} p(v_2 | x_1)^{\frac{1}{1+\rho}} \right]^{1+\rho} \right] \\
 &= -\ln \left[\sum_{v_1^R, v_2^R} \sum_{v_1^I, v_2^I} \left[\sum_{x_1^R} \sum_{x_1^I} \frac{1}{M} [p(v_1^R | x_1^R) p(v_1^I | x_1^I) p(v_2^R | x_1^R) p(v_2^I | x_1^I)]^{\frac{1}{1+\rho}} \right]^{1+\rho} \right] \\
 &= -\ln \left[\sum_{v_1^R, v_2^R} \sum_{v_1^I, v_2^I} \left[\sum_{x_1^R} \frac{1}{\sqrt{M}} [p(v_1^R | x_1^R) p(v_2^R | x_1^R)]^{\frac{1}{1+\rho}} \right]^{1+\rho} \times \right. \\
 &\quad \left. \left[\sum_{x_1^I} \frac{1}{\sqrt{M}} [p(v_1^I | x_1^I) p(v_2^I | x_1^I)]^{\frac{1}{1+\rho}} \right]^{1+\rho} \right] \\
 &= -\ln \left[\sum_{v_1^R, v_2^R} \left[\sum_{x_1^R} \frac{1}{\sqrt{M}} [p(v_1^R | x_1^R) p(v_2^R | x_1^R)]^{\frac{1}{1+\rho}} \right]^{1+\rho} \right. \\
 &\quad \left. - \ln \left[\sum_{v_1^I, v_2^I} \left[\sum_{x_1^I} \frac{1}{\sqrt{M}} [p(v_1^I | x_1^I) p(v_2^I | x_1^I)]^{\frac{1}{1+\rho}} \right]^{1+\rho} \right] \right] \\
 &= E_0^*(\rho) + E_0^{**}(\rho) \\
 &= 2E_0^*(\rho)
 \end{aligned} \tag{3.31}$$

where $p(v_k^R | x_1^R)$ and $p(v_k^I | x_1^I)$, for $k = 1, 2$, are given in (3.28) and (3.29), respectively. With these settings (3.30) becomes

$$E_{r,QF}(R_1) = \max_{0 \leq \rho \leq 1} [2E_0^*(\rho) - \rho R_1]. \tag{3.32}$$

3.2.3 Error Exponent analysis for Two Sources Case

In this section, we analyze the error exponent performances of DF, CF and QF relaying strategies for two-source (i.e., $M = 2$), two-relay (i.e., $K = 2$) and a single destination AWGN PRN setup. In the following derivations, for simplicity, we assume symmetric channels from each source to the RSs and equal backhaul capacity from each RS to the destination.

For DF relaying, we assume that wireless medium is shared by the sources in an *orthogonal* fashion (i.e., orthogonal MAC). During the access time of each source, each RS performs the same steps as in single source PRN case wherein

Gaussian codebooks are used by each source. For the CF and QF relaying strategies, the same assumptions are done as in single source case. Here, we analyze the error exponents using joint ML decoding which was derived by Gallager in [71].

Definition 22. For a given MAC, let $P_{e,sys}(n, R_1, R_2)$ denote the smallest average probability of system error of any length- n block-code and rates R_1, R_2 for source 1 and source 2, respectively. Then, the random coding EE for a MAC is defined as

$$E_{sys}(R_1, R_2) \triangleq \lim_{n \rightarrow \infty} -\frac{\log_2 P_{e,sys}(n, R_1, R_2)}{n}. \quad (3.33)$$

In [71], Gallager derived an upper bound on the average probability of system error using joint ML decoding rule. Let (w_1, w_2) be the message pair sent from the sources and (\hat{w}_1, \hat{w}_2) be the decoded message pair. Consider an ensemble of $(n, 2^{nR_1}, 2^{nR_2})$ codes where each codeword is selected independently for a given joint input distribution $f(x_1, x_2) = f(x_1)f(x_2)$. Then, the probability of system error can be written as

$$\begin{aligned} P_{e,sys}(n, R_1, R_2) &= P(\hat{w}_1 \neq w_1 \cup \hat{w}_2 \neq w_2) \\ &= P(\hat{w}_1 \neq w_1 \cap \hat{w}_2 = w_2) + P(\hat{w}_1 = w_1 \cap \hat{w}_2 \neq w_2) \\ &\quad + P(\hat{w}_1 \neq w_1 \cap \hat{w}_2 \neq w_2) \\ &= P_1 + P_2 + P_3 \end{aligned} \quad (3.34)$$

where

$$\begin{aligned} P_1 &\triangleq P(\hat{w}_1 \neq w_1 \cap \hat{w}_2 = w_2) \\ P_2 &\triangleq P(\hat{w}_1 = w_1 \cap \hat{w}_2 \neq w_2) \\ P_3 &\triangleq P(\hat{w}_1 \neq w_1 \cap \hat{w}_2 \neq w_2). \end{aligned} \quad (3.35)$$

We have the following bounds on P_i , for $i = 1, 2, 3$ [71]

$$P_i \leq 2^{-n[-\rho R_i + E_{0i}(\rho, f(x_1, x_2))]} \quad (3.36)$$

for all $\rho, 0 \leq \rho \leq 1$, where $R_3 = R_1 + R_2$ and

$$\begin{aligned} E_{01}(\rho, f(x_1, x_2)) &= -\log_2 \left[\int_{-\infty}^{\infty} \int_{-\infty}^{\infty} f(\mathbf{x}_2) \left(\int_{-\infty}^{\infty} f(\mathbf{x}_1) f(\mathbf{y}|\mathbf{x}_1, \mathbf{x}_2)^{\frac{1}{1+\rho}} d\mathbf{x}_1 \right)^{1+\rho} d\mathbf{x}_2 d\mathbf{y} \right] \\ E_{02}(\rho, f(x_1, x_2)) &= -\log_2 \left[\int_{-\infty}^{\infty} \int_{-\infty}^{\infty} f(\mathbf{x}_1) \left(\int_{-\infty}^{\infty} f(\mathbf{x}_2) f(\mathbf{y}|\mathbf{x}_1, \mathbf{x}_2)^{\frac{1}{1+\rho}} d\mathbf{x}_2 \right)^{1+\rho} d\mathbf{x}_1 d\mathbf{y} \right] \\ E_{03}(\rho, f(x_1, x_2)) &= -\log_2 \left[\int_{-\infty}^{\infty} \left(\int_{-\infty}^{\infty} \int_{-\infty}^{\infty} f(\mathbf{x}_1) f(\mathbf{x}_2) f(\mathbf{y}|\mathbf{x}_1, \mathbf{x}_2)^{\frac{1}{1+\rho}} d\mathbf{x}_1 d\mathbf{x}_2 \right)^{1+\rho} d\mathbf{y} \right] \end{aligned} \quad (3.37)$$

where $f(\mathbf{x}_1, \mathbf{x}_2) = \prod_{i=1}^n f(x_{1i})f(x_{2i})$ is the joint input distribution and $f(\mathbf{y}|\mathbf{x}_1, \mathbf{x}_2)$ is the channel output distribution conditioned on the inputs.

Then for an input distribution $f(x_1, x_2) = f(x_1)f(x_2)$ we can bound the probability of system error as follows

$$\begin{aligned} P_{e,sys}(n, R_1, R_2) &= P_1 + P_2 + P_3 \\ &\leq 2^{-n \left(E_r(R_1, R_2, f(x_1, x_2)) - \frac{\log_2(3)}{n} \right)} \end{aligned} \quad (3.38)$$

where

$$E_r(R_1, R_2, f(x_1, x_2)) = \min_{1 \leq i \leq 3} \max_{0 \leq \rho \leq 1} [E_{0i}(\rho, f(x_1, x_2)) - \rho R_i] \quad (3.39)$$

with $R_3 = R_1 + R_2$.

In general, the input-output relation for a MAC with two sources and a multiple-antenna destination can be expressed as

$$\mathbf{y} = \mathbf{H}_1 \mathbf{x}_1 + \mathbf{H}_2 \mathbf{x}_2 + \mathbf{z} \quad (3.40)$$

where $\mathbf{x}_i \in \mathbb{C}^{M \times 1}$, $\mathbf{y} \in \mathbb{C}^{N \times 1}$ and $\mathbf{H}_i \in \mathbb{C}^{N \times M}$, for $i = 1, 2$. Assume $\mathbf{x}_i \sim \mathcal{CN}(\mathbf{0}, P_i \mathbf{I}_M)$ and $\mathbf{z} \sim \mathcal{CN}(\mathbf{0}, \sigma^2 \mathbf{I}_N)$. Then,

$$\begin{aligned} E_{01}(\rho) &= \rho \log_2 \mathbb{E}_{\mathbf{H}} |\mathbf{I} + \frac{P_1}{(1+\rho)\sigma^2} \mathbf{H}_1 \mathbf{H}_1^H| \\ E_{02}(\rho) &= \rho \log_2 \mathbb{E}_{\mathbf{H}} |\mathbf{I} + \frac{P_2}{(1+\rho)\sigma^2} \mathbf{H}_2 \mathbf{H}_2^H| \\ E_{03}(\rho) &= \rho \log_2 \mathbb{E}_{\mathbf{H}} |\mathbf{I} + \frac{P_1}{(1+\rho)\sigma^2} \mathbf{H}_1 \mathbf{H}_1^H + \frac{P_2}{(1+\rho)\sigma^2} \mathbf{H}_2 \mathbf{H}_2^H|. \end{aligned} \quad (3.41)$$

DF relaying with Gaussian Inputs

For multi-source ($M = 2$) case, in order to simplify the relay processing we assume time-division (TD) MAC with $\alpha_1 n$ duration for source 1 and $\alpha_2 n$ duration for source 2, where $\alpha_1 + \alpha_2 = 1$. During the access of each source, both RSs perform the same steps as in the single source case. For TD-MAC, we define the following probability of system error

$$\begin{aligned} P_{e,DF}(n, R_1, R_2, \alpha_1, \alpha_2) &= P(\hat{w}_1 \neq w_1) + P(\hat{w}_2 \neq w_2) \\ &= P_{e,DF,1}(n, R_1, \alpha_1) + P_{e,DF,2}(n, R_2, \alpha_2) \\ &\leq 2^{-\alpha_1 n E_{DF,1}(R_1, \alpha_1)} + 2^{-\alpha_2 n E_{DF,2}(R_2, \alpha_2)} \\ &\leq 2^{-n \left(\min \{ \alpha_1 E_{DF,1}(R_1, \alpha_1), \alpha_2 E_{DF,2}(R_2, \alpha_2) \} - \frac{1}{n} \right)} \end{aligned} \quad (3.42)$$

and the corresponding EE

$$\begin{aligned} E_{DF}(R_1, R_2) &\triangleq \lim_{n \rightarrow \infty} \max_{\alpha_1 + \alpha_2 = 1} -\frac{\log_2 P_{e,DF}(n, R_1, R_2, \alpha_1, \alpha_2)}{n} \\ &= \max_{\alpha_1 + \alpha_2 = 1} \min \{ \alpha_1 E_{DF,1}(R_1, \alpha_1), \alpha_2 E_{DF,2}(R_2, \alpha_2) \} \end{aligned} \quad (3.43)$$

where $\alpha_1 + \alpha_2 = 1$, $E_{DF,i}(R_i, \alpha_i)$, $i = 1, 2$, will be specified. We assume that the w_i -th message, $w_i \in \{1, \dots, 2^{\alpha_i n R_i}\}$, is encoded into the codeword $\mathbf{x}_i(w_i)$ of length $\alpha_i n$, $i = 1, 2$.

The average power constraint, due to power control at the transmitting nodes, at the i -th source is P_s/α_i . With symmetric channel assumption from each source to the RSs and using (3.20), the probability of error for the i -th source can be expressed as follows

$$\begin{aligned}
 P_{e,DF,i}(n, R_i, \alpha_i) &\leq P_{ML,i}^2 + 2 P_{ML,i} 2^{-\alpha_i n T(\Gamma_i(\alpha_i))} \\
 &\leq 2^{-\alpha_i n (2 E_{r,i}(R_i, \alpha_i))} + 2^{-\alpha_i n \left(E_{r,i}(R_i, \alpha_i) + T(\Gamma_i(\alpha_i)) - \frac{1}{\alpha_i n} \right)} \\
 &\leq 2 \cdot 2^{-\alpha_i n \min \left\{ 2 E_{r,i}(R_i, \alpha_i), E_{r,i}(R_i, \alpha_i) + \frac{\log_2(e)}{2} - T(\Gamma_i(\alpha_i)) - \frac{1}{\alpha_i n} \right\}} \\
 &\leq 2^{-\alpha_i n \left(\min \left\{ 2 E_{r,i}(R_i, \alpha_i), E_{r,i}(R_i, \alpha_i) + T(\Gamma_i(\alpha_i)) - \frac{1}{\alpha_i n} \right\} - \frac{1}{\alpha_i n} \right)} \\
 &\leq 2^{-\alpha_i n \min \left\{ 2 E_{r,i}(R_i, \alpha_i) - \frac{1}{\alpha_i n}, E_{r,i}(R_i, \alpha_i) + T(\Gamma_i(\alpha_i)) - \frac{2}{\alpha_i n} \right\}} \quad (3.44)
 \end{aligned}$$

where

$$T(\Gamma_i(\alpha_i)) = \frac{\log_2(e)}{2} - \frac{\log_2(e)(1 + 2\Gamma_i(\alpha_i))^2}{1 + (1 + 2\Gamma_i(\alpha_i))^4}$$

with $\Gamma_i(\alpha_i) = \frac{h_i^2 P_s}{\alpha_i \sigma^2}$, and $P_{ML,i} = 2^{-\alpha_i n E_{r,i}(R_i, \alpha_i)}$ being the standard ML error probability at each RS. Hence, the corresponding EE, as $n'_i = \alpha_i n \rightarrow \infty$ for fixed $\alpha_i > 0$, becomes

$$E_{DF,i}(R_i, \alpha_i) = \min \{ 2 E_{r,i}(R_i, \alpha_i), E_{r,i}(R_i, \alpha_i) + T(\Gamma_i(\alpha_i)) \} \quad (3.45)$$

and the overall EE $E_{DF}(R_1, R_2)$ given in (3.43) can be calculated accordingly.

For *symmetric* channel conditions from each source to the RSs, i.e., $\alpha_1 = \alpha_2 = 1/2$ and $\Gamma_1(1/2) = \Gamma_2(1/2) = \Gamma$, and assuming both users communicate with the same rate $R_1 = R_2 = R$, then the EE becomes

$$\begin{aligned}
 E_{DF}(R_1 = R, R_2 = R) &= \frac{1}{2} \min \{ 2 E_r(R, 1/2), E_r(R, 1/2) + T(\Gamma) \} \\
 &= \begin{cases} E_r(R, 1/2) & \text{if } E_r(R, 1/2) < T(\Gamma), \\ \frac{E_r(R, 1/2)}{2} + \frac{T(\Gamma)}{2} & \text{if } E_r(R, 1/2) \geq T(\Gamma). \end{cases} \quad (3.46)
 \end{aligned}$$

CF relaying with Gaussian Signaling

For CF relaying, we assume all the sources access the wireless medium simultaneously, hence the system probability of error can be upper bounded as in MAC defined in (3.34) with modified channel matrices and noise assumptions.

The general input-output relation for the CF is given by

$$\begin{aligned} \mathbf{v} &= \mathbf{y}_R + \mathbf{z}_q \\ &= \begin{bmatrix} h_{11}e^{j\Phi_{11}} \\ h_{21}e^{j\Phi_{21}} \end{bmatrix} x_1 + \begin{bmatrix} h_{12}e^{j\Phi_{12}} \\ h_{22}e^{j\Phi_{22}} \end{bmatrix} x_2 + \mathbf{z} + \mathbf{z}_q \\ &= \tilde{\mathbf{h}}_1 x_1 + \tilde{\mathbf{h}}_2 x_2 + \mathbf{z} + \mathbf{z}_q \end{aligned}$$

where $z_k \sim \mathcal{CN}(0, \sigma^2)$ and $z_{q,k} \sim \mathcal{CN}(0, D_k)$ for $k = 1, 2$. Define $\mathbf{W} = \text{diag}\{\sigma^2 + D_1, \sigma^2 + D_2\}$.

Then, for an i.i.d. Gaussian input distribution with $x_i \sim \mathcal{CN}(0, P_i)$, we can bound the probability of system error $P_{e,sys}(n, R_1, R_2)$ given in (3.38) with the corresponding random coding EEs given by

$$E_{r,CF}(R_1, R_2) = \min_{1 \leq i \leq 3} \max_{0 \leq \rho \leq 1} [E_{0i}(\rho) - \rho R_i], \quad (3.47)$$

with $R_3 = R_1 + R_2$ and

$$\begin{aligned} E_{01}(\rho) &= \rho \log_2 \mathbb{E}_{\tilde{\mathbf{h}}_1} \left| \mathbf{I} + \frac{P_s}{(1+\rho)} \mathbf{W}^{-1} \tilde{\mathbf{h}}_1 \tilde{\mathbf{h}}_1^H \right| \\ &= \rho \log_2 \mathbb{E}_{\tilde{\mathbf{h}}_1} \left[1 + \frac{P_s}{(1+\rho)} \tilde{\mathbf{h}}_1^H \mathbf{W}^{-1} \tilde{\mathbf{h}}_1 \right] \\ &= \rho \log_2 \left(1 + \frac{P_s}{(1+\rho)} \left[\frac{h_{11}^2}{\sigma^2 + D_1} + \frac{h_{21}^2}{\sigma^2 + D_2} \right] \right), \\ E_{02}(\rho) &= \rho \log_2 \mathbb{E}_{\tilde{\mathbf{h}}_2} \left| \mathbf{I} + \frac{P_s}{(1+\rho)} \mathbf{W}^{-1} \tilde{\mathbf{h}}_2 \tilde{\mathbf{h}}_2^H \right| \\ &= \rho \log_2 \mathbb{E}_{\tilde{\mathbf{h}}_2} \left[1 + \frac{P_s}{(1+\rho)} \tilde{\mathbf{h}}_2^H \mathbf{W}^{-1} \tilde{\mathbf{h}}_2 \right] \\ &= \rho \log_2 \left(1 + \frac{P_s}{(1+\rho)} \left[\frac{h_{12}^2}{\sigma^2 + D_1} + \frac{h_{22}^2}{\sigma^2 + D_2} \right] \right), \\ E_{03}(\rho) &= \rho \log_2 \mathbb{E}_{\tilde{\mathbf{h}}_1, \tilde{\mathbf{h}}_2} \left| \mathbf{I} + \frac{P_s}{(1+\rho)} \mathbf{W}^{-1} \tilde{\mathbf{h}}_1 \tilde{\mathbf{h}}_1^H + \frac{P_s}{(1+\rho)} \mathbf{W}^{-1} \tilde{\mathbf{h}}_2 \tilde{\mathbf{h}}_2^H \right| \\ &\stackrel{(a)}{=} \rho \log_2 \left(1 + \frac{P_s}{(1+\rho)} \left[\frac{h_{11}^2}{\sigma^2 + D_1} + \frac{h_{21}^2}{\sigma^2 + D_2} \right] \right. \\ &\quad \left. + \frac{P_s}{(1+\rho)} \left[\frac{h_{12}^2}{\sigma^2 + D_1} + \frac{h_{22}^2}{\sigma^2 + D_2} \right] \right. \\ &\quad \left. + \frac{P_s^2}{(1+\rho)^2} \left[\frac{h_{11}^2 h_{22}^2 + h_{12}^2 h_{21}^2}{(\sigma^2 + D_1)(\sigma^2 + D_2)} \right] \right) \end{aligned} \quad (3.48)$$

where (a) follows from i.i.d. uniform (ergodic) phase fading assumption. As in the process of achievable rate calculation, we have the compression rate constraints given in (3.23).

QF relaying with Non-Gaussian Signaling

Again, assuming all the sources access the wireless medium simultaneously and having in mind the conditional probabilities given by (2.47), we will bound

the system probability of error defined in (3.34) with modified channel matrices and noise assumptions. The i -th source transmits $(n, R_i), i = 1, 2$, block code where each letter of each codeword is independently selected with probability assignment $p(x_i)$ and M-QAM constellation is used where 2^{nR_i} messages (alphabet size) are encoded over blocks of length n . The received signals at the RSs are simply quantized by using uSQ, where correlation information is discarded (no compression is done). We assume that each symbol $x_i = (x_i^R, x_i^I) = x_i^R + jx_i^I$ on the M-QAM constellation has equal probability $p(x_i) = 1/M$, and $p(x_i^R) = 1/\sqrt{M}, p(x_i^I) = 1/\sqrt{M}$.

The channel output at each RS has been expressed in (2.45) each decomposed into real and imaginary parts. The quantization process at each RS follows the same steps as in Section-2.4.3. Then, for a given source input signal vector $\mathbf{x} = (x_1, x_2)$, the probability that the quantizer output is in the $\underline{l} = (l^R, l^I)$ -th quantizing interval, i.e., $\underline{V}_k = (V_k^R, V_k^I) = \underline{v}_{k,\underline{l}} = (v_{k,l^R}^R, v_{k,l^I}^I), k = 1, 2$, is given by (2.47).

The destination performs ML decoding on the observations v_1, v_2 , which are the representation points corresponding to the received signals at each RS. Then, we have the following EE for the QF relaying with uniform M-QAM at the sources and uSQ at the RSs

$$E_{r,QF}(R_1, R_2) = \min_{1 \leq i \leq 3} \max_{0 \leq \rho \leq 1} [E_{0i}(\rho) - \rho R_i] \quad (3.49)$$

with $R_3 = R_1 + R_2$ where $E_{0i}(\rho)$, for all $i = 1, 2, 3$ is defined as

$$\begin{aligned} E_{01}(\rho) &= -\log_2 \left[\sum_{v_1, v_2} \sum_{x_2} \frac{1}{M} \left[\sum_{x_1} \frac{1}{M} p(v_1, v_2 | x_1, x_2)^{\frac{1}{1+\rho}} \right]^{1+\rho} \right] \\ &= -\log_2 \left[\sum_{v_1, v_2} \sum_{x_2} \frac{1}{M} \left[\sum_{x_1} \frac{1}{M} p(v_1 | x_1, x_2)^{\frac{1}{1+\rho}} p(v_2 | x_1, x_2)^{\frac{1}{1+\rho}} \right]^{1+\rho} \right] \\ &= -\log_2 \left[\sum_{v_1^R, v_2^R} \sum_{v_1^I, v_2^I} \sum_{x_2} \frac{1}{M} \right. \\ &\quad \left. \left[\sum_{x_1} \frac{1}{M} \left[p(v_1^R | x_1, x_2) p(v_2^R | x_1, x_2) p(v_1^I | x_1, x_2) p(v_2^I | x_1, x_2) \right]^{\frac{1}{1+\rho}} \right]^{1+\rho} \right] \quad (3.50) \end{aligned}$$

and similarly

$$\begin{aligned}
E_{02}(\rho) &= -\log_2 \left[\sum_{v_1, v_2} \sum_{x_1} \frac{1}{M} \left[\sum_{x_2} \frac{1}{M} p(v_1, v_2 | x_1, x_2)^{\frac{1}{1+\rho}} \right]^{1+\rho} \right] \\
&= -\log_2 \left[\sum_{v_1, v_2} \sum_{x_1} \frac{1}{M} \left[\sum_{x_2} \frac{1}{M} p(v_1 | x_1, x_2)^{\frac{1}{1+\rho}} p(v_2 | x_1, x_2)^{\frac{1}{1+\rho}} \right]^{1+\rho} \right] \\
&= -\log_2 \left[\sum_{v_1^R, v_2^R} \sum_{v_1^I, v_2^I} \sum_{x_1} \frac{1}{M} \right. \\
&\quad \left. \left[\sum_{x_2} \frac{1}{M} \left[p(v_1^R | x_1, x_2) p(v_2^R | x_1, x_2) p(v_1^I | x_1, x_2) p(v_2^I | x_1, x_2) \right]^{\frac{1}{1+\rho}} \right]^{1+\rho} \right] \quad (3.51)
\end{aligned}$$

and

$$\begin{aligned}
E_{03}(\rho) &= -\log_2 \left[\sum_{v_1, v_2} \left[\sum_{x_1} \sum_{x_2} \frac{1}{M^2} p(v_1, v_2 | x_1, x_2)^{\frac{1}{1+\rho}} \right]^{1+\rho} \right] \\
&= -\log_2 \left[\sum_{v_1, v_2} \left[\sum_{x_1} \sum_{x_2} \frac{1}{M^2} p(v_1 | x_1, x_2)^{\frac{1}{1+\rho}} p(v_2 | x_1, x_2)^{\frac{1}{1+\rho}} \right]^{1+\rho} \right] \\
&= -\log_2 \left[\sum_{v_1^R, v_2^R} \sum_{v_1^I, v_2^I} \right. \\
&\quad \left. \left[\sum_{x_1} \sum_{x_2} \frac{1}{M^2} \left[p(v_1^R | x_1, x_2) p(v_2^R | x_1, x_2) p(v_1^I | x_1, x_2) p(v_2^I | x_1, x_2) \right]^{\frac{1}{1+\rho}} \right]^{1+\rho} \right] \quad (3.52)
\end{aligned}$$

where $p(v_k^R | x_1, x_2)$ and $p(v_k^I | x_1, x_2)$, for $k = 1, 2$, are given by (2.47). With these settings (3.49) can be calculated.

3.3 Numerical Results

For error exponent analysis we only consider the orthogonal MAC where each RS has limited capacity link to the destination.

3.3.1 Single Source Case

We compare the random coding EE performances of the relaying strategies studied above for the symmetric system model case where the channel gains from the source to RSs are the same, i.e., $h = h_1 = h_2 = 1$, and the link capacities from the RSs to the destination are the same, $C = C_1 = C_2$.

In Figure 3.2 and Figure 3.3, we plot the EEs given by (3.21), (3.24) and (3.32) corresponding to DF, CF and QF (with 4-QAM at the source and uSQ at the RSs) relaying strategies with respect to transmission rate R [bits/transmission]

for fixed $\Gamma = \frac{P_s h^2}{\sigma^2} = \{0, 10\}$ [dB]. In Figure 3.2, which corresponds to a low SNR regime, we see that at rates above 0.2 [bits/transmission] the proposed simple and practical QF relaying has better EE than both DF and CF. However, when we operate at rates lower than 0.2 [bits/transmission], the EE for the proposed DF relaying strategy outperforms the others. This might be explained as follows: as the source codebook size (i.e., transmission rate) get smaller while the network can provide higher transmission rates, the minimum distance between two different codewords will be sufficient enough for the decoders at the RSs to make more reliable decision. Beside this as opposed to the DF relaying, for CF and QF relaying, there is quantization noise factor which worsens the decoding performance at the final destination. Due to these two reasons, the DF relaying outperforms the others as low rate operating regime.

In Figure 3.3, which corresponds to a high SNR regime, we see that at all rates our proposed QF relaying performs the worst, which can be explained as follows: since the backhaul rate is fixed whilst the SNR is increased, the proposed QF strategy cannot fully exploit the inherent structure of the modulation scheme used at the source, i.e. the selected alphabet size (transmission rate) does not match to the system conditions. Hence, one needs to be careful while selecting the transmission rate in order to harvest the best profit from the network. From this plot we can also see that the achieved EE with the proposed DF relaying is better than that of the CF relaying strategy at low to moderate rates.

3.3.2 Two Sources Case

We consider $T = 2$ source, $K = 2$ RS phase fading AWGN PRN with orthogonal relay-to-destination links with limited capacity $C = C_1 = C_2$. We take a sample channel matrix from sources to RSs as

$$\mathbf{H} = \frac{1}{\sqrt{2}} \begin{bmatrix} 1 & \exp\{-j\pi/3\} \\ \exp\{-j2\pi/3\} & 1 \end{bmatrix}. \quad (3.53)$$

In Figure 3.4 and Figure 3.5, we plot the EEs given by (3.46), (3.47) and (3.49) corresponding to DF, CF and QF (with 4-QAM at the source and uSQ at the RSs) relaying strategies with respect to sum-rate $R_{sum} = R_1 + R_2$ [bits/transmission] for fixed $\frac{P_s}{\sigma^2} = \{0, 10\}$ [dB] where $R_1 = R_2 = R_{sum}/2$. In Figure 3.4, which corresponds to a low SNR regime, we see that the proposed simple and practical QF relaying has better EE than both DF and CF over all operating sum-rates. However, from Figure 3.5, which corresponds to a high SNR regime, we see that at all rates the proposed QF relaying performs the worse than CF relaying scheme, which can be explained as in single source case. From this plot we can also see that the achieved EE with the proposed DF relaying is the worst.

3.4 Conclusions and Future Directions

In this chapter, we evaluated the random coding error exponents corresponding to DF, BQRB and QF relaying strategies for the single- and two-source PRN se-

tups, consisting of two relay nodes which are connected to the destination via an error-free finite capacity backhaul, in order to have thorough characterization of system performance. Moreover, through numerical analysis we illustrated that the EEs achieved by using QF relaying along with non-Gaussian signaling (i.e., finite constellation codebooks) at the source(s) and symbol-by-symbol uSQs at the relays is better than that achieved by DF and CF relaying strategies when the system is in the low SNR regime and the backhaul capacity is large enough. Using a finite constellation, such as M-QAM, at the source node(s) along with simple processing at the relay nodes, such as the proposed QF scheme, can provide better EEs compared to more complex schemes. This is due to the structure inherent in the considered modulation scheme, which Gaussian signaling lacks.

With the light shed on the potentials of practical relaying strategies, it would be interesting to analyze block error rates (BLER) performance of practical channel coding schemes, i.e., the standard LTE transmitter blocks consisting of turbo encoder, interleaver and M-QAM might be used, for the relaying strategies studied above. In this chapter, for DF relaying case we assume that each RS passes the reliability information to the destination in a cost-free manner. However, in practical case each RS would perform a cyclic redundancy check (CRC) operation right after the decoding step and depending on the result it might use the backhaul to send the decoded bits to the destination (or send an automatic repeat request (ARQ) to the source(s)). Opposed to the BQRB and QF relaying strategies the backhaul resources are not exploit by the RSs *constantly* in DF relaying case. Hence, it might be interesting to examine the relation between relaying strategies and the corresponding backhaul utilization.

Another interesting future work might be the case where system engineer wishes to keep the RSs as simple as possible and leave the decoding step to the destination. In this case, the RSs might generate log-likelihood ratios (LLRs) and send quantized versions to the destination which combines all *soft* information and perform final decoding. The question would be if using quantization on received signal (BQRB relaying) or on soft information (partial DF relaying) will give the the better performance.

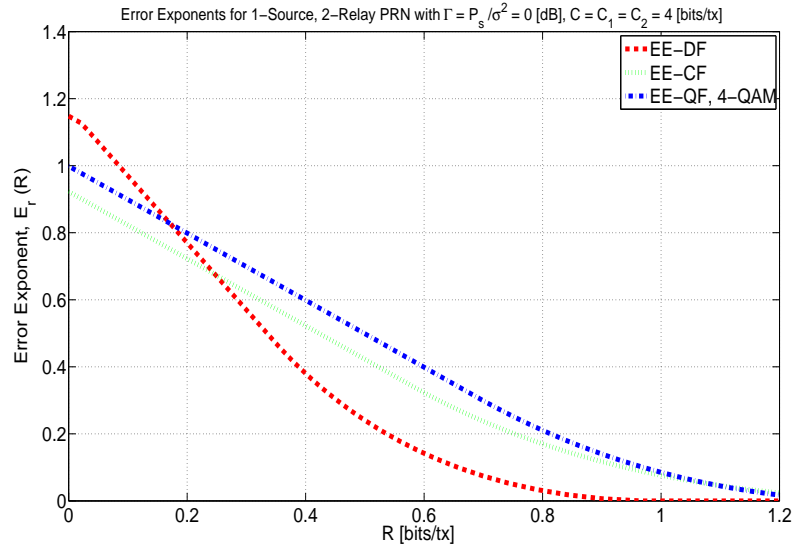


Figure 3.2: Random coding EEs for 1-Source, 2-Relay PRN with $\Gamma = \frac{P_s h^2}{\sigma^2} = 0$ [dB] and $C = C_1 = C_2 = 4$ [bits/transmission].

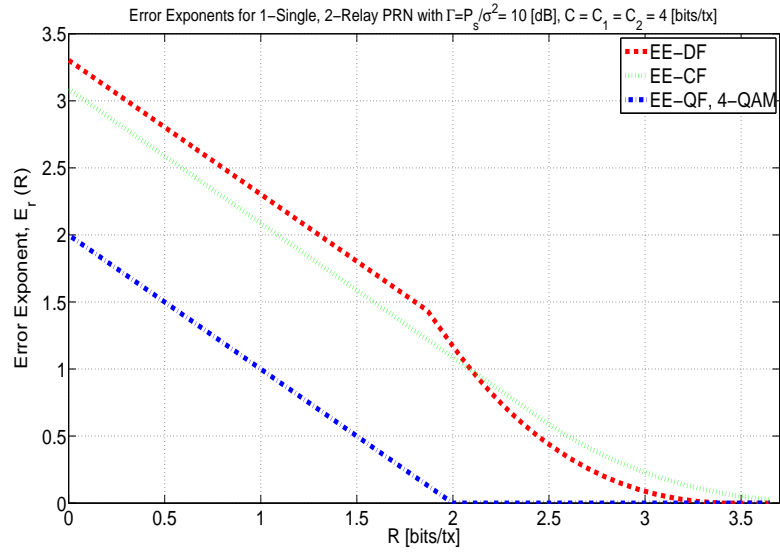


Figure 3.3: Random coding EEs for 1-Source, 2-Relay PRN with $\Gamma = \frac{P_s h^2}{\sigma^2} = 10$ [dB] and $C = C_1 = C_2 = 4$ [bits/transmission].

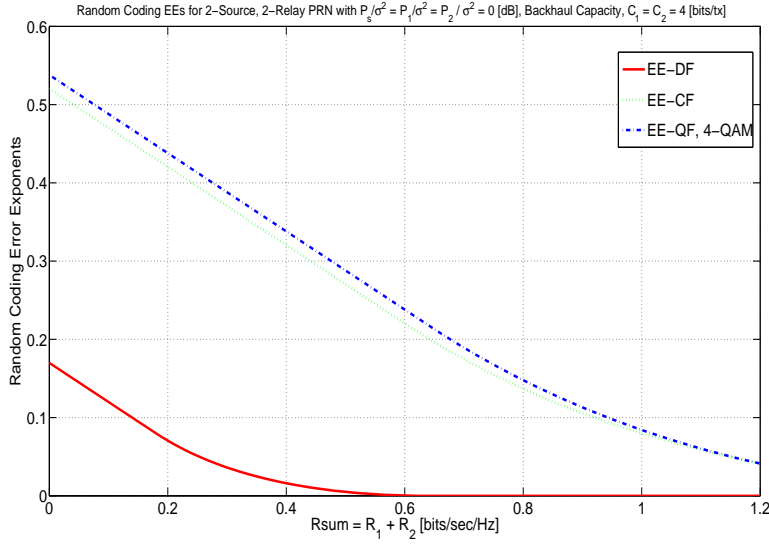


Figure 3.4: Random coding EEs for 2-Source, 2-Relay PRN with $\frac{P_s}{\sigma^2} = \frac{P_1}{\sigma^2} = \frac{P_2}{\sigma^2} = 0$ [dB] and $C = C_1 = C_2 = 4$ [bits/transmission].

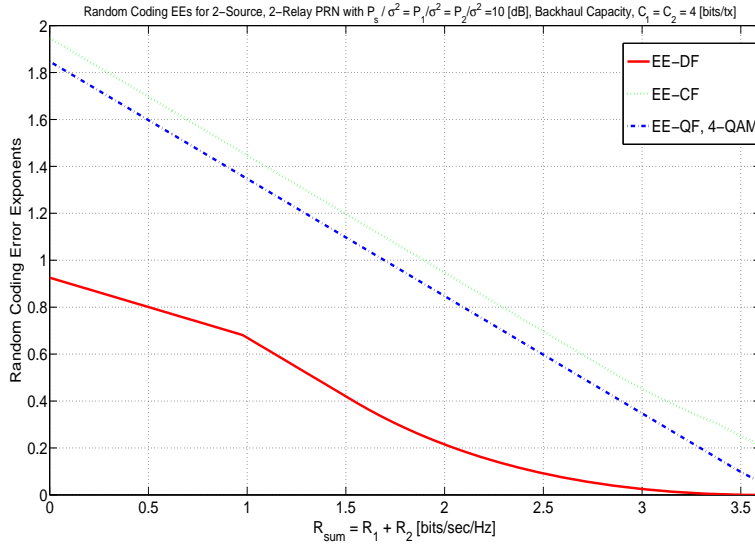


Figure 3.5: Random coding EEs for 2-Source, 2-Relay PRN with $\frac{P_s}{\sigma^2} = \frac{P_1}{\sigma^2} = \frac{P_2}{\sigma^2} = 10$ [dB] and $C = C_1 = C_2 = 4$ [bits/transmission].

3.A The pdf of difference of exponentially distributed Random variables

Let F and Y be two independent exponentially distributed RVs with respective means $\mathbb{E}[F] = \lambda_f$ and $\mathbb{E}[Y] = \lambda_y$. Now define a new RV Z as follows

$$Z = F - Y.$$

We want to find the pdf of Z . The cdf of Z is calculated as follows:

$$\begin{aligned}
 F_Z(z) &= P(Z \leq z) = P(F - Y \leq z) \\
 &= \begin{cases} \int_0^\infty \int_0^{z+y} f(f)f(y)dfdy & , z \geq 0 \\ \int_{-z}^\infty \int_0^{z+y} f(f)f(y)dfdy & , z < 0 \end{cases} \\
 &= \begin{cases} \int_0^\infty \lambda_y e^{-\lambda_y y} \int_0^{z+y} \lambda_f e^{-\lambda_f f} df dy & , z \geq 0 \\ \int_{-z}^\infty \lambda_y e^{-\lambda_y y} \int_0^{z+y} \lambda_f e^{-\lambda_f f} df dy & , z < 0 \end{cases} \\
 &= \begin{cases} \int_0^\infty \lambda_y e^{-\lambda_y y} (1 - e^{-\lambda_f (z+y)}) dy & , z \geq 0 \\ \int_{-z}^\infty \lambda_y e^{-\lambda_y y} (1 - e^{-\lambda_f (z+y)}) dy & , z < 0 \end{cases} \\
 &= \begin{cases} 1 - \frac{\lambda_y}{\lambda_y + \lambda_f} e^{-\lambda_f z} & , z \geq 0 \\ \frac{\lambda_f}{\lambda_y + \lambda_f} e^{\lambda_y z} & , z < 0 \end{cases} . \tag{3.54}
 \end{aligned}$$

Then the pdf of Z is given by:

$$f_Z(z) = \frac{\partial F_Z(z)}{\partial z} = \begin{cases} \frac{\lambda_f \lambda_y}{\lambda_f + \lambda_y} e^{-\lambda_f z} & , z \geq 0 \\ \frac{\lambda_f \lambda_y}{\lambda_f + \lambda_y} e^{\lambda_y z} & , z < 0 \end{cases} \tag{3.55}$$

Then, the mean and variance of Z are given by

$$\begin{aligned}
 \mu_Z &= \mathbb{E}[Z] = \int_{-\infty}^{\infty} z f(z) dz \\
 &= \int_{-\infty}^0 \frac{\lambda_f \lambda_y}{\lambda_f + \lambda_y} z e^{\lambda_y z} dz + \int_0^{\infty} \frac{\lambda_f \lambda_y}{\lambda_f + \lambda_y} z e^{-\lambda_f z} dz \\
 &= \frac{\lambda_y}{\lambda_f(\lambda_f + \lambda_y)} - \frac{\lambda_f}{\lambda_y(\lambda_f + \lambda_y)} = \frac{1}{\lambda_f} - \frac{1}{\lambda_y} \\
 \sigma_Z^2 &= \text{VAR}[Z] = \mathbb{E}[(Z - \mu_Z)^2] = \left(\frac{\lambda_y}{\lambda_f(\lambda_f + \lambda_y)} \right)^2 + \left(\frac{\lambda_f}{\lambda_y(\lambda_f + \lambda_y)} \right)^2 \\
 &= \frac{1}{(\lambda_f + \lambda_y)^2} \left[\frac{\lambda_y^2}{\lambda_f^2} + \frac{\lambda_f^2}{\lambda_y^2} \right]. \tag{3.56}
 \end{aligned}$$

3.B The exact expression and an upper bound on the $\Pr\{\beta_2 > \beta_1\}$

The exact expression for the *reliability* function:

$$\begin{aligned}
 \Pr\{\beta_2 > \beta_1\} &= \Pr\{Y > F\} = 1 - \Pr\{Y \leq F\} \\
 &= 1 - \int_0^{\infty} f(f) \left[\int_0^f f(y) dy \right] df \\
 &= 1 - \int_0^{\infty} f(f) F_Y(f) df \\
 &= 1 - \int_0^{\infty} \frac{\lambda_f (\lambda_f f)^{n-1}}{(n-1)!} e^{-\lambda_f f} \left[1 - \sum_{k=0}^{n-1} \frac{(\lambda_y f)^k e^{-\lambda_y f}}{k!} \right] df \\
 &= \sum_{k=0}^{n-1} \int_0^{\infty} \frac{\lambda_f^n \lambda_y^k f^{n+k-1}}{(n-1)! k!} e^{-(\lambda_f + \lambda_y) f} df \\
 &= \sum_{k=0}^{n-1} \frac{\lambda_f^n \lambda_y^k (n+k-1)!}{(\lambda_f + \lambda_y)^{n+k} (n-1)! k!} \int_0^{\infty} \frac{(\lambda_f + \lambda_y)^{n+k} f^{n+k-1}}{(n+k-1)!} e^{-(\lambda_f + \lambda_y) f} df \\
 &= \frac{\lambda_f^n}{(\lambda_f + \lambda_y)^n (n-1)!} \sum_{k=0}^{n-1} \frac{\lambda_y^k (n+k-1)!}{(\lambda_f + \lambda_y)^k k!} \\
 &= \left(\frac{\lambda_y}{\lambda_f + \lambda_y} \right)^n \sum_{k=0}^{n-1} \left(\frac{\lambda_f}{\lambda_f + \lambda_y} \right)^k \binom{n+k-1}{k}. \tag{3.57}
 \end{aligned}$$

Hence the exact expression for the probability of error in (3.13) is given by:

$$\begin{aligned}
 P_e &\leq P_{ML,1}P_{ML,2} + P_{ML,1}(1 - P_{ML,2}) \Pr\{\beta_2 > \beta_1\} \\
 &\quad + P_{ML,2}(1 - P_{ML,1}) \Pr\{\beta_1 > \beta_2\} \\
 &= P_{ML,1}P_{ML,2} + P_{ML,1}(1 - P_{ML,2}) \Pr\{\beta_2 > \beta_1\} \\
 &\quad + P_{ML,2}(1 - P_{ML,1})(1 - \Pr\{\beta_2 > \beta_1\}) \\
 &= P_{ML,1} \Pr\{\beta_2 > \beta_1\} + P_{ML,2}(1 - \Pr\{\beta_2 > \beta_1\}). \tag{3.58}
 \end{aligned}$$

Next, we evaluate an upper bound on the the *reliability* function $\Pr\{\beta_2 > \beta_1\}$. We will give an upper bound on the tail probability of a random variable consisting of n independent identically distributed RVs with the same mean μ_Z and variance σ_Z^2 . As $n \rightarrow \infty$ we can apply the central limit theorem and get upper bound on the tail probability. Define $Z = \sum_{i=1}^n Z_i$ where each of Z_i has mean μ_Z and variance σ_Z^2 . Then, from the central limit theorem for $Z = \sum_{i=1}^n Z_i = \sum_{i=1}^n F_i - Y_i$ we have

$$\begin{aligned}
 \lim_{n \rightarrow \infty} \Pr \left(\sum_{i=1}^n Z_i \leq \epsilon \right) &= \lim_{n \rightarrow \infty} \Pr \left(\frac{\sum_{i=1}^n Z_i - n\mu_Z}{\sqrt{n\sigma_Z^2}} \leq \frac{\epsilon - n\mu_Z}{\sqrt{n\sigma_Z^2}} \right) \\
 &\leq Q \left(\frac{n\mu_Z - \epsilon}{\sqrt{n\sigma_Z^2}} \right) \leq e^{-\frac{(n\mu_Z - \epsilon)^2}{2n\sigma_Z^2}}. \tag{3.59}
 \end{aligned}$$

Hence, we have the following bound on $\Pr(Z \leq 0)$ (i.e., $\epsilon = 0$), for sufficiently large n :

$$\begin{aligned}
 \Pr(Z \leq 0) &\leq e^{-n \frac{\mu_Z^2}{2\sigma_Z^2}} \\
 &= e^{-n \left(\frac{1}{2} - \frac{\lambda_f^2 \lambda_y^2}{\lambda_f^4 + \lambda_y^4} \right)}. \tag{3.60}
 \end{aligned}$$

We note that $\Pr(Z \leq 0) \rightarrow 0$ exponentially with increasing n .

Chapter 4

Relay Deployment in Cellular Uplink Communications

4.1 Introduction

With the next generation wireless systems, end-users will be able to use various applications, ranging from multi-media messaging and video conferencing to the Internet access, which however requires a smarter and more complex system architecture than the conventional cellular systems. In particular, in next generation cellular systems better link quality, coverage and higher network throughput are predicted by using recently emerged technologies such as OFDM and MIMO. Lately, multi-hopping (or relaying) in cellular networks has been considered as a promising solution since it improves the overall system performance by providing coverage extension, power saving which is crucial especially in UL communications, and spatial-reuse [2–4, 12, 15, 17, 18].

In addition to relaying, there have been some other proposals for next generation wireless networks to increase system capacity and coverage fairness such as distributed antenna systems (DASs), cell-splitting and multi-cell coordination. The impact of limited-capacity backhaul on both multi-cell processing and mobile station (MS) cooperation for the UL and DL under non-fading Gaussian scenario assumptions have been studied in [56, 57, 72, 73].

4.1.1 Motivation

Even though the above proposals (i.e., ideal DAS and cell-splitting) provide huge system performance gains, relay station (RS) deployment in cellular networks is preferable due to the affordable, and relatively less, cost requirement since there is no need for infrastructure links and flexible site acquisition. As stated above, with relay-assisted infrastructure based cellular networks it is possible to reduce deployment cost and required transmission power at mobile terminals, enhance network capacity, extend radio range, mitigate shadowing effect and have spatial-reuse [2–7, 74].

Due to high link budget requirements in the next generation cellular systems, power constraints at the MSs will be a bottleneck for UL communications especially for the MSs close to the cell boundary. Moreover, had the MSs have higher power levels, then the system would be in interference limited regime and the MSs at the cell-edges would still suffer. Also, the processing capability and size constraint at the MSs prevent them from performing fancy MIMO precoding (or beamforming) techniques [75, 76].

Relay deployment is one of the feasible and efficient solutions to the problems stated above. Hence, in this chapter we concentrate on UL communications for relay-aided cellular systems and assess the effects of relay deployment regarding various parameters such as number of deployed relays in each cell, their locations and powers they use.

4.1.2 Prior Work

In [33], the capacity benefits of in-band backhaul relaying for UL cellular network is considered wherein a Decode-and-forward (DF) relaying scheme is proposed to exploit *full spatial-reuse* in the system, which increases with the number of RSs operating in half-duplex (HD) mode. In [34], different communication modes have been proposed for RS deployed cellular systems in order to increase spatial reuse, and consequently spectral efficiency. In [35], the power savings achieved by HD low power RSs in cellular system is studied for DL communications and it has been observed that *interference* is a big obstacle for power saving. Hence, in interference limited regime, one should be more careful in deploying RSs in cellular systems which brings extra power (or say interference to the other user) into the system. Coordinated transmission should be a promising solution in order to tackle the interference effect in RS deployed cellular systems.

4.1.3 Contributions

In this chapter, we consider a cellular network assisted by fixed RSs, which are used by MSs to access the base station (BS) via a relaying strategy, namely Amplify-and-forward (AF), DF, Compress-and-forward (CF) and Quantize-and-forward (QF). We analyze the achievable sum-of-rates for UL communications. We compare the relaying strategies with two well-known cellular systems where in the first case the BS antennas are assumed to be co-located (conventional

cellular systems) and in the second case they are assumed to be distributed in the cell and be connected to the BS via very high capacity wired links, i.e., ideal DAS. It is assumed that the MS and RS signals are emitted on *orthogonal* frequency bands, with the possibility of having a larger bandwidth (BW) on the RS-to-BS links.

The contributions of this chapter are:

- Generalized orthogonal relay channel (GORC) model is introduced. Outer bounds and achievable rates for different relaying strategies are derived.
- We propose a theoretical analysis of the gains brought by fixed relays in a multi-cell scenario, where the key point is in exploiting the ability of the system designer to engineer near line-of-sight (LOS) links between the relays and the base at deployment time.
- We explicitly take into account the inter-cell interference impact on the relay performance and compare leading forms of relaying strategies, namely AF, DF and QF. Among these relaying strategies, it is observed that the QF outperforms the others.
- We assess the gains brought by fixed RSs when compared with the conventional cellular systems.
- With proper choice of system parameters such as bandwidth, power and relaying mechanism, we show that multi-hop relaying performs quite well compared to the ideal DAS.

4.1.4 Outline of the chapter

We first start with a general orthogonal relay channel (GORC) model and give information theoretic expressions for different relaying strategies in Section-4.2. The results derived in this section are used for the cellular relaying model, which are the main focus of this chapter, in Section-4.3. We continue with numerical results in Section-4.10 and conclude with Section-9.6.1.

4.2 The Generalized Orthogonal Relay Channel

In this chapter, we consider a cellular network consisting of frequency-division duplex (FDD) RSs¹ where the frequency band used by the MSs to communicate with the RSs and the BSs is orthogonal to the frequency band used by the RSs to access the BSs. This channel model is the multi-source and multi-relay generalization of the orthogonal relay channel model studied in [77, 78]. In [78], orthogonal time and frequency allocation to separate source-access (links to relay and destination) and relay-access (link to destination) links was studied in order to maximize the information rate. As in [78], for the GORC model,

¹Note that for the considered system model in chapter, assuming Time-Division Duplex (TDD) relaying also provides the same performance as FDD relaying.

the sources transmit to the RSs and the destination in one orthogonal channel (say in channel 1), and the RSs access to the destination in the other orthogonal channel (say in channel 2), with channel 1 and 2 being orthogonalized in the frequency domain.

In this section, we simply consider a single-cell GORC model defined above; hence, circumvent interference effect arising in cellular networks, and derive an outer bound for this channel model and give achievable rate expressions corresponding to different relaying strategies. Then, in the following sections we will use the obtained results for the multi-cell cellular networks, where inter- and intra-cell interference will be taken into account.

4.2.1 Model

Consider a GORC model where a set of sources $\mathcal{M} = \{1, 2, \dots, M\}$ simultaneously transmit information to the destination with the help of a set of RSs $\mathcal{K} = \{1, 2, \dots, K\}$. Assume the sources transmit to the RSs and the destination in one orthogonal channel (channel 1), and the RSs transmit to the destination in the other orthogonal channel (channel 2) and no connection between the RSs. This channel model is shown in Figure 4.1.

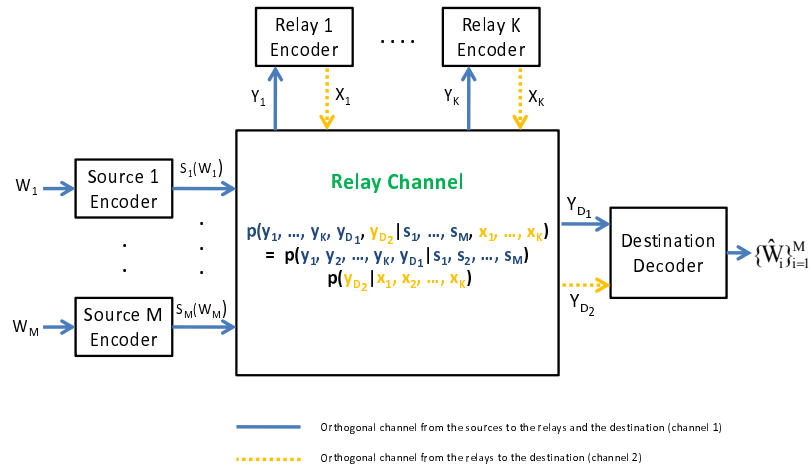


Figure 4.1: A d.m. GORC with M sources, K RSs where the channel from the sources to the RSs and destination (channel 1) is orthogonal to the channels from the RSs to the destination (channel 2).

In this section, we give an outer bound and some achievable rates for discrete memoryless (d.m.) GORCs with multiple sources and RSs. Then, in the fol-

lowing section, we will generalize the results derived for the d.m. relay channel model to the Gaussian case.

Now we define the d.m. GORC, consisting of multiple sources and RSs (where channel components from the sources to the RSs and destination and from the RSs to the destination are orthogonal). This channel model is parallel to the multi-hop cellular system setup we examine in the proceeding sections of this chapter.

Definition 23. An M -source, K -relay d.m. GORC denoted by

$$\left(\left(\prod_{m=1}^M \mathcal{S}_m \times \prod_{k=1}^K \mathcal{X}_k \right), p(y_{1:K}, y_D | s_{1:M}, x_{1:K}), \left(\prod_{k=1}^K \mathcal{Y}_k \times \mathcal{Y}_D \right) \right)$$

consists of finite sets $\{\mathcal{S}_m\}_{m=1}^M$, $\{\mathcal{X}_k\}_{k=1}^K$, $\{\mathcal{Y}_k\}_{k=1}^K$ and $\mathcal{Y}_D = \mathcal{Y}_{D_1} \times \mathcal{Y}_{D_2}$; and the channel transition probability given by

$$\begin{aligned} p(y_1, \dots, y_K, y_D | s_1, \dots, s_M, x_1, \dots, x_K) \\ = p(y_1, \dots, y_K, y_{D_1} | s_1, \dots, s_M) p(y_{D_2} | x_1, \dots, x_K) \end{aligned} \quad (4.1)$$

for all

$$\begin{aligned} (s_1, \dots, s_M, x_1, \dots, x_K, y_1, \dots, y_K, y_{D_1}, y_{D_2}) \\ \in \{\mathcal{S}_m\}_{m=1}^M \times \{\mathcal{X}_k\}_{k=1}^K \times \{\mathcal{Y}_k\}_{k=1}^K \times \{\mathcal{Y}_{D_i}\}_{i=1}^2 \end{aligned} \quad (4.2)$$

where $\{s_m\}_{m=1}^M$ are the source inputs to the orthogonal channel allocated to them, $\{y_k\}_{k=1}^K$ are the relay outputs and y_{D_1} is the destination output in the channel allocated to the sources; $\{x_k\}_{k=1}^K$ are the RS inputs to the orthogonal channel allocated to them and y_{D_2} is the destination output in the channel allocated to the RSs as shown in Figure 4.1 where solid and dashed lines refer to the orthogonal channels allocated to the sources and RSs, respectively.

Definition 24. A $(2^{nR_1}, 2^{nR_2}, \dots, 2^{nR_M}, n)$ code for the d.m. GORC with M sources, K RSs and a single destination consists of the followings:

- M message sets $\mathcal{W}_m = \{1, 2, \dots, 2^{nR_m}\}$ and M signal spaces \mathcal{S}_m , for $m = 1, 2, \dots, M$.
- M source encoding functions that map each message $W_m \in \mathcal{W}_m$ into a codeword $\mathcal{S}_m^n(W_m)$

$$f_m : \mathcal{W}_m \rightarrow \mathcal{S}_m^n, \quad m = 1, 2, \dots, M, \quad (4.3)$$

- K (causal) RS encoding functions $\{f_{R_k, i}\}_{i=1}^n$, for $k = 1, 2, \dots, K$, such that

$$x_{k, i} = f_{R_k, i}(Y_{k, 1}, Y_{k, 2}, \dots, Y_{k, i-1}), \quad 1 \leq i \leq n, \quad (4.4)$$

- and a decoding function

$$g : \mathcal{Y}_{D_1}^n \times \mathcal{Y}_{D_2}^n \rightarrow \mathcal{W}_1 \times \mathcal{W}_2 \times \cdots \times \mathcal{W}_M. \quad (4.5)$$

Each source selects an index W_m uniformly from the set \mathcal{W}_m and sends the corresponding codeword $S_m^n(W_m)$ over the channel. A rate tuple (R_1, \dots, R_M) is said to be achievable for the d.m. GORC if there exists a sequence of $(2^{nR_1}, \dots, 2^{nR_M}, n)$ codes with the average probability of error

$$P_e^{(n)} = \Pr \left(\{\hat{W}_m\}_{m=1}^M \neq \{W_m\}_{m=1}^M \right) \rightarrow 0.$$

4.2.2 Outer Region

Here, we give an outer region on the achievable rates for the GORC defined above by using max-flow min-cut theorem [1, Theorem 15.10.1]. We have the following cut-set outer rate region

Theorem 25 (General Outer Rate Region). *The general outer rate region of relay channel consisting of M -source, K -relay and single destination is the union of the sets of rate-tuples (R_1, R_2, \dots, R_M) satisfying*

$$\begin{aligned} \mathcal{R}^* = \left\{ (R_1, \dots, R_M) : \right. \\ \left. \sum_{i \in \mathcal{T}} R_i \leq \sup_{p(s_1, \dots, s_M, x_1, \dots, x_K)} \left\{ \min_{\mathcal{J} \subseteq \mathcal{K}} I(S_{(\mathcal{T})}, X_{(\mathcal{J})}; Y_{(\mathcal{J}^c)}, Y_D | S_{(\mathcal{T}^c)}, X_{(\mathcal{J}^c)}) \right\} \mid \forall \mathcal{T} \subseteq \mathcal{M} \right\} \end{aligned} \quad (4.6)$$

where $S_{(\mathcal{T})} = \{S_m : m \in \mathcal{T} \subseteq \mathcal{M}\}$ and $X_{(\mathcal{J})} = \{X_k : k \in \mathcal{J} \subseteq \mathcal{K}\}$, and \mathcal{T}^c (\mathcal{J}^c) is the complement of \mathcal{T} (\mathcal{J}) in \mathcal{M} (\mathcal{K}).

Proof. The proof follows from the max-flow min-cut theorem [1, Theorem 15.10.1]. \square

Now consider the GORC model defined above. Let $Y_D = (Y_{D_1}, Y_{D_2})$ be the received signals at the destination where Y_{D_1} (Y_{D_2}) represents the received signal in the orthogonal channel 1 (channel 2). With the channel transition probability given in (4.1), we have the following cut-set outer rate region for the d.m. GORC:

Theorem 26 (Outer Rate Region for the d.m. GORC). *The outer rate region of M -source, K -relay and single destination GORC is the union of the sets of rate-tuples (R_1, \dots, R_M) satisfying*

$$\begin{aligned} \mathcal{R}_{O-OR} = \left\{ (R_1, \dots, R_M) : \right. \\ \left. \sum_{i \in \mathcal{T}} R_i \leq \sup_{\substack{p(s_1, \dots, s_M) \\ p(x_1, \dots, x_K)}} \min_{\mathcal{J} \subseteq \mathcal{K}} \left\{ I(S_{(\mathcal{T})}; Y_{(\mathcal{J}^c)}, Y_{D_1} | S_{(\mathcal{T}^c)}) + I(X_{(\mathcal{J})}; Y_{D_2} | X_{(\mathcal{J}^c)}) \right\}, \right. \\ \left. \forall \mathcal{T} \subseteq \mathcal{M} \right\} \end{aligned} \quad (4.7)$$

where $S_{(\mathcal{T})} = \{S_m : m \in \mathcal{T} \subseteq \mathcal{M}\}$ and $X_{(\mathcal{J})} = \{X_k : k \in \mathcal{J} \subseteq \mathcal{K}\}$ and \mathcal{T}^c is the complement of \mathcal{T} in \mathcal{M} .

Proof. Consider the general outer region given in (4.6). For the orthogonal relay network, let $Y_D = (Y_{D_1}, Y_{D_2})$ be the received signals at the destination. Consider the channel transition probability defined in (4.1), then the mutual information term in (4.6) becomes:

$$\begin{aligned}
& I(S_{(\mathcal{T})}, X_{(\mathcal{J})}; Y_{(\mathcal{J}^c)}, Y_D | S_{(\mathcal{T}^c)}, X_{(\mathcal{J}^c)}) \\
&= I(S_{(\mathcal{T})}, X_{(\mathcal{J})}; Y_{(\mathcal{J}^c)}, Y_{D_1}, Y_{D_2} | S_{(\mathcal{T}^c)}, X_{(\mathcal{J}^c)}) \\
&= H(Y_{(\mathcal{J}^c)}, Y_{D_1}, Y_{D_2} | S_{(\mathcal{T}^c)}, X_{(\mathcal{J}^c)}) - H(Y_{(\mathcal{J}^c)}, Y_{D_1}, Y_{D_2} | S_{\mathcal{M}}, X_{\mathcal{K}}) \\
&\stackrel{(a)}{\leq} H(Y_{(\mathcal{J}^c)}, Y_{D_1} | S_{(\mathcal{T}^c)}) + H(Y_{D_2} | X_{(\mathcal{J}^c)}) \\
&\quad - H(Y_{(\mathcal{J}^c)}, Y_{D_1} | S_{(\mathcal{M})}) - H(Y_{D_2} | X_{(\mathcal{K})}) \\
&= I(S_{(\mathcal{T})}; Y_{(\mathcal{J}^c)}, Y_{D_1} | S_{(\mathcal{T}^c)}) + I(X_{(\mathcal{J})}; Y_{D_2} | X_{(\mathcal{J}^c)}) \tag{4.8}
\end{aligned}$$

where (a) follows from conditioning can only reduces entropy and the channel transition probability defined in (4.1). Note that this inequality becomes equality when the source transmit signals $\{S_m\}_{m=1}^M$ are independent from the RS transmit signals $\{X_k\}_{k=1}^K$; hence, the input probability distribution

$$p(s_1, \dots, s_M, x_1, \dots, x_K) = p(s_1, \dots, s_M)p(x_1, \dots, x_K)$$

yields a tighter outer region. \square

If we just consider the broadcast cut, i.e., $\mathcal{J} = \emptyset$, and the multiple-access cut, i.e., $\mathcal{J} = \mathcal{K}$, we have the following loose outer rate region for the d.m. GORC:

$$\begin{aligned}
\mathcal{R}_{O-OR} &= \left\{ (R_1, \dots, R_M) : \right. \\
&\left. \sum_{i \in \mathcal{T}} R_i \leq \sup_{\substack{p(s_1, \dots, s_M) \\ p(x_1, \dots, x_K)}} \min \left\{ \begin{array}{l} I(S_{(\mathcal{T})}; Y_{1:K}, Y_{D_1} | S_{(\mathcal{T}^c)}), \\ I(S_{(\mathcal{T})}; Y_{D_1} | S_{(\mathcal{T}^c)}) + I(X_{1:K}; Y_{D_2}) \end{array} \right\} \mid \forall \mathcal{T} \subseteq \mathcal{M} \right\}. \tag{4.9}
\end{aligned}$$

4.2.3 Achievable Rates

DF Relaying

Assume that a subset $\mathcal{J} \subseteq \mathcal{K}$ of RSs are selected to cooperate with the sources. All of the RSs in set \mathcal{J} decode and forward the source messages to the destination in an orthogonal channel. We have the following achievable rate for the DF relaying strategy.

Proposition 1 (Full DF Relaying). *The DF achievable rate region for the M -source, K -relay and single destination GORC is given by*

$$\sum_{i \in \mathcal{T}} R_i \leq \sup_{\mathcal{J} \subseteq \mathcal{K}} \min \left\{ \min_{k \in \mathcal{J}} \{ I(S_{(\mathcal{T})}; Y_k | S_{(\mathcal{T}^c)}) \}, I(S_{(\mathcal{T})}; Y_{D_1} | S_{(\mathcal{T}^c)}) + I(X_{(\mathcal{J})}; Y_{D_2} | X_{(\mathcal{J}^c)}) \right\} \tag{4.10}$$

for all $\mathcal{T} \subseteq \mathcal{M}$.

Proof. The achievability proof of the DF relaying for an orthogonal relay channel consisting of one source and one RS is provided in [78]. To extend the proof to the multi-source, multi-relay case, we need to look at all RS selection possibilities that gives the maximum rate region. It can be easily shown that it is not necessary to use block-Markov encoding to achieve the rate region (4.11). Parallel Gaussian channel arguments for decoding at the destination can be used for the achievability. \square

Note that forcing all RSs to decode all transmitted signals not only results in a smaller rate region, but also requires more complexity at the RS side. However, with a simple scheduler assigning a distinct source to each RS and letting them just decode the message of the assigned source, regarding the other user signals as noise, would offer better rate region with less complicated RS processing. We have the following rate region for the DF scheme defined above, which we call partial DF relaying. Assume $M \geq K$, let \mathcal{M}^* be the scheduled source set, where $|\mathcal{M}^*| = K$, and \mathcal{K}' denote the RS set which holds the indexes of RSs for the scheduled sources. Then we have the following achievable rate-region:

Proposition 2 (Partial DF Relaying). *By treating part of the interference signals as noise, the DF achievable rate region for the d.m. GORC with M -source, K -relay ($M \geq K$) and single destination is given by*

$$\begin{aligned} \sum_{j \in \mathcal{U}} R_j &\leq I(S_{(\mathcal{U})}; Y_{D_1} | S_{(\mathcal{U}^c)}) \\ \sum_{i \in \mathcal{T}} R_i &\leq \min \left\{ \sum_{i \in \mathcal{T}} I(S_i; Y_{\mathcal{K}'_i}), I(S_{(\mathcal{T})}; Y_{D_1} | S_{(\mathcal{T}^c)}, S_{(\mathcal{M}^{*c})}) \right. \\ &\quad \left. + I(X_{(\mathcal{K}'(\mathcal{T}))}; Y_{D_2} | X_{(\mathcal{K}' \setminus \mathcal{K}'(\mathcal{T}))}) \right\} \end{aligned} \quad (4.11)$$

for all $\mathcal{T} \subseteq \mathcal{M}^*$ and $\mathcal{U} \subseteq \mathcal{M}^{*c} = \mathcal{M} \setminus \mathcal{M}^*$.

Proof. Assume \mathcal{M}^{*c} , where $\mathcal{M}^{*c} \cup \mathcal{M}^* = \mathcal{M}$, is the set of non-relayed sources whose messages are directly decoded at the destination. In the first phase of the communication, the destination decodes the messages corresponding to the sources assigned to itself regarding the other sources' signals as interference. Then, the remaining messages which are decoded at the RSs are decoded at the destination. \square

Remark 27. *Assignment of sources to the RSs can be done in several ways: 1) location based assignment where each RS schedules the sources fallen in their pre-assigned regions, 2) received power based scheduling (or channel strength base). We note that each RS selects a unique source.*

CF Relaying

For the CF (BQRB) relaying strategy we use the Wyner-Ziv source coding [32] where side information at the destination is used to have better compression at the RSs by exploiting correlation between the signals.

We have the following achievable rate region for the CF relaying strategy:

Proposition 3 (CF Relaying). *For the d.m. GORC using the CF relaying the following rate region is achievable where all RSs participate in communications between the sources and the destination*

$$\sum_{i \in \mathcal{J}} R_i \leq I(S_{(\mathcal{J})}; \hat{Y}_{1:K}, Y_{D_1} | S_{(\mathcal{J}^c)}), \quad \forall \mathcal{J} \subseteq \mathcal{M} \quad (4.12)$$

such that

$$I(\hat{Y}_{(\mathcal{J})}; Y_{(\mathcal{J})} | Y_{D_1}, \hat{Y}_{(\mathcal{J}^c)}) \leq I(X_{(\mathcal{J})}; Y_{D_2} | X_{(\mathcal{J}^c)}), \quad \forall \mathcal{J} \subseteq \mathcal{K}. \quad (4.13)$$

Proof. The achievability proof of the CF relaying for the constraint multiple-access relay channel (MARC) with single RS (where the RS is assumed to be HD) has been proved in [79]. Considering the orthogonality and multiple RS case, we can easily obtain the achievable rate region given in (4.12) by exploiting the Wyner-Ziv source coding [32]. \square

QF Relaying

In the CF relaying strategy, each RS needs to know the correlation information between its received signal and the received signals at the other RSs and at the destination in order to preform Wyner-Ziv compression. In practice, this assumption is hard to implement since each RS needs to have full CSI corresponding to the all other RSs and the destination. Hence, CF relaying imposes extra complexity on the system setup. To overcome this issue, we look at the QF relaying where each RS just quantizes its received signal without exploiting correlation, i.e., regular rate-distortion theory applies, and forwards the bin indexes corresponding to the quantized signals to the destination².

In the QF relaying, each RS quantizes the received signal with a rate that falls in the MAC rate region for the communication from the RSs to the destination on the orthogonal channel. We have the following achievable rate region for the QF relaying where all RSs participate in communications between the sources and the destination:

Proposition 4 (QF Relaying). *For the d.m. GORC using the QF relaying the following rate region can be achieved where all RSs participate in communications between the sources and the destination*

$$\sum_{i \in \mathcal{J}} R_i \leq I(S_{(\mathcal{J})}; \hat{Y}_{1:K}, Y_{D_1} | S_{(\mathcal{J}^c)}), \quad \forall \mathcal{J} \subseteq \mathcal{M} \quad (4.14)$$

²Note that in this chapter by QF relaying we mean Gaussian codebooks at the sources and Gaussian mapping (for quantization) at the RSs.

such that

$$\sum_{k \in \mathcal{J}} I(\hat{Y}_k; Y_k) \leq I(X_{(\mathcal{J})}; Y_{D_2} | X_{(\mathcal{J}^c)}), \quad \forall \mathcal{J} \subseteq \mathcal{K}. \quad (4.15)$$

Proof. The proof can be simply derived as in the CF relaying strategy case. \square

Remark 28 (Mixed DF and CF Relaying). *Considering UL communications in a cellular system with RS deployment, channel qualities between a given source (e.g., mobile stations) and all RSs in a given cell will be different. Hence, assuming high quality RS-to-BS links, it makes sense that the RSs that have good received signal quality decode the source message and the other RSs which have inferior link qualities compress the received signal and send to the BS, instead of decoding the source signal. Since this relaying strategy is more complex than the above mentioned ones, we do not consider mixed DF and CF relaying strategy in this chapter.*

4.3 Cellular Networks with Relay Deployment: System Model

We consider UL communication (from MSs to the BS) in a multi-cell cellular network topology comprising infrastructure RSs where channels from MSs to RSs and BSs are orthogonal to the channels from RSs to BSs. This channel model is called *GORC* in the previous section. We assume $B + 1$ cells each having M MSs which want to communicate with the BS in the center of the cell through K RSs which are placed arbitrarily in the cell. In this section, the AF, DF, CF and QF relaying strategies are considered.

The UL communications takes place in two phases (hops): MSs access the RSs and the BS in the first phase of the communication while the RSs backhaul the MSs data to the BS via a wireless channel in the second phase with the access and backhaul channels having orthogonal frequency bands: frequency division duplex (FDD) relaying is adopted. RS-to-RS communication is not allowed as it requires more intelligent high-layer routing protocols. We assume that the BW allocated to the first hop (the second hop) is W_1 (W_2) with a total BW constraint W_{tot} where $W_{tot} = W_1 + W_2$. We define the BW ratio as $F = W_2/W_1 \in \mathcal{R}^+$, see Figure 9.4. As shown in the numerical results later, resource allocation, i.e. controlling F , directly impacts the system performance.

Due to the frequency reuse of 1 assumption, communications in a specific cell face with inter-cell interference. Assuming statistical interference CSI at each receiver, we modeled inter-cell interference signals as Gaussian noise with zero mean and variance determined by mean channel gain between an interfering transmitter and a specific receiver. Note however that having full interference CSI at the receiver (CSIR) might improve the performance.

The BSs are equipped with N directional antennas each directed to a unique RS around it and each MS is assumed to have single omnidirectional antenna. For the RSs, we will consider both omnidirectional and directional antenna

cases. Each case corresponds to a different RS deployment scenario which will be clarified in Section-4.9. We note that in the preceding sections all derivations are generic and cover both scenarios.

We will analyze the system performance in terms of achievable *sum-rate*. We choose the *central* cell for performance evaluation. Hence, in the following we will give a general channel and signal model at the central cell. Note that as opposed to single-cell networks [80], here we want to see the effects of inter-cell and inter-relay interference on the performance of infrastructure relaying schemes.

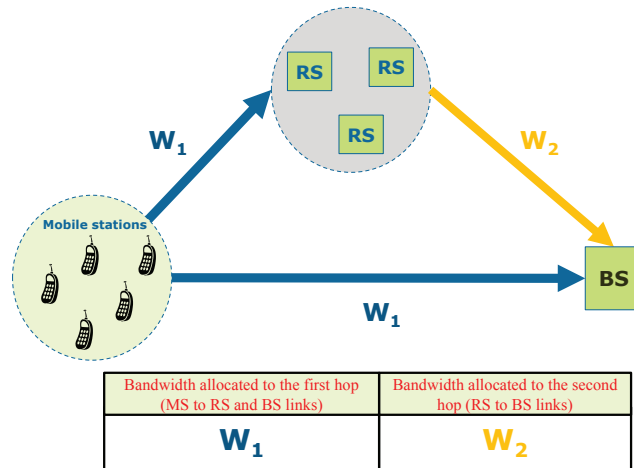


Figure 4.2: The bandwidth allocation in the first and second hop.

4.3.1 Channel Model

Here we give the channel model corresponding to UL communications from MSs to the BS with the aid of the RSs. We denote $h_{n,m}$ and $f_{k,m}$, for $n = 1, 2, \dots, N$, $k = 1, 2, \dots, K$, $m = 1, 2, \dots, M$ as the channel coefficient in the first phase of communication from m -th MS in the central cell to the n -beam of the central BS and the k -th RS in the central cell, respectively:

$$h_{n,m} = \sqrt{\Upsilon_{n,m,0}} \tilde{h}_{n,m} \quad (4.16)$$

$$f_{k,m} = \sqrt{\Psi_{k,m,0}} \tilde{f}_{k,m} \quad (4.17)$$

where each entry of $\tilde{h}_{n,m}$ and $\tilde{f}_{k,m}$ is an i.i.d. zero-mean complex Gaussian random variable (ZMCSCG) with unit variance; $\Upsilon_{n,m,b}$ and $\Psi_{k,m,b}$, $b = 0, 1, \dots, B$, is the parameter representing channel gain from m -th MS in the b -th cell to the n -beam of the central BS and k -th RS in the central cell, respectively, including

path-loss, transmitter and receiver antenna gains and shadowing effects. The specifications of channel gains are explained in details in Section-4.9. In what follows, we will consider average rates and thus the single coefficient channel model is sufficient even to characterize wide-band channels (e.g. OFDM).

We denote $g_{n,k}$ as the channel coefficient at the second hop (from the RSs to the BSs) between the k -th RS and the n -th beam of the central BS,

$$g_{n,k} = \sqrt{\Phi_{n,k,0}} \tilde{g}_{n,k} \quad (4.18)$$

where each entry of $\tilde{g}_{n,k}$ is an i.i.d. complex Gaussian random variable with non-zero mean (due to line-of-sight (LOS) component between the terminals) and unit variance and $\Phi_{n,k,b}$, $b = 0, 1, \dots, B$, is the parameter representing channel gain from the k -th RS in the b -th cell to the n -th beam of the BS, $\forall k \in \{1, 2, \dots, K\}$ and $\forall n \in \{1, 2, \dots, N\}$, including path-loss, transmitter and receiver antenna gains and shadowing effects.

4.3.2 Signal Model

In the first hop, the MSs communicate with the RSs and the BS while the RSs communicate with the BS in the second hop. Due to no CSIR assumption for the interfering channels, we modeled the interference terms as white Gaussian noise with zero mean and variance which is specified by channel gains.

In the first hop, the received signal at the n -th beam of the central BS is given by

$$\begin{aligned} y_{D_1,n} &= \sum_{k=1}^M h_{n,m} s_m + \chi_n^{(1)} + z_n^{(1)} \\ &= \mathbf{h}_n^T \mathbf{s} + \chi_n^{(1)} + z_n^{(1)}, \quad n = 1, 2, \dots, N \end{aligned} \quad (4.19)$$

where $\mathbf{s} = [s_1, s_2, \dots, s_M]^T$ is the vector of transmitted signals from MSs in the central cell and $\mathbf{h}_n = [h_{n,1}, h_{n,2}, \dots, h_{n,M}]^T$ is the channel vector from all MSs in the central cell to the n -th beam of the central BS. All MSs in the system are subject to average transmit power constraint $\mathbb{E}[|s_m|^2] = P_s, \forall m$. $z_n^{(1)} \sim \mathcal{CN}(0, \sigma_1^2)$ is ZMCSCG noise term at the n -th beam of the BS with variance $\sigma_1^2 = N_0 W_1$, and $\chi_n^{(1)} \sim \mathcal{CN}(0, \xi_{1,n}^2)$ with $\xi_{1,n}^2 = \sum_{b=1}^B \sum_{m=1}^M \Upsilon_{n,m,b} P_s$ is the interference random variable.

Combining all of the received signals at each beam in a vector form, i.e. $\mathbf{y}_{D_1} = [y_{D_1,1}, y_{D_1,2}, \dots, y_{D_1,N}]^T$, we have the following compact form

$$\mathbf{y}_{D_1} = \begin{bmatrix} \mathbf{h}_1^T \\ \mathbf{h}_2^T \\ \vdots \\ \mathbf{h}_N^T \end{bmatrix} \mathbf{s} + \begin{bmatrix} \chi_1^{(1)} \\ \chi_2^{(1)} \\ \vdots \\ \chi_N^{(1)} \end{bmatrix} + \mathbf{z}^{(1)} = \mathbf{H} \mathbf{s} + \chi^{(1)} + \mathbf{z}^{(1)} \quad (4.20)$$

where $\mathbf{H} \in \mathbb{C}^{N \times M}$ is the channel matrix from all MSs to the all RSs in the central cell, and $\chi^{(1)} = [\chi_1^{(1)}, \chi_2^{(1)}, \dots, \chi_N^{(1)}]^T$ is the total interference vector seen at the BS.

In the first hop, the received signal at the k -th RS on the central cell is given by

$$\begin{aligned} y_k &= \sum_{m=1}^M f_{k,m} s_m + \chi_k^{(R)} + z_k^{(R)} \\ &= \mathbf{f}_k^T \mathbf{s} + \chi_k^{(R)} + z_k^{(R)}, \quad k = 1, 2, \dots, K \end{aligned} \quad (4.21)$$

where $\mathbf{s} = [s_1, s_2, \dots, s_M]^T$ is the vector of transmitted signals from MSs in the central cell and $\mathbf{f}_k = [f_{k,1}, f_{k,2}, \dots, f_{k,M}]^T$ is the channel vector from all MSs in the central cell to the i -th RS in the central cell. All MSs in the system are subject to average transmit power constraint $\mathbb{E}[|s_m|^2] = P_s, \forall m$. $z_k^{(R)} \sim \mathcal{CN}(0, \sigma_R^2)$ is ZMCSCG noise at the k -th RS with variance $\sigma_R^2 = N_0 W_1$, and $\chi_k^{(R)} \sim \mathcal{CN}(0, \xi_{r,k}^2)$ with $\xi_{r,k}^2 = \sum_{b=1}^B \sum_{m=1}^M \Psi_{k,m,b} P_s$ is the interference random variable.

Considering the received signals of all RSs, i.e. $\mathbf{y} = [y_1, y_2, \dots, y_K]^T$, we have the following compact form

$$\mathbf{y} = \begin{bmatrix} \mathbf{f}_1^T \\ \mathbf{f}_2^T \\ \vdots \\ \mathbf{f}_K^T \end{bmatrix} \mathbf{s} + \begin{bmatrix} \chi_1^{(R)} \\ \chi_2^{(R)} \\ \vdots \\ \chi_K^{(R)} \end{bmatrix} + \mathbf{z}^{(R)} = \mathbf{F} \mathbf{s} + \chi^{(R)} + \mathbf{z}^{(R)} \quad (4.22)$$

where $\mathbf{F} \in \mathbb{C}^{K \times M}$ is the channel matrix from all MSs to the all RSs in the central cell, and $\chi^{(R)} = [\chi_1^{(R)}, \chi_2^{(R)}, \dots, \chi_K^{(R)}]^T$ is the total interference vector seen at the RSs in the central cell.

At the second hop, the communication between the RSs and the BSs, we assume that the channel qualities are relatively good compared to the first hop as the RSs need to convey all the data streams it has received from the MSs in the first hop. Assuming the BSs has N directional antennas the received signal at the n -th beam of the BS in the central cell is given by

$$\begin{aligned} y_{D_2,n} &= \sum_{k=1}^K g_{n,k} x_k + \chi_n^{(2)} + z_n^{(2)} \\ &= \mathbf{g}_n^T \mathbf{x} + \chi_n^{(2)} + z_n^{(2)}, \quad n = 1, 2, \dots, N \end{aligned} \quad (4.23)$$

where $\mathbf{x} = [x_1, x_2, \dots, x_K]^T$ with x_k being the transmitted signal from the k -th RS in the central cell with average power constraint $\mathbb{E}[|x_k|^2] = P_r$ for $k = 1, 2, \dots, K$; $\chi_n^{(2)} \sim \mathcal{CN}(0, \xi_{2,n}^2)$ with $\xi_{2,n}^2 = \sum_{b=1}^B \sum_{k=1}^K \Phi_{n,k,b} P_r$, and $z_n^{(2)} \sim \mathcal{CN}(0, \sigma_2^2)$ is the noise at the n -th beam of the BS with variance $\sigma_2^2 = N_0 W_2$.

Combining all of the received signals in a vector form we get

$$\mathbf{y}_{D_2} = \mathbf{G} \mathbf{x} + \chi^{(2)} + \mathbf{z}^{(2)} \quad (4.24)$$

where $\mathbf{G} \in \mathbb{C}^{N \times K}$ is the channel matrix from all RSs to the BS in the central cell, $\chi^{(2)} = [\chi_1^{(2)}, \chi_2^{(2)}, \dots, \chi_N^{(2)}]^T$ is the total interference vector seen at the BSs in the central cell, and $\mathbf{z}^{(2)} = [z_1^{(2)}, z_2^{(2)}, \dots, z_N^{(2)}]^T$ is the noise vector at the BS.

From now on we will only consider the achievable rates for UL communications in the central cell (i.e., $c = 0$) for different relaying schemes.

4.4 Amplify-and-Forward Relaying

In this section, we will give input-output relations for AF relaying strategy in cellular systems under the following CSI assumptions: each RS has its corresponding backward CSI and each BS has full CSI of the cell it is located; in each cell the RSs and the BS treat the interfering signals coming from surrounding cells as Gaussian distributed random variables with zero mean and some variance depending on the channel gain between corresponding transmitter and the receiver.

In AF relaying, the received signal at each RS is scaled according to the relay power constraint and then is forwarded to the BSs. AF relaying is simple, however it suffers from noise amplification. Note that for AF relaying, the signaling dimensions should be the same both in the first and the second phases, i.e., $W = W_1 = W_2 = W_{tot}/2$, hence $\sigma_d^2 = \sigma_r^2 = N_0W$.

Received signal power at the k -th RS, for $k = 1, 2, \dots, K$, is given by

$$\begin{aligned} \mathbb{E}[|y_k|^2 | \mathbf{f}_k] &= \|\mathbf{f}_k\|^2 P_s + \sum_{b=1}^B \sum_{m=1}^M \Upsilon_{k,m,b} P_s + \sigma_r^2 \\ &= \|\mathbf{f}_k\|^2 P_s + \xi_{r,k}^2 + \sigma_r^2. \end{aligned} \quad (4.25)$$

And according to the received signal at the RSs given in (4.21), the scaling factors are given by

$$\alpha_k = \sqrt{\frac{P_r}{\mathbb{E}[|y_k|^2 | \mathbf{f}_k]}} = \sqrt{\frac{P_r}{\|\mathbf{f}_k\|^2 P_s + \xi_{r,k}^2 + \sigma_r^2}} \quad (4.26)$$

and the signal transmitted by the k -th RS on the central cell is given by

$$\begin{aligned} x_k &= \alpha_k y_k \\ &= \alpha_k \left(\mathbf{f}_k^T \mathbf{s} + \chi_k^{(R)} + \mathbf{z}_k^{(R)} \right) \end{aligned} \quad (4.27)$$

for $k = 1, 2, \dots, K$, which has the following compact form

$$\begin{aligned} \mathbf{x} &= \mathbf{D} \mathbf{y} = \mathbf{D} \left(\mathbf{F} \mathbf{s} + \chi^{(R)} + \mathbf{z}^{(R)} \right) \\ &= \mathbf{D} \mathbf{F} \mathbf{s} + \mathbf{D} \chi^{(R)} + \mathbf{D} \mathbf{z}^{(R)} \end{aligned} \quad (4.28)$$

where $\mathbf{x} = [x_1, x_2, \dots, x_K]^T$, $\chi^{(R)} = [\chi_1^{(R)}, \chi_2^{(R)}, \dots, \chi_K^{(R)}]^T$ is the noise plus total interference vector at the RSs on the central cell, and

$$\mathbf{D} = \text{diag}\{\alpha_1, \alpha_2, \dots, \alpha_N\}. \quad (4.29)$$

The received signal at the n -th beam of the central BS is given by (4.24) by which we have the following vector form for the received signals at the BS

$$\begin{aligned} \mathbf{y}_{D_2} &= \mathbf{G} \mathbf{x} + \chi^{(2)} + \mathbf{z}^{(2)} \\ &= \mathbf{G} \mathbf{D} \mathbf{F} \mathbf{s} + \underbrace{\mathbf{G} \mathbf{D} \chi^{(R)} + \mathbf{G} \mathbf{D} \mathbf{z}^{(R)}}_{\mathbf{z}_{eq}^{(2)}} + \chi^{(2)} + \mathbf{z}^{(2)} \\ &= \mathbf{G} \mathbf{D} \mathbf{F} \mathbf{s} + \mathbf{z}_{eq}^{(2)} \end{aligned} \quad (4.30)$$

where $\mathbf{G} \in \mathbb{C}^{N \times K}$ channel matrix from all RSs on central cell to the BS, $\mathbf{z}_{eq}^{(2)} \in \mathbb{C}^{N \times 1}$ is the equivalent noise term which has the following covariance matrix

$$\Lambda_2 = \mathbb{E} \left[\mathbf{z}_{eq}^{(2)} \mathbf{z}_{eq}^{(2)H} \right] = \mathbf{G} \mathbf{D} (\Delta_r + \sigma_r^2 \mathbf{I}_N) \mathbf{D}^H \mathbf{G}^H + \Delta_2 + \sigma_d^2 \mathbf{I}_N \quad (4.31)$$

where

$$\begin{aligned} \Delta_r &= \mathbb{E} \left[\chi^{(R)} \chi^{(R)H} \right] = \text{diag}\{\xi_{r,1}^2, \xi_{r,2}^2, \dots, \xi_{r,K}^2\} \\ \Delta_2 &= \mathbb{E} \left[\chi^{(2)} \chi^{(2)H} \right] = \text{diag}\{\xi_{2,1}^2, \xi_{2,2}^2, \dots, \xi_{2,N}^2\}. \end{aligned}$$

We can combine the received signals at the BS in the central cell as follows

$$\mathbf{y}_D = \begin{bmatrix} \mathbf{y}_{D_1} \\ \mathbf{y}_{D_2} \end{bmatrix} = \begin{bmatrix} \mathbf{H} \\ \mathbf{G} \mathbf{D} \mathbf{F} \end{bmatrix} \mathbf{s} + \begin{bmatrix} \chi^{(1)} + \mathbf{z}^{(1)} \\ \mathbf{z}_{eq}^{(2)} \end{bmatrix} = \overline{\mathbf{H}} \mathbf{s} + \overline{\mathbf{z}} \quad (4.32)$$

where $\overline{\mathbf{H}} \in \mathbb{C}^{2N \times K}$ is the overall channel from the MSs in the central cell to the BS and $\overline{\mathbf{z}} \in \mathbb{C}^{2N \times 1}$ is the noise and interference vector seen at the BS which has the following covariance matrix

$$\Lambda = \mathbb{E} [\overline{\mathbf{z}} \overline{\mathbf{z}}^H] = \text{diag}\{\Lambda_1, \Lambda_2\} \in \mathbb{C}^{2N \times 2N} \quad (4.33)$$

where $\Lambda_1 = \Delta_1 + \sigma_d^2 \mathbf{I}_N$ and

$$\Delta_1 = \mathbb{E} \left[\chi^{(1)} \chi^{(1)H} \right] = \text{diag}\{\xi_{1,1}^2, \xi_{1,2}^2, \dots, \xi_{1,N}^2\}.$$

Considering the channel model in (4.32), for given channel realizations the achievable sum-of-rates (in [bits/sec]) for UL communications on the central cell is given by

$$\begin{aligned} R_{AF} &= W \log_2 \det \left(\mathbf{I}_K + P_s \overline{\mathbf{H}}^H \Lambda^{-1} \overline{\mathbf{H}} \right) \\ &= W \log_2 \det \left(\mathbf{I}_N + P_s \mathbf{H} \Lambda_1^{-1} \mathbf{H}^H + \mathbf{G} \mathbf{D} \mathbf{F} \Lambda_2^{-1} \mathbf{F}^H \mathbf{D}^H \mathbf{G}^H \right). \end{aligned} \quad (4.34)$$

The average achievable rate for AF relaying is given by

$$\overline{R}_{AF} = \mathbb{E}_{\{\mathbf{H}, \mathbf{F}, \mathbf{G}\}} [R_{AF}]. \quad (4.35)$$

4.5 Decode-and-Forward Relaying

In this relaying strategy, we assume that each RS selects a distinct MS to help. The way the selection is done will be specified in Section-4.9.1.

Now we give the sum-rate expression for the DF relaying strategy where each RS decodes the message of the selected MS by considering other MSs' signals as noise³. The messages of the non-selected MSs which access the BS directly are decoded at the BS jointly.

Let \mathcal{M} denote the set of active MSs, and \mathcal{U} and \mathcal{J} be two distinct sets, where $\mathcal{M} = \mathcal{U} \cup \mathcal{J}$, holding respective indexes of the MSs sending messages to the BS directly and through a RS, where $|\mathcal{U}| = M - K$. Assume that the i -th MS is assigned to the r_i -th RS where $i \in \mathcal{J}$. Regarding the signal model and achievable rate region (4.11), we have the following sum-rate for this DF relaying strategy

$$\begin{aligned} R_{DF}^{sum} &\leq \min \left\{ I(S_{(\mathcal{U})}; Y_{D_1}) + \sum_{i \in \mathcal{J}} I(S_i; Y_{r_i}), \right. \\ &\quad \left. I(S_{(\mathcal{U})}; Y_{D_1}) + I(S_{(\mathcal{J})}; Y_{D_1} | S_{(\mathcal{U})}) + I(X_{(\mathcal{X})}; Y_{D_2}) \right\} \\ &= \min \left\{ I(S_{(\mathcal{U})}; Y_{D_1}) + \sum_{i \in \mathcal{J}} I(S_i; Y_{r_i}), I(S_{(\mathcal{M})}; Y_{D_1}) + I(X_{(\mathcal{X})}; Y_{D_2}) \right\} \end{aligned} \quad (4.36)$$

where

$$I(s_{(\mathcal{U})}; \mathbf{y}_{D_1}) = W_1 \log_2 \det \left(\mathbf{I}_N + P_s \mathbf{H}_{(\mathcal{U})} \left(P_s \mathbf{H}_{(\mathcal{J})} \mathbf{H}_{(\mathcal{J})}^H + \Lambda \right)^{-1} \mathbf{H}_{(\mathcal{U})}^H \right) \quad (4.37)$$

$$I(s_i; y_{r_i}) = W_1 \log_2 \left(1 + \frac{|f_{r_i,i}|^2 P_s}{\sum_{j \neq i} |f_{r_i,j}|^2 P_s + \xi_{r,r_i}^2 + \sigma_r^2} \right), \quad \forall i \quad (4.38)$$

$$I(s_{(\mathcal{M})}; \mathbf{y}_{D_1}) = W_1 \log_2 \det \left(\mathbf{I}_N + P_s \mathbf{H} (\Delta_1 + \sigma_1^2 \mathbf{I}_N)^{-1} \mathbf{H} \right) \quad (4.39)$$

$$I(x_{(\mathcal{X})}; \mathbf{y}_{D_2}) = W_2 \log_2 \det \left(\mathbf{I}_N + P_r \mathbf{G} \mathbf{G}^H (\Delta_2 + \sigma_2^2 \mathbf{I}_N)^{-1} \right) \quad (4.40)$$

where $\Lambda = \Delta_1 + \sigma_1^2 \mathbf{I}_N$, $\mathbf{H}_{(\mathcal{U})}$ is channel matrix from all mobiles in the set \mathcal{U} to the BS and $\Delta_1, \Delta_2, \xi_{r,k}^2$ are defined in the previous sections.

4.6 Compress-and-Forward Relaying

In the CF relaying strategy, the RSs compress their observations and send the corresponding bin indexes to the BS. With the CF relaying as the RS-to-BS links improve, the system mimics single-input multiple-output (SIMO) performance

³One might also consider a system model where the system is loaded such that multiple distinct active MSs, instead of one, are selected by each RS. With this setting it might be possible to increase the sum-rate performance since each MS comes with their power. The sum-rate performance also depends on the system's operating regime, e.g., noise limited or interference limited regimes, and the relaying capabilities, e.g., RS-to-BS link qualities and decoding complexity.

[18]. Hence, the scenario we consider here is well suited for usage of CF relaying. In [23] and [81], distributed source coding followed by compression is considered for parallel relay networks for Gaussian and phase fading cases, respectively.

In this section, we assume that each RS knows its corresponding backward CSI and each BS knows just the CSIs for the MSs that are located in its cell, and it treats the interfering signals coming from the surrounding cells as Gaussian random variable with zero mean and some variance depending on the channel gain between each BS and interfering nodes.

The RSs first invert the channel gains to have unit-variance i.i.d. ZMCSCG source \tilde{y}_i , i.e.,

$$\tilde{y}_k = A_k y_k, \quad k = 1, 2, \dots, K \quad (4.41)$$

where

$$A_k = \sqrt{\frac{1}{\mathbb{E}[|y_k|^2 | \mathbf{f}_k]}} = \sqrt{\frac{1}{\|\mathbf{f}_k\|^2 P_s + \xi_{r,k}^2 + \sigma_r^2}}. \quad (4.42)$$

Then, the RSs generate the quantized codewords, without claiming optimality, according to the distribution $f(\hat{y}_k | \tilde{y}_k) \sim \mathcal{CN}(\tilde{y}_k, D_k)$, where D_k is the noise variance due to the distortion in reconstructing \tilde{y}_k as in [82], i.e.,

$$\hat{y}_k = \tilde{y}_k + z_{d,k} \quad (4.43)$$

where $z_{d,k} \sim \mathcal{CN}(0, D_k)$ for $k = 1, 2, \dots, K$. The BS jointly decodes the MSs messages using the quantized signals in (4.43) which have the following compact form

$$\begin{aligned} \hat{y}_k &= \tilde{y}_k + z_{d,k} \\ &= A_k \mathbf{f}_k^T \mathbf{s} + A_k \chi_k^{(R)} + A_k z_k + z_{d,k} \end{aligned} \quad (4.44)$$

and putting all of the representations together, we have

$$\hat{\mathbf{y}} = \mathbf{A} \mathbf{F} \mathbf{s} + \mathbf{A} \boldsymbol{\chi}^{(R)} + \mathbf{A} \mathbf{z} + \mathbf{z}_d \quad (4.45)$$

where $\mathbf{A} = \text{diag}\{A_1, A_2, \dots, A_K\}$ and $\mathbf{D} = \mathbb{E}[\mathbf{z}_d \mathbf{z}_d^H] = \text{diag}\{D_1, D_2, \dots, D_K\}$.

We can combine (4.45) with the direct received signal (4.20) at the BS and get the following form

$$\begin{aligned} \bar{\mathbf{y}} &= \begin{bmatrix} \mathbf{y}_{D_1} \\ \hat{\mathbf{y}} \end{bmatrix} = \begin{bmatrix} \mathbf{H} \\ \mathbf{A} \mathbf{F} \end{bmatrix} \mathbf{s} + \begin{bmatrix} \chi^{(1)} + \mathbf{z}^{(1)} \\ \mathbf{A} \boldsymbol{\chi}^{(R)} + \mathbf{A} \mathbf{z} + \mathbf{z}_d \end{bmatrix} \\ &= \bar{\mathbf{H}} \mathbf{s} + \bar{\mathbf{z}} \end{aligned} \quad (4.46)$$

where $\bar{\mathbf{H}} \in \mathbb{C}^{(N+K) \times M}$ is the equivalent channel matrix and $\bar{\mathbf{z}} \in \mathbb{C}^{(N+K) \times 1}$ is the equivalent noise and interference vector seen at the BS which has the following covariance matrix

$$\Lambda = \mathbb{E}[\bar{\mathbf{z}} \bar{\mathbf{z}}^H] = \begin{bmatrix} \Lambda_1 & 0 \\ 0 & \mathbf{A} (\Delta_r + \sigma_r^2 \mathbf{I}_N) \mathbf{A}^H + \mathbf{D} \end{bmatrix} \in \mathbb{C}^{(N+K) \times (N+K)}. \quad (4.47)$$

Considering (4.46), the instantaneous achievable sum-rate (in [bit/sec]) for CF relaying strategy, where all RSs participate in the communications between the MSs and the BS, is given by

$$\begin{aligned}
 R_{CF} &= I(s_{(\mathcal{M})}; \hat{y}_{(\mathcal{X})}, \mathbf{y}_{D_1}) \\
 &= W_1 \log_2 \det \left(\mathbf{I}_M + P_s \bar{\mathbf{H}}^H \Lambda^{-1} \bar{\mathbf{H}} \right) \\
 &= W_1 \log_2 \det \left(\mathbf{I}_M + P_s \mathbf{H}^H \Lambda_1^{-1} \mathbf{H} + \mathbf{F}^H \mathbf{A}^H (\mathbf{A} (\Delta_r + \sigma_r^2 \mathbf{I}_N) \mathbf{A}^H + \mathbf{D})^{-1} \mathbf{A} \mathbf{F} \right).
 \end{aligned} \tag{4.48}$$

The average achievable sum-rate for the CF relaying is given by

$$\bar{R}_{CF} = \mathbb{E}_{\{\mathbf{H}, \mathbf{F}, \mathbf{G}\}} [R_{CF}]. \tag{4.49}$$

Assuming that each RS wants to send the compressed signal to the BS with rate R_k , $k = 1, 2, \dots, K$, according to the conditional distribution $f(\hat{y}_k | \tilde{y}_k)$, we have the following constraints

$$I(\hat{y}_{(\mathcal{J})}; y_{(\mathcal{J})} | y_{D_1}, \hat{y}_{(\mathcal{J}^c)}) \leq \sum_{k \in \mathcal{J}} R_k, \quad \forall \mathcal{J} \subseteq \mathcal{K} \tag{4.50}$$

where LHS of the above expression can be calculated as follows, assuming Gaussian signalling at the MSs:

$$\begin{aligned}
 &I(\hat{y}_{(\mathcal{J})}; y_{(\mathcal{J})} | \mathbf{y}_{D_1}, \hat{y}_{(\mathcal{J}^c)}) \\
 &= h(\hat{y}_{(\mathcal{J})} | \mathbf{y}_{D_1}, \hat{y}_{(\mathcal{J}^c)}) - h(\hat{y}_{(\mathcal{J})} | y_{(\mathcal{J})}, \mathbf{y}_{D_1}, \hat{y}_{(\mathcal{J}^c)}) \\
 &= I(s_{(\mathcal{M})}; \hat{y}_{(\mathcal{J})} | \mathbf{y}_{D_1}, \hat{y}_{(\mathcal{J}^c)}) + h(\hat{y}_{(\mathcal{J})} | s_{(\mathcal{M})}, \mathbf{y}_{D_1}, \hat{y}_{(\mathcal{J}^c)}) - h(\hat{y}_{(\mathcal{J})} | y_{(\mathcal{J})}, \mathbf{y}_{D_1}, \hat{y}_{(\mathcal{J}^c)}) \\
 &= I(s_{(\mathcal{M})}; \hat{y}_{(\mathcal{J})} | \mathbf{y}_{D_1}, \hat{y}_{(\mathcal{J}^c)}) + h(\hat{y}_{(\mathcal{J})} | s_{(\mathcal{M})}, \mathbf{y}_{D_1}, \hat{y}_{(\mathcal{J}^c)}) - h(\hat{y}_{(\mathcal{J})} | s_{(\mathcal{M})}, y_{(\mathcal{J})}, \mathbf{y}_{D_1}, \hat{y}_{(\mathcal{J}^c)}) \\
 &= I(s_{(\mathcal{M})}; \hat{y}_{(\mathcal{J})} | \mathbf{y}_{D_1}, \hat{y}_{(\mathcal{J}^c)}) + I(\hat{y}_{(\mathcal{J})}; y_{(\mathcal{J})} | s_{(\mathcal{M})}, \mathbf{y}_{D_1}, \hat{y}_{(\mathcal{J}^c)}) \\
 &= I(s_{(\mathcal{M})}; \hat{y}_{(\mathcal{X})}, \mathbf{y}_{D_1}) - I(s_{(\mathcal{M})}; \hat{y}_{(\mathcal{J}^c)}, \mathbf{y}_{D_1}) + I(\hat{y}_{(\mathcal{J})}; y_{(\mathcal{J})} | s_{(\mathcal{M})}, \mathbf{y}_{D_1}, \hat{y}_{(\mathcal{J}^c)})
 \end{aligned} \tag{4.51}$$

where the mutual information term $I(s_{(\mathcal{M})}; \hat{y}_{(\mathcal{X})}, \mathbf{y}_{D_1})$ is given by (4.48) and

$$I(s_{(\mathcal{M})}; \hat{y}_{(\mathcal{J}^c)}, \mathbf{y}_{D_1}) = W_1 \log_2 \det \left(\mathbf{I}_K + P_s \mathbf{H}^H \Lambda_1^{-1} \mathbf{H} + \sum_{k \in \mathcal{J}^c} \frac{A_k^2 \mathbf{f}_k^* \mathbf{f}_k^T}{A_k^2 (\xi_{r,k}^2 + \sigma_r^2) + D_k} \right)$$

and

$$I(\hat{y}_{(\mathcal{J})}; y_{(\mathcal{J})} | s_{(\mathcal{M})}, \mathbf{y}_{D_1}, \hat{y}_{(\mathcal{J}^c)}) = \sum_{k \in \mathcal{J}} W_1 \log_2 \left(1 + \frac{\sigma_r^2}{D_k} \right).$$

To be able to send compressed signals reliably to the BS, the RSs should select the compression rates, R_k , according to the MAC rate region on the second hop. We note that the bandwidth allocated to second hop is W_2 [Hz].

For the scheme considered here, the achievable MAC rate region on the second hop is given by [1]

$$\sum_{k \in \mathcal{J}} R_k \leq I(x_{(\mathcal{J})}; \mathbf{y}_{D_2} | x_{(\mathcal{J}^c)}), \quad \forall \mathcal{J} \subseteq \mathcal{K}. \quad (4.52)$$

Assuming that all RSs operate on equal-rate point inside the achievable rate region, i.e. $R_1 = R_2 = \dots = R_K = R_c$, we have the following individual rates for each RSs:

$$\begin{aligned} R_c &= \frac{W_2}{K} I(x_{(\mathcal{K})}; \mathbf{y}_{D_2}) \\ &= \frac{W_2}{K} \mathbb{E} \left[\log_2 \det \left(\mathbf{I}_N + P_r \mathbf{G} \mathbf{G}^H (\Delta_2 + \sigma_2^2 \mathbf{I}_N)^{-1} \right) \right]. \end{aligned} \quad (4.53)$$

Provided that we select the quantization rates according to the MAC limits, we can represent the RS received signals with certain fidelity at the BS. As our aim is to find the sum-of-rates from the MSs to the BS, having multiple independent representations of the received signals at the RSs will help us to improve the network capacity.

4.7 Quantize-and-Forward Relaying

In QF relaying strategy, the RSs do not exploit side information of the received signal seen at the BS. Hence, compression done at the RSs boils down to the standard rate-distortion scheme. We note that higher performance gains are achievable by exploiting correlations between the compressed signals at the RSs (distributed source coding [58]) and the received signal at the BS, e.g. the CF relaying. However, from a system designer point of view the CF relaying is more complicated than the QF counterpart. Thus, in the numerical results section we will just analyze QF relaying performance.

As detailed in Section-4.2.3, each RS quantizes its received signal according to a rate that falls in the MAC rate region given by (4.15).

As in the CF relaying case, the RSs first invert the channel gains to have unit-variance and then generate the quantized codewords according to the distribution $f(v_k | \tilde{y}_k) \sim \mathcal{CN}(\tilde{y}_k, D_k)$, where D_k is the noise variance. Let each RS send its compressed signal to the BS with rate R_k , where (see (4.15))

$$R_k = I(\tilde{y}_k; v_k) = W_1 \log_2 \left(1 + \frac{1}{D_k} \right) \quad (4.54)$$

or in terms of distortion

$$D_k = \frac{1}{2^{R_k/W_1} - 1}, \quad \forall k \in \{1, 2, \dots, K\}. \quad (4.55)$$

As in the CF relaying, we assume that all of the RSs operates on the *equal-rate point* inside the achievable rate region, i.e. $R_1 = R_2 = \dots = R_K = R_c$, (see (4.53)). Then, corresponding distortion values, given by (4.15), and achievable sum-rates, given by (4.48), can be calculated for the QF relaying strategy.

4.8 Conventional Cellular Systems

In this section, we look at both conventional cellular system where the BS antennas are co-located, and ideal DAS where the antennas are distributed in space and connected to the BS via noiseless links. We note that for both cases there is no RS in the system anymore. The ideal DAS should provide better performance due to different shadowing and path-loss at each antenna [56]. These two schemes provide benchmark for relaying strategies considered above.

4.8.1 Co-Located Antenna Cellular System

Each BS is assumed to have N co-located antennas. Considering UL communication, the received signal vector at the central-cell BS is given by

$$\mathbf{y}_D = \mathbf{H} \mathbf{s} + \chi^{(1)} + \mathbf{z} \quad (4.56)$$

where $\mathbf{y} \in \mathbb{C}^{N \times 1}$ is the received signal at the central-cell BS, $\mathbf{z} \in \mathbb{C}^{N \times 1}$ is the noise vector, $\mathbf{s} \in \mathbb{C}^{N \times 1}$ is the transmitted signal vector. Note that for the conventional case only N active MSs are present in each cell.

Considering the above conventional cellular system, the MAC sum-rate is given by

$$\bar{R}_{conv} = \mathbb{E}_{\{\mathbf{H}\}} \left[W_{tot} \log_2 \det \left(\mathbf{I} + P_s \mathbf{H} \mathbf{H}^H \Lambda_1^{-1} \right) \right] \quad (4.57)$$

where

$$\Lambda = \mathbb{E} \left[\chi^{(1)} \chi^{(1)H} \right] + \mathbb{E} [\mathbf{z} \mathbf{z}^H] = \Delta_1 + \sigma_d^2 \mathbf{I}_N. \quad (4.58)$$

with $\sigma_d^2 = W_{tot} N_0$.

4.8.2 Ideal Distributed Antenna System (DAS)

For this case, we assume that the antennas are placed at the same locations as the RSs⁴. Comparing to conventional co-located antenna case, the only difference is in channel characteristics. Each channel element for this case is the same as in the relaying schemes and is given by (4.16). With this channel characteristics, corresponding sum-rate expression can be calculated as in the co-located antenna case.

Remark 29. *We note that the achievable sum-rate expression for the ideal DAS is the same as the first term of the outer bound (4.6) which corresponds to the BC cut.*

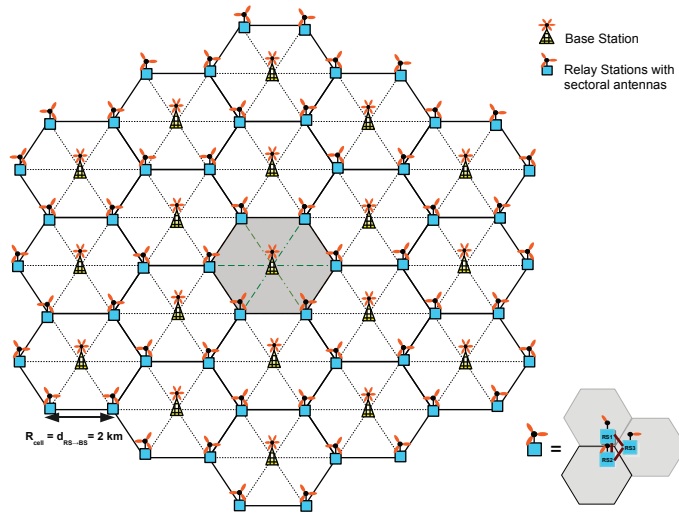


Figure 4.3: A RS deployment scenario in $B = 19$ cells network. The BSs have $N = 6$ sectoral antennas each directed to a unique RS. Each RS consists of 3 RF elements each serving a unique cell.

4.9 Simulation Setup

4.9.1 User Loading

Once the general expressions of sum-rates are given, for numerical analysis we will introduce a naive user loading procedure, which might be thought of as a link-layer scheduler. This will enable some relaying strategies, e.g. the DF relaying, to reveal their potentials in enhancing the system performance. We assume the same user loading procedure as in [33] where MSs are uniformly spread across the cells and each of them is assigned to the antenna, e.g. the BS or RSs, with the *strongest* received signal strength provided that the antenna is not already serving another MS. This procedure is continued until all network antennas are loaded with a single MS. With this procedure there will be the same number of active MSs in each cell as the total receiving antennas. Hence, the network can serve more MSs simultaneously, as the number of antennas in the system increases. As explained in [33], the system might benefit from a *spatial-reuse* gain provided by the presence of spatially distributed RSs.

Since we assume N sectoral antennas at the BSs and single (omni or sectoral antennas) antenna at the RSs, the total number of active MSs in the each cell will be $M = N + K$ where K is the number of deployed RSs. Note that for conventional cellular scheme only N MSs are selected to be active.

⁴Note that optimal antenna placement is a tough issue that is out of scope of this paper.

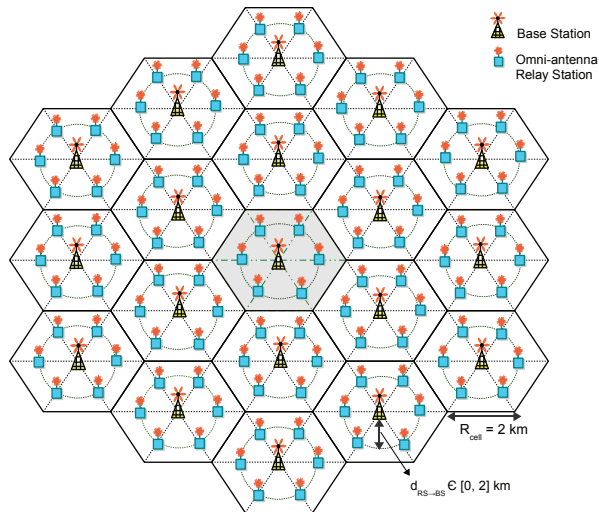


Figure 4.4: A RS deployment scenario in $B = 19$ cells network. The BSs have $N = 6$ sectoral antennas each directed to a unique RS. Each RS is equipped with a single omnidirectional antenna.

4.9.2 Parameters

In this section, we give *two* cellular system setups which differ from each other by the way the RSs are positioned and the antenna pattern they used. Specifically, for the first RS deployment scenario, the RSs are placed at the cell-edges, along the main lobe of each BS sectoral antenna, and equipped with a single *sectoral* antenna directed towards the BS, see Figure 4.3. The main reason we select this set-up for evaluation is due to the significant interference elimination inherent in the system design. For the second RS deployment scenario, the RSs equipped with a single *omnidirectional* antenna are uniformly placed on circle around the BS, see Figure 4.4. The main reasons we use this setup are to see the effects of interference added to the system with RSs and positioning of RSs.

For both cases we consider a multi-cell wrap-around cellular system with K RSs where the BSs are equipped with N directional antennas and $M = K + N$ single omni-antenna MSs are randomly and uniformly distributed on the cell area (as explained in Section-4.9.1).

All channel gains include path-loss, shadowing and antenna gain terms which is given by

$$\Upsilon(\text{dB}) = -PL(\text{dB}) + G_{TX} + G_{RX} + \xi \quad (4.59)$$

where $G_{TX}[\text{dB}]$ is the transmit antenna gain, $G_{RX}[\text{dB}]$ is the receiver antenna gain, and the log-normal shadowing term, ξ , is a random variable with a normal

distribution with mean of 0[dB] and standard deviation of σ_{sh} [dB]. It is assumed that each link undergoes path-loss according to simplified COST 231 model [83], given by

$$PL(\text{dB}) = 138 + 39.6 \log_{10}(d) \quad (4.60)$$

where d is distance between communicating nodes in km . All parameters used in the simulations are specified in Table-4.1.

For the terminals equipped with sectoral antennas, we assume the following parabolic antenna pattern

$$A(\theta) = G_c - \min \left\{ 12 \left(\frac{\theta}{\theta_{3dB}} \right)^2, A_{max} \right\} \quad (4.61)$$

where $A(\theta)$ is the antenna gain in dBi in the direction θ , $-180 \leq \theta \leq 180$, θ_{3dB} is the 3 [dB] beam-width, A_{max} is the maximum attenuation and G_c [dBi] is the antenna gain at zero degree horizontal angle. The antenna gain pattern is shown in Figure 4.5 for $A_{max} = 20$ [dBi] and $\theta_{3dB} = 30$.

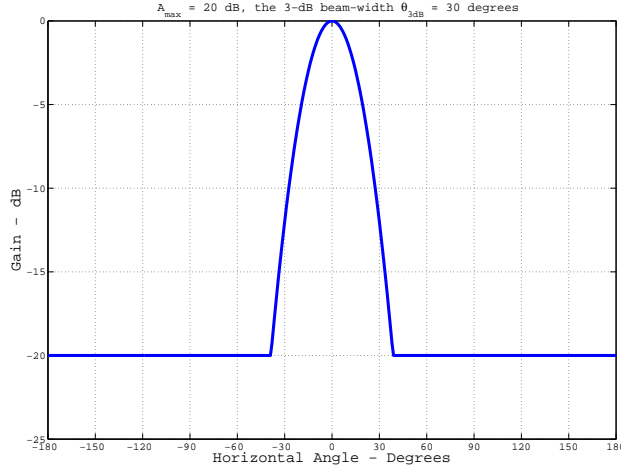


Figure 4.5: Antenna gain pattern for $A_{max} = 20$ dB and $\theta_{3dB} = 30$ as a function of the horizontal angle.

4.10 Numerical Results

In this section, we give some numerical results for the achievable average sum-of-rates for the schemes described above for the two system setups.

Common to the both setups, hexagonal cellular layout with $B = 19$ cells is considered with the cell radius $R_{cell} = 2$ km. The BSs are assumed to have N

sectoral antennas each directed to a unique RS. $M = K + N$ MSs with single omnidirectional antenna are randomly and uniformly distributed in each cell. All channel gains include path-loss, shadowing and antenna gain terms. All parameters used in the simulations are specified in Table-4.1.

4.10.1 Relays with Sectoral Antennas

In this section, we consider the RS deployment scenario illustrated in Figure-4.3 where RSs are equipped with directional antennas with main lobe towards the BSs.

In Figure 4.6, we plot the achievable average sum-of-rates in [bits/sec] for the MSs in the central cell with respect to BW allocations ratios, F , for the relay transmit power $P_r = 10$ [dBW] and fixed MS transmit powers $P_s = \{-5, 0\}$ [dBW]. In this plot, it can be seen that resource allocation, here bandwidth, have profound influence on the sum-rates achieved by the DF and QF relaying strategies. For both cases, the best sum-rates are achievable in the low BW ratio regime, i.e., allocating more bandwidth to the channels from the MSs to the RSs and the BSs.

In Figure 4.7, we plot the achievable sum-rates with respect to the relay transmit power, P_r in [dBW] for fixed MS transmit power $P_s = 0$ [dBW] and BW ratio $F = W_2/W_1 = 0.3$. The system performance improvement over the no relay deployment case are about 10% and 20% for the DF and QF relaying, respectively. At low RS power, the AF relaying performs worse than the conventional case. For this specific parameters, we also plot the outer bound corresponding to the system model we consider. Regarding this, the QF might be a promising relaying strategy to utilize in cellular systems as providing close to optimal performance. We also note that with increasing RS power, the sum-rate performance of both DF and AF saturates.

4.10.2 Relays with Omnidirectional Antennas

In this section, we consider the RS deployment scenario illustrated in Figure 4.4 where RSs are equipped with omnidirectional antennas and located uniformly on a circle, with a radius $d_{RS \rightarrow BS}$, around BSs.

In Figure 4.8, we demonstrate the achievable average sum-of-rates in [bits/sec] for the MSs in the central cell with respect to BW allocations ratios, F , where the transmit powers of the RSs and MSs are fixed to $P_r = 10$ [dBW] and $P_s = -5$ [dBW], respectively, and the RSs are located uniformly on a circle of radius $d_{RS \rightarrow BS} = 1.2$ km. Similar behaviors as in the previous setup are observed.

In Figure 4.9, for fixed $P_r = 10$ [dBW], $P_s = -5$ [dBW] and BW ratio $F = W_2/W_1 = 0.3$ we plot the achievable average sum-of-rates with respect to the distance between the RSs and the BS. For these selected parameters, the best location for RSs, considering the achievable sum-rate as our figure of merit, is about a distance ~ 1.2 km from the BSs. When the RSs are positioned close to the cell-edge the system will be interference limited due to the omnidirectional

antenna utilization at the RSs, and the achievable performance will be lowered. For the case where the RSs are located close to the BSs, the MSs at the cell-edge will suffer due to the path-loss and inter-cell interference effects. And hence the system will be insufficient to provide coverage with high QoS requirements.

In Figure 4.10, we plot the achievable average sum-rates with respect to the RS transmit power, P_r , for fixed MS transmit power $P_s = -5$ [dBW], BW ratio $F = W_2/W_1 = 0.2$ and $d_{RS \rightarrow BS} = 1.2$ km. Although the DF and AF relaying strategies achieve better rates than the no relay case, increasing RS power does not help them a lot. This might be explained as the system performance is limited by access links from MSs to the BSs and RSs. On the other side, for the QF relaying we see a linear increase in achievable sum-rate with the RS transmit power. We may conclude that, also for this RS deployment scenario, one should prefer the QF relaying strategy for cellular UL communications. This result is, to some extent, parallel to the insights given in [17, 18].

4.11 Conclusions

In this chapter, we consider relay-aided cellular UL communications under inter-cell interference. Assuming orthogonal frequencies for the MS-to-RS and RS-to-BS links, the achievable average sum-of-rates are analyzed for the AF, DF, CF and QF relaying strategies and compared with two well-known cellular systems, namely the conventional cellular system and the ideal DAS.

We observe that system parameter selection, such as positions of relay stations and the antenna patterns they used, plays an important role on the achievable rate performance. Given the system parameters, resource allocation on the access and backhauling links plays a crucial role on the system performance, as well. Among all relaying strategies, we see that the CF is the most favorable one as harnessing the potentials offered by multi-hop relaying.

Although we provide some analysis, a thorough examination of relay positioning in cellular systems is also a crucial topic to address. One might also look at the fairness issues since the one of the reasons for relaying is to stabilize the system load. To this end, our proposed procedure in [84], based on successive interference cancellation (SIC), might be improved.

Table 4.1: Simulation Parameters

Cell layout	Hexagonal (B=19 cells wrap-around)
Link Analysis	Uplink (UL)
Cell radius	$R_{cell} = 2$ km
RSs per cell	$K = 6$
MSs per cell	$M = 12$
Antenna Type	$N = 6$ sectoral antennas at BSs 1 sectoral or omni antenna at RSs 1 omnidirectional antenna at MSs
Antenna Pattern	parabolic with $\theta_{3dB} = 60^\circ$ and $A_{max} = 20$ [dBi] for all BS and RS
Antenna Gains, in [dBi]	$G_{BS} = 15, G_{RS} = 10, G_{MS} = 0$
Boltzmann constant	$k_B = 1.38 \cdot 10^{-23}$
Operating temperature	$T = 290$ Kelvin
Band-width (first hop)	$W_{tot} = 20$ [MHz]
Rician fading factor	10[dB] (only the links from RS to BS)
Log-normal Shadowing	0 [dB] mean and $\sigma_{sh} = 2$ [dB] (RS to BS) 0 [dB] mean and $\sigma_{sh} = 8$ [dB] (RS and MS to BS)

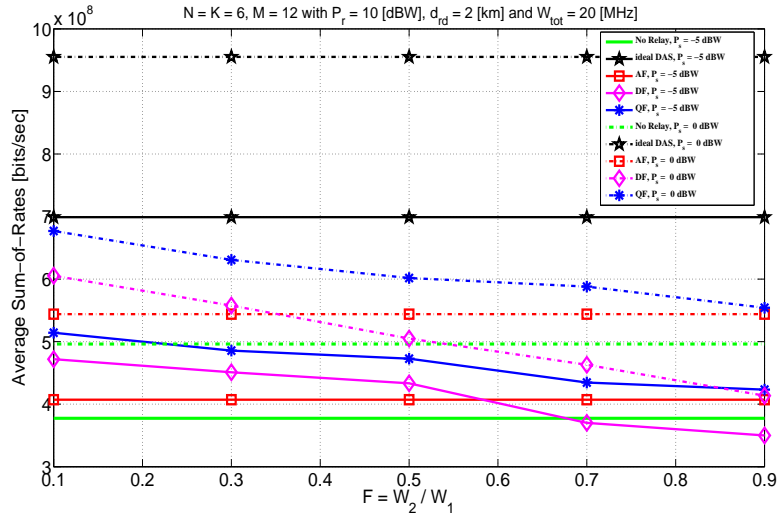


Figure 4.6: The average sum-of-rates [bits/sec] versus $F = W_2/W_1$ for fixed $P_s = \{-5, 0\}$ [dBW] and $P_r = 10$ [dBW]. The RSs are located at the cell-edges.

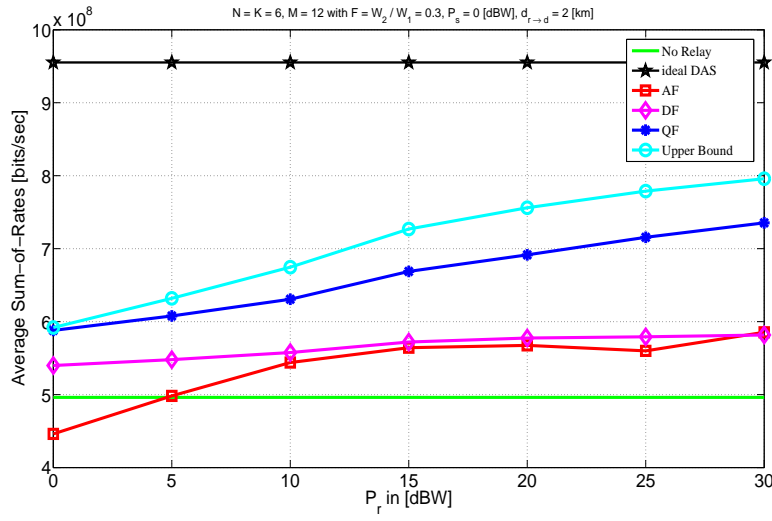


Figure 4.7: The average sum-of-rates with respect to P_r for fixed $P_s = 0$ [dBW] and $F = W_2/W_1 = 0.3$ where the RSs are located at the cell-edges.

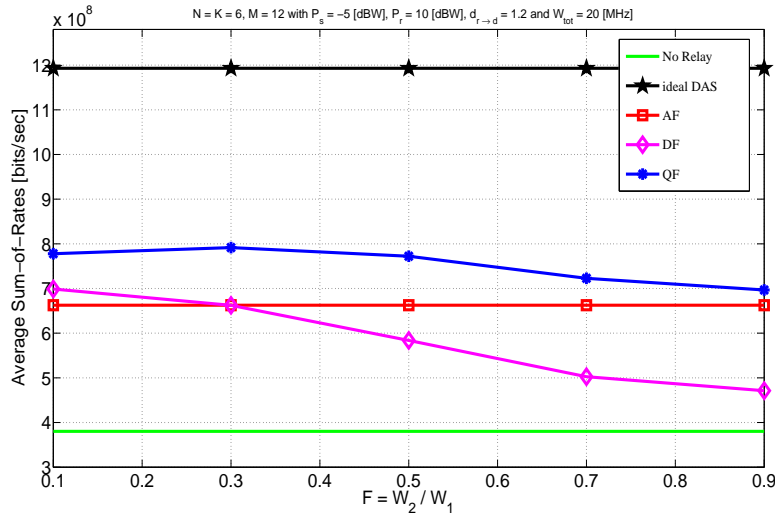


Figure 4.8: The average sum-of-rates [bits/sec] versus bandwidth ratio, F for $P_s = -5$ [dBW] and $P_r = 10$ [dBW]. The RS-to-BS distance is $d_{RS \rightarrow BS} = 1.2$ km

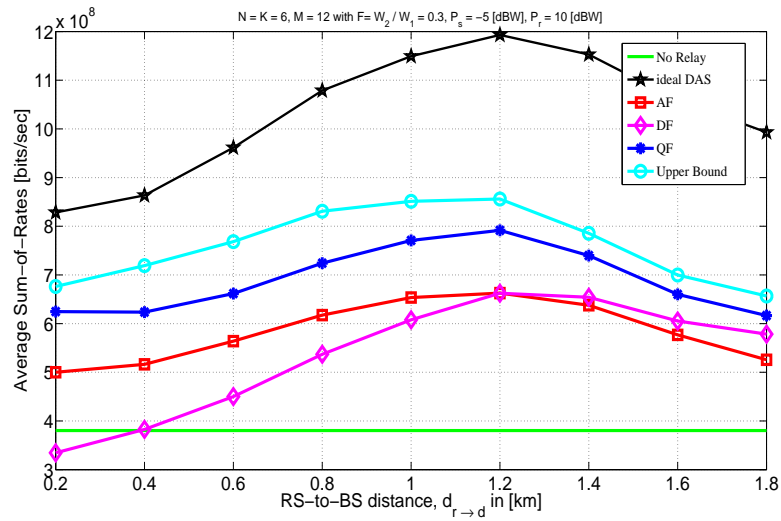


Figure 4.9: The average sum-of-rates [bits/sec] versus the RS-to-BS distance $d_{RS \rightarrow BS}$ for fixed $P_s = -5$ [dBW], $P_r = 10$ [dBW] and $F = W_2/W_1 = 0.3$.

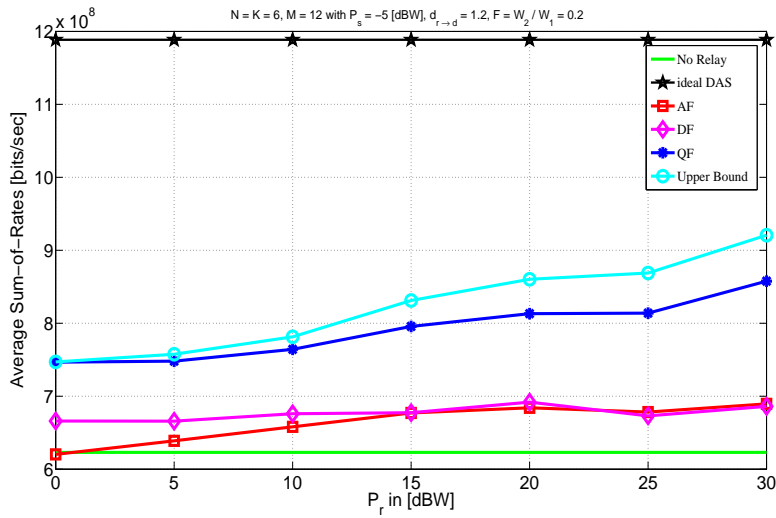


Figure 4.10: The average sum-of-rates with respect to P_r for fixed $P_s = -5$ [dBW] and $F = W_2/W_1 = 0.2$ where the RS-to-BS distance is $d_{RS \rightarrow BS} = 1.2$ km.

Chapter 5

Relay Deployment in Cellular Downlink Communications

5.1 Introduction

The research led to this chapter was conducted during my internship at Bell-Labs Alcatel-Lucent.

In the last years, wireless relay networks have attracted much attention, since they can provide better coverage and/or higher network throughput, and hence improve the overall system performance [12, 13, 15, 17, 18]. When multiple relays are available, they can be further exploited to obtain macroscopic diversity, multiplexing gain. In other words, they can be utilized to further combat fading and improve coverage, link quality and system capacity. Different relaying strategies, mainly AF, DF and CF relaying, have been widely studied to improve the spectral efficiency and system performance. The relays (RSs) are often assumed to be HD (half-duplex), since FD (full-duplex) RSs are difficult and expensive to implement. This, however, generates a pre-log factor of 1/2 for the overall system throughput and may therefore limit the achievable spectral efficiency.

Recently, a big effort has been spent on relay-assisted infrastructure based networks due to the potential improvements in system performance provided by RSs [2–4, 33, 34]. Also, the impact of limited-capacity backhaul on both multi-cell processing and mobile station (MS) cooperation for the UL and the DL for non-fading Gaussian scenarios have been studied in [56, 57, 72, 73].

The main factors that limit the gain achievable in relay-aided cellular systems are:

- The RS-to-BS (base station) link, that must be able to support the amount of data of all the MSs associated to a given RS.
- The efficient exploitation of the spatial reuse, by enabling multiple MSs to be served at the same time by different RSs without degrading the performance of individual MSs.
- The effect of the interference, that can limit the relaying gains if an appropriate coordination is not introduced in the system, by means of centralized or distributed-cooperative algorithms.
- The effect of the feedback overhead, especially in centralized solutions that require an estimate of the channel state information (CSI) at the BS side.

5.1.1 Related Work

References [4], [33] and [35] tackle some of the issues listed above. In [4], a centralized DL scheduling scheme is proposed, that guarantees the stability of the MS queues for the largest set of arrival rates and achieves a significant gain with respect to a system without RSs. It has been also shown that by increasing number of RSs and multi-hops the achievable gain boosts up due to the increasing reuse efficiency in the system, which is achieved by simultaneous multiple transmission. However, with more RS in the system the interference will be much more and this will limit the system performance. Hence, one should be aware of the interference associated with adding extra RSs into the system. In [33] the capacity benefits of in-band backhaul relaying for cellular UL communications is studied under the assumption of a common maximum rate achievable by all the users in the network and of orthogonal separation of resources between BS to RSs links and BS/RSs to MSs links. They proposed a relaying scheme to exploit full *spatial-reuse* in the system which increase with increasing number of HD RSs, wherein DF relaying strategy is used. Simulation results show the benefit of the proposal with respect to the base line without RSs. Similarly, in [34] different communication modes are proposed in order to increase spatial reuse (i.e., increasing spectral efficiency) in a cellular system for the cases of one and two RSs in each cell sector with one- or two-hop transmission. Also, the optimal assignment of the proposed modes to the MSs is provided. In [35], the power saving collaborative relaying schemes are proposed for cellular DL communications systems with HD low-power RSs. There they pointed out that coordinated transmission should be a promising solution to tackle the interference effect which is a big obstacle for power saving.

5.1.2 Motivation for Relaying in Cellular Systems

Above some recent works on RS deployment in cellular networks is summarized. It can be easily seen that there are many open problems needed to be solved. In

relay-assisted cellular systems, the main factors that limit the achievable gains are the quality of the link between RSs and BS, the multiplexing-loss due to multi-hopping, the effect of the interference which increases with the number of deployed RSs, and the feedback overhead especially in centralized solutions where an estimate of the CSI is required at the BS side.

In this section, some of RS deployment issues are going to be pointed out regarding the realistic instruments in wireless cellular networks. Due to realistic assumptions, in this chapter RSs are considered to operate in HD mode, i.e., they can not transmit and receive simultaneously. Whilst deploying RSs in cellular networks, the following issues seem to be promising fields that should be addressed:

- Compared to [33] where the number of MSs is quadrupled in system, we can try to see if the similar gains achievable when number of MSs in relaying case is the same as that of without relaying case (baseline case). With this assumption is it still possible to have full spatial-reuse gain?
- Spatial-Reuse versus Interference: Assuming enough receiving terminals, e.g., MS and/or RSs, the number of simultaneous transmissions is limited by the number of transmitting antennas (BS and/or RSs) at each cell. However, the more simultaneous transmission in the cellular system, the more the interference created within the cells and to the other cells which consequently limits the spatial-reuse gain. Hence, there should be a subtle coordination/control mechanism in the system for getting more profit.
- The cellular relaying scheme proposed in [35] may be improved by utilizing RSs for helping the MSs that are not assigned to them when they finished their missions for their associated MSs.
- Is it better to have sectoral or omnidirectional antennas at RSs? One might predict that using sectoral antennas would provide additional degrees of freedom to avoid inter- and intra- cell interference created by RSs.
- Distributed actions at RSs: Own decision on to be ON or OFF. As we have seen, in the interference limited regime the gains brought by relaying is limited when there is no coordination and cooperation. Also, local cooperation may bring good gains due to leveraging interference in the system.
- Self-organizing RSs: Plug&Play RSs

Considering the problems listed above, in this chapter we propose a *two-level distributed scheduling algorithm* which provides spatial-reuse gain, fairness, throughput improvement and potential interference cancellation via locally coordinated RSs. With this scheduling algorithm we can assure that RS deployment would be easier, cheaper and more flexible.

5.1.3 Our Contributions

In this chapter, we investigate a RS deployment issue in cellular networks for DL communications where we take into account realistic cellular network characteristics in order to fill some gaps of the schemes proposed in [2, 4, 33–36]. Specifically, we focus our attention on a distributed relaying scheme for DL transmissions, where a given MS can be either served by the BS or by a RS (up to two hops are considered). This scheme, as will be detailed in the following sections, requires a reduced amount of feedback with respect to the centralized case, especially when multiple antennas are deployed in each node and a simple scalar feedback is not sufficient. As a result of the reduced feedback requirements the system is more scalable, as new RSs can be deployed where needed. Moreover, by moving the processing towards the RS side, local cooperation between RSs becomes possible. Like in the centralized case considered in [4] (and differently from [33] where the notion of maximum common rate is used), we guarantee user-fairness by making scheduling decisions based on the state of the MSs' queues and on the estimate of instantaneous signal to interference-plus-noise ratios (SINRs). Also, differently from [33], we do not assume an orthogonal separation of resources between BS-to-RS links and BS/RS-to-MS links. The proposed technique works in two phases. In the first phase, the BS makes its scheduling decisions for that time slot taking into account the channel conditions and the RSs and MSs' queue states. The selected destination could be either a RS or an MS. In the second phase, each RS, if it had not been scheduled by the BS in the first phase, schedules a MS taking into account channel conditions and queue states. We study the performance of the proposal by means of a multicell simulator.

5.1.4 Outline of the chapter

This chapter is organized as follows. In Section-5.2 we give the system model considered in this chapter and proceed with a brief review of the centralized algorithm proposed in [4] in Section-5.3. In Section-5.4 we present our proposed technique. In Section-5.5 we describe the system simulator used to assess the performance and some simulation results. Finally, in Section-5.6 we conclude this chapter.

5.2 System Model

We consider a relay-deployed cellular system for DL communication where several fixed RSs are present in each cell and frequency reuse of one is used. Considering wrap-around hexagonal cell-layout, we focus on the cell in center for the performance evaluation. Data packets corresponding to each MS in the cell arrive at the corresponding BS and then are placed in the appropriate queues. The RSs also have queues corresponding to each MS assigned to them where they receive data from the BS via wireless link (there are no backhaul connections between BSs and RSs). We consider *at most* two-hop communication from

the BSs to the MSs as this is provisioned for future cellular systems consisting of RSs. This assumption has the following consequences: there is no link (or communication) between RSs and MSs whether directly receive data from the BS or via one RS. Each MS is assigned to one transmitter, i.e., the BS or one of the RSs. The MSs' assignments can be done in different ways. We are going to use received power at the MS as a metric as explained in the Section-5.5.

For relaying, DF is adopted, which is the best relaying strategy when the BS-to-RS links are better than the other links [18]. Decoding the signal they received, then they retransmit the same data to one of the MSs assigned to them. As will be explained below, the RSs can also make scheduling decisions in our scheme. At the start of each time frame, for centralized scheduling at the BS is assumed to have the knowledge of the instantaneous transmission rates on all links during that frame, and also a knowledge of the sizes of the queues corresponding to each RS at all the transmitters (BS and RSs) in the cell. For decentralized scheduling algorithm, we assume the BS just receives queue state information from each RS. Also, it does not require any instantaneous transmission rates on the links between the RSs and MSs which means a great *feedback reduction* from RSs to the BS.

5.3 Centralized Scheduling Algorithm

In this section, we give a brief overview of the throughput-optimal scheduling algorithm proposed by Harish, *et al.* in [4]. We try to follow the same notation. Note that user loading and assignment is totally different from the one in [4]. As explained before, there are regions corresponding to each transmitter, the BS and the RS, that MSs falling in this region are assigned to the corresponding transmitter.

Differently from [4], we consider at most 2-hop communications, i.e., the RSs can not exchange information. The MSs fallen in the BS region directly receive from the BS, as so the MSs fallen in the RS region just receive data from that RS. Hence, the model considered is much more simple and practical compared to the one in [4]. As we would like to have spatial-reuse opportunity of multi-hopping, there would be multiple concurrent transmission at a given time, i.e., while BS is transmitting to some MSs, some RSs can be transmitting to the MSs at their regions. Moreover, we assume that neither a MS nor a RS receives from more than one source simultaneously.

The set of all transmitters is denoted as $\mathcal{T} = \{1, \dots, N+1\}$, corresponding to the N RSs and the single BS and the set of all MSs is denoted as $\mathcal{M} = \{1, \dots, K\}$. Note that depending on a higher layer scheduler/policy, MSs might be pre-assigned to different transmitters as we consider, without loss of generality, the following partitioning of MSs to the transmitters, i.e., the BS and the RSs. Let the set of all MSs assigned to the BS be $\mathcal{M}_0 = \{1, \dots, K_0\}$, the set of all MSs assigned to the n -th RS be $\mathcal{M}_n = \{1, \dots, K_n\}$ for $n = 1, \dots, N$. If we use assume non-partitioning of the MSs than all sets will be equal to the set \mathcal{M} , also $K_n = K, \forall n$. However, if a geographical partitioning is done, then the sets

of MSs corresponding to each transmitter will be disjoint, i.e., $\mathcal{M}_i \cap \mathcal{M}_j = \emptyset$, $\forall i \neq j$ and $\mathcal{M} = \cup_{i=0}^N \mathcal{M}_i$ where the cardinality of the set $|\mathcal{M}|$ is $K = \sum_{i=0}^N K_i$.

The total number of links, including the links from the BS to MSs and RSs, and links from RSs to MSs, is given by

$$L = N + K_0 + \sum_{i=1}^N K_i = N + K_0 + (K - K_0) = N + K. \quad (5.1)$$

Due to the transmission and reception constraints specified above the actual number of feasible links may be less than L . We use ϕ to denote an arbitrary set of simultaneously active links, and Ω to denote the set of all feasible ϕ . Note that Ω can have at most $2^L - 1$ elements as there are at most $2^L - 1$ possible nonempty sets of simultaneously active links. Number all links in the system (whether feasible or not) from 1 through L . A link l is an ordered pair consisting of an origin (the BS or a RS), denoted $orig(l)$, and a destination (another RS or a MS), denoted $dest(l)$.

Given a set ϕ of simultaneously active links, we denote by $R_l(t; \phi)$ the transmission rate from origin to destination on link $l \in \phi$ at the start of time frame t . For simplicity, the transmission rates are computed from Shannon's formula as

$$R_l(t; \phi) = \log_2 \left(1 + SINR_{orig(l)}^{dest(l)}(t) \right) [bits/sec/Hz] \quad (5.2)$$

where $SINR_{orig(l)}^{dest(l)}(t)$ is the SINR at the destination of this link when receiving from the origin of this link, assuming that all other simultaneously active links (i.e., all other members of ϕ) are interfering. The notation for the rate therefore includes, as a parameter, the set ϕ of simultaneously active links during time frame t .

Let $Q_{BS}^j(t)$ for $j \in \mathcal{M}$ and $Q_{RS,i}^j(t), \forall i$ for $j \in \mathcal{M}_i$ denote the size of the queues at the BS for MS j in the cell and at the i -th RS for MS j assigned to it, respectively, at the start of time frame t . Note that the arrival process of packets for the MSs at the queues of the BS are assumed independent and identically distributed (i.i.d.) from each time frame to the next.

Now we describe the throughput-optimal scheduling policy proposed in [4]. Define for a given set $\phi \in \Omega$ of simultaneously active links in time frame t and $l \in \phi$

$$D_l(t; \phi) = \begin{cases} R_l(t; \phi) Q_{BS}^j(t) & \text{if } orig(l) = \text{BS}, j = dest(l) \in \mathcal{M}_0, \\ R_l(t; \phi) Q_{BS-RS}^i(t) & \text{if } orig(l) = \text{BS}, dest(l) = \text{RS}_i, \\ R_l(t; \phi) Q_{RS,i}^j(t) & \text{if } orig(l) = \text{RS}_i, j = dest(l) \in \mathcal{M}_i, \end{cases} \quad (5.3)$$

where $Q_{BS-RS}^i(t) = \max_{j \in \mathcal{M}_i} \left\{ \max\{Q_{BS}^j(t) - Q_{RS,i}^j(t), 0\} \right\}, \forall i$, and the first case corresponds to the BS transmission to one of its assigned MSs, the second

case corresponds to the BS transmission to i -th RS and the last case is the transmission from i -th RS to one of its assigned MSs.

The optimal set $\phi(t)$ of simultaneously active links for the next time frame is selected from Ω as follows:

$$\hat{\phi}(t) = \arg \max_{\phi \in \Omega} \sum_{l \in \phi} D_l(t; \phi) \quad (5.4)$$

If more than one ϕ achieves the maximum in (5.4), one of them is chosen arbitrarily. If a link l between the BS and the i -th RS is chosen to be active in time frame t , the MS whose packets will be transmitted over this link is

$$j_i^*(t) = \arg \max_{j \in \mathcal{M}_i} \left\{ \max\{Q_{BS}^j(t) - Q_{RS,i}^j(t), 0\} \right\} \quad \text{for } \text{dest}(l) = \text{RS}_i. \quad (5.5)$$

This therefore determines the set of MSs to be scheduled in this time frame.

5.4 Decentralized Scheduling Algorithm

In this section, we propose a *distributed* two-phase scheduling algorithm intended to be suitable for easy and flexible RS deployment in cellular networks. RS deployment should not create big changes in the existing communication structure. Hence, it is unavoidable to consider plug&play RSs in the next generation cellular system due to reasons explained above. We note that the user loading and assignment in the system are the same as before where some MSs are assigned to the BS and some assigned to the RSs depending on the assignment policy we use.

In the first phase of the proposed distributed scheduling algorithm, the BS makes its scheduling decisions for that time slot taking into account the *channel* conditions and the RSs' and MSs' *queue* states. The selected destination could be either a RS or a MS. If the BS schedules a RS, then that RS just switches to receiving mode. In the second phase each RS, if it had not been scheduled by the BS in the first phase, schedules a MS taking into account *channel* conditions and *queue* states. We observe that, as in the centralized scheduling case, the BS and non-receiving RSs transmit at the same time, allowing *full* spatial reuse by utilizing the RSs in an opportunistic fashion. Unlike in the centralized case, here a transmitter set is activated without taking into account the interference generated to the scheduled receivers.

With the distributed scheduling algorithm, the scheduling at the BS can be seen as a conventional single hop cellular system scheduling algorithm with some users associated with multiple queues. And the scheduling at the RSs are exactly the same as the conventional case. Hence, we can say that we are staying compatible with the existing cellular system when deploying RSs.

Following the same notations used in Section-5.3, the description of the first phase (RSs and MSs' scheduling at the BS side) can be given as follows. The total number of links that the BS considers, the links from the BS to MSs and

RSs, is given by

$$L = N + K_0. \quad (5.6)$$

Similar to the centralized scheduling case, we define $D_l(t)$ as

$$D_l(t) = \begin{cases} R_l(t)Q_{BS}^j(t), & \text{if } j = \text{dest}(l) \in \mathcal{M}_0 \\ R_l(t) \max_{j \in \mathcal{M}_i} \left\{ \max\{Q_{BS}^j(t) - Q_{RS,i}^j(t), 0\} \right\}, & \text{if } \text{dest}(l) = \text{RS}_i \end{cases} \quad (5.7)$$

where the first case corresponds to the BS transmission to one of the MSs assigned to it, whereas the second case corresponds to the transmission to the i -th RS. The optimal active link for the next time frame is selected as follows:

$$l^*(t) = \arg \max_{l=\{1,\dots,L\}} D_l(t). \quad (5.8)$$

If a link l between the BS and the i -th RS is chosen to be active in time frame t , the MS whose packets will be transmitted over this link is given by

$$j_{l^*}^*(t) = \arg \max_{j \in \mathcal{M}_i} \left\{ \max\{Q_{BS}^j(t) - Q_{RS,i}^j(t), 0\} \right\} \quad \text{if } \text{orig}(l^*) = \text{RS}_i \quad (5.9)$$

which determines the scheduled MS or RS in this time frame. After the scheduling decision of the BS, at least $N - 1$ RSs, as the BS schedules only one MS at a time due to single antenna assumption, will make their own scheduling independently. We assume that the scheduling decision of the BS is passed to the RSs.

The description of the second scheduling phase (MSs' scheduling at the RSs' side) can be given considering the i -th RS RS_i for $i \in \{1, \dots, N\}$, which is not scheduled by the BS for a given time slot, as follows. There are K_i possible links from the i -th RS to the MSs assigned to it. Let us define $D_{l_i}(t)$ as

$$D_{l_i}(t) = R_{l_i}(t; l^*(t))Q_{RS,i}^j(t), \quad \text{if } j = \text{dest}(l_i) \in \mathcal{M}_i, \quad (5.10)$$

for $l_i = 1, \dots, K_i$ where $R_{l_i}(t; l^*(t))$ is the rate for the link l_i taking into account the scheduling decision of the BS. The optimal active link for the next time frame is selected as follows:

$$l_i^*(t) = \arg \max_{l_i=\{1,\dots,K_i\}} D_{l_i}(t). \quad (5.11)$$

We repeat the same procedure for each RS. We note that for the case of distributed scheduling each RS needs to feedback to the BS only an update of queue values. Unlike in the centralized case, a feedback concerning the CSI is not required. We emphasize that a feedback concerning the CSI can require a considerable amount of bits, especially when multiple antennas are deployed at BS, RS or MS side and a scalar feedback is not sufficient to estimate the SINR of a given link.

Remark 30. *We aim to have the following characteristics in our system model while proposing the above RS deployment scheme in cellular systems: 1) Full spatial reuse with multi-hopping (here we consider two-hop systems), 2) Small amount of feedback exchange between the RSs and the BS, 3) Easy and flexible to deploy and reconfigure plug&play RSs, and 4) Strong RS-to-BS wireless links which play a crucial role on the system performance [33].*

However, while trying to address (some of) these problems by the proposed distributed scheduling algorithm, due to no coordination in the transmissions some RSs may become a strong interferer to others which causes system performance degradation. This problem might be handled by allowing the RSs to coordinate locally. One simple way to mitigate the interference among the RSs is to equip RSs with multiple fixed beams where depending on the channel condition and MS positions each RS switches ON or OFF some of its beams in a coordinated way with the neighboring RSs.

5.4.1 Feedback Reduction with Decentralized Scheduling Algorithm

As we already stressed, one of the main goals in proposing the decentralized scheduling algorithm is to reduce the amount of feedback required at the BS while exploiting the spatial reuse in the system. Note that for dense networks scalability is one of the main issues that need special attention. Suppose there is no user partitioning in the system. Then, in order to be able to perform centralized scheduling the BS needs $L = N + K + NK$ channel coefficient feedback along with the queue states of the RSs. However, for the decentralized scheduling the BS needs only $L = N + K$ channel coefficient feedback. The feedback reduction is pronounced when the terminals have multiple antennas.

5.5 Numerical Results

In this section, we would like to see the performance of the proposed distributed scheduling for relay-deployed cellular systems. A system simulator has been developed with 7 BSs and wrap-around for a DL transmission. N RSs are uniformly placed in the cell with a half cell radius distance from the BS. The K MSs are dropped with uniform probability inside each cell (see Figure 5.1 for an example of a multi-cell setup with 7 BSs, $N = 6$ and $K = 30$ in each cell). All the nodes are assumed to have a single omnidirectional antenna.

The channel model includes path-loss, shadowing, antenna gains, Rice fading for the BSs-to-RS links and Rayleigh fading for the BS-to-MS and RS-to-RS links. We express all channel gains as follows

$$\Upsilon(\text{dB}) = -PL(\text{dB}) + G_{TX} + G_{RX} + \xi \quad (5.12)$$

where G_{TX} [dB] is the transmit antenna gain, G_{RX} [dB] is the receiver antenna gain, and the log-normal shadowing term, ξ , is a random variable with a normal

distribution with mean of 0 [dB] and standard deviation of σ_{sh} [dB]. The path-loss is simulated according to the COST 231 model [83] for a small to medium-sized city, given by

$$PL(\text{dB}) = 46.3 + 33.9 \log_{10}(f_c) - 13.82 \log_{10}(h_b) - a(h_r) + (44.9 - 6.55 \log_{10}(h_b)) \log_{10}(d) \quad (5.13)$$

where f_c is the carrier frequency in MHz, d is distance between the transmitter and the receiver in km; h_b and h_r are the transmitter and the receiver antenna heights above the ground level in meters, respectively. $a(h_r)$ is a correction factor for the receiver antenna height based on the size of the coverage area, given by

$$a(h_r) = (1.1 \log_{10}(f_c) - 0.7) h_r - (1.56 \log_{10}(f_c) - 0.8). \quad (5.14)$$

A new packet arrives at the BS for each MS with equal probability and independently at each time frame with packet length following an exponential distributed with mean μ [bits/sec/Hz] which is the same for all MSs. We define the the total average arrival rate $\mu_{TOT} = K\mu$ (i.e., the overall system load). In the simulations all of the queues are assumed unlimited. The main parameters used in the simulations are specified in Table-5.6.

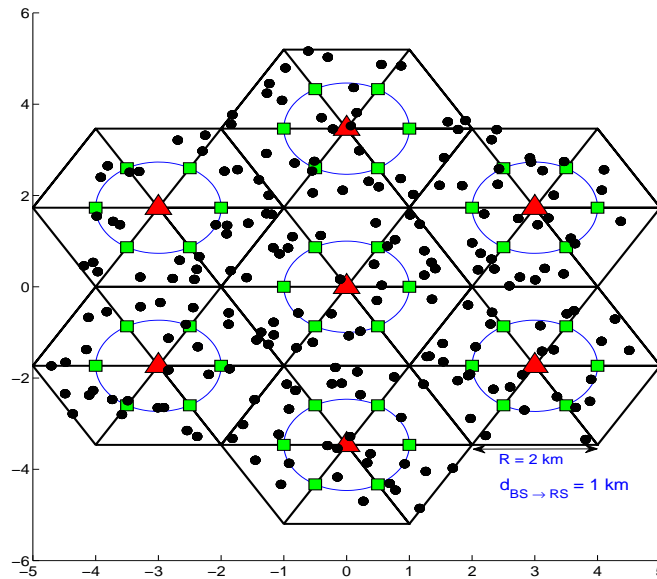


Figure 5.1: Multi-cell hexagonal layout, $R = 2$ km, $d_{BS \rightarrow RS} = 1$ km with $N = 6$ RSs and uniformly distributed $K = 30$ mobile stations.

5.5.1 Simulation Setup

In the simulations, we assume that in each cell all the transmitters, the BS and RSs, can serve any MS in the cell, i.e. there is *no* MS partitioning among the transmitter. Each MS can only select one transmitter. After this assignment some MSs will be directly assigned to the BSs while some other MSs will be assigned to one of the RSs. Packets intended for each MS first arrive at the BS and are placed in the appropriate queues, one for each MS in the cell. Each RS has a queue corresponding to each MSs assigned to itself.

5.5.2 Simulation Methodology

In this subsection, we describe the simulation methodology in order to determine the throughput for both centralized and distributed scheduling algorithms proposed above. Depending on the MSs' positions and queue sizes, scheduling decisions will be different from time to time. Also due to the independent actions at the surround cells the inter-cell interference will have varying second order statistics (we assume only statistical knowledge of interference at the cell under consideration). In order to capture these effects in our simulator we used the following methodology.

Firstly, we consider a single isolated cell, i. e., no inter-cell interference. We randomly drop K MSs with a spatially uniform distribution in this region and calculate the scheduling decisions and assess which transmitters are active (or silent). We repeat this procedure until the statistics of transmitters' activations (probabilities of transmission of each transmitter, the BS and the RS) are stabilized and calculate. Note that these probabilities depend on the power used by the transmitters, system load, RS locations, etc.

We then use these transmitter activation probabilities (depending on the underlined scheduler), and generate inter-cell interference terms by selecting a random transmitter set for the core simulation.

5.5.3 Results

Figure 5.2 shows the average cell throughput [bps/Hz] versus BS transmit power [dBm], for $N = 6$, $K = 30$ and for two different values of total packet arrival rate μ_{TOT} . We consider three set of curves: the solid blue line represents the performance of the centralized algorithm, the dashed red line represents the performance of the distributed algorithm and the dotted green line represents the performance of a system without RSs. We firstly observe that the gap between centralized and distributed schemes is small when the total packet arrival rate is small, while it grows as function of the total packet arrival rate. This is due to the fact that the distributed scheme is limited by the intra-cell interference. For the same reason, the gap between centralized and distributed schemes gets smaller as a function of the BS transmit power: for a low transmit power the percentage of MSs served by the RSs is bigger. We also observe that both the centralized scheme and the distributed schemes outperform the

scheme without RSs for average to high transmission power. On the other hand, at low transmission power and for a high total packet arrival rate value, the conventional scheme outperforms the distributed one in terms of average cell throughput: we will see from Figure 5.4 that such a loss in terms of average cell throughput corresponds to a fairer per-user rate allocation.

Figure-5.3 shows the total average cell throughput versus the total packet arrival rate μ_{TOT} for BS transmit powers $P_{bs} = \{40, 50\}$ [dBm]. We observe that for a low traffic value the performance of the three schemes are similar. For average traffic values the two RS-based schemes give an advantage with respect to the no RS case. For high traffic values the distributed scheme becomes interference limited for lower values of μ_{TOT} than the centralized scheme, as it suffers from both intra- and inter-cell interference, whilst the centralized one only suffers from inter-cell interference.

Figure 5.4 shows the sorted long-term average user rates for $R = 2$ km, $d_{BS \rightarrow RS} = 1$ km, $P_{bs} = \{40, 50\}$ [dBm], $P_{rs} = 35$ [dBm], $\mu_{TOT} = \{4, 8\}$ [bps/Hz], with $N = 6$ relays. The main message of Figure 5.4 is that the proposed scheme is fairer in terms of long-term average user rate and gives a substantial improvement with respect to the conventional scheme without RSs.

5.6 Conclusion and Outlook

We proposed a distributed relaying scheme for DL transmissions, where a given MS can be either served by the BS or by a RS, in an opportunistic way. Such a distributed approach, allow a *reduced* feedback with respect to the centralized case, especially when a simple scalar feedback is not sufficient for estimating the channel quality. As a result of the reduced feedback requirements, the system becomes more *scalable*, and hence new RSs can be deployed without the need of a careful network planning. We also studied the performance of the proposal by means of a multicell simulator.

Table 5.1: Simulation Parameters

Cell layout	Hexagonal (7 cells wrap-around)
Cell radius, R	2 km
BS to RS distance, $d_{BS \rightarrow RS}$	1 km
Number of RSs per cell	$N = 6$
Number of MSs per cell	$K = 30$
Link Analysis	Downlink (DL)
Antenna Type	Omni-Directional
TX and RX Antenna Gains	$G_{TX} = 0$ [dB], $G_{RX} = 0$ [dB]
BS, RS and MS heights	10m, 3m and 1.5m, respectively
Carrier Frequency, f_c	1900 MHz
Thermal noise power, N_0	-121 [dBm]
TX power (BS), P_{bs}	[35, 40, 45, 50] [dBm]
TX power (RS), P_{rs}	35 [dBm]
Rician fading factor	8 [dB] (only for BS to RS links)
Log-normal Shadowing	0 [dB] mean and $\sigma_{sh} = 8$ [dB] (BS to RS) 0 [dB] mean and $\sigma_{sh} = 2$ [dB] (BS and RS to MS)
Packet arrivals	1 [packet/sec/Hz] (constant)
Packet size	exponentially distributed with mean $\mu_{TOT} = \frac{1}{K} [0.1, 0.5, 1, 2, 4, 6, 8, 10]$ [bits/packet]

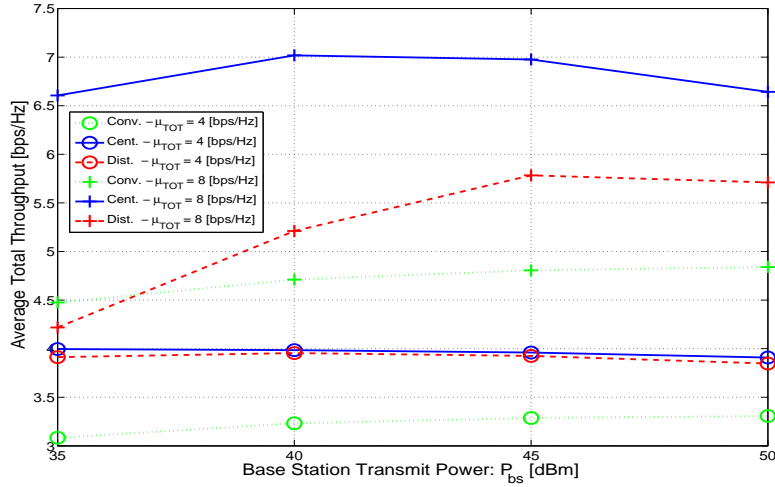


Figure 5.2: Total Average throughput versus BS transmit power, P_{bs} , for total packet arrival rate $\mu_{TOT} = \{4, 8\}$ [bps/Hz], $R = 2$ km, $d_{BS \rightarrow RS} = 1$ km, $P_{rs} = 35$ [dBm] with $N = 6$ RSs and $K = 30$ mobile stations.

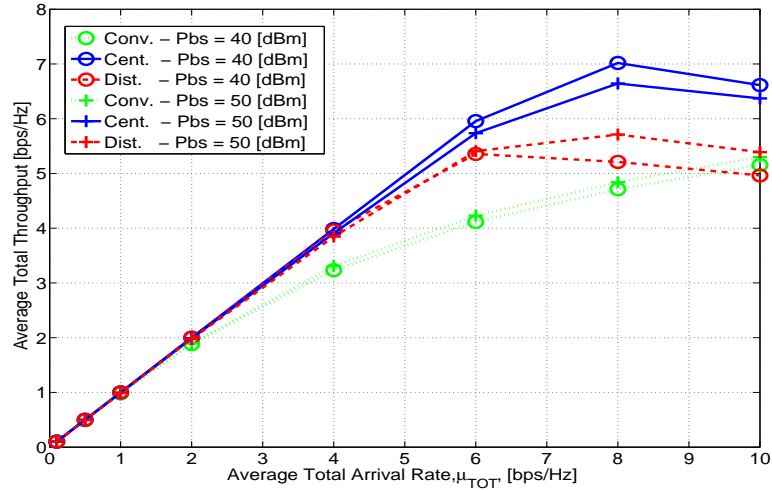


Figure 5.3: Total Average throughput versus total packet arrival rate μ_{TOT} for BS transmit powers $P_{bs} = \{40, 50\}$ [dBm], $R = 2$ km, $d_{BS \rightarrow RS} = 1$ km, $P_{rs} = 35$ [dBm] with $N = 6$ RSs and $K = 30$ mobile stations.

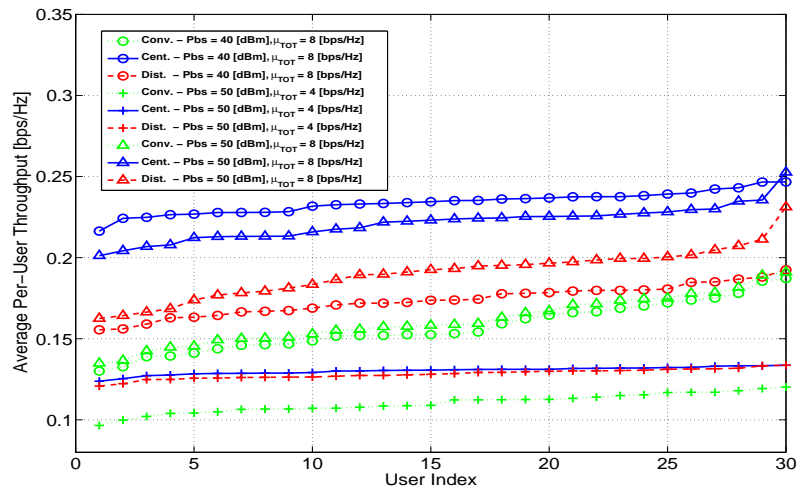


Figure 5.4: Sorted average user rates for $R = 2$ km, $d_{BS \rightarrow RS} = 1$ km, $P_{bs} = \{40, 50\}$ [dBm], $P_{rs} = 35$ [dBm], $\mu_{TOT} = \{4, 8\}$ [bps/Hz], with $N = 6$ RSs.

Chapter 6

Coding Strategies for Two-way Relay Channels

6.1 Introduction

In this chapter we consider a communication network comprised of nodes communicating two-way with the aid of a common RS. The nodes are assumed to have no direct communication links. A cut-set outer bound for the set of rates in the context of this network topology is given for two special cases assuming FD (full-duplex) transmission capabilities. We study first a binary adder channel with additive noise at the nodes and the RS, and then generalize this to an additive white Gaussian multi-user channel at the RS and additive Gaussian noise at the nodes where we improve upon recent achievability results for lattice codes and partial decoding at the RS. We also show that the outer bound is virtually achievable by *physical-layer* network coding, using group codes and partial decoding at the RS under both channel models. We then compare such coding schemes to binning (hashing and compression with side information) where the RS does not attempt to partially decode the sum signal and amplify-and-forward (AF) relaying strategies at the RS. It is shown that for strong RS-to-node links compression-based strategies can provide near optimal performance without the need for full CSI at the transmission end.

6.1.1 Related Work on Two-Way Relaying

Up to now, different transmission schemes are proposed for two-way relaying (TWR) channels [38, 42, 45, 47, 50, 51, 53, 85]. However, the capacity region for general TWR channel remains open. The simplest transmission scheme for

TWR channel consists of four phases where the two nodes transmit their messages to the RS successively and then the RS decodes and forwards each mobile's message in the following two time slots. However, using ideas from network coding (NC) [46], it is shown in [47] that the last two transmissions may be merged into a single transmission, resulting in three time slots and hence a pre-log factor of $2/3$ with respect to the sum-rate. The number of required time slots for the communication between the two nodes can be reduced even further to two time slots by allowing them to simultaneously access the RS [41, 44, 48–53].

In [41, 48, 49, 54] AF, DF and CF based relaying schemes consisting only of two time slots are proposed for TWR channel. A NC scheme that requires three time slots is considered in [47] where in the first two time slots the mobiles send their messages to the RS in orthogonal time slots, the RS decodes both messages and then combines them by means of the bit-wise XOR operation and retransmits it to the mobiles. There the mobiles are assumed to use the bit-wise XOR operation on the decoded message and the own transmitted message to obtain the message sent from the other mobile. Requiring three time slots, this bit-wise XOR based TWR scheme provides a pre-log factor of $2/3$ with respect to the sum-rate. In [44] an analog network coding (ANC) scheme, where the RS amplifies and forwards mixed received signals, is proposed and compared to the traditional and digital network coding (bit-wise XOR at the RS) schemes in terms of network throughput. In [41, 49] the denoise-and-forward (DNF) relaying is proposed for TWR channel where the RS removes the noise from the combined mobiles' messages (on the multiple-access channel) before broadcasting and compared with AF, DF based TWR schemes as well as the traditional four phase scheme.

6.1.2 Application Scenarios

The results considered here could find application in wireless networks requiring robust high-bandwidth links, for instance, for first or second tier infrastructure links. The first primary application is a high-capacity satellite relay, a similar application to the work considered in [86], where the distributed source coding and reconstruction problem was considered for correlated sources and noiseless links. Here we consider uncorrelated sources and noisy channels in both directions. In this type of application, the ground stations are fixed and in LOS with the satellite. The ground stations clearly do not have reliable communication links, otherwise the use of satellite would not be warranted.

The second application is a rapidly-deployable high-bandwidth RS for emergency communications (police, army, fire brigade, etc). Here we imagine a scenario where two networks (e.g. WiMax, WiFi) have been set up but do not have a physical link to be interconnected. This could be due to obstructions in the propagation environment (e.g. mountains, buildings) or due to an indoor/outdoor deployment. The authority places a "WiMax RS" between both networks to link them (e.g. with a helicopter on the mountaintop, or by placing an indoor/outdoor antenna.). Again this would be a fixed station, along with the gateways in the two WiFi/WiMax networks.

A third application scenario would be a wireless mesh for infrastructure networks, for example to interconnect BSs or ADSL DSLAMS in rural areas. Here we could imagine the deployment of a linear network of BSs (e.g. down a valley) which take in traffic from their cells and relay it to the operator's network via their neighboring BSs. In addition, they relay the traffic from/to the adjacent BSs along the line.

6.2 The channel model

Consider the general wireless network with a single RS shown in Figure 9.5, where nodes are assumed to exchange all information via a RS since no direct communication links are available¹. If we restrict ourselves to a 2-user network, we are ultimately interested in considering channel models of the form

$$y_R = \sqrt{P_1}|h_{1R}|x_{12} + \sqrt{P_2}|h_{2R}|x_{21} + z_R, \quad (6.1)$$

$$y_a = \sqrt{P_R}|h_{Ra}|x_R + z_a, \quad a = 1, 2 \quad (6.2)$$

where P_a , P_R , h_{aR} and h_{Ra} are the transmit power at node $a \in \{1, 2\}$, the transmit power at the RS, complex channel gain from node a to the RS and complex channel gain from the RS to node a , respectively. x_{ab} , y_a and z_a (x_R , y_R and z_R) are the transmitter input from node a to node b (from the RS to the nodes), receiver output and additive Gaussian noise with unit variance at node a (at the RS), respectively. We assume quasi-static LOS channels from the outset which is motivated by the propagation environments associated with the target applications that are envisaged for this type of system. As a result, we assume that the complex channel gains (amplitude and phase) are deterministic and known to the transmitters. This is justified given that we have a two-way channel and that bandwidth for CSI on the DL will be negligible, in comparison to the rate of information transfer. The latter is reasonable if the channels are quasi-stationary, which may not be the case in practice (see Section-6.7).

For the multiuser coding strategies we consider in this work, the most important practical aspect by far, is the ability of the system to control the phases of the incoming signals at RS. In a real wireless communication system this will vary quickly due to factors other than the propagation medium, primarily clock drift, carrier frequency-offsets and phase noise. The ability to track the phase of the signal received by the RS at the transmitters is therefore an issue of great practical importance related to the results presented here, but is beyond the scope of this preliminary study.

Were we to consider a slowly-varying channel, the communication model would change significantly to incorporate a more sophisticated use of CSI at

¹It should be noted from the outset that in the problem considered herein the RS is not an access-point to another network as is primarily the case for a cellular BS or a WiFi access-point. In these two-way link examples, the amount of traffic exchanged between users in the same cell is usually negligible compared to the amount relayed by the access-point through the operator's network to another cell or to the Internet.

transmission which would include power-control and would greatly complicate matters. We also leave this type of channel model to future work.

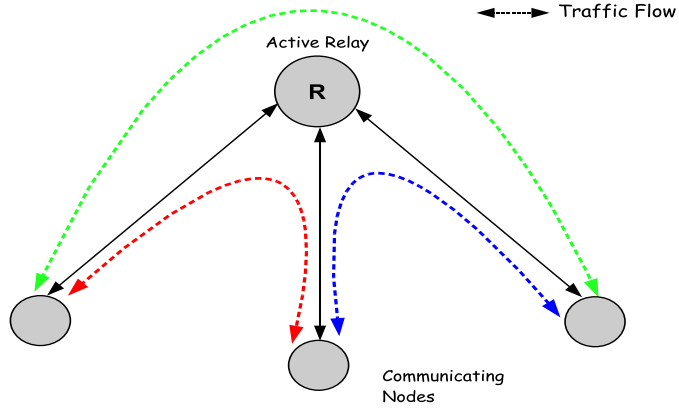


Figure 6.1: Two-way relay network

6.3 Outer Bound on Achievable Rates

6.3.1 Information-Theoretic System Model

Consider the network in Figure 6.2 comprising a pair of nodes communicating two-way via a RS. Node a generates n -dimensional codewords X_{ab}^n based on an index $W_{ab} \in \{1, 2, \dots, 2^{nR_{ab}}\}$ where R_{ab} is the information rate in bits/dimension in the direction ab . Similarly, node 2 generates X_{ba}^n based on $W_{ba} \in \{1, 2, \dots, 2^{nR_{ba}}\}$. Each letter of the transmitted codewords, $X_{ab,i}$, $i = 1, 2, \dots, n$ belongs to an alphabet \mathcal{X}_{ab} and is chosen according to a deterministic encoding function $X_{ab,i} = f_{ab,i}(W_{ab}, Y_a^{i-1})$ which includes the possibility for exploiting the past observations of the relay channel output (downlink)². The RS also uses a deterministic transcoder which generates an n -dimensional output sequence X_R^n based on the observed noisy multiuser (uplink) channel output Y_R^n . The transcoding function at the RS is causal and written as $X_{R,i} = f_{R,i}(Y_R^{i-1}) \in \mathcal{X}_R$, where \mathcal{X}_R is the alphabet of the RS transmitter. The multiuser channel is memoryless and successive outputs are identically distributed according to the conditional probability $p(y_R|x_{ab}, x_{ba})$. The observed sequences at the nodes, Y_a^n and Y_b^n , are independent conditioned on the

²In order to avoid repeating expressions, from this point onwards, we will use the subscripts a and b to represent the two nodes arbitrarily.

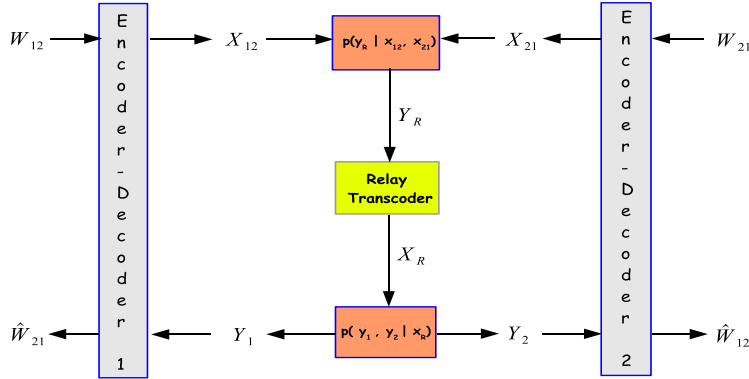


Figure 6.2: Two-user two-way relay network

RS output and identically distributed according to the conditional probability $p(y_a, y_b | x_R) = p(y_a | x_R)p(y_b | x_R)$. Receiver b decodes its message based on the observed sequence Y_b^n using a decoding function $\hat{W}_{ab} = g(Y_b^n, W_{ba})$ with probability of error $P_{e,b} = \Pr(\hat{W}_{ab} \neq W_{ab})$.

6.3.2 Outer Bound

Let us first derive an outer-bound on the capacity region from first principles. Using Fano's inequality twice (see Appendix-6.A) we have the following outer-bound on achievable rates,

$$R_{ab} \leq \min(I(X_{ab}; Y_R | X_{ba}), I(X_R; Y_b)). \quad (6.3)$$

The first term (uplink) in (6.3) corresponds to the outer-bound of the two-way channel with a common output [87] with which no coding strategy is known to coincide, except for additive channels and some special cases [88]. In our system, the achievable rates would be limited to this rate if the DL channels were capable enough to allow the RS to forward a sufficient characterization of Y_R to the nodes. In the case of a noiseless DL channel our system boils down to a two-way channel with a common output [87]. For a weak DL, the information rates will be limited by the second term in (6.3). Again, were the uplink channel noiseless, an outer-bound to the achievable rates would be given by the second term.

6.4 Coding Strategies for Additive Channels using Group Codes

We now restrict our treatment to two specific additive channel models, namely the binary adder channel and the AWGN channel in (6.1)-(6.2).

6.4.1 Binary Adder Channel

The input/output relationships for the binary adder channel are given by

$$\begin{aligned} y_{R,n} &= x_{12,n} \oplus x_{21,n} \oplus z_{R,n}, \\ y_{i,n} &= x_{R,n} \oplus z_{i,n}, \quad i = 1, 2 \end{aligned} \quad (6.4)$$

where all variables are binary and $x \oplus y$ denotes the modulo-2 sum of x and y . The probability of taking on the value 1 for the noise terms are denoted $\epsilon_R, \epsilon_a, \epsilon_b$. Here the outer bound from Section-6.3 is

$$\begin{aligned} R_{ab} &\leq \min \{I(X_{ab}; Y_R | X_{ba}), I(X_R; Y_b)\} \\ &= \min \{H(Y_R | X_{ba}) - H(Y_R | X_{ab}, X_{ba}), H(Y_b) - H(Y_b | X_R)\} \\ &\leq \min \{1 - \mathcal{H}(\epsilon_R), 1 - \mathcal{H}(\epsilon_b)\} \end{aligned} \quad (6.5)$$

where the last inequality becomes equality when the input distributions are uniform, i.e., $p(x_{ab} = 1) = p(x_{ba} = 1) = 1/2$.

To show the achievability of (6.5) we assume that uplink and DL encoding occur in subsequent periods of n output symbols, where n is the length of code sequences. That is to say that after decoding a message from a group of n symbols, the RS transmits the DL message while it receives the next UL message. Suppose without loss of generality that $R_{ab} \geq R_{ba}$. Consider two random codebooks C_{ab} with rate $R_{ab} - R_{ba}$ and C_c with rate R_{ba} . C_c is the *common codebook*. We now time-share between both codebooks as shown in Figure-6.3 with $0 \leq \alpha \leq 1$. During the first time-slot of duration $(1 - \alpha)n$ dimensions user a transmits alone to the RS using C_{ab} . Call the information sequence $X_{ab}^{(1)}$. Using standard random coding arguments, arbitrarily small error probability for detection of $X_{ab}^{(1)}$ is achievable if

$$R_{ab} - R_{ba} < (1 - \alpha)I(X_{ab}; Y_R) \leq (1 - \alpha)(1 - \mathcal{H}(\epsilon_R)).$$

During the second time-slot of duration αn dimensions, both users transmit their information sequences $X_{ab}^{(2)}$ and X_{ba} which are codewords belonging to the *same linear code* over $\text{GF}(2)$, C_c . As a result the RS receives the modulo-2 sum of the two codewords which is itself a codeword in C_c . Linear codes achieve the capacity of the BSC (see [69]) and thus an arbitrarily small average error probability for the detection of $X_{ab}^{(2)} \oplus X_{ba}$ is possible if

$$R_{ba} \leq \alpha(1 - \mathcal{H}(\epsilon_R)).$$

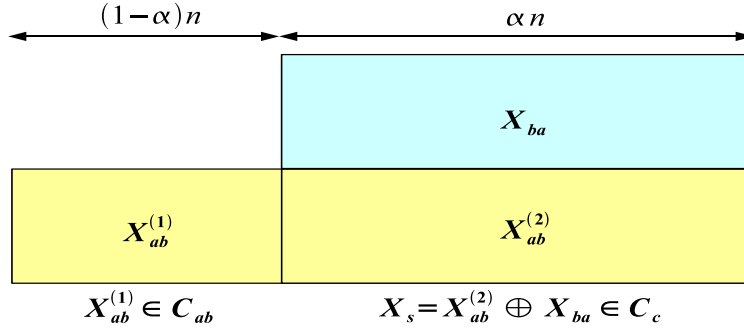


Figure 6.3: Binary Adder Channel Codebook Time-Sharing

The RS encodes with a two-dimensional codebook of cardinality $2^{nR_{ab}}$, indexed by column and row pair (i, j) , $i = 1, \dots, 2^{n(R_{ab}-R_{ba})}$, $j = 1, \dots, 2^{nR_{ba}}$. Column i is used to encode $X_{ab}^{(1)}$ and row j to encode $X_{ab}^{(2)} \oplus X_{ba}$. At receiver 1 (weak receiver), X_{ab} is known and so the column i of the transmitted codeword is known. Arbitrarily small error probability is achievable for detection of j or $X_{ab}^{(2)} \oplus X_{ba}$ (and consequently X_{ba}) if

$$R_{ba} < I(X_R; Y_a) \leq 1 - \mathcal{H}(\epsilon_a).$$

At receiver 2 (strong receiver) X_{ba} is known. Arbitrarily small error probability for detection of (i, j) (or X_{ab}) is achievable if

$$R_{ab} < I(X_R; Y_b) \leq 1 - \mathcal{H}(\epsilon_b).$$

Consider first the “strong relay” case where $\epsilon_R \geq \max(\epsilon_1, \epsilon_2)$. Here we let $\alpha = 1$ so that both users can achieve $1 - \mathcal{H}(\epsilon_R)$. For the “medium relay” case where $\epsilon_a \geq \epsilon_R \geq \epsilon_b$ we choose $\alpha = \frac{1 - \mathcal{H}(\epsilon_a)}{1 - \mathcal{H}(\epsilon_R)}$, so that $R_{ab} = 1 - \mathcal{H}(\epsilon_R)$ and $R_{ba} = 1 - \mathcal{H}(\epsilon_a)$ are achievable. Finally in the “weak relay” case when $\epsilon_a \geq \epsilon_b \geq \epsilon_R$ we choose $\alpha = \frac{1 - \mathcal{H}(\epsilon_a)}{1 - \mathcal{H}(\epsilon_b)}$, resulting in $R_{ab} = 1 - \mathcal{H}(\epsilon_b)$ and $R_{ba} = 1 - \mathcal{H}(\epsilon_a)$.

6.4.2 AWGN Channel

Now consider the main channel model of interest given in (6.1)-(6.2) and incorporate the UL channel gains in the transmit powers. The $P_{1R} = P_1|h_{1R}|^2$ and $P_{2R} = P_2|h_{2R}|^2$ therefore now represent received powers and the channel gains can be ignored. If we further incorporate the received powers in the received

codeword strengths for the DL signals we have the following set of power constraints, $\mathbb{E}[|X_1|^2] \leq P_{1R}$, $\mathbb{E}[|X_2|^2] \leq P_{2R}$, $\mathbb{E}[|X_R|^2] \leq 1$. Let $P_{Ra} = P_R |h_{Ra}|^2$ denote the received power at node a . Now suppose again, without loss of generality, that $R_{ab} \geq R_{ba}$, which implies a particular configuration of received powers at the RS and nodes, namely that $P_{aR} > P_{bR}$ or $P_{Ra} < P_{Rb}$. In this case, the outer-bounds become

$$R_{ab} \leq \frac{1}{2} \min \{ \log_2(1 + P_{aR}), \log_2(1 + P_{Rb}) \}. \quad (6.6)$$

Weak Relay Case

A weak relay is defined by the condition

$$\log_2(1 + P_{R1}) + \log_2(1 + P_{R2}) \leq \log_2(1 + P_{1R} + P_{2R}). \quad (6.7)$$

In this case, the RS can decode the UL multi-user signal and then re-encode the two signals jointly on the DL, i.e., *decode-and-forward* relaying which will be studied in Section-6.5.2. The nodes will make use of the knowledge they have about their own transmitted signal in the previous block to decode the message. On the UL, the RS can decode reliably provided [1], refer to (6.23),

$$\begin{aligned} R_{12} &\leq \frac{1}{2} \log_2(1 + P_{1R}), \\ R_{21} &\leq \frac{1}{2} \log_2(1 + P_{2R}), \\ R_{12} + R_{21} &\leq \frac{1}{2} \log_2(1 + P_{1R} + P_{2R}). \end{aligned} \quad (6.8)$$

On the DL, the RS uses a random codebook of cardinality $2^{n(R_{12}+R_{21})}$, drawn from a Gaussian distribution with variance P_R in each dimension of each codeword. For convenience, arrange the codewords in a two-dimensional grid where the column index corresponds to the decoded index of user 1's signal (W_{12}), and the row index corresponds to the decoded index of user 2's signal (W_{21}). User 1 decodes its message (\hat{W}_{21}) by looking at the code of cardinality $2^{nR_{21}}$ contained in the column corresponding to W_{12} . User 2 proceeds in an identical fashion on the row corresponding to W_{21} . Because of the side information from their own signals, the DL is decoupled into two orthogonal channels and the users can decode their messages provided

$$R_{ab} \leq \frac{1}{2} \log_2(1 + P_{Rb}). \quad (6.9)$$

Because of the weak relay definition, the sum DL rate will always be less than the sum UL rate, and thus the achievable DL rate-pair lies within the multiple-access capacity region in (6.8). This rate-pair coincides with the outer-bound and thus constitutes the capacity region for this special case.

General Case

In the general case, we must exploit the fact that the RS need not decode the entire UL message, as was the case in the binary-adder channel by letting the nodes use the same linear code and allow the channel to combine the two signals. This is a generalization of *physical-layer* network coding as described in [52]. The group structure of the linear code allows the cardinality of the sum-codebook seen by the RS to be much smaller than $2^{n(R_{12}+R_{21})}$ and thus decoding of the sum sequence can be achieved more reliably than decoding of the individual code sequences. Proceeding similarly to the binary case, we introduce a group structure on the transmitted codewords in Euclidean space by building them up from a *common* lattice. This approach was recently considered independently by Narayanan *et al* in [89] for the case of equal rates between the two stations. The nodes use different size codebooks, according to their powers, by bounding the lattice by appropriate hyperspheres.

Theorem 31. *An achievable rate region for the two-way relay channel using group codes and partial decoding at the RS is given by the closure of the following set of inequalities*

$$R_{12} = \min \left[\frac{1}{2} \log_2 (1 + P_{R2}), \frac{1}{2} \log_2 (1 - \alpha + P_{1R}) \right], \quad (6.10a)$$

$$R_{21} = \min \left[\frac{1}{2} \log_2 (1 + P_{R1}), \frac{1}{2} \log_2 (\alpha + P_{2R}) \right] \quad (6.10b)$$

for any $\alpha \in [0, 1]$.

Proof. To prove the achievability of decoding the sum codeword at the RS, we rely on the coding theorem for lattice codes with minimum-distance decoding from [90]. Consider two sequences of n -dimensional lattice codes built from the same sequence of lattices Λ_n which are bounded by the n -dimensional balls $T_{n,1}$ of radius $\sqrt{nP_{1R}}$ and $T_{n,2}$ of radius $\sqrt{nP_{2R}}$. The sequence of lattices are characterized by the sequence of fundamental volumes $d_n = \det(\Lambda_n)$. Suppose $R_{12} < \frac{1}{2} \log_2 (1 - \alpha + P_{1R})$ and $R_{21} < \frac{1}{2} \log_2 (\alpha + P_{2R})$, $\alpha \in [0, 1]$, or, equivalently,

$$R_{12} = \frac{1}{2} \log_2 \left(\frac{nP_{1R}}{d_n} \right) < \frac{1}{2} \log_2 (1 - \alpha + P_{1R})$$

$$R_{21} = \frac{1}{2} \log_2 \left(\frac{nP_{2R}}{d_n} \right) < \frac{1}{2} \log_2 (\alpha + P_{2R}).$$

Simple manipulation of these inequalities gives us a condition on the rate of the “sum-codebook” seen by the RS

$$\frac{1}{2} \log_2 \left(\frac{n(P_{1R} + P_{2R})}{d_n} \right) < \frac{1}{2} \log_2 (1 + P_{1R} + P_{2R}). \quad (6.11)$$

Now since the rate of the sum-codebook at the RS, R_s , is clearly upper-bounded by the left-hand side of (6.11) (since not all lattice points in the ball of radius

$\sqrt{n(P_{1R} + P_{2R})}$ are possible outcomes), we have that

$$R_s < \frac{1}{2} \log_2 (1 + P_{1R} + P_{2R}) \quad (6.12)$$

With (6.12) we can now make use of the result in [90] which guarantees the existence of a sequence of lattices such that the probability of error for decoding the sum codeword can be made arbitrarily small by increasing the number of dimensions n . As a result, the RS can decode the sum codeword and re-encode it on the DL in a similar fashion as in the case of the weak relay using a codebook of rate $\max(R_{12}, R_{21})$ (by reducing the decoded sum codeword index modulo- $2^{n \max(R_{12}, R_{21})}$).

Here we have the same condition on the DL rates, namely (6.9), and thus the rates in (6.10) are achievable for any $\alpha \in [0, 1]$. This coincides with Narayanan's result [89] for $\alpha = 0.5$ and with Nam's result [91] for $\alpha = \frac{\gamma_{1,R}}{\gamma_{1,R} + \gamma_{2,R}}$. Moreover, compared to the achievable rate region in [91] where time-sharing with DF relaying is used, our scheme achieves larger rate region even without time-sharing. \square

6.5 Decode-, Hash- and Compress-and-Forward Schemes at the Relay

At the node-1 and node-2 assuming coding schemes which do not exploit the DL signal in the encoding of the UL data so that the data streams are independent, we now consider coding schemes at the RS which do not attempt to decode or partially decode the transmitted data streams, but rather perform binning (hashing) or quantization of the received sequence. UL codebooks are generated randomly at each node according to $p(x_{12})$ and $p(x_{21})$. At the RS we will consider two different encoding strategies, namely hash-and-forward and decode-and-forward. Prior to discussing these further, we consider two possibilities for DL coding which will be needed for the probability of error analysis for data transmission on the DL.

6.5.1 Degraded BC with successive refinement

We consider the case where the DL channel is degraded and a DL channel code where the two users are required to decode the same information but with different degrees of refinement (here two). By this we mean that the user with the weaker channel only receives the heavily-protected data stream, while the user with the stronger channel receives both. This is the general BC where there is common information for both users and extra information for the stronger user. We make use of standard multi-level coding [1], and let $R_{R,1}$ and $R_{R,2}$ denote the information rates of the RS to nodes 1 and 2 respectively, and assume further that $R_{R,1} \geq R_{R,2}$. The random codebook, $\{X_R(i, j), i = 1, 2, \dots, 2^{n(R_{R,1} - R_{R,2})}, j = 1, 2, \dots, 2^{nR_{R,2}}\}$, is generated according to the

distributions $p(u)$ and $p(x_R|u)$ in the standard-way so that the achievable DL rates are given by the convex hull (with respect to the parameter α and $p(x_R, u)$) of

$$(R_{R,1}, R_{R,2}) = \{(R_{R,1}, R_{R,2}) : \arg \max_{\substack{p(x_R, u) \\ 0 \leq \alpha \leq 1}} \{\alpha(R_{R,1} - R_{R,2}) + (1 - \alpha)R_{R,2}\}\},$$

where

$$R_{R,2} = I(U; Y_2), \quad (6.13a)$$

$$R_{R,1} - R_{R,2} = I(X_R; Y_1|U). \quad (6.13b)$$

6.5.2 Decode-and-Forward Relaying

In this section, we provide a more complete view of the achievable rates for the digital single-relay network with two communicating nodes. We begin with a discrete-memoryless channel model and then give an achievable rate region which makes use of a generalized form of network-coding for noisy channels.

Discrete-Memoryless Network Model

Consider the discrete-memoryless channel model as shown in Figure 6.2. User 1 and user 2 generate indexes W_{12} and W_{21} , respectively, for the codeword to be transmitted via the RS to the other user. Each encoder generates codewords comprising n dimensions on the alphabets \mathcal{X}_{12} and \mathcal{X}_{21} for transmission during the UL. The cardinality of the two codebooks are $2^{nR_{12}}$ and $2^{nR_{21}}$. The channel from the nodes to the RS is a classical MAC (multiple access channel) described by the transition probability on the received symbols $p(y_R|x_{12}, x_{21})$.

The RS employs a multi-user receiver to decode the transmitted codeword indices yielding the estimates $(\hat{W}_{12}, \hat{W}_{21})$ at its output. Based on these indices, it then encodes the two indices using a codebook of dimensionality n on the alphabet \mathcal{X}_R . The cardinality of the RS's codebook is at most $2^{n(R_{12}+R_{21})}$. We assume that the codebooks at the nodes and RS are fixed. This implies that the codebook of the RS cannot be a function of the received sequence y_R^n .

Remark 32. *We note that compared to the "structures codes" and limited decoding case, the DF relaying strategy requires more complexity at the RS.*

The DL channel is a classical BC except for the fact that the decoders have side information to exploit, namely the transmitted codeword indices that they themselves sent during the UL portion. For simplicity, we assume that the two channel outputs are conditionally independent so that they can be separated into two transition probabilities $p(y_i|x_R), i = 1, 2$. Each node decodes the received sequence y_1^n (y_2^n) using the side information from its own transmission to yield the estimates \hat{W}_{21} (\hat{W}_{12}).

An Achievable Rate Region

In the following theorem we provide an achievable rate region for the above channel model.

Theorem 33. *An achievable rate region for the two-user single relay network using DF relaying strategy is given by the closure of the following set of inequalities*

$$R_{12} \leq \min \{I(X_{12}; Y_R | X_{21}), I(X_R; Y_2)\}, \quad (6.14a)$$

$$R_{21} \leq \min \{I(X_{21}; Y_R | X_{12}), I(X_R; Y_1)\}, \quad (6.14b)$$

$$R_{12} + R_{21} \leq I(X_{12}, X_{21}; Y_R). \quad (6.14c)$$

Proof. The probability of decoding error at each receiver assuming $(W_{ab}, W_{ba}) = (1, 1)$ are sent is given by

$$\begin{aligned} P_{e,a} &= \Pr(\hat{W}_{ba} \neq 1) \\ &\leq \Pr(\hat{W}_{ba} \neq 1 | \hat{W}_{ab} = \hat{W}_{ba} = 1) + \Pr((\hat{W}_{ab}, \hat{W}_{ba}) \neq (1, 1)). \end{aligned} \quad (6.15)$$

where $a, b \in \{1, 2\}$ and $a \neq b$. The second term in the sum in (6.15) is the probability of decoding error at the RS for the MAC on the UL. As a result, the following set of rates are achievable in the sense of vanishing $\Pr((\hat{W}_{ab}, \hat{W}_{ba}) \neq (1, 1))$ (see [1]),

$$R_{12} \leq I(X_{12}; Y_R | X_{21}), \quad (6.16a)$$

$$R_{21} \leq I(X_{21}; Y_R | X_{12}), \quad (6.16b)$$

$$R_{12} + R_{21} \leq I(X_{12}, X_{21}; Y_R). \quad (6.16c)$$

The first term in the sum in (6.15) is the probability of decoding error at the node given that the RS has correctly decoded both transmitted indices. To show the rates for which these probabilities vanish, consider the following two-dimensional coding scheme between the RS and the two nodes, under the assumption that $R_{ab} \geq R_{ba}$:

1. From the UL, the RS decodes \hat{W}_{ab} and \hat{W}_{ba} . The DL codewords at the RS are organized in the two-dimensional codebook $\mathcal{X}_R = \{X_R^n(W_R^{(1)}, W_R^{(2)}), W_R^{(1)} = 1, \dots, 2^{n(R_{ab}-R_{ba})}, W_R^{(2)} = 1, \dots, 2^{nR_{ba}}\}$. The $2^{nR_{ab}}$ n -dimensional codewords are generated i.i.d. according to $p(X_R^n(W_R^{(1)}, W_R^{(2)})) = \prod_{m=1}^n p(x_{R,m})$.
2. Let $x \oplus y$ denote $(x + y) \bmod 2^{nR_{ba}}$. To send indices $W_R^{(1)}$ and $W_R^{(2)}$ choose $X_R^n(W_R^{(1)}, W_R^{(2)})$ where $W_R^{(1)} = \lfloor \hat{W}_{ab} 2^{-nR_{ba}} \rfloor$, $W_R^{(2)} = \hat{W}_{ab} \oplus \hat{W}_{ba}$ [Network Coding].
3. Let $A_{\epsilon,k}^n$ denote the set of jointly-typical sequences $\{x_R(w_R^{(1)}, w_R^{(2)}), y_k\}$, $k = 1, 2$ (see [1]).

6.5 Decode-, Hash- and Compress-and-Forward Schemes at the Relay135

4. Receiver a (the weak receiver) has knowledge of W_{ab} (side information due to its own transmission on the UL) so it chooses the unique \hat{W}_{ba} such that

$$\{X_R^n(\lfloor W_{ab}2^{-nR_{ba}} \rfloor, W_{ab} \oplus \hat{W}_{ba}), Y_a^n\} \in A_{\epsilon, a}^n. \quad (6.17)$$

Note that due to the side information $W_R^{(1)}$ is known to receiver a so the cardinality of the search space is limited to $2^{nR_{ba}}$. If none or more than one exist an error is declared. The decoded index is then $W_{ab} \oplus \hat{W}_{ba}$.

5. Receiver b (the stronger receiver) has knowledge of W_{ba} (side information due to its own transmission on the UL) so it chooses the unique \hat{W}_{ab} such that

$$\{X_R^n(\lfloor \hat{W}_{ab}2^{-nR_{ba}} \rfloor, \hat{W}_{ab} \oplus W_{ba}), Y_b^n\} \in A_{\epsilon, b}^n. \quad (6.18)$$

Note that the cardinality of the search space is $2^{nR_{ab}}$. If none or more than one exist an error is declared. Due to the side information W_{ba} the decoded index at the receiver b is then $\hat{W}_{ab}2^{-nR_{ba}} + \hat{W}_{ab} \oplus W_{ba}$.

Define the conditional events

$$E_{i,j,k} = \left\{ (X_R^n(\lfloor i2^{-nR_{ba}} \rfloor, i \oplus j), Y_k) \in A_{\epsilon, k}^n | \hat{W}_{ab} = \hat{W}_{ba} = 1 \right\} \quad (6.19)$$

to calculate the error probabilities. Then, by the union of events bound and the joint asymptotic equipartition property (AEP) (see [1])

$$\begin{aligned} \Pr(\hat{W}_{ba} \neq 1 | \hat{W}_{ab} = \hat{W}_{ba} = 1) &\leq \Pr(E_{11,a}^c) + \sum_{j'=2}^{2^{nR_{ba}}} \Pr(E_{1j',a}) \\ &\leq \epsilon + 2^{-n(I(X_R; Y_a) - R_{ba} - 3\epsilon)} \end{aligned} \quad (6.20)$$

and

$$\begin{aligned} \Pr(\hat{W}_{ab} \neq 1 | \hat{W}_{ab} = \hat{W}_{ba} = 1) &\leq \Pr(E_{11,b}^c) + \sum_{(i',j') \neq (1,1)} \Pr(E_{i'j',b}) \\ &\leq \epsilon + 2^{-n(I(X_R; Y_b) - R_{ab} - 3\epsilon)}. \end{aligned} \quad (6.21)$$

Note that both $\Pr(\hat{W}_{ba} \neq 1 | \hat{W}_{ab} = \hat{W}_{ba} = 1)$ and $\Pr(\hat{W}_{ab} \neq 1 | \hat{W}_{ab} = \hat{W}_{ba} = 1)$ go to zero if $n \rightarrow \infty$ and

$$\begin{aligned} R_{12} &\leq I(X_R; Y_2), \\ R_{21} &\leq I(X_R; Y_1) \end{aligned} \quad (6.22)$$

are satisfied. We see that both users can benefit from the full DL rate. Combining (6.22) with (6.16) yields (6.14). \square

Corollary 34. For an AWGN TWR channel, the achievable rate region corresponding to the DF relaying strategy is given by the closure of the following set of inequalities

$$R_{12} \leq \min \{ \log_2(1 + P_{1R}), \log_2(1 + P_{R2}) \}, \quad (6.23a)$$

$$R_{21} \leq \min \{ \log_2(1 + P_{2R}), \log_2(1 + P_{R1}) \}, \quad (6.23b)$$

$$R_{12} + R_{21} \leq \log_2(1 + P_{1R} + P_{2R}). \quad (6.23c)$$

6.5.3 Hash-and-Forward Relaying

If the RS does not attempt to decode the received sequence Y_R^n , it may still attempt to reduce the amount of information needed to convey it to both users, and moreover with a higher degree of refinement for the user with the stronger DL channel. We will proceed similarly to distributed source coding as originally described by Slepian and Wolf in [58]. This was recently referred to as *Hashing* at the RS, resulting in an *hash-and-forward* transmission scheme. The set of ϵ -typical sequences Y_R^n is partitioned into $2^{nR_{R,1}}$ bins $B_{ij}, i = 1, \dots, 2^{n(R_{R,1}-R_{R,2})}, j = 1, \dots, 2^{nR_{R,2}}$, such that $\bigcup_{i,j} B_{ij} = A_\epsilon^n$ and $B_{ij} \cap B_{i'j'} = \emptyset$, for $i \neq i'$ or $j \neq j'$. Let $\mathcal{B}(y_R^n) = (i, j)$ be a random hash-function which assigns a received sequence to a particular bin.

Encoding at the RS is done in two steps. First, if $y_R^n \in A_\epsilon^n$, we hash y_R^n and let $W_{R,1} = i$ and $W_{R,2} = j$. If $y_R^n \notin A_\epsilon^n$, we set $(W_{R,1}, W_{R,2}) = (e, e)$ to indicate an error condition at the RS encoder. Then, we generate the transmitted sequence X_R^n according to the multilevel-coding strategy for the (degraded) BC.

Decoder 1 creates a list, $L_1(y_R^n)$ of candidate y_R^n based on the decoded (\hat{i}, \hat{j}) . The number of candidates in the list, $N_1(y_R^n)$ is bounded by

$$2^{n(H(Y_R) - R_{R,1} - \epsilon)} \leq N_1(y_R^n) \leq 2^{n(H(Y_R) - R_{R,1} + \epsilon)} \quad (6.24)$$

Similarly, decoder 2 has a list based solely on \hat{j} , $L_2(y_R^n)$, for which the number of elements is bounded by

$$2^{n(H(Y_R) - R_{R,2} - \epsilon)} \leq N_2(y_R^n) \leq 2^{n(H(Y_R) - R_{R,2} + \epsilon)} \quad (6.25)$$

Knowing x_{12}^n , decoder 1 tries to find an x_{21}^n such that $(x_{12}^n, x_{21}^n, y^n) \in A_\epsilon^n$ for at least one $y^n \in L_1(y_R^n)$. If more than one x_{21}^n or none are jointly ϵ -typical, then an error is declared. Decoder 2 proceeds similarly and tries to find an x_{12}^n knowing x_{21}^n such that $(x_{12}^n, x_{21}^n, y^n) \in A_\epsilon^n$ for at least one $y^n \in L_2(y_R^n)$. Assuming $(W_{12}, W_{21}) = (1, 1)$, the probability of decoding error (conditioned on receiving (i, j) without error and $i \neq e, j \neq e$) for decoder 1 is given by

$$\begin{aligned} P_e^{(1)} &\leq \Pr((x_{12}^n(1), x_{21}^n(1), y_R^n) \notin A_\epsilon^n) + 2^{nR_{21}} \{ \Pr((x_{12}^n(1), x_{21}^n(i \neq 1), y_R^n) \in A_\epsilon^n) \\ &\quad + N_1(y_R^n) \Pr((x_{12}^n(1), x_{21}^n(i \neq 1), y_R'^n) \in A_\epsilon^n) \} \\ &\quad + \Pr((\hat{W}_{R,1}, \hat{W}_{R,2}) \neq (i, j)) + \Pr(W_{R,1} = e). \end{aligned} \quad (6.26)$$

The first element in the sum can be made arbitrarily small by increasing n . The probability in the second term is the probability over the random ensemble of

6.5 Decode-, Hash- and Compress-and-Forward Schemes at the Relay137

codebooks that an $x_{21}^n(i), i \neq 1$ is jointly ϵ -typical with the true RS output (which is always in $L_1(y_R^n)$ if (i, j) are received without error at the RS) and is given by

$$\begin{aligned} \Pr((x_{12}^n(1), x_{21}^n(i), y_R^n) \in A_\epsilon^n) &= \sum_{(x_{12}^n(1), x_{21}^n(i), y_R^n) \in A_\epsilon^n} p(x_{12}^n(1), y_R^n) p(x_{21}^n(i)) \\ &\leq 2^{n(H(X_{12}, X_{21}, Y_R) - H(X_{12}, Y_R) - H(X_{21}) - 3\epsilon)} \\ &\leq 2^{-n(I(X_{21}; Y_R | X_{12}) + 3\epsilon)} \end{aligned} \quad (6.27)$$

The probability in the third term reflects the event that another $y_R'^n \in L_1(y_R^n)$ sequence from the random list of candidates is jointly ϵ -typical with $x_{12}(1)$ and $x_{21}(i)$. Note that this sequence is independent of both code sequences and thus

$$\begin{aligned} \Pr((x_{12}^n(1), x_{21}^n(i), y_R'^n) \in A_\epsilon^n) &= \sum_{(x_{12}^n(1), x_{21}^n(i), y_R'^n) \in A_\epsilon^n} p(x_{12}^n(1)) p(y_R'^n) p(x_{21}^n(i)) \\ &\leq 2^{n(H(X_{12}, X_{21}, Y_R) - H(X_{12}) - H(Y_R) - H(X_{21}) - 4\epsilon)} \\ &\leq 2^{-n(I(X_{21}, X_{12}; Y_R) - 4\epsilon)} \end{aligned} \quad (6.28)$$

Combining the two probabilities and the size of the list in (6.26) yields

$$\begin{aligned} P_e^{(1)} &\leq \Pr((\hat{i}, \hat{j}) \neq (i, j)) + 2\epsilon + 2^{n(R_{21} - I(X_{21}; Y_R | X_{12}) - 3\epsilon)} \\ &\quad + 2^{n(R_{21} - R_{R,1} + H(Y_R | X_{12}, X_{21}) - 5\epsilon)} \end{aligned} \quad (6.29)$$

Proceeding in an identical fashion for decoder 2 yields

$$\begin{aligned} P_e^{(2)} &\leq \Pr(\hat{j} \neq j) + 2\epsilon + 2^{n(R_{12} - I(X_{12}; Y_R | X_{21}) - 3\epsilon)} \\ &\quad + 2^{n(R_{12} - R_{R,2} + H(Y_R | X_{12}, X_{21}) - 5\epsilon)} \end{aligned} \quad (6.30)$$

We now turn to the remaining error event in the overall error probability, namely the event that the bin indices (i, j) for decoder 1 and j for decoder 2 are incorrectly decoded. For the degraded BC with successive refinement (see Section-6.5.1) we have the two error probabilities vanish if (6.13) are satisfied yielding the overall achievable rate region with hashing (for UL joint probability $p(x_{12})p(x_{21})p(y_R | x_{12}, x_{21})$):

$$\begin{aligned} \{(R_{12}, R_{21}) : (R_{12}, R_{21}) &= \operatorname{argmax}_{p_{X,U}(x,u)} (\beta R_{12} + (1 - \beta) R_{21}), 0 \leq \beta \leq 1\} \\ R_{12} &= \min \left\{ I(X_{21}; Y_R | X_{12}), [I(X_R; Y_1 | U) + I(U; Y_2) - H(Y_R | X_1, X_2)]^+ \right\} \\ R_{21} &= \min \left\{ I(X_{12}; Y_R | X_{21}), [I(U; Y_2) - H(Y_R | X_1, X_2)]^+ \right\}. \end{aligned} \quad (6.31)$$

Discussion 35. Consider the special case where $p(y_1 | x_R) = p(y_2 | x_R)$, and thus $R_{R,1} = R_{R,2} = I(X_R; Y_1) = I(X_R; Y_2)$. Assume further the DL channels are very strong in the sense that

$$I(X_R; Y_1) \geq \max \{H(Y_R | X_{12}), H(Y_R | X_{21})\}.$$

Under these conditions, the overall rate region coincides with Shannon's inner-bound for the two-way channel [87] with a common output (which is not tight due to the statistical independence of the input sequences) and is achievable by binning at the RS in the sense of Slepian-Wolf [58] with the only difference being that the two destinations now recover Y_R without error using their own DL side information from the UL sequences.

6.5.4 Compress-and-Forward Relaying

If the RS does not attempt to decode the received sequence Y_R^n , it could still attempt to reduce the amount of information needed to convey it to both users, and moreover with a higher degree of refinement for the user with the stronger DL channel. We will proceed similarly to rate distortion with side information as originally described by Wyner and Ziv in [32].

Proposition 5. *Using 2-level Wyner-Ziv compression technique [32] with binning at the RS and assuming degraded BC, we can achieve the rate region $\cup\{R_{12}, R_{21}\}$ with*

$$\begin{aligned} R_{12} &\leq I(X_{12}; \hat{Y}_{R_2} | X_{21}, U), \\ R_{21} &\leq I(X_{21}; \hat{Y}_R | X_{12}, U, X_R) \end{aligned} \quad (6.32)$$

provided that

$$\begin{aligned} \max\{I(\hat{Y}_{R_2}; Y_R | X_{21}, U), I(\hat{Y}_{R_2}; Y_R | X_{12}, U)\} &< I(U; Y_2), \\ \max\{I(\hat{Y}_R; Y_R | \hat{Y}_{R_2}, X_{12}, X_R, U) + I(\hat{Y}_{R_2}; Y_R | X_{21}, X_R, U), \\ I(\hat{Y}_R; Y_R | X_{12}, X_R, U)\} &< I(X_R; Y_1 | X_{12}, U) + I(U; Y_2) \end{aligned} \quad (6.33)$$

and the joint probability distribution of the random variables factor as

$$p(x_{12})p(x_{21})p(u, x_R)p(y_1, y_2, y_R | x_{12}, x_{21}, x_R)p(\hat{y}_{R_2} | u, y_R)p(\hat{y}_R | \hat{y}_{R_2}, x_R).$$

Proof. See Appendix-6.B for the proof. \square

6.5.5 AWGN Channel

Consider the AWGN TWR channel given in equations (6.1) and (6.2). We focus now on the symmetric UL and symmetric DL channel case where the transmit power constraints at the node-1, node-2 and the RS are $P_1 = P_2 = P$ and $P_R = KP$ with $\mathbb{E}[|X_{12}|^2] = \mathbb{E}[|X_{21}|^2] = \mathbb{E}[|X_R|^2] = 1$. The condition $K \gg 1$ would reflect the scenario where the DL is strong in addition to being symmetric. We assume the additive Gaussian noise at the node-1 and node-2 with variance σ_1^2 and σ_2^2 . The RS generates the quantized codewords according to the distribution $f(\hat{y}_R | y_R) \sim \mathcal{CN}(y_R, D_1)$ and $f(\hat{y}_{R_2} | \hat{y}_R) \sim \mathcal{CN}(\hat{y}_R, D_2)$ as in [82], i. e.,

$$\hat{y}_R = y_R + z_{D_1} = \sqrt{P_1}h_{1R}|x_{12} + \sqrt{P_2}h_{2R}|x_{21} + z_R + z_{D_1} \quad (6.34)$$

$$\hat{y}_{R_2} = \hat{y}_R + z_{D_2} = \sqrt{P_1}h_{1R}|x_{12} + \sqrt{P_2}h_{2R}|x_{21} + z_R + z_{D_1} + z_{D_2} \quad (6.35)$$

6.5 Decode-, Hash- and Compress-and-Forward Schemes at the Relay139

where $z_{D_i} \sim \mathcal{CN}(0, D_i)$ for $i = 1, 2$ and $z_R \sim \mathcal{CN}(0, \sigma_R^2)$. We use the following SNR definitions $\gamma_{i,R} = \frac{P_i |h_{iR}|^2}{\sigma_R^2}$ and $\gamma_{R,i} = \frac{P_R |h_{Ri}|^2}{\sigma_i^2}$ for $i = 1, 2$. And $\gamma_{R,1} \geq \gamma_{R,2}$ is assumed to have degraded BC. At the RS superposition coding is used for DL transmission where the transmitted signal is constructed as $X_R = \sqrt{\alpha P_R} X_{R,1} + \sqrt{(1-\alpha)P_R} X_{R,2}$ with $\mathbb{E}[|X_{R,i}|^2] = 1$ for $i = 1, 2$. With these assumptions the achievable rates are given by

$$R_{12} \leq \log_2 \left(1 + \frac{\gamma_{1,R}}{1 + \frac{D_1 + D_2}{\sigma_R^2}} \right) \quad (6.36a)$$

$$R_{21} \leq \log_2 \left(1 + \frac{\gamma_{2,R}}{1 + \frac{D_1}{\sigma_R^2}} \right) \quad (6.36b)$$

provided that

$$\log_2 \left(1 + \frac{1 + \gamma_{1,R}}{\frac{D_1 + D_2}{\sigma_R^2}} \right) < \log_2 \left(1 + \frac{(1-\alpha)\gamma_{R,2}}{1 + \alpha\gamma_{R,2}} \right) \quad (6.37)$$

$$\log_2 \left(1 + \frac{1 + \gamma_{2,R}}{\frac{D_1}{\sigma_R^2}} \right) < \log_2(1 + \alpha\gamma_{R,1}) + \log_2 \left(1 + \frac{(1-\alpha)\gamma_{R,2}}{1 + \alpha\gamma_{R,2}} \right) \quad (6.38)$$

which results in following bounds for the distortion noise powers:

$$\frac{D_1 + D_2}{\sigma_R^2} \geq \frac{(1 + \gamma_{1,R})(1 + \alpha\gamma_{R,2})}{(1 - \alpha)\gamma_{R,2}} \quad (6.39)$$

$$\frac{D_1}{\sigma_R^2} \geq \frac{(1 + \gamma_{2,R})(1 + \alpha\gamma_{R,2})}{(1 - \alpha)\gamma_{R,2} + \alpha\gamma_{R,1}(1 + \gamma_{R,2})}. \quad (6.40)$$

Now with the above bounds we can achieve the following rates

$$R_{12}(\alpha) \leq \log_2 \left(1 + \frac{\gamma_{1,R}}{1 + \frac{(1 + \gamma_{1,R})(1 + \alpha\gamma_{R,2})}{(1 - \alpha)\gamma_{R,2}}} \right) \quad (6.41a)$$

$$R_{21}(\alpha) \leq \log_2 \left(1 + \frac{\gamma_{2,R}}{1 + \frac{(1 + \gamma_{2,R})(1 + \alpha\gamma_{R,2})}{(1 - \alpha)\gamma_{R,2} + \alpha\gamma_{R,1}(1 + \gamma_{R,2})}} \right) \quad (6.41b)$$

Note that the achievable rates depends on the parameter α which is defined for superposition coding for DL channel (degraded BC). If we assume the DL channels are symmetric ($\gamma_{R,1} = \gamma_{R,2} = \gamma_R$) then the $\alpha = 0$, i.e. there is no refinement information. Then for fixed $\gamma_{1,R}$ and $\gamma_{2,R}$ if $\gamma_R \rightarrow \infty$, we can achieve the capacity of the two-way channel.

6.5.6 Amplify-and-Forward Relaying

We now consider analog relaying for two-way relay channel which has been called as *Analog Network Coding* in [44]. In this relaying strategy, the RS does not

attempt to decode the messages between the two nodes, but simply forwards them by normalizing the noisy received signal and amplifying it to transmit at the desired power [54]. This RS turns the channel into Shannon's Gaussian two-way channel [87] with a noise variance at the terminals dependent on the terminals' and RS's signal strengths and the RS's noise variance. The advantage here is that the RS does not have to decode the multi-user UL signal and thus does not incur a multiplexing-loss. However, this will clearly be sub-optimal because of noise accumulation.

The signal received by the RS at time slot $k - 1$ is

$$y_{R,k-1} = \sqrt{P_1}|h_{1R}|x_{12,k-1} + \sqrt{P_2}|h_{2R}|x_{21,k-1} + z_{R,k-1}$$

where $\mathbb{E}[|x_{12}|^2] = \mathbb{E}[|x_{21}|^2] = 1$ and P_1 and P_2 are the transmit powers at user 1 and user 2, respectively, and $z_{R,k-1}$ is the noise at the RS which is assumed to be an i.i.d. complex Gaussian sequence with variance σ_R^2 . The RS transmits the signal

$$\begin{aligned} x_{R,k} &= \frac{y_{R,k-1}}{\sqrt{P_1|h_{1R}|^2 + P_2|h_{2R}|^2 + \sigma_R^2}} \\ &= \frac{\sqrt{P_1}|h_{1R}|x_{12,k-1} + \sqrt{P_2}|h_{2R}|x_{21,k-1} + z_{R,k-1}}{\sqrt{P_1|h_{1R}|^2 + P_2|h_{2R}|^2 + \sigma_R^2}}. \end{aligned}$$

The received signal at user a in time slot k is

$$y_{a,k} = \sqrt{P_R}|h_{R,a}|x_{R,k} + z_{a,k}, \quad a = 1, 2 \quad (6.42)$$

where P_R is the transmit power at the RS and $z_{a,k}$ is the noise at node a , and is also assumed to be an i.i.d. complex Gaussian sequence with variance σ_a^2 .

Since each user knows its own transmitted signal, they can strip their own transmitted signal out from the received sequence leaving only the signal originating from the corresponding node. The interference-free signals received at the user a is given by

$$\hat{y}_{a,k} = \sqrt{\frac{P_R|h_{R,a}|^2}{P_1|h_{1R}|^2 + P_2|h_{2R}|^2 + \sigma_R^2}} \left(\sqrt{P_b}|h_{bR}|x_{ba,k-1} + z_{R,k-1} \right) + z_{a,k}$$

for $a, b \in \{1, 2\}$, and $a \neq b$. The achievable rates are therefore given by the single-user capacities

$$\begin{aligned} R_{ba} &= \log_2 \left(1 + \frac{P_b|h_{bR}|^2 P_R|h_{R,a}|^2}{P_R|h_{R,a}|^2 \sigma_R^2 + (P_1|h_{1R}|^2 + P_2|h_{2R}|^2 + \sigma_R^2) \sigma_a^2} \right) \\ &= \log_2 \left(1 + \frac{\gamma_{R,a} \gamma_{b,R}}{1 + \gamma_{R,a} + \gamma_{1,R} + \gamma_{2,R}} \right) \end{aligned} \quad (6.43)$$

for $a, b \in \{1, 2\}$ and $a \neq b$. Note that for fixed $\gamma_{a,R}$ and $\gamma_{b,R}$ if $\gamma_{R,a} \rightarrow \infty$, we can achieve the capacity of the two-way channel.

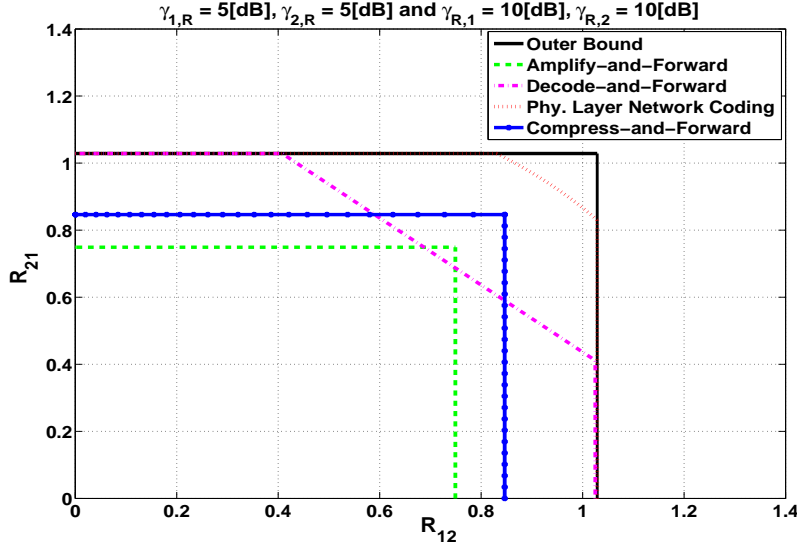


Figure 6.4: Rate regions for TWR channel.

6.6 Numerical Examples

For numerical examples, we consider symmetric UL and symmetric DL AWGN channel with $\gamma_{1,R} = \gamma_{2,R} = \gamma_{UL}$ and $\gamma_{R,1} = \gamma_{R,2} = \gamma_{DL}$. In Figure 6.4, the achievable rate regions of all the relaying schemes are plotted for $\gamma_{UL} = 5[\text{dB}]$ and $\gamma_{DL} = 10[\text{dB}]$. In Figure 6.5, the sum rates of the relaying schemes are plotted with respect to DL SNR, γ_{DL} , for $\gamma_{UL} = 5[\text{dB}]$. Here we can see that at high DL SNR regime, CF and AF performances converge to that of outer bound and physical-layer network coding achieves the best performance at the medium DL SNR regime.

6.7 Conclusions

In this chapter, we compared different coding strategies for TWR channels. For the lattice-based partial decoding strategy, the most important practical aspect by far, is the ability of the system to control the phases of the incoming signals at RS. In a real wireless communication system, this will vary quickly due to factors other than the propagation medium, primarily clock drift, carrier frequency-offsets and phase noise. As a result, the use of binning-type strategies may be a more practical approach, despite the loss in spectral efficiency, since phase coherence of the signals at the RS is not required. Our current work examines the use of feedback in the coding strategy at the terminals, an issue that was neglected here.

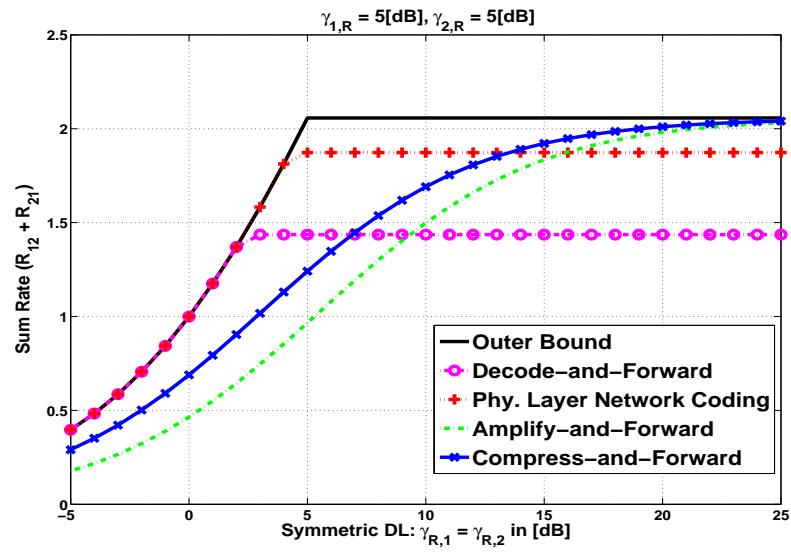


Figure 6.5: Sum-rates for TWR channel.

6.A Outer Bound

From the Fano inequality [1], we have the following series of inequalities:

$$\begin{aligned}
nR_{ab} &\leq I(W_{ab}; Y_b^n | W_{ba}) + n\epsilon_n \\
&\leq I(W_{ab}, X_R^n; Y_b^n | W_{ba}) + n\epsilon_n \\
&= \sum_{i=1}^n H(Y_{b,i} | W_{ba}, Y_b^{i-1}) - H(Y_{b,i} | W_{ba}, Y_b^{i-1}, W_{ab}, X_R^n) + n\epsilon_n \\
&\stackrel{(a)}{\leq} \sum_{i=1}^n H(Y_{b,i}) - H(Y_{b,i} | X_{R,i}) + n\epsilon_n \\
&= \sum_{i=1}^n I(X_{R,i}; Y_{b,i}) + n\epsilon_n, \tag{6.44}
\end{aligned}$$

where (a) follows from the fact that conditioning reduces the entropy of the first term in the sum and that $Y_{b,i}$ is independent of all other variables conditioned on $X_{R,i}$. In addition, we have the following series of inequalities for the same pairwise rate

$$\begin{aligned}
nR_{ab} &\leq I(W_{ab}; Y_b^n | W_{ba}) + n\epsilon_n \\
&\leq I(W_{ab}; Y_b^n, Y_R^n | W_{ba}) + n\epsilon_n \\
&= \sum_{i=1}^n H(Y_{b,i}, Y_{R,i} | W_{ba}, Y_b^{i-1}, Y_R^{i-1}) - H(Y_{b,i}, Y_{R,i} | W_{ba}, Y_b^{i-1}, Y_R^{i-1}, W_{ab}, X_R^n) + n\epsilon_n \\
&\stackrel{(a)}{\leq} \sum_{i=1}^n H(Y_{b,i}, Y_{R,i} | X_{ba,i}, X_{R,i}) - H(Y_{b,i}, Y_{R,i} | X_{ba,i}, X_{R,i}, X_{ab,i}) + n\epsilon_n \\
&= \sum_{i=1}^n H(Y_{R,i} | X_{ba,i}, X_{R,i}) + H(Y_{b,i} | Y_{R,i}, X_{ba,i}, X_{R,i}) \\
&\quad - H(Y_{R,i} | X_{ba,i}, X_{R,i}, X_{ab,i}) - H(Y_{b,i} | Y_{R,i}, X_{ba,i}, X_{R,i}, X_{ab,i}) + n\epsilon_n \\
&\stackrel{(b)}{\leq} \sum_{i=1}^n H(Y_{R,i} | X_{ba,i}) - H(Y_{R,i} | X_{ab,i}, X_{ba,i}) \\
&= \sum_{i=1}^n I(X_{ab,i}; Y_{R,i} | X_{ba,i}) \tag{6.45}
\end{aligned}$$

where (a) follows from the definition of the encoding and transcoding functions and that conditioning reduces the entropy of the second term in the sum, and (b) follows first from the fact that conditioned on $X_{R,i}$, $Y_{b,i}$ is independent of all other variables canceling the second and fourth terms, second that conditioning reduces the entropy of the first term and third that conditioned on $X_{ab,i}$ and $X_{ba,i}$, $Y_{R,i}$ is independent of $Y_{R,j < i}$ and thus $X_{R,i}$. After invoking standard timesharing arguments we have (6.3).

6.B Achievable rates with CF relaying strategy

We follow the same coding structure as in [10]. We consider K blocks each of n symbols. A sequence of $K - 1$ messages $w_{12,k} \in [1, 2^{nR_{12}}]$ and $w_{21,k} \in [1, 2^{nR_{21}}]$, $k = 1, 2, \dots, K - 1$ will be sent over the 2-way channel in nK transmissions.

Random Codebooks: Node-1 and Node-2 choose $2^{nR_{12}}$ and $2^{nR_{21}}$ i.i.d. $x_{12}^n(w_{12})$ and $x_{21}^n(w_{21})$ each with probability $p(x_{12}^n) = \prod_{i=1}^n p_{X_{12}}(x_{12,i})$ and $p(x_{21}^n) = \prod_{i=1}^n p_{X_{21}}(x_{21,i})$. Label these with $x_{12}^n(w_{12})$ and $x_{21}^n(w_{21})$, $w_{12} \in [1, 2^{nR_{12}}]$ and $w_{21} \in [1, 2^{nR_{21}}]$.

The relay node chooses $2^{nR_{R,2}}$ i.i.d. $u^n(c)$ each with probability $p(u^n) = \prod_{i=1}^n p_U(u_i)$. Label these $u^n(c)$, $c \in [1, 2^{nR_{R,2}}]$. And for each $u^n(c)$, the relay node chooses $2^{n(R_{R,1}-R_{R,2})}$ i.i.d. x_R^n each with probability $p(x_R^n|u^n(c)) = \prod_{i=1}^n p_{X_{R|U}}(x_{R,i}|u_i)$. Label these $x_R^n(f|c)$, $f \in [1, 2^{n(R_{R,1}-R_{R,2})}]$. Note that we assume a degraded broadcast channel with $X_R \rightarrow Y_1 \rightarrow Y_2$ forms a Markov chain where Y_i is received signal the i -th node for $i = 1, 2$.

Now we will choose our codebook at the relay node for compression. There are two levels of refinement for compression as in the channel code for degraded BC. For each $u^n(c)$ choose $2^{n\hat{R}_c}$ i.i.d. \hat{y}_{R_2} (coarse compressed signal) with $p(\hat{y}_{R_2}^n|u^n(c)) = \prod_{i=1}^n p_{\hat{Y}_{R_2,i}|U_i}(\hat{y}_{R_2,i}|u_i)$ and label these $\hat{y}_{R_2}^n(r|c)$, $r \in [1, 2^{n\hat{R}_c}]$. Then, for finer compression, for all $x_R^n(f|c)$, $u^n(c)$, $\hat{y}_{R_2}^n(r|c)$ choose $2^{n(\hat{R}-\hat{R}_c)}$ i.i.d. \hat{y}_R^n with

$$p(\hat{y}_R^n|u^n(c), x_R^n(f|c), \hat{y}_{R_2}^n(r|c)) = \prod_{i=1}^n p(\hat{y}_{R,i}|u_i(c), x_{R,i}(f|c), \hat{y}_{R_2,i}(r|c))$$

and label these $\hat{y}_R^n(z|r, f, c)$, $z \in [1, 2^{n(\hat{R}-\hat{R}_c)}]$.

For the course compression, randomly partition the set $\{1, 2, \dots, 2^{n\hat{R}_c}\}$ into $2^{nR_{R,2}}$ cells S_c where $c \in [1, 2^{nR_{R,2}}]$. And for the finer compression randomly partition the set $\{1, 2, \dots, 2^{n(\hat{R}-\hat{R}_c)}\}$ into $2^{n(R_{R,1}-R_{R,2})}$ cells S_f where $f \in [1, 2^{n(R_{R,1}-R_{R,2})}]$.

Encoding: Node-1 and Node-2 send $x_{12}^n(w_{12})$ and $x_{21}^n(w_{21})$ in block $k - 1$, respectively. Upon receiving $y_{R,k-1}^n$, the relay node sends $x_R^n(f_k, c_k)$ in block k such that $\{\hat{y}_{R_2}^n(r_k|c_k), y_{R,k-1}^n, u^n(c_k)\}$ are jointly ϵ -typical and $r_k \in S_{c_k}$, and $\{\hat{y}_R^n(z_k|r_k, f_k, c_k), \hat{y}_{R_2}^n(r_k|c_k), y_{R,k-1}^n, x_R^n(f_k|c_k), u^n(c_k)\}$ are jointly ϵ -typical and $z_k \in S_{f_k}$.

Decoding: At the end of block k we have the following.

Decoding at the Node-2 (Weak user):

1. The node-2 estimates c_k by \hat{c}_k by looking for the unique typical $u^n(c_k)$ with $y_{2,k}^n$. If

$$R_{R,2} \leq I(U; Y_2 | X_{21}) = I(U; Y_2) \quad (6.46)$$

and $n \rightarrow \infty$, then corresponding error probability will be small.

2. Then the node-2 calculates a set $L(x_{21}^n)$ of r such that $r \in L(x_{21}^n)$ if $\{\hat{y}_{R_2}^n(r_k|\hat{c}_k), x_{21}^n(w_{21}), u^n(\hat{c}_k)\}$ are jointly ϵ -typical. The node-2 declares r_k was sent if

$$\hat{r}_k \in S_{\hat{c}_k} \cap L(x_{21}^n). \quad (6.47)$$

With high probability $r_k = \hat{r}_k$ if $n \rightarrow \infty$ and

$$\hat{R}_c \leq I(\hat{Y}_{R_2}; X_{21}|U) + R_{R,2}. \quad (6.48)$$

3. Using $\hat{y}_{R_2}^n(\hat{r}_k|\hat{c}_k)$ with the side information $x_{21}^n(w_{21})$, the node-2 decides that $\hat{w}_{12,k-1}$ was sent in block $k-1$ if

$$R_{12} \leq I(X_{12}; \hat{Y}_{R_2}|U, X_{21}) \quad (6.49)$$

and $n \rightarrow \infty$.

4. For the relay node, upon receiving $y_{R,k-1}^n$, it decides that r_k is received if $\{\hat{y}_{R_2}^n(r_k|c_k), y_{R,k-1}^n, u^n(c_k)\}$ are jointly ϵ -typical. From rate-distortion theory, there exists such r_k with high probability if

$$\hat{R}_c > I(\hat{Y}_{R_2}; Y_R|U) \quad (6.50)$$

and $n \rightarrow \infty$.

5. Now if we combine the results for compression rates we have

$$I(\hat{Y}_{R_2}; Y_R|U) < \hat{R}_c \leq I(\hat{Y}_{R_2}; X_{21}|U) + R_{R,2} \quad (6.51)$$

which leads to

$$\begin{aligned} R_{R,2} &> I(\hat{Y}_{R_2}; Y_R|U) - I(\hat{Y}_{R_2}; X_{21}|U) \\ &= H(\hat{Y}_{R_2}|U) - H(\hat{Y}_{R_2}|Y_R, U) - H(\hat{Y}_{R_2}|U) + H(\hat{Y}_{R_2}|U, X_{21}) \\ &= H(\hat{Y}_{R_2}|U, X_{21}) - H(\hat{Y}_{R_2}|Y_R, U) \\ &= H(\hat{Y}_{R_2}|U, X_{21}) - H(\hat{Y}_{R_2}|Y_R, X_{21}, U) \\ &= I(\hat{Y}_{R_2}; Y_R|U, X_{21}). \end{aligned} \quad (6.52)$$

Hence using (6.46) and (6.52) we have

$$I(\hat{Y}_{R_2}; Y_R|X_{21}, U) < R_{R,2} \leq I(U; Y_2). \quad (6.53)$$

Decoding at the Node-1 (Strong user):

1. The node-1 first estimates c_k by \hat{c}_k by looking for the unique typical $u^n(c_k)$ with $y_{1,k}^n$. If

$$R_{R,2} \leq I(U; Y_1|X_{12}) = I(U; Y_1) \quad (6.54)$$

and $n \rightarrow \infty$, then corresponding error probability will be small. Note that due to the degradedness of the BC we have $I(U; Y_1) > I(U; Y_2) > R_{R,2}$.

2. After decoding \hat{c}_k (the cloud centers) the node-2 looks for f_k (the refinement points) such that $x_R^n(f_k|\hat{c}_k)$ is jointly ϵ -typical with $y_{1,k}^n$ given $u^n(\hat{c}_k)$, i.e., $\{x_R^n(f_k|\hat{c}_k), y_{1,k}^n | u^n(\hat{c}_k)\}$ are jointly ϵ -typical. If

$$R_{R,1} \leq I(X_R; Y_1|U) + R_{R,2} \quad (6.55)$$

and $n \rightarrow \infty$, then corresponding error probability will be small.

3. Then the node-1 calculates a set $L_1(x_{12}^n)$ of r such that $r \in L_1(x_{12}^n)$ if $\{\hat{y}_{R_2}^n(r_k|\hat{c}_k), x_{12}^n(w_{12}), u^n(\hat{c}_k)\}$ are jointly ϵ -typical. The node-1 declares r_k was sent if

$$\hat{r}_k \in S_{\hat{c}_k} \cap L_1(x_{12}^n). \quad (6.56)$$

With high probability $r_k = \hat{r}_k$ if $n \rightarrow \infty$ and

$$\hat{R}_c \leq I(\hat{Y}_{R_2}; X_{12}|U) + R_{R,2}. \quad (6.57)$$

Using the lower bound for \hat{R}_c , we have

$$R_{R,2} > I(\hat{Y}_{R_2}; Y_R|X_{12}, U) \quad (6.58)$$

and combining (6.53) with (6.58) we have the following lower bound for $R_{R,2}$:

$$R_{R,2} > \max\{I(\hat{Y}_{R_2}; Y_R|X_{21}, U), I(\hat{Y}_{R_2}; Y_R|X_{12}, U)\}. \quad (6.59)$$

4. After finding \hat{r}_k , the node-1 now calculates a set $L_2(x_{12}^n)$ of z such that $z \in L_2(x_{12}^n)$ if $\{\hat{y}_R^n(z_k|\hat{r}_k, \hat{c}_k, \hat{f}_k), \hat{y}_{R_2}^n(\hat{r}_k|\hat{c}_k), x_{12}^n(w_{12}), u^n(\hat{c}_k), x_R^n(\hat{f}_k|\hat{c}_k)\}$ are jointly ϵ -typical. The node-1 declares z_k was sent if

$$\hat{z}_k \in S_{\hat{f}_k} \cap L_2(x_{12}^n). \quad (6.60)$$

With high probability $z_k = \hat{z}_k$ if $n \rightarrow \infty$ and

$$\hat{R} - \hat{R}_c \leq I(\hat{Y}_R; X_{12}|\hat{Y}_{R_2}, X_R, U) + R_{R,1} - R_{R,2}. \quad (6.61)$$

5. Using $\hat{y}_2^n(\hat{z}_k|\hat{r}_k, \hat{c}_k, \hat{f}_k)$ and $\hat{y}_{R_2}^n(\hat{r}_k|\hat{c}_k)$ with the side information $x_{12}^n(w_{12})$, the node-1 decides that $\hat{w}_{21,k-1}$ was sent in block $k-1$ if

$$\{x_{21}^n(w_{21}), \hat{y}_R^n(z_k|\hat{r}_k, \hat{c}_k, \hat{f}_k), \hat{y}_{R_2}^n(r_k|\hat{c}_k), u^n(\hat{c}_k), x_{R,k}^n(\hat{f}_k|\hat{c}_k)|x_{12}^n(w_{12})\}$$

are jointly ϵ -typical. Thus, $w_{21} = \hat{w}_{21}$ with high probability if

$$\begin{aligned} R_{21} &\leq I(X_{21}; \hat{Y}_R, \hat{Y}_{R_2}|U, X_R, X_{12}) \\ &= I(X_{21}; \hat{Y}_R|U, X_R, X_{12}) + \underbrace{I(X_{21}; \hat{Y}_{R_2}|\hat{Y}_R, U, X_R, X_{12})}_{=0} \\ &= I(X_{21}; \hat{Y}_R|U, X_R, X_{12}) \end{aligned} \quad (6.62)$$

and $n \rightarrow \infty$.

6. For the relay node, upon receiving $y_{R,k}^n$, it decides that z_k is received if $\{\hat{y}_R^n(z_k|r_k, f_k, c_k), \hat{y}_{R_2}^n(r_k|c_k), y_{R,k}^n, x_R^n(f_k|c_k), u^n(c_k)\}$ are jointly ϵ -typical. From rate-distortion theory, there exists such z_k with high probability if $n \rightarrow \infty$ and

$$\hat{R} - \hat{R}_c > I(\hat{Y}_R; Y_R | \hat{Y}_{R_2}, X_R, U). \quad (6.63)$$

7. Now if we combine (6.61) and (6.63) we have

$$I(\hat{Y}_R; Y_R | \hat{Y}_{R_2}, X_R, U) < I(\hat{Y}_R; X_{12} | \hat{Y}_{R_2}, X_R, U) + R_{R,1} - R_{R,2} \quad (6.64)$$

which leads to

$$\begin{aligned} R_{R,1} - R_{R,2} &> I(\hat{Y}_R; Y_R | \hat{Y}_{R_2}, X_R, U) - I(\hat{Y}_R; X_{12} | \hat{Y}_{R_2}, X_R, U) \\ &= H(\hat{Y}_R | \hat{Y}_{R_2}, X_R, U) - H(\hat{Y}_R | Y_R, \hat{Y}_{R_2}, X_R, U) \\ &\quad - H(\hat{Y}_R | \hat{Y}_{R_2}, X_R, U) + H(\hat{Y}_R | X_{12}, \hat{Y}_{R_2}, X_R, U) \\ &= H(\hat{Y}_R | X_{12}, \hat{Y}_{R_2}, X_R, U) - H(\hat{Y}_R | Y_R, \hat{Y}_{R_2}, X_R, U) \\ &= H(\hat{Y}_R | X_{12}, \hat{Y}_{R_2}, X_R, U) - H(\hat{Y}_R | Y_R, X_{12}, \hat{Y}_{R_2}, X_R, U) \\ &= I(\hat{Y}_R; Y_R | \hat{Y}_{R_2}, X_{12}, X_R, U), \end{aligned} \quad (6.65)$$

equivalently, using the lower bound on $R_{R,2}$ we have the following lower bound for $R_{R,1}$

$$\begin{aligned} R_{R,1} &> I(\hat{Y}_R; Y_R | \hat{Y}_{R_2}, X_{12}, X_R, U) + R_{R,2} \\ &> I(\hat{Y}_R; Y_R | \hat{Y}_{R_2}, X_{12}, X_R, U) + \max\{I(\hat{Y}_{R_2}; Y_R | X_{21}, U), I(\hat{Y}_{R_2}; Y_R | X_{12}, U)\} \\ &= I(\hat{Y}_R; Y_R | \hat{Y}_{R_2}, X_{12}, X_R, U) + \max\{I(\hat{Y}_{R_2}; Y_R | X_{21}, X_R, U), I(\hat{Y}_{R_2}; Y_R | X_{12}, X_R, U)\} \\ &= \max\{I(\hat{Y}_R; Y_R | \hat{Y}_{R_2}, X_{12}, X_R, U) + I(\hat{Y}_{R_2}; Y_R | X_{21}, X_R, U), I(\hat{Y}_R, \hat{Y}_{R_2}; Y_R | X_{12}, X_R, U)\} \\ &\stackrel{(a)}{=} \max\{I(\hat{Y}_R; Y_R | \hat{Y}_{R_2}, X_{12}, X_R, U) + I(\hat{Y}_{R_2}; Y_R | X_{21}, X_R, U), I(\hat{Y}_R; Y_R | X_{12}, X_R, U)\} \end{aligned} \quad (6.66)$$

where (a) follows since $(X_{12}, X_{21}) \rightarrow Y_R \rightarrow \hat{Y}_R \rightarrow \hat{Y}_{R_2}$ forms a Markov chain.

At the end, for the two-way relay channel using Wyner-Ziv compression technique [32] with the degraded broadcast channel assumption (i.e., $U \rightarrow X_R \rightarrow Y_1 \rightarrow Y_2$ forms a Markov chain), combining (6.46), (6.55), (6.59) and (6.66) we get the conditions for (6.33) which concludes the proof.

Chapter 7

Multi-pair Two-way Relay Channel with Multiple Antenna Relay Station

7.1 Introduction

In this chapter, we consider a practical relaying scenario where all the nodes in the system, e.g. the mobile stations (MSs) and relay station (RS), operate in HD mode. Although providing the advantages specified in the previous chapter, the half-duplex constraint at the RS imposes a well-known pre-log factor $1/2$ for the overall system throughput and therefore limits the achievable spectral efficiency.

To circumvent the spectral efficiency loss in the one-way relay channel, the two-way relay channel (TWRC) has recently been proposed where both MSs exchange information via the intermediate RS [43, 44, 48–50, 52, 53, 85]. This kind of scenario can occur in satellite communications where different ground stations want to exchange information or in public safety networks where different intervening entities (e.g. fire-fighters) want to communicate with each other (to gain information about the current status at different parts of the disaster area for example) for example [43]. The MSs send their messages to the RS, which then processes the received signals according to a given relaying strategy and broadcasts to the MSs. This two-way relaying, assuming only two MSs, provides interference-free reception since at each MS the self-interference can be canceled before decoding the unknown message. For the TWRC, analog network coding where the mobiles' signals are combined in the air and digital network

coding where the RS first decodes the MSs' signals and combines the decoded bits using the bit-wise XOR operation are the main schemes considered. [92,93] study the single pair TWRC with multiple antenna RS and propose different RS precoding schemes.

In this chapter, we consider a multi-pair two-way relay channel (TWRC) where the single-antenna MS on each pair seek to communicate, and can do so, via a common multiple antenna RS. In the multi-pair TWRC, the main bottleneck on system performance is the interference seen by each MS due to the other communicating MS pairs. We try to tackle this problem in the spatial domain by using multiple antennas at the RS. Recently there has been research effort on the multi-pair TWRC [94–96]. Both [94] and [96] deal with a multi-pair multi-antenna RS TWRC with DF relaying followed by digital network coding (bitwise XOR) scheme. In [94], a precoding matrix optimization algorithm is developed for maximizing the sum-rate of the system, whereas [96] propose a multi-group multi-cast aware beamforming scheme for the transmission in the second phase. Both separate MSs spatially using a multi-antenna RS. In [95], on the other hand, a multi-pair TWRC is studied where a single antenna RS orthogonalizes the users in the studied multi-pair TWRC using Code Division Multiple Access (CDMA). However, in [94,96] the MSs are separated spatially by a multi-antenna RS.

In this chapter, we focus on AF and QF relaying strategies: these are particularly attractive when there is a complexity constraint at the relay node or when the latter is oblivious to the codebooks of the MSs, in which case DF would not be possible. Moreover, as our simulations will show there are SNR ranges over which they outperform the DF strategy. We thus propose specific schemes for both types of relaying and analyze their achievable sum-rate performance. In particular, two beamforming schemes are proposed for AF relaying: a simple Tx-Rx zero-forcing (ZF) scheme and a Tx-Rx block-diagonalization (BD)-based scheme, adapted to our specific setup. We show that the BD achieves better sum-rate than the ZF since in the BD scheme the relay does not need to invert the whole channel as opposed to the ZF scheme and save power. Then, for QF based relaying, we let the RS separate the signals corresponding to the MSs in each pair and quantize the processed received signals as accurately as allowed by the achievable rates in the second hop of communication. Here, by taking into account the side information at each MS, we quantize a scalar which is an appropriately selected linear combination of the processed RS received signal vector, thereby avoiding vector quantization. This approach may be seen as an analog form of network coding facilitating self interference cancelation at each MS.

7.2 System Model

The communication scenario considered is depicted in Figure 9.6 where K pairs of single-antenna MSs each communicate bi-directionally via a single M -antenna RS; there are no direct links between any of the $N = 2K$ single antenna MSs,

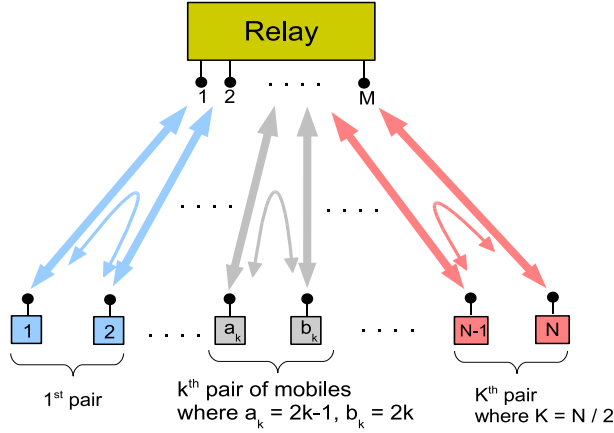


Figure 7.1: K -pair ($N = 2K$ MSs) TWRC with an M antenna RS.

as is standardly assumed, e.g. in [43, 92, 94].

Transmission is divided into two phases with *equal* time duration. In the first phase, the nodes simultaneously transmit their messages to the RS (UL communication from the MSs to the RS); in this phase, as in [94], CSI is not available at the MSs but is available at the RS. In the second phase, the RS transmits some processed version of the received signal (DL communication from the RS to the MSs); here CSI is available at both the transmitting RS and the receiving MSs. The exact relaying schemes used will be detailed in the next two sections.

Each node knows its own signal and can thus cancel it out of the DL received signal, and since it only needs the message of its pair, the remaining $N - 2$ messages from the other $K - 1$ pairs thus constitute interference. Note that due to the side information available at each receiver this scheme is different from, but could be related to, multi-user MIMO broadcasting.

Denote by \mathbf{h}_i the channel coefficients vector between MS i and the RS in the UL direction, \mathbf{g}_i the corresponding channel in the DL direction; both \mathbf{h}_i and $\mathbf{g}_i \in \mathbb{C}^M$. Further, let the k -th communicating pair consist of MS a_k and MS b_k where $a_k = 2k - 1$ and $b_k = 2k$, $k = 1, \dots, K$.

The signal received at the RS in the first phase is given by:

$$\mathbf{y}_R = \sum_{i=1}^N \mathbf{h}_i x_i + \mathbf{n}_R \quad (7.1)$$

where x_i is the signal transmitted from MS i , and is subject to an average power

constraint $p_i := \mathbb{E}[|x_i|^2]$, for $i = 1, \dots, N$. The noise vector \mathbf{n}_R is assumed to have i.i.d. components which are zero-mean complex circularly symmetric Gaussian variables of variance σ_R^2 , $\mathcal{CN}(0, \sigma_R^2)$. Similarly, the signal received at MS i in the second phase is given by:

$$y_i = \mathbf{g}_i^T \mathbf{x}_R + n_i \quad (7.2)$$

where $\mathbf{x}_R \in \mathbb{C}^M$ is the RS transmit signal and is subject to an average power constraint P_R . The noise n_i is $\mathcal{CN}(0, \sigma^2)$.

Our main performance measure is the overall sum-rate:

$$R_{sum} = \frac{1}{2} \sum_{i=1}^N \log_2(1 + \gamma_i), \quad (7.3)$$

where $1/2$ is due to the HD (half-duplex) relaying and γ_i is the receive SNR (or SINR) at MS i . The γ_i 's, as well as the signals transmitted depending on the exact relaying strategy adopted, and are specified in the next two sections.

7.3 Amplify-and-forward (AF) Relaying Schemes

In AF relaying, the RS transmit signal, \mathbf{x}_R , is given by

$$\mathbf{x}_R = \mathbf{A}_R \mathbf{y}_R \quad (7.4)$$

where the linear processing matrix $\mathbf{A}_R \in \mathbb{C}^{M \times M}$ is selected so as to meet the RS power constraint:

$$\begin{aligned} \mathbb{E}[\mathbf{x}_R^H \mathbf{x}_R] &= \mathbb{E}[\mathbf{y}_R^H \mathbf{A}_R^H \mathbf{A}_R \mathbf{y}_R] \\ &= \mathbb{E} \left[\left(\sum_{i=1}^N \mathbf{h}_i x_i + \mathbf{n}_R \right)^H \mathbf{A}_R^H \mathbf{A}_R \left(\sum_{i=1}^N \mathbf{h}_i x_i + \mathbf{n}_R \right) \right] \\ &= \text{Tr} \left[\left(\sum_{i=1}^N p_i \mathbf{h}_i \mathbf{h}_i^H + \sigma^2 \mathbf{I} \right) \mathbf{A}_R^H \mathbf{A}_R \right] \leq P_R \end{aligned} \quad (7.5)$$

After eliminating its own signal (recall that we assume CSIR), the SINR at MS $a_k, \forall k$ will be given by:

$$\gamma_{a_k} = \frac{p_{b_k} |\mathbf{g}_{a_k}^T \mathbf{A}_R \mathbf{h}_{b_k}|^2}{\sigma^2 + \sigma_R^2 \|\mathbf{g}_{a_k}^T \mathbf{A}_R\|^2 + \sum_{j \neq a_k, b_k} p_j |\mathbf{g}_{a_k}^T \mathbf{A}_R \mathbf{h}_j|^2}. \quad (7.6)$$

7.3.1 General structure of the linear processing matrix \mathbf{A}_R

The structure of the linear processing matrix at the RS, \mathbf{A}_R , has yet to be specified. The optimal structure given our performance metric would maximize the sum rate subject to the given power constraint at the RS. To avoid a

non-tractable optimization problem, we instead resort to suboptimal structures, which ensure that inter-pair interference is eliminated. To guarantee the feasibility of such a solution, we assume that $M \geq N = 2K$. Moreover, to formulate the proposed suboptimal solutions, we find it useful to decompose \mathbf{A}_R into:

$$\mathbf{A}_R = \mathbf{M} \mathbf{D} \mathbf{F} \quad (7.7)$$

where $\mathbf{M} \in \mathbb{C}^{M \times \bar{R}}$, $\mathbf{D} \in \mathbb{C}^{\bar{R} \times \bar{L}}$ and $\mathbf{F} \in \mathbb{C}^{\bar{L} \times M}$, (\bar{R} and \bar{L} will be specified later) and have the following forms:

$$\begin{aligned} \mathbf{M} &= [\mathbf{M}_1 \ \mathbf{M}_2 \ \dots \ \mathbf{M}_K], \\ \mathbf{D} &= \text{diag}\{\mathbf{D}_1, \mathbf{D}_2, \dots, \mathbf{D}_K\}, \\ \mathbf{F} &= [\mathbf{F}_1^T \ \mathbf{F}_2^T \ \dots \ \mathbf{F}_K^T]^T, \end{aligned} \quad (7.8)$$

where $\mathbf{M}_k \in \mathbb{C}^{M \times \bar{R}_k}$, $\mathbf{D}_k \in \mathbb{C}^{\bar{R}_k \times \bar{L}_k}$ and $\mathbf{F}_k \in \mathbb{C}^{\bar{L}_k \times M}$, $k = 1, 2, \dots, K$. Thus $\bar{R} = \sum_{k=1}^K \bar{R}_k$ and $\bar{L} = \sum_{k=1}^K \bar{L}_k$ where \bar{R}_k and \bar{L}_k are specified later. Letting $\mathbf{A}_k = \mathbf{M}_k \mathbf{D}_k \mathbf{F}_k$, one can rewrite \mathbf{A}_R as

$$\mathbf{A}_R = \sum_{k=1}^K \mathbf{M}_k \mathbf{D}_k \mathbf{F}_k = \sum_{k=1}^K \mathbf{A}_k. \quad (7.9)$$

7.3.2 Receive and Transmit Zero-Forcing at the Relay

The simplest RS precoding scheme which satisfies the no inter-pair interference constraint we want to impose is one that only allows its intended signal to reach each receiver (thus even its own transmitted signal is canceled out by the RS). In the first hop the RS implements the well-known ZF receive filter then it permutes the signal position so as to ensure that each signal arrives at its destination. After that it uses a ZF transmit filter to send the signals to the MSs in the second hop.

The ZF receive filter is given by:

$$\mathbf{F} = \mathbf{H}^\dagger = (\mathbf{H}^H \mathbf{H})^{-1} \mathbf{H}^H. \quad (7.10)$$

Then, the RS permutes the received signals with the following matrix:

$$\underline{\mathbf{D}} = \text{diag}(\underline{\mathbf{D}}_1, \dots, \underline{\mathbf{D}}_K) \quad \text{where} \quad \underline{\mathbf{D}}_k = \begin{bmatrix} 0 & 1 \\ 1 & 0 \end{bmatrix}, \quad \forall k$$

and we define $\mathbf{D} = \rho \underline{\mathbf{D}}$ where ρ is for transmit power scaling. For transmission the RS chooses the following ZF transmit filter:

$$\mathbf{M} = \mathbf{G}^\dagger = \mathbf{G}^H (\mathbf{G} \mathbf{G}^H)^{-1} \quad (7.11)$$

and the corresponding RS precoding matrix is given by:

$$\mathbf{A}_R = \mathbf{M} \mathbf{D} \mathbf{F} = \rho \mathbf{M} \underline{\mathbf{D}} \mathbf{F} = \rho \underline{\mathbf{A}}_R \quad (7.12)$$

where

$$\rho = \sqrt{\frac{P_R}{\text{Tr} \left[\left(\sum_{i=1}^N p_i \mathbf{h}_i \mathbf{h}_i^H + \sigma^2 \mathbf{I} \right) \underline{\mathbf{A}}_R^H \underline{\mathbf{A}}_R \right]}}$$

and the SNR at the MS a_k is given by

$$\gamma_{a_k} = \frac{\rho^2 p_{b_k}}{\sigma^2 + \rho^2 \sigma_R^2 \|\mathbf{f}_{a_k}\|^2}, \quad \forall k \quad (7.13)$$

where $\mathbf{F} = [\mathbf{f}_{a_1} \quad \mathbf{f}_{b_1} \quad \dots \quad \mathbf{f}_{a_K} \quad \mathbf{f}_{b_K}]^T$.

7.3.3 Block-Diagonalization (BD) for the TWRC

The ZF structure in the previous section does not consider the fact that the RS should worry solely about eliminating inter-pair interference, but not the intra-pair interference since the individual MSs can take care of that themselves. A natural way to take this into consideration is to by adapting the BD technique of [97] to the TWRC problem, which we do in the following.

If we define $\tilde{\mathbf{H}}_k$ as

$$\tilde{\mathbf{H}}_k = [\mathbf{H}_1 \quad \dots \quad \mathbf{H}_{k-1} \quad \mathbf{H}_{k+1} \quad \dots \quad \mathbf{H}_K], \quad (7.14)$$

where $\mathbf{H}_k = [\mathbf{h}_{a_k} \quad \mathbf{h}_{b_k}]$ is the UL channel matrix of the k -th pair, then \mathbf{F}_k should lie in the null space of $\tilde{\mathbf{H}}_k$ so as to separate the UL signals of each pair. Define $\tilde{L}_k = \text{rank}(\tilde{\mathbf{H}}_k) \leq N - 2$, as in [97]. We can define the singular value decomposition (SVD) of $\tilde{\mathbf{H}}_k$ as follows:

$$\tilde{\mathbf{H}}_k = \left[\mathbf{U}_{\tilde{\mathbf{H}}_k}^{(1)} \quad \mathbf{U}_{\tilde{\mathbf{H}}_k}^{(0)} \right] \Sigma_{\tilde{\mathbf{H}}_k} \mathbf{V}_{\tilde{\mathbf{H}}_k}^H \quad (7.15)$$

where $\mathbf{U}_{\tilde{\mathbf{H}}_k}^{(1)}$ holds the first \tilde{L}_k left singular vectors, and $\mathbf{U}_{\tilde{\mathbf{H}}_k}^{(0)}$ holds the last $M - \tilde{L}_k$ left singular vectors and forms an orthogonal basis for the null space of $\tilde{\mathbf{H}}_k$. Define the following SVD for the channels of the k -th pair:

$$\mathbf{U}_{\tilde{\mathbf{H}}_k}^{(0)H} \mathbf{H}_k = \left[\mathbf{U}_{\mathbf{H}_k}^{(1)} \quad \mathbf{U}_{\mathbf{H}_k}^{(0)} \right] \begin{bmatrix} \Sigma_{\mathbf{H}_k} & \mathbf{0} \\ \mathbf{0} & \mathbf{0} \end{bmatrix} \mathbf{V}_{\mathbf{H}_k}^H \quad (7.16)$$

where $\Sigma_{\mathbf{H}_k}$ is $\bar{L}_k \times \bar{L}_k$, $\mathbf{U}_{\mathbf{H}_k}^{(1)}$ holds the first \bar{L}_k left singular vectors. The product of $\mathbf{U}_{\mathbf{H}_k}^{(1)H}$ and $\mathbf{U}_{\tilde{\mathbf{H}}_k}^{(0)H}$ produces an orthogonal basis of dimension \bar{L}_k .

Then, in order to be able to have zero interference at each MS pairs, the RS selects \mathbf{F}_k as follows:

$$\mathbf{F}_k = \mathbf{U}_{\mathbf{H}_k}^{(1)H} \mathbf{U}_{\tilde{\mathbf{H}}_k}^{(0)H} = \left(\mathbf{U}_{\tilde{\mathbf{H}}_k}^{(0)} \quad \mathbf{U}_{\mathbf{H}_k}^{(1)} \right)^H \in \mathbb{C}^{\bar{L}_k \times M}. \quad (7.17)$$

In second hop, the signal received at the i -th MS is given by (7.2). Let $\mathbf{G} = [\mathbf{g}_1 \ \mathbf{g}_2 \ \dots \ \mathbf{g}_N]^T \in \mathbb{C}^{N \times M}$ for $\mathbf{g}_k \in \mathbb{C}^{M \times 1}$ be the overall channel matrix from the RS to the MSs in the second hop. If we define $\mathbf{G}_k = [\mathbf{g}_{a_k} \ \mathbf{g}_{b_k}]^T \in \mathbb{C}^{2 \times M}$, for $k = 1, 2, \dots, K$, and let $\tilde{\mathbf{G}}_k$ be equal to

$$\tilde{\mathbf{G}}_k = [\mathbf{G}_1^T \ \dots \ \mathbf{G}_{k-1}^T \ \mathbf{G}_{k+1}^T \ \dots \ \mathbf{G}_K^T]^T, \quad (7.18)$$

then \mathbf{M}_k should lie in the null space of $\tilde{\mathbf{G}}_k$ for no inter-pair interference. With the above signal models we can write received signals for each pair of MSs as follows:

$$\begin{aligned} \mathbf{y}_k &= \mathbf{G}_k \mathbf{x}_R + \mathbf{n}_k = \mathbf{G}_k \mathbf{A}_R \left(\sum_{j=1}^K \mathbf{H}_j \mathbf{x}_j + \mathbf{n}_R \right) + \mathbf{n}_k \\ &= \mathbf{G}_k \mathbf{A}_R \mathbf{H}_k \mathbf{x}_k + \mathbf{G}_k \mathbf{A}_R \left(\sum_{\substack{j=1 \\ j \neq k}}^K \mathbf{H}_j \mathbf{x}_j + \mathbf{n}_R \right) + \mathbf{n}_k \end{aligned} \quad (7.19)$$

Define $\tilde{R}_k = \text{rank}(\tilde{\mathbf{G}}_k) \leq N - 2$. We can express the SVD of $\tilde{\mathbf{G}}_k$ as follows:

$$\tilde{\mathbf{G}}_k = \mathbf{U}_{\tilde{\mathbf{G}}_k} \Sigma_{\tilde{\mathbf{G}}_k} \begin{bmatrix} \mathbf{V}_{\tilde{\mathbf{G}}_k}^{(1)} & \mathbf{V}_{\tilde{\mathbf{G}}_k}^{(0)} \end{bmatrix}^H \quad (7.20)$$

where $\mathbf{V}_{\tilde{\mathbf{G}}_k}^{(1)}$ holds the first \tilde{R}_k right singular vectors, and $\mathbf{V}_{\tilde{\mathbf{G}}_k}^{(0)}$ holds the last $M - \tilde{R}_k$ right singular vectors and forms an orthogonal basis for the null space of $\tilde{\mathbf{G}}_k$.

Define the following SVD for the channels of the k -th pair in the second hop:

$$\mathbf{G}_k \mathbf{V}_{\tilde{\mathbf{G}}_k}^{(0)} = \mathbf{U}_{\mathbf{G}_k} \begin{bmatrix} \Sigma_{\mathbf{G}_k} & \mathbf{0} \\ \mathbf{0} & \mathbf{0} \end{bmatrix} \begin{bmatrix} \mathbf{V}_{\mathbf{G}_k}^{(1)} & \mathbf{V}_{\mathbf{G}_k}^{(0)} \end{bmatrix}^H \quad (7.21)$$

where $\Sigma_{\mathbf{G}_k}$ is $\bar{R}_k \times \bar{R}_k$, $\mathbf{V}_{\mathbf{G}_k}^{(1)}$ holds the first \bar{R}_k right singular vectors. The product of $\mathbf{V}_{\mathbf{G}_k}^{(1)}$ and $\mathbf{V}_{\tilde{\mathbf{G}}_k}^{(0)}$ produces an orthogonal basis of dimension \bar{R}_k . Then, for the RS operation we select \mathbf{M}_k as follows:

$$\mathbf{M}_k = \mathbf{V}_{\tilde{\mathbf{G}}_k}^{(0)} \mathbf{V}_{\mathbf{G}_k}^{(1)} \in \mathbb{C}^{M \times \bar{R}_k}. \quad (7.22)$$

After defining $\mathbf{F}_k \in \mathbb{C}^{\bar{L}_k \times M}$ and $\mathbf{M}_k \in \mathbb{C}^{M \times \bar{R}_k}$, we now give the structure for $\mathbf{D}_k \in \mathbb{C}^{\bar{R}_k \times \bar{L}_k}$. Define $\bar{Q}_k = \min\{\bar{R}_k, \bar{L}_k\}$ and let the RS power scaling factor be ρ , then we assume the following structure for \mathbf{D}_k :

$$\mathbf{D}_k = \rho \underline{\mathbf{D}}_k = \rho \begin{bmatrix} \mathbf{I}_{\bar{Q}_k \times \bar{Q}_k} & \mathbf{0} \\ \mathbf{0} & \mathbf{0} \end{bmatrix} \in \mathbb{C}^{\bar{R}_k \times \bar{L}_k}. \quad (7.23)$$

The RS transmit signal power is given by:

$$\mathbb{E} [\mathbf{x}_R^H \mathbf{x}_R] = \text{Tr} \left[\sum_{k=1}^K \mathbf{A}_k \mathbf{H}_k \mathbf{Q}_k \mathbf{H}_k^H \mathbf{A}_k^H + \sigma_R^2 \mathbf{A}_R \mathbf{A}_R^H \right]$$

where $\mathbf{Q}_k = \mathbb{E}[\mathbf{x}_k \mathbf{x}_k^H] = \text{diag}(p_{a_k}, p_{b_k})$. To meet the RS power constraint we need to select ρ as

$$\rho = \sqrt{\frac{P_R}{\text{Tr} \left[\sum_{k=1}^K \underline{\mathbf{A}}_k \mathbf{H}_k \mathbf{Q}_k \mathbf{H}_k^H \underline{\mathbf{A}}_k^H + \sigma_R^2 \underline{\mathbf{A}}_R \underline{\mathbf{A}}_R^H \right]}}$$

where $\underline{\mathbf{A}}_R = \sum_{k=1}^K \mathbf{M}_k \underline{\mathbf{D}}_k \mathbf{F}_k$.

With the structures given by (7.17), (7.22) and (7.23) each pair of MSs is guaranteed to receive inter-pair interference-free signals. After canceling the self-interference (using the knowledge of transmit signal), the received signal at MS a_k and the corresponding received SINR are given by:

$$y_{a_k} = \mathbf{g}_{a_k}^T \mathbf{A}_k \mathbf{h}_{b_k} x_{b_k} + \mathbf{g}_{a_k}^T \mathbf{A}_k \mathbf{n}_R + n_{a_k}, \quad (7.24)$$

$$\gamma_{a_k} = \frac{p_{b_k} |\mathbf{g}_{a_k}^T \mathbf{A}_k \mathbf{h}_{b_k}|^2}{\sigma^2 + \sigma_R^2 \|\mathbf{g}_{a_k}^T \mathbf{A}_k\|^2} \quad \forall k \quad (7.25)$$

where a_k and b_k are the MSs in the k -th pair willing to exchange information through the RS.

7.4 Quantize-and-Forward (QF) Relaying

In this section, we consider QF relaying where the RS quantizes the signal vector it receives in the first phase and sends the corresponding bin-index to the MSs in the second phase. Though sub-optimal, QF relaying is less complex than the CF relaying strategy in which the RS exploits the correlation between its received signal and the transmitted signal of each MS. We are lead to consider this scheme by the fact shown in [18] that as the DL channel quality improves, the system performance approaches the outer bound for the three-node relay channel. Here too, to avoid inter-pair interference, we resort to BD processing.

As each pair is only interested in part of the signal received at the RS, the latter first separates the received signals corresponding to each MS pair by using the receive BD filter \mathbf{F} given by (7.8) and (7.17), then proceeds to quantize each of the resulting signals independently. Thus, the processed received signal at the RS corresponding to the k -th pair is given by:

$$\bar{\mathbf{y}}_{R_k} = \mathbf{F}_k \mathbf{y}_R = \mathbf{F}_k \mathbf{H}_k \mathbf{x}_k + \mathbf{F}_k \mathbf{n}_R. \quad (7.26)$$

Moreover, since while decoding, each MS is able to subtract its own signal, we reduce the dimension of the source to be quantized from a two-dimensional vector, $\bar{\mathbf{y}}_{R_k}$ in (7.26), to a scalar, z_k , which is an appropriately selected linear combination of $\bar{\mathbf{y}}_{R_k}$'s components and send that to both MSs in the corresponding pair. Thus:

$$z_k = \mathbf{d}_k^H \bar{\mathbf{y}}_{R_k} = \mathbf{d}_k^H \mathbf{F}_k \mathbf{H}_k \mathbf{x}_k + \mathbf{d}_k^H \mathbf{F}_k \mathbf{n}_R \quad (7.27)$$

where the combining vector \mathbf{d}_k is selected so that the resulting pair sum-rate is maximized; this is illustrated below. In QF relaying, for each MS pair, the RS wants to reliably forward the quantized signal \hat{z}_k to the corresponding MSs in the pair where the quantized signal is selected according to the distribution $f(\hat{z}_k|z_k) \sim \mathcal{CN}(z_k, \sigma_{D_k}^2)$, where $\sigma_{D_k}^2$ is the noise variance due to the distortion in reconstructing z_k , i.e., $\hat{z}_k = z_k + n_{D_k}$ where $n_{D_k} \sim \mathcal{CN}(0, \sigma_{D_k}^2)$.

Now we need to reliably communicate from the RS to each MS pair a single signal s_k corresponding to that pair; signals corresponding to different pairs are independent. To do this, we use the multicast aware transmit beamforming scheme of [96] with a slight modification. The RS thus transmits

$$\mathbf{x}_R = [\mathbf{M}_1 \mathbf{b}_1 \dots \mathbf{M}_K \mathbf{b}_K] \begin{bmatrix} s_1 \\ \vdots \\ s_K \end{bmatrix} = \sum_{k=1}^K \mathbf{M}_k \mathbf{b}_k s_k \quad (7.28)$$

where \mathbf{M}_k was defined in the previous section (i.e. here too inter-pair interference is eliminated in the DL) and \mathbf{b}_k is selected so as to minimize distortion as will become clear in the following. With this structure the received signal at the MSs in the k -th pair is given by:

$$\mathbf{y}_k = \begin{bmatrix} y_{a_k} \\ y_{b_k} \end{bmatrix} = \mathbf{G}_k \mathbf{M}_k \mathbf{b}_k s_k + \mathbf{n}_k = \begin{bmatrix} \mathbf{g}_{a_k}^T \\ \mathbf{g}_{b_k}^T \end{bmatrix} \mathbf{M}_k \mathbf{b}_k s_k + \mathbf{n}_k. \quad (7.29)$$

For each pair, in order to be able to forward the quantized signal to both MSs, the following quantization rate constraint must be satisfied:

$$I(\hat{z}_k; z_k) \leq \min_{i \in \{a_k, b_k\}} I(s_k; y_i) \quad (7.30)$$

or equivalently, assuming Gaussian codebooks for transmission at the RS with $\mathbb{E}[|s_k|^2] = 1$, the quantization variance should be lower bounded by

$$\sigma_{D_k}^2 \geq \frac{\sigma^2 \mathbb{E}[|z_k|^2]}{\min_{i \in \{a_k, b_k\}} |\mathbf{g}_i^T \mathbf{M}_k \mathbf{b}_k|^2} \quad (7.31)$$

where $\mathbb{E}[|z_k|^2] = P_s \|\mathbf{d}_k^H \mathbf{F}_k \mathbf{H}_k\|^2 + \sigma_R^2 \|\mathbf{d}_k^H \mathbf{F}_k\|^2$. Then, for the a_k -th MS we have the following SNR expression:

$$\gamma_{a_k} = \frac{P_s \|\mathbf{d}_k^H \mathbf{F}_k \mathbf{h}_{b_k}\|^2}{\sigma_R^2 \|\mathbf{d}_k^H \mathbf{F}_k\|^2 + \sigma_{D_k}^2}. \quad (7.32)$$

A similar equation holds for the SNR of b_k by interchanging a_k and b_k in (7.32).

It was mentioned that \mathbf{b}_k is selected so as to minimize distortion: referring to (7.31) and assuming equal power allocation to each pair, it is the solution of the following optimization problem:

$$\begin{aligned} & \text{maximize}_{\mathbf{b}_k} \min_{i \in \{a_k, b_k\}} |\mathbf{g}_i^T \mathbf{M}_k \mathbf{b}_k|^2 \\ & \text{such that } \|\mathbf{M}_k \mathbf{b}_k\|^2 = \frac{P_R}{K} \end{aligned} \quad (7.33)$$

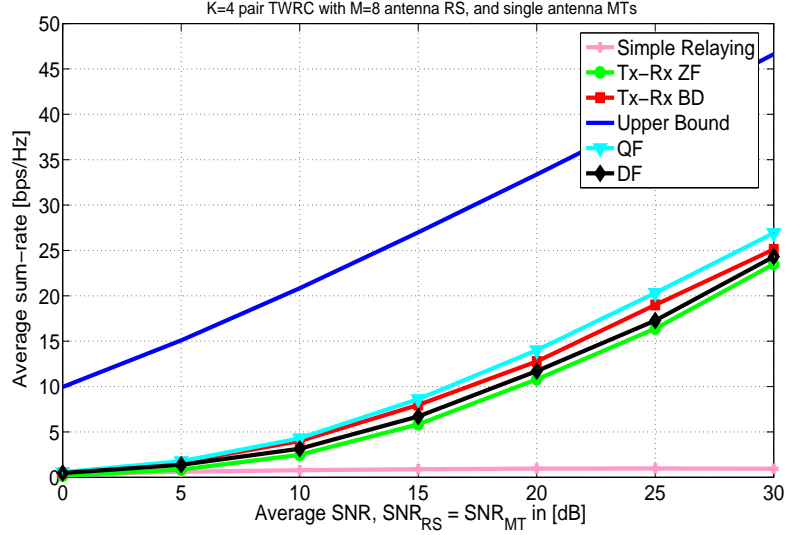


Figure 7.2: Average sum-rate vs. SNR_{RS} for $K = 4$ pair TWRC with $M = 8$ antenna RS and single antenna MSs with $SNR_{MS} = SNR_{RS}$.

Also, \mathbf{d}_k is selected so as to maximize the resulting sum rate of the k -th pair. Details of how this optimization problem and that in (7.33) are solved are given in the Appendix-(7.A) and -(7.B).

7.5 Simulation Results

Assume all MSs have equal power constraint $p_i = P_s, \forall i$ and $\sigma^2 = \sigma_R^2 = 1$. We define the average SNR at the RS as $SNR_{RS} = P_s/\sigma_R^2$ and at the MSs as $SNR_{MS} = P_R/\sigma^2$. The communication phases are divided into equivalent orthogonal time durations, i.e., all nodes are HD. We note that resource partitioning (time duration) at the first and second hop of the communication might increase the overall system performance for DF and QF/CF relaying schemes. Reciprocal flat Rayleigh fading channels with unit variance for all of the channels on both phases are assumed. For the simulations, a $K = 4$ pair ($N = 8$ MSs) TWRC with $M = 8$ antenna RS is considered.

We analyze and compare the average achievable sum-rates for the simple AF relaying scheme where the RS simply scales and forwards its received signal, the Tx-Rx ZF scheme, the Tx-Rx BD scheme and the proposed QF relaying scheme. As a benchmark we compare our proposed schemes to the ZF based DF relaying scheme from [96, Section 3.1].

Figure 7.2 illustrates the achievable average sum-rate versus SNR_{RS} with $SNR_{MS} = SNR_{RS}$. The proposed QF based relaying scheme achieves the best performance among the schemes considered. However, it is still far away from

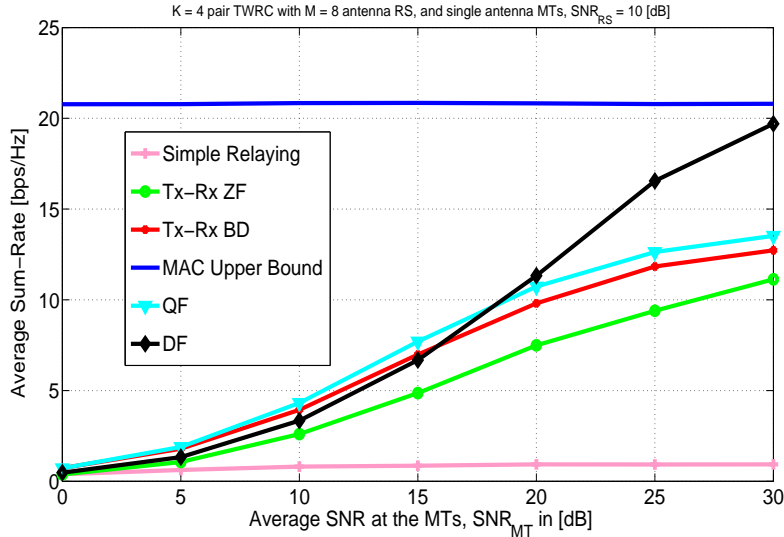


Figure 7.3: Average sum-rate vs. SNR_{MS} for $K = 4$ pair TWRC with $M = 8$ antenna RS and single antenna MSs with $SNR_{RS} = 10$ [dB].

the MAC outer bound. Note that the performance of DF scheme is even inferior to the AF based Tx-Rx BD scheme because of using a ZF precoder on the DL.

In Figure 7.3, we plot the achievable average sum-rate versus SNR_{MS} for $SNR_{RS} = 10$ [dB]. As the channel quality in the second phase, a bottleneck for the DF scheme, increases with SNR_{MS} , its achievable rate performance improves accordingly. However, the performance improvements in the AF and QF based schemes saturate with increasing SNR_{MS} due to noise amplification and power consumption in channel inversion for the AF based schemes and not exploiting superposition coding in the second phase for the QF based scheme (assuming single user decoding capabilities for the MSs). But still for low SNR_{MS} , the QF is the best.

Note that the BD always outperforms the ZF scheme because ZF consumes additional degrees of freedom unnecessarily as it does not exploit the fact that each mobile has side information (its own signal). Moreover, the performance of simple relaying is heavily interference limited.

7.6 Conclusion

In a multi-pair TWRC, the main bottleneck on the system performance is the interference seen by each MS from other communicating MS pairs. This chapter has tried to tackle this problem in the spatial domain by using multiple antennas at the RS. Beamforming schemes for the RS using either AF or QF relaying strategies, were proposed. Moreover, for the QF relaying we proposed

a signal combination scheme for each MS pair at the RS, which may be seen as an analog form of network coding to facilitate self-interference cancelation at each MS. The sum-rate performance of the different schemes was illustrated via simulations and compared to the DF relaying strategy.

7.A Optimizing over \mathbf{d}_k

Recall

$$\gamma_{a_k} = \frac{P_s \|\mathbf{d}_k^H \mathbf{F}_k \mathbf{h}_{b_k}\|^2}{\sigma_R^2 \|\mathbf{d}_k^H \mathbf{F}_k\|^2 + \sigma_{D_k}^2}. \quad (7.34)$$

and

$$\sigma_{D_k}^2 = \frac{\sigma^2 \mathbb{E} [|z_k|^2]}{\min_{i \in \{a_k, b_k\}} |\mathbf{g}_i^T \mathbf{M}_k \mathbf{b}_k|^2} \quad (7.35)$$

where $\mathbb{E} [|z_k|^2] = P_s \|\mathbf{d}_k^H \mathbf{F}_k \mathbf{H}_k\|^2 + \sigma_R^2 \|\mathbf{d}_k^H \mathbf{F}_k\|^2$. Letting $c_k = \min_{i \in \{a_k, b_k\}} |\mathbf{g}_i^T \mathbf{M}_k \mathbf{b}_k|^2$, γ_{a_k} becomes

$$\begin{aligned} \gamma_{a_k} &= \frac{P_s \|\mathbf{d}_k^H \mathbf{F}_k \mathbf{h}_{b_k}\|^2}{\sigma_R^2 \|\mathbf{d}_k^H \mathbf{F}_k\|^2 + \frac{\sigma^2}{c_k} \left[P_s \|\mathbf{d}_k^H \mathbf{F}_k \mathbf{H}_k\|^2 + \sigma_R^2 \|\mathbf{d}_k^H \mathbf{F}_k\|^2 \right]} \\ &= \frac{\mathbf{d}_k^H P_s \mathbf{F}_k \mathbf{h}_{b_k} \mathbf{h}_{b_k}^H \mathbf{F}_k^H \mathbf{d}_k}{\mathbf{d}_k^H \left[\sigma_R^2 \mathbf{F}_k \mathbf{F}_k^H + \frac{\sigma^2}{c_k} \left[P_s \mathbf{F}_k \mathbf{H}_k \mathbf{H}_k^H \mathbf{F}_k^H + \sigma_R^2 \mathbf{F}_k \mathbf{F}_k^H \right] \right] \mathbf{d}_k} \\ &= \frac{\mathbf{d}_k^H \mathbf{A}_{a_k} \mathbf{d}_k}{\mathbf{d}_k^H \mathbf{D}_k \mathbf{d}_k}, \end{aligned} \quad (7.36)$$

where $\mathbf{A}_{a_k} = P_s \mathbf{F}_k \mathbf{h}_{b_k} \mathbf{h}_{b_k}^H \mathbf{F}_k^H$ and $\mathbf{D}_k = \sigma_R^2 \left(1 + \frac{\sigma^2}{c_k} \right) \mathbf{F}_k \mathbf{F}_k^H + \frac{\sigma^2}{c_k} P_s \mathbf{F}_k \mathbf{H}_k \mathbf{H}_k^H \mathbf{F}_k^H$.

Maximizing a given pair's sum rate over \mathbf{d}_k is equivalent to maximizing

$\gamma_{a_k} + \gamma_{b_k} + \gamma_{a_k} \gamma_{b_k}$. Taking the derivative with respect to \mathbf{d}_k^H , we get

$$\begin{aligned}
& \frac{\mathbf{A}_{a_k} \mathbf{d}_k}{\mathbf{d}_k^H \mathbf{D}_k \mathbf{d}_k} - \frac{\mathbf{d}_k^H \mathbf{A}_{a_k} \mathbf{d}_k}{\left(\mathbf{d}_k^H \mathbf{D}_k \mathbf{d}_k\right)^2} \mathbf{D}_k \mathbf{d}_k \\
& + \frac{\mathbf{A}_{b_k} \mathbf{d}_k}{\mathbf{d}_k^H \mathbf{D}_k \mathbf{d}_k} - \frac{\mathbf{d}_k^H \mathbf{A}_{b_k} \mathbf{d}_k}{\left(\mathbf{d}_k^H \mathbf{D}_k \mathbf{d}_k\right)^2} \mathbf{D}_k \mathbf{d}_k \\
& + \left[\frac{\mathbf{A}_{a_k} \mathbf{d}_k}{\mathbf{d}_k^H \mathbf{D}_k \mathbf{d}_k} - \frac{\mathbf{d}_k^H \mathbf{A}_{a_k} \mathbf{d}_k}{\left(\mathbf{d}_k^H \mathbf{D}_k \mathbf{d}_k\right)^2} \mathbf{D}_k \mathbf{d}_k \right] \frac{\mathbf{d}_k^H \mathbf{A}_{b_k} \mathbf{d}_k}{\mathbf{d}_k^H \mathbf{D}_k \mathbf{d}_k} \\
& + \left[\frac{\mathbf{A}_{b_k} \mathbf{d}_k}{\mathbf{d}_k^H \mathbf{D}_k \mathbf{d}_k} - \frac{\mathbf{d}_k^H \mathbf{A}_{b_k} \mathbf{d}_k}{\left(\mathbf{d}_k^H \mathbf{D}_k \mathbf{d}_k\right)^2} \mathbf{D}_k \mathbf{d}_k \right] \frac{\mathbf{d}_k^H \mathbf{A}_{a_k} \mathbf{d}_k}{\mathbf{d}_k^H \mathbf{D}_k \mathbf{d}_k} = 0. \tag{7.37}
\end{aligned}$$

Rearranging and multiplying by $\mathbf{d}_k^H \mathbf{D}_k \mathbf{d}_k$

$$\begin{aligned}
& \underbrace{\left[\left(1 + \frac{\mathbf{d}_k^H \mathbf{A}_{b_k} \mathbf{d}_k}{\mathbf{d}_k^H \mathbf{D}_k \mathbf{d}_k} \right) \mathbf{A}_{a_k} + \left(1 + \frac{\mathbf{d}_k^H \mathbf{A}_{a_k} \mathbf{d}_k}{\mathbf{d}_k^H \mathbf{D}_k \mathbf{d}_k} \right) \mathbf{A}_{b_k} \right] \mathbf{d}_k}_{\triangleq \mathbf{T}_1} \\
& = \underbrace{\left[2 \frac{\mathbf{d}_k^H \mathbf{A}_{a_k} \mathbf{d}_k \mathbf{d}_k^H \mathbf{A}_{b_k} \mathbf{d}_k}{\left(\mathbf{d}_k^H \mathbf{D}_k \mathbf{d}_k\right)^2} + \frac{\mathbf{d}_k^H (\mathbf{A}_{a_k} + \mathbf{A}_{b_k}) \mathbf{d}_k}{\mathbf{d}_k^H \mathbf{D}_k \mathbf{d}_k} \right] \mathbf{D}_k \mathbf{d}_k}_{\triangleq \mathbf{T}_2} \tag{7.38}
\end{aligned}$$

Thus,

$$\mathbf{d}_k = \mathbf{T}_2^{-1} \mathbf{T}_1 \mathbf{d}_k \tag{7.39}$$

We solve for a stationary point \mathbf{d}_k by the following iterative algorithm

$$\mathbf{d}_k^{(i)} = \left(\mathbf{T}_2^{(i-1)} \right)^{-1} \mathbf{T}_1^{(i-1)} \mathbf{d}_k^{(i-1)}, \tag{7.40}$$

where $\mathbf{d}_k^{(i-1)}$ denotes the solution at the i th iteration and $\mathbf{d}_k^{(0)}$ is a randomly selected vector. Simulations show that this algorithm converges.

7.B Solving Problem (7.33)

Define \mathbf{x} as $\mathbf{M}_k \mathbf{b}_k$ and solve

$$\begin{aligned}
& \text{maximize}_{\mathbf{x}} \min_{i \in \{a_k, b_k\}} |\mathbf{g}_i^T \mathbf{x}|^2 \\
& \text{such that } \|\mathbf{x}\|^2 = \frac{P_R}{K} \tag{7.41}
\end{aligned}$$

\mathbf{x} can be written as

$$\mathbf{x} = \alpha \frac{\mathbf{g}_{a_k}^*}{\|\mathbf{g}_{a_k}\|} + \beta \frac{\Pi_{\mathbf{g}_{a_k}^*}^\perp \mathbf{g}_{b_k}^*}{\|\Pi_{\mathbf{g}_{a_k}^*}^\perp \mathbf{g}_{b_k}^*\|} \quad (7.42)$$

such that

$$|\alpha|^2 + |\beta|^2 = \frac{P_R}{K}. \quad (7.43)$$

Thus

$$|\mathbf{g}_{a_k}^T \mathbf{x}|^2 = |\alpha|^2 \|\mathbf{g}_{a_k}\|^2 \quad (7.44)$$

and

$$|\mathbf{g}_{b_k}^T \mathbf{x}|^2 = \left| \alpha \frac{\mathbf{g}_{b_k}^T \mathbf{g}_{a_k}^*}{\|\mathbf{g}_{a_k}\|} + \beta \frac{\mathbf{g}_{b_k}^T \Pi_{\mathbf{g}_{a_k}^*}^\perp \mathbf{g}_{b_k}^*}{\|\Pi_{\mathbf{g}_{a_k}^*}^\perp \mathbf{g}_{b_k}^*\|} \right|^2 \quad (7.45)$$

$$\begin{aligned} &= |\alpha|^2 \frac{|\mathbf{g}_{b_k}^T \mathbf{g}_{a_k}^*|^2}{\|\mathbf{g}_{a_k}\|^2} + |\beta|^2 \frac{\left(\mathbf{g}_{b_k}^T \Pi_{\mathbf{g}_{a_k}^*}^\perp \mathbf{g}_{b_k}^*\right)^2}{\|\Pi_{\mathbf{g}_{a_k}^*}^\perp \mathbf{g}_{b_k}^*\|^2} \\ &+ 2\text{Re} \left[\alpha \beta^* \mathbf{g}_{b_k}^T \mathbf{g}_{a_k}^* \right] \frac{\mathbf{g}_{b_k}^T \Pi_{\mathbf{g}_{a_k}^*}^\perp \mathbf{g}_{b_k}^*}{\|\Pi_{\mathbf{g}_{a_k}^*}^\perp \mathbf{g}_{b_k}^*\| \|\mathbf{g}_{a_k}\|} \end{aligned} \quad (7.46)$$

Without loss of generality we can assume that α is real and positive. Moreover, let $\beta = |\beta|e^{\sqrt{-1}\theta}$, and let $\phi = \angle \mathbf{g}_{b_k}^T \mathbf{g}_{a_k}^*$. $|\mathbf{g}_{b_k}^T \mathbf{x}|^2$ is maximized by selecting $\theta = \phi$ without affecting $|\mathbf{g}_{a_k}^T \mathbf{x}|^2$. Combining this with the power constraint, we get

$$\begin{aligned} |\mathbf{g}_{a_k}^T \mathbf{x}|^2 &= \alpha^2 \|\mathbf{g}_{a_k}\|^2 \\ |\mathbf{g}_{b_k}^T \mathbf{x}|^2 &= \alpha^2 \left[\frac{|\mathbf{g}_{b_k}^T \mathbf{g}_{a_k}^*|^2}{\|\mathbf{g}_{a_k}\|^2} - \frac{\left(\mathbf{g}_{b_k}^T \Pi_{\mathbf{g}_{a_k}^*}^\perp \mathbf{g}_{b_k}^*\right)^2}{\|\Pi_{\mathbf{g}_{a_k}^*}^\perp \mathbf{g}_{b_k}^*\|^2} \right] + \frac{P_R}{K} \frac{\left(\mathbf{g}_{b_k}^T \Pi_{\mathbf{g}_{a_k}^*}^\perp \mathbf{g}_{b_k}^*\right)^2}{\|\Pi_{\mathbf{g}_{a_k}^*}^\perp \mathbf{g}_{b_k}^*\|^2} \\ &+ 2\alpha \sqrt{\frac{P_R}{K} - \alpha^2} |\mathbf{g}_{b_k}^T \mathbf{g}_{a_k}^*| \frac{\mathbf{g}_{b_k}^T \Pi_{\mathbf{g}_{a_k}^*}^\perp \mathbf{g}_{b_k}^*}{\|\Pi_{\mathbf{g}_{a_k}^*}^\perp \mathbf{g}_{b_k}^*\| \|\mathbf{g}_{a_k}\|} \end{aligned} \quad (7.47)$$

The first is clearly increasing in positive α , the second increases then decreases, its maximum occurring for α such that

$$\begin{aligned} &\alpha \sqrt{\frac{P_R}{K} - \alpha^2} \left[\frac{|\mathbf{g}_{b_k}^T \mathbf{g}_{a_k}^*|^2}{\|\mathbf{g}_{a_k}\|^2} - \frac{\left(\mathbf{g}_{b_k}^T \Pi_{\mathbf{g}_{a_k}^*}^\perp \mathbf{g}_{b_k}^*\right)^2}{\|\Pi_{\mathbf{g}_{a_k}^*}^\perp \mathbf{g}_{b_k}^*\|^2} \right] \\ &+ \left[\frac{P_R}{K} - 2\alpha^2 \right] |\mathbf{g}_{b_k}^T \mathbf{g}_{a_k}^*| \frac{\mathbf{g}_{b_k}^T \Pi_{\mathbf{g}_{a_k}^*}^\perp \mathbf{g}_{b_k}^*}{\|\Pi_{\mathbf{g}_{a_k}^*}^\perp \mathbf{g}_{b_k}^*\| \|\mathbf{g}_{a_k}\|} = 0. \end{aligned} \quad (7.48)$$

If $\frac{|\mathbf{g}_{b_k}^T \mathbf{g}_{a_k}^*|^2}{\|\mathbf{g}_{a_k}\|^2} \geq \|\mathbf{g}_{a_k}\|^2$, then the optimum is achieved by setting $\alpha = \sqrt{\frac{P_R}{K}}$. Otherwise, the two curves intersect at an α such that

$$\begin{aligned}
& 2\alpha\sqrt{\frac{P_R}{K}} - \alpha^2 |\mathbf{g}_{b_k}^T \mathbf{g}_{a_k}^*| \frac{\mathbf{g}_{b_k}^T \Pi_{\mathbf{g}_{a_k}^*}^\perp \mathbf{g}_{b_k}^*}{\|\Pi_{\mathbf{g}_{a_k}^*}^\perp \mathbf{g}_{b_k}^*\| \|\mathbf{g}_{a_k}\|} \\
&= \alpha^2 \left(\|\mathbf{g}_{a_k}\|^2 - \frac{|\mathbf{g}_{b_k}^T \mathbf{g}_{a_k}^*|^2}{\|\mathbf{g}_{a_k}\|^2} + \frac{(\mathbf{g}_{b_k}^T \Pi_{\mathbf{g}_{a_k}^*}^\perp \mathbf{g}_{b_k}^*)^2}{\|\Pi_{\mathbf{g}_{a_k}^*}^\perp \mathbf{g}_{b_k}^*\|^2} \right) \\
&\quad - \frac{P_R}{K} \frac{(\mathbf{g}_{b_k}^T \Pi_{\mathbf{g}_{a_k}^*}^\perp \mathbf{g}_{b_k}^*)^2}{\|\Pi_{\mathbf{g}_{a_k}^*}^\perp \mathbf{g}_{b_k}^*\|^2}. \tag{7.49}
\end{aligned}$$

If the intersection occurs before the maximum of the second function, the optimal α corresponds to that maximum. Otherwise it is the intersection point.

Chapter 8

Conclusions

The main focus of this thesis has been the RS development for potential wireless communication scenarios with achievable rates and reliability being our main figures of merit. Insufficiency of the current conventional cellular systems to address the overgrowing wireless application demands constitutes the motivation for this study. To deliver ubiquitous, reliable, high data rate wireless services requires smart and complex network architecture designs, integrating various air interfaces to form large networks. It is therefore important to search for cost-effective approaches and technologies that will improve spectral efficiency and reliability. Although integrating recently developed advanced transmission techniques, such as MIMO, OFDM and interference cancellation techniques, into the wireless systems offers better throughput, reliability and coverage performance, these techniques alone cannot meet future demands of wireless systems without further deployment of infrastructure devices. It is therefore necessary to change the way the wireless systems are designed and deployed. To this end, the integration of multi-hopping (or relaying) into the conventional wireless networks has been considered as a promising solution. Thus, we have given our attention to the use of RSs in different wireless communication systems where various relaying and coding strategies were considered.

The following approaches have been investigated in this thesis.

We initially focused on parallel relay networks, which might find wide range of wireless *applications*, and examined possibility of having good achievable rate performance by using *simple* and *cheap* RSs. We provided an outer bound based on cross-cuts, and achievable rate analysis for various relaying strategies. Considering phase fading channel models, we showed that the proposed block quantization and random binning (BQRB) relaying strategy performs quite well due to the antenna pooling effect at the receiver side. We also showed the pos-

sibility of achieving relatively good performance with simplified assumptions at the source and RSs. Specifically, we showed that in certain regimes the rates achieved by simple relaying strategies (wherein finite-alphabet modulation and simple symbol-by-symbol uSQ are used at the sources and RSs, respectively), are better than the rates achieved by more complex relaying strategies (wherein Gaussian codebooks, VQ and ML decoding are used at the sources, relays and destination, respectively). This therefore shows that the *structure* inherent in the finite modulation alphabets used by the sources can be helpful in the quantization process at the RSs.

In order to have thorough performance characterization of the parallel relay networks, we also studied the random coding error exponents corresponding to the DF, BQRB and QF relaying strategies. We proposed practical DF relaying strategies and derived the corresponding error exponents. Akin to the achievable rate analysis, it was observed that using a finite alphabets, e.g. M-QAM, at the source nodes along with uniform scalar quantization at the RSs could provide better error exponents than more complex and non-practical relaying strategies, again thanks to the structure inherent in the considered modulation scheme.

Next, we directed our attention to a relay-assisted cellular network and analyzed the achievable sum-of-rates for uplink communications assuming that MS and RS signals are emitted on *orthogonal* frequency bands. Explicitly take into account the inter-cell interference impact on the relay performance, we derived the achievable rate expressions for the AF, DF, CF and QF relaying strategies and showed that the CF provides the best achievable rate performance. Moreover, the importance of resource allocation in relay-assisted cellular systems was assessed.

Continuing with DL communications in relay-deployed cellular systems, we proposed a distributed scheduling algorithm wherein a given MS can be either served by the BS or by a RS, in an opportunistic way. With this distributed scheduling algorithm we tried to address some of the drawbacks that arise with RS deployment: the multiplexing loss due to multi-hopping, the effect of the interference which increases with the number of deployed RSs, and the feedback overhead. It was shown that such a distributed approach fully exploits the spatial reuse in the system and allows *reduced* feedback with respect to the centralized case, especially when a simple scalar feedback is not sufficient for estimating the channel quality. As a result of the reduced feedback requirements the system becomes more *scalable*, as new RSs can be deployed where needed without need of a careful network planning. Moreover, by moving the processing towards the RS side, local cooperation between RSs becomes possible.

In the thesis, we continued with analyzing different coding strategies for TWRCs. Assuming full-duplex transmission capabilities a cut-set outer bound has been derived and it has been shown that this outer bound is virtually achievable by *physical-layer* network coding, using group codes and partial decoding at the relay station under both binary adder and Gaussian channel models. We have then proposed coding schemes based on binning (hashing and compression with side information) where the relay does not attempt to partially decode the sum signal. It has been shown that for strong relay to node links compression-

based strategies can provide near optimal performance without the need for *full* channel state information at the transmission end.

Finally, we extended the single-pair TWRC model to a multi-pair case. In the multi-pair TWRC, the main bottleneck on system performance is the interference seen by each MS due to the other communicating MS pairs. We have proposed different transmit/receive beamforming schemes at the RS in order to tackle this problem in the *spatial* domain by using multiple antennas at the RS.

8.1 Future Work Directions

Although we have tried to solve some of the problems that arose from RS deployment in several wireless communication systems, a number of issues still need closer look. The most notable of these is to see the performance of the proposed relaying mechanisms through a detailed system simulator. For example, with the light shed on the potentials of the proposed practical relaying strategies for parallel relay networks, it might be interesting to deploy practical channel codes by using the standard LTE transmitter/receiver blocks, and analyze the corresponding block error rates (BLER). Investigating error control mechanism at the relay stations and their consequences on the backhaul utilization would also be an interesting research topic.

For the relay-assisted cellular UL framework a number of issues also remain to be investigated. The most notable of these is the notion of *fairness*, since one of the potentials offered by relaying is to stabilize the system load. For the cellular DL framework, we have shown that the proposed distributed scheduling approach performs quite close to the centralized one when the cell load is not too high. A future study might be to improve the performance in the interference-limited region by means of multiple antenna processing and local-cooperation between RSs.

In conventional communication systems, e.g. no RS, communication between two nodes is facilitated in two steps where in the first step one node transmits and the other node receives and in the next step with the reversed roles on transmission and reception. Note that even though this communication scheme seems to be simple compared to the modern communication schemes, in cellular networks (or WLAN) it might be necessary for a MS to have high transmit power capability to access a BS (or an access-point). However, with the deployment of an intermediate RS, the MS transmit power problem might be solved, and moreover by multiplexing forward (DL) and backward (UL) communications via two-way relaying higher spectral efficiencies might be achieved.

Chapter 9

Appendix: Summary of the thesis in French

9.1 Abstract en français

Dans les futurs réseaux de communication sans fil, l'une des préoccupations majeures des fournisseurs de service d'accès est de fournir une connectivité transparente pour les utilisateurs finaux ainsi que la meilleure qualité de service (QoS) possible. Toutefois, atteindre un niveau donné de QoS pour tous les utilisateurs du réseau n'est pas simple. Ceci est dû notamment aux caractéristiques variables dans le temps des canaux de communication, causées par l'affaiblissement multi-trajet, l'affaiblissement de parcours et les effets de masque. Récemment, le déploiement de stations relais (RS) et la coopération entre stations de bases (BSs) ont été proposés afin d'améliorer les performances des systèmes sans fil de la prochaine génération en termes d'équité, de couverture, de consommation d'énergie, de coût de déploiement et d'efficacité spectrale.

Dans cette thèse, nous nous intéressons à l'utilisation de RSs dans les différents systèmes de communication sans fil tels que la téléphonie cellulaire, les réseaux ad-hoc et les réseaux satellites. Nos objectifs principaux étant la fiabilité et les débits réalisables. En particulier, nous adaptons l'analyse des techniques de relayage, réalisée dans le domaine de la théorie de l'information, aux paramètres du monde réel, et évaluons l'efficacité et potentiels du relayage dans diverses applications sans fil.

Dans la première partie de la thèse, nous nous concentrons sur les réseaux parallèles de relais (PRN) et examinons s'il est possible d'avoir de bonnes performances à l'aide de RSs simples et pas chères dans des PRNs à backhaul limité

vers la destination. En particulier, nous proposons une technique de quantification simple et pratique, au niveau des RSs, qui repose sur la quantification scalaire uniforme (uSQ) symbole-par-symbole. Pour le même modèle de réseau, nous caractérisons également les exposants d'erreurs (EE) du codage aléatoire, correspondant à différentes stratégies de relais utilisées par les RSs. Nous montrons que, dans certains régimes, les EEs réalisés par de simples stratégies de relais sont meilleurs que les EEs de plusieurs pièces complexes.

Inspiré par la configuration du PRN, nous considérons, dans la deuxième partie de la thèse, des réseaux cellulaires assistés par des RSs fixes pour les liens de communication ascendant (UL) et descendant (DL). En particulier, nous analysons la somme des taux réalisables pour les communications UL en supposant que les signaux de la station mobile (MS) et ceux de la RS sont émis sur des bandes de fréquences orthogonales. De plus, nous évaluons de manière intensive l'influence du déploiement de la RS sur la somme des taux, compte tenu de plusieurs paramètres utilisés par le système, tel que le nombre de RSs déployées dans chaque cellule, leur emplacement et la puissance qu'elles utilisent. Pour les communications DL assistées par les relais, nous proposons un algorithme d'ordonnancement distribué réparti en deux étapes où une MS donnée peut être servie, d'une façon opportuniste, soit par la BS soit par l'une des RSs déployées. Une telle approche permet d'avoir un feedback de signalisation réduit par rapport au cas centralisé, surtout lorsqu'un feedback scalaire simple n'est pas suffisant pour estimer la qualité du canal.

Dans la dernière partie de la thèse, nous proposons plusieurs stratégies de codages pour les canaux relais bidirectionnels. Nous montrons plus particulièrement que les stratégies de décodage à base lattice atteignent une performance quasi optimale. Cependant, en raison de sa forte dépendance à la déficience du canal, ce schéma de codage ne peut pas s'appliquer pour des scénarios réels. Par conséquent, nous démontrons que les stratégies de type "binning" peuvent être une approche plus pratique car la phase de cohérence au niveau de la station de relais n'est pas nécessaire. Enfin, nous étendons le modèle "à pair unique" en un modèle "à pairs multiples" où les stations mobiles à antenne unique pour chaque pair cherchent à communiquer via une station de relais à antennes multiples commune. Dans les canaux relais bidirectionnels multi-pairs, le goulet d'étranglement vis à vis de la performance système est l'interférence constatée par chaque station mobile provenant des autres pairs communicants. Concernant ce problème, nous proposons des solutions à domaines spatiaux en exploitant les antennes multiples de la station relais.

9.2 Introduction

9.2.1 Motivation

L'introduction des systèmes de communication cellulaire de nouvelle génération, telle que WiMAX et 3GPP LTE/LTE-A par les opérateurs vise, entre autres, à offrir aux clients une connectivité transparente assurant une meilleure qualité

de service (QOS) en termes de fiabilité, de stabilité et de débits comparé à celles offerte par l'architecture des systèmes conventionnels. Par ailleurs, le nombre croissant d'applications, couvrant l'accès sans fil, l'accès à Internet ainsi que les services d'urgence et de reprise après sinistre requièrent la mise en place d'une architecture plus complexe et plus intelligente intégrant différentes interfaces sans-fils tels que les réseaux locaux sans fils (WLAN) et les réseaux Ad-hoc/mesh afin de former un unique et vaste réseau sans fil. L'intégration de techniques de transmission récemment développé (telles que MIMO, OFDM, l'annulation d'interférences, etc) dans le système permet d'offrir de meilleurs débits, une meilleure fiabilité et des performances de couverture améliorées. Ces techniques ne suffisent cependant pas à répondre aux besoins futurs des systèmes sans fil et nécessitent la poursuite du déploiement d'équipements d'infrastructure. L'une des solutions prometteuses pour résoudre ces problèmes consiste à intégrer un mécanisme "multi-sauts" (ou relais) dans les réseaux sans fil conventionnels [2-7].

Dans les réseaux sans fil, le "multi-sauts" offre plusieurs avantages tels que la réduction des coûts, l'économie d'énergie, l'extension de la couverture, l'augmentation des taux de données offerts ainsi qu'un gain de diversité, comme expliqué ci-après.

Tout d'abord, grâce à des liaisons sans fil de longueur réduites et à un gain de diversité de coopération, des économies d'énergie importantes peuvent être réalisées avec le "multi-hop". En effet, d'une part il y a de fortes contraintes sur le bilan de liaison dans les systèmes cellulaires de nouvelle génération. D'autre part, on a des contraintes de puissance au niveau des stations mobiles (MSs) qui représente un goulot d'étranglement pour la liaison montante (UL) en particulier pour les communications des mobiles à proximité de la bordure de cellule. En outre, même si ces contraintes de puissance n'existaient pas et que les utilisateurs disposaient d'autant d'énergie que nécessaire et communiquaient à des niveaux de puissance plus élevés, le système se retrouverait dans un régime limitée par l'interférence et les MSs à sur la bordure de cellule serait encore défavorisés. En plus, la capacité de traitement réduite et de contrainte de dimension des terminaux mobiles peut empêcher la mise en place de techniques de précodage MIMO (ou beamforming).

Ensuite, si l'objectif est d'obtenir des débits de données plus élevés, une solution naïve dans les systèmes classiques serait d'augmenter la densité des stations de base (BS) (Subdivision de cellules). Toutefois, cela entraîne des coûts de déploiement prohibitif, car chaque BS exige non seulement de nouvelles liaisons terrestres mais surtout les frais pour les baux des sites. Comparé à la subdivision des cellules, les coûts de déploiement pour la station relais (RS) moindres car il n'est pas nécessaire de mettre en place des liaisons filaires et l'acquisition des sites reste flexible. Si un utilisateur dans une cellule est beaucoup plus proche de l'un des RSs dans cette dernière que de la BS, alors l'atténuation du signal est plus importante vers la BS de vers la RS à proximité. De ce fait les débits offerts sur le lien entre la RS et les MSs sont plus élevés et donc permet de résoudre le problème de la *couverture* pour les hauts débits dans les grandes cellules [2].

Enfin, en exploitant le potentiel de *réutilisation spatiale* de la technique

”multi-hop” où les BS et les RSs peuvent transmettre simultanément à différents MSs en utilisant les mêmes ressources. De ce fait, des débits plus élevés peuvent être atteints.

Scénarios possibles pour le déploiement de station relais

Étant donné les avantages du ”multi-sauts”, nous allons considérer plusieurs scénarios de déploiement RS considérés pour IEEE 802.16j. Tous les schémas de relai possibles sont illustrés à la Figure 9.1.

L’un des scénarios possibles de déploiement des RS est d’opter pour des RS fixes. Dans ce cas ils sont destinés à augmenter la couverture et le débit. Dans la plupart des cas, le lien entre une BS et chaque RS fixe est conçu pour avoir une ligne-de-visée directe (LOS). Les RSs peut-être omni-directionnelles ou avoir des antennes dirigées vers la BS. Ce dernier nécessite besoin de plus d’effort puisqu’en fonction de la configuration du trafic, il peut être nécessaire de déplacer les RSs et/ou d’orienter les antennes en conséquence.

Trasmettre de l’extérieur vers l’intérieur (ou vice versa) avec une qualité de service élevée est difficile à réaliser vu que le signal électromagnétique subit des pertes de puissance importantes en traversant les murs des bâtiments. En installant une station relai, ce problème pourrait facilement être résolu. Ce type de RS peut également être déployé à proximité de tunnels souterrains afin d’assurer une extension de la couverture.

Les RSs peuvent aussi être déployés dans des situations d’urgence (comme les tremblements de terre, les inondations, etc), ou encore dans le cas où certaines BSs endommagées. Ce type de RS est appelée RS temporaire (ou RS nomades). Une autre forme de relais peut être utilisée pour fournir une connexion sans fil pour les utilisateurs finaux situés dans les trains ou les bus.

Principaux défis à la conception multi-hop réseaux

Comme démontré précédemment, les relais multi-hop ont la possibilité d’accroître les performances du système en termes de débit, d’équité et de couverture. Toutefois, l’introduction de relais multi-hop est également livré avec des défis spécifiques liés à la conception aussi bien de la couche physique que MAC [2,4,8].

Les principaux facteurs qui limitent les gains réalisables peuvent être classés comme suit

- la perte de multiplexage en raison des sauts multiples
- la qualité du lien entre les relais et la station de base
- l’effet de l’interférence qui augmente avec le nombre de relais déployés
- des entêtes de retour d’informations plus larges, en particulier dans les solutions centralisées où une estimée de l’état du canal d’information (CSI) est nécessaire au niveau de la station de base.

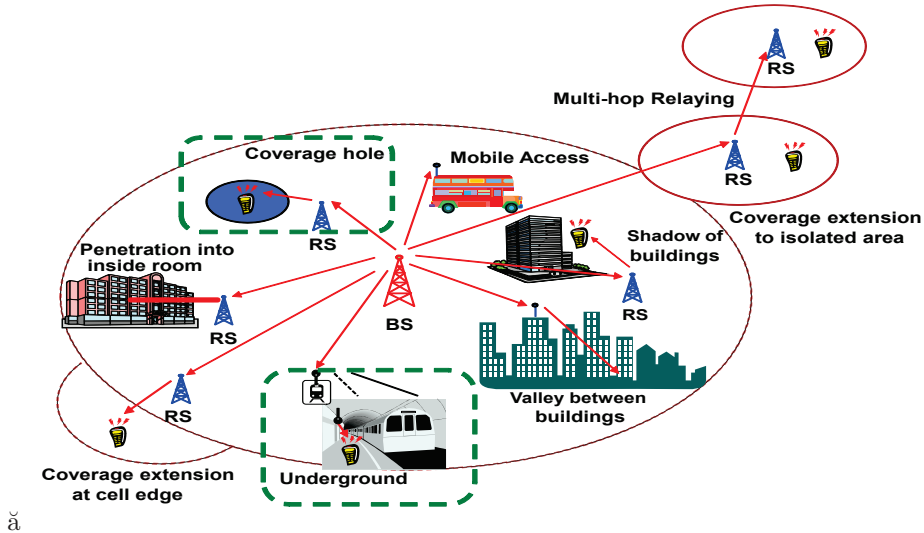


Figure 9.1: Une illustration de scénarios possibles relais.

Pour surmonter la perte de multiplexage, et par conséquent respecter certaines contraintes de QoS tels que la fiabilité, l'équité et de la latence, l'affectation intelligente des ressources joue un rôle crucial dans les réseaux cellulaires à saut multiples. En conséquence, il faut accorder une attention particulière à la définition des algorithmes de routage et de sélection des utilisateurs. Selon la complexité et le niveau d'intelligence incorporée dans les stations relais, l'allocation des ressources peut être effectuée soit d'une manière centralisée ou distribuée. Dans le cas d'une gestion centralisée, la station de base prend toutes les décisions, le système est entièrement coordonné et dans ce cas, tous les avantages du multi-sauts peuvent être exploités.

Toutefois, l'allocation des ressources centralisées s'appuie fortement sur une connaissance parfaite la parfaite du CSI global à la station de base. Ceci augmente de ce fait considérablement les entêtes contenant des retours d'informations dans le système. Une telle approche peut devenir insolubles en présence d'évanouissements rapides avec des terminaux équipés d'antennes multiples, ce qui limite non seulement les performances du système mais aussi son évolutivité.

Dans le cas d'allocation distribuée des ressources, les relais sont autorisés à faire la planification, l'allocation des ressources et la gestion des interférences. Les RSs effectuent la répartition des ressources entre les utilisateurs dans leur zones respectifs, sans aucune influence de la station de base. Dans le Chapitre 5, nous abordons ce problème et proposons un algorithme d'ordonnancement distribué nécessitant moins de retours d'informations vers station de base tout en offrant de meilleurs débits.

Avec un nombre croissante d'utilisateurs, la RS pourrait avoir besoin d'acheminer

des données de différents utilisateurs vers la station de base ce qui nécessite de prévoir une ligne de visée directe entre la station de base et le relai lors de la conception du système. La sectorisation des relais, permettant de contrôler le niveau d'interférence dans la cellule représente un important degré de liberté exploitable à travers des schémas optimisés de réutilisation de l'espace pour maximiser le débit. Dans le Chapitre 4, nous nous intéressons aux communications en lien montant. Des questions liées à l'affectation des ressources aux liens entre les mobiles et la station de base à travers les RSs sont abordées. D'autres problématiques concernant les liaisons terrestres reliant relais et station de base ainsi que les effets des modèles d'antenne utilisés au niveau des relais sont également étudiées.

En outre, l'introduction RSs dans des systèmes cellulaires permet de réutiliser l'espace des ressources qui est un facteur important permettant d'augmenter le débit du système. Cependant, si l'ajout n'est pas bien étudié, les RSs introduits pourraient augmenter l'interférence intracellulaire et intercellulaire. Dans le Chapitre 4, nous avons également abordé ce problème.

En dehors de ce qui précède, il y a encore d'autres problèmes d'ordre pratiques qui doivent être abordés lors du déploiement du réseau de relais. Parmi ces derniers on peut citer la synchronisation des antennes spécialement séparées et l'acquisition des CSI distribués. Bien que ces questions soient fondamentales dans les réseaux sans fil Ad-hoc, dans cette thèse, nous faisons des simplifications et assumons que ces problèmes ont été résolus.

9.2.2 Background

Le relai entre les nœuds radio permet de réduire les pertes à cause du canal de transmission et d'améliorer les performances dans les canaux sans fil. Ce concept exploite la nature inhérente de *diffusion* d'un canal sans fil qui est plus connu sous le nom de système à saut multiples (multi-hopping en anglais). Les canaux des systèmes à relais ainsi que les protocoles associés ont été étudiés dans divers ouvrages dans lesquels on observe des gains considérables réalisables grâce à la coopération. Dans les sous-parties suivantes nous allons présenter brièvement le processus d'évolution des relais classiques (aller simple) et continuer avec les protocoles, récemment introduits, introduisant des relais fonctionnant dans les deux sens pour terminer avec un résumé des études des relais se focalisant sur les applications pour les réseaux cellulaires de nouvelle génération.

La chaîne de relais à sens unique

Le réseau classique à relais avec trois terminaux qui est au cIJur des réseaux de coopération a été initialement développée par Van der Muelen dans [9]: un nœud agit comme une source et une station relai(RS) n'ayant pas d'informations propres à transmettre l'y aide. Cover et El Gamal fait de nouveaux progrès en développant des limites supérieure et inférieure de la capacité d'un tel système, qui reste encore un problème ouvert, et a proposé trois stratégies de relais: la coopération, la facilitation et l'estimation [10]. Carleial a examiné la coopération

des utilisateurs dans les canaux à accès multiples à travers des voie généralisée (différentes sorties des canaux) de retours d'information du destinataire final vers les émetteurs. [11]. Récemment, la diversité de coopération entre les utilisateurs ont reçu une grande attention car elle offre un gain de diversité spatiale de manière distribuée. En d'autres termes, la source coopère avec un partenaire pour transmettre ses informations vers la destination. Ce système constitue un réseau d'antennes de transmission virtuel assurant une transmission plus fiable qu'une transmission que de la source toute seule [12–14]. La diversité coopérative est aussi attrayante à cause de la bande passante occupée. En effet, contrairement au cas de la diversité d'espace (ou antenne), aucune bande passante supplémentaire n'est nécessaire. Pour augmenter la capacité de transmission de plusieurs modes de coopération au RS ont été proposées [12, 15, 16].

Jusqu'à présent, différents protocoles et stratégies de relais ont été proposés et largement étudiés dans la littérature afin d'améliorer l'efficacité spectrale et la fiabilité des systèmes sans fil [12, 15, 17, 18]. En fonction des connaissances et la complexité des RSs, ces derniers peuvent traiter les signaux reçus de différentes manières parmi lesquels on retrouve les stratégies fondamentales suivantes: amplifier et retransmettre (AF), décoder et retransmettre (DF) ou encore compresser et retransmettre (CF). En AF, les RSs simplement amplifient le signal reçu en fonction d'une contrainte de puissance et transmettent la version amplifiée vers le nœud destination. En DF, les RSs décodent les signaux reçus, les ré-encodent et transmettent au nœud destination. Notez que, l'exécution de la stratégie de DF est limitée par les liens de la source au-relais en raison du processus de décodage. En CF, les RSs compressent (ou estiment/quantifient) les signaux reçus avec une certaine fidélité et les transmettent au nœud destination.

La conception des codes espace-temps distribués et les limites de la théorie de l'information pour le rendement des relais à antenne unique dans le cas d'un canal à évanouissement (avec un nombre fini de nœuds) ont été étudiés dans [12, 15, 18, 19]. Les résultats obtenus pour les canaux de relais MIMO avec un nombre fini de relais ont été donnés dans [20–22].

Dans [23], Schein a introduit un réseau de relais en parallèle (PRN), où un nœud source communique avec un nœud de destination à travers deux flux parallèles. Il a également étudié les limites inférieure et supérieure de la capacité. Ce canal peut être un modèle pour les réseaux de relais à sauts multiples où les MSs qui se trouvent dans un trou de couverture et ne peuvent voir que des RSs. Dans la littérature, il existe plusieurs ouvrages où les différents aspects de PRN sont étudiés [24–31]. Gastpar a montré dans [24] que la capacité des canaux à relais parallèles multiples évolue proportionnellement au logarithme du nombre de relais pour les canaux de Rayleigh. Une variante du PRN, où les relais sont raccordées par des liaisons sans perte de capacité limitée indépendamment de la destination, est considéré par Sanderovich *et. al.* dans [28, 29] où les auteurs ont évalué les taux réalisables avec des relais en mode compression et retransmission en utilisant une compression Wyner Ziv distribuée [32] au niveau du relais. Il a également été démontré par Sanderovich *et. al.* [28] que pour un émetteur nomade où un nœud source communique avec un nœud destination à travers deux RSs intermédiaires et où chacun a un lien sans perte de capacité limitée

à 1 [bit/lien capacité de transmission] vers la destination. Le taux atteint avec une signalisation BPSK au niveau du nœud source associée à un décodage fixe à 2-niveau (par symbole) au niveau de chaque RS dépasse le taux obtenu par l'utilisation de signalisation Gaussienne par le nœud source et un codage binaire à symbole de type gaussien au niveau des RSs. Motivé par ces observations, nous étudions dans le deuxième chapitre différentes stratégies de relais dans des scénarios simplifiés et réalistes.

Dans la dernière décennie, il y a eu beaucoup de recherche sur l'infrastructure des réseaux basés sur des relais en raison des améliorations possibles, discutées dans les sections précédentes offertes par les relais [2–4, 33–36].

Les références [4], [33] et [35] abordent certaines des questions énumérées ci-dessus. Dans [4], un système de planification centralisé en lien descendant est proposé. Cette solution garantit la stabilité des files d'attente d'utilisation pour le plus grand ensemble de taux d'arrivée et réalise un gain significatif comparé au cas d'un système sans relais. Il a été démontré qu'une augmentation du nombre des RSs en sauts multiples, on a une augmentation du gain réalisable en raison de l'efficacité de la réutilisabilité qui s'accroît qui peut être réalisée par des transmissions multiples simultanées. Cependant, avec plus de RSs dans les cellules, les interférences seront plus importantes, ce qui limite les performances du système. Par conséquent, il faut être conscient de l'interférence associée avec l'ajout de relais supplémentaires dans le système. Dans [33] des améliorations de capacités en liaison montante sont obtenues grâce à l'utilisation d'un réseau sans fils utilisant la même bande de fréquences que le système considéré pour interconnecter les RSs au système (BS). L'étude a été faite en considérant une séparation orthogonale des ressources entre les deux catégories de liens BS-à-RS et BS/Rs-à-MS et sous l'hypothèse d'un taux maximal commun réalisables par tous les utilisateurs du réseau. Ils ont proposé un schéma de relais exploitant pleinement la réutilisation spatiale dans le système pour lequel le gain augmente avec le nombre de RSs half-duplex. Le mode DF a été considéré pour les relais dans cette étude. Les résultats de simulation montrent l'intérêt de la proposition à une configuration de base sans relais. De même, dans [34] divers modes de communication sont proposés afin d'accroître la réutilisation spatiale (i.e., accroître l'efficacité spectrale) dans un système cellulaire pour les cas d'un et deux RSs dans chaque secteur cellulaire avec un saut ou deux sauts de transmission. En outre, l'affectation optimale des modes proposés aux utilisateurs mobiles est décrite.

Comme expliqué ci-dessus, les relais peuvent être utilisés dans les réseaux sans fil pour étendre la couverture ou améliorer la qualité du canal. Vu que le déploiement des relais est une solution rentable pour de nombreuses applications, plusieurs comités de normalisation, y compris l'IEEE 802.16j [7, 37], travaillent sur l'ajout de la fonctionnalité de relais à leurs standards actuels. Par exemple, IEEE 802.16j adopte une connexion réseau à deux-sauts sans lien direct entre la source et le destinataire [7].

La chaîne de relais dans les deux sens

En raison de la complexité des problèmes, considérer des RSs fonctionnant en mode half-duplex (HD) (où ils ne peuvent transmettre et recevoir en même temps) est plus pratique que des RSs en mode full-duplex (FD). Cependant, la contrainte de RSs en HD introduit un facteur pré-log de $1/2$ sur le débit global du système et limite donc l'efficacité spectrale réalisable. Récemment, pour compenser la perte spectrale dans le canal de relais à sens unique, le concept de canal de relais à double sens (bidirectionnel) a été mis en place. Dans ce type de canal, noté TWRC, deux mobiles échangent des informations via une interface RS intermédiaires [38–45]. En bref, les mobiles voulant communiquer envoient d'abord leurs messages à la RS et puis dans une deuxième phase de la RS traite les signaux reçus selon une stratégie de relai donnée et les diffuse vers les mobiles. TWR offre une réception sans interférences à chaque mobile en annulant l'auto-interférence avant de décoder les messages inconnus. La région de capacité pour la TWRC dans le cas général reste une question ouverte.

Le schéma le plus simple de transmission pour la TWRC est composé de quatre phases où les deux nœuds transmettent successivement leurs messages à la RS, puis le RS décode et retransmet les messages de chaque mobile dans les deux intervalles de temps suivants. Cependant, en utilisant des concepts de codage de réseau (NC) [46]. Un autre système de relais bidirectionnel qui n'exige que trois intervalles de temps est pris en compte dans [47] où dans les deux premiers intervalles temporels les mobiles envoient leurs messages à la RS dans des créneaux orthogonaux, le RS décode les messages et les combine par le biais de l'opération XOR bit-à-bit et les retransmet vers les mobiles. Là, les mobiles sont supposés utiliser l'opération XOR bit-à-bit sur le message décodé et le message transmis afin d'obtenir le message envoyé par l'autre mobile. Ne nécessitant que trois intervalle temporels, régime TWR basé sur un XOR bit à bit offre un facteur pré-log de $2/3$ par rapport à la somme totale des débits.

Le nombre de créneaux horaires nécessaires à la communication entre les deux nœuds peuvent être encore réduits d'avantage à seulement deux créneaux horaires en leur permettant d'accéder simultanément au RS [41,44,48–53]. Dans [41,48,49,54] des solutions de relai en modes AF, DF et CF avec seulement deux intervalles temporels sont proposés pour la TWRC. Dans [44] un schéma pour un réseau avec un codage analogique (ANC) est décrit. La RS amplifie et transmet tous les signaux mélangés qu'il reçoit. Cette solution est comparée aux réseaux traditionnel et avec codage numérique (XOR bit-à-bit par le RS) en termes de le débit. Dans [41,49], un relais qui nettoyer le signal du bruit et retransmettre (DNF: Denoise and Forward) est proposé pour la TWRC où la RS supprime le bruit des messages combinés des mobiles (sur le canal d'accès multiple) avant de las rediffuser. Cette méthode est omparé aux régimes AF, DF de TWR ainsi que le régime traditionnelle en quatre phases.

9.2.3 Contributions et cadre de cette thèse

L'objectif de cette thèse est de proposer des architectures de relais simples et souples pour différents réseaux sans fil avec comme objectifs principaux la maximisation des débits et l'amélioration de la fiabilité. Plus précisément, nous allons essayer d'appliquer les connaissances acquises à partir des analyses des différentes stratégies de relais en terme de théorie de l'information dans le monde réel et d'analyser l'efficacité et le potentiel que présentent les relais dans diverses applications sans fil. En particulier, nous analysons les réseaux parallèles de relais (PRN), qui pourrait servir à modéliser plusieurs scénarios de communication sans fil tels que les liaisons montantes avec contraintes sur les liaisons entre les équipements des réseaux (BSs et RSs), relais multi sauts en liaison montante et descendante, et les réseaux de relais bidirectionnels pouvant représenter différents systèmes de communications sans fils comme les satellites.

Dans le Chapitre 2, nous étudions les limites supérieures et inférieures des débits de diverses stratégies réalisables pour les relais, comme AF, DF, quantification et encapsulation aléatoire en bloc (BQRB) et QF, pour le PRN AWGN avec atténuation de phase en se basant sur deux différents modèles de canaux d'accès entre les RSs et la destination. Nous montrons également la possibilité de réaliser des performances relativement bonnes avec des hypothèses de traitement simplifiées au niveau de la source et des RSs. Les résultats ont été publiés dans

- Erhan Yilmaz, David Gesbert and Raymond Knopp, "**Parallel Relay Networks with Phase Fading**", *in the proceedings of IEEE Global Communications Conference (GLOBECOM)*, New Orleans, USA, 2008.

et sera présenté comme une partie de

- Erhan Yilmaz, Raymond Knopp and David Gesbert, "**Coding strategies and Error exponents for multi-source Parallel Relay Networks**", under preparation.

Dans le Chapitre 3, nous nous concentrons sur les exposants d'erreur de codage aléatoires pour les stratégies de relai: DF, BQRB et QF dans les deux cas de configurations monosource et PRN avec deux sources. Ces scénarios considèrent deux RSs qui sont connectés à la destination à travers un réseau à capacité finie sans erreurs. Le but ici est d'avoir une caractérisation approfondie des performances du système. Nous montrons que l'utilisation d'une modulation à constellation finie, par exemple, M-QAM, au niveau de la source combiné avec un traitement simple au niveau des RSs, qui consiste en une quantification scalaire uniforme, peut fournir des exposants d'erreur meilleures que certaines stratégies plus complexes et non-pratique. Ceci est obtenu grâce à la structure inhérente au régime de modulation considérée. Une partie de ce travail a été publié en

- Erhan Yilmaz, Raymond Knopp and David Gesbert, "**Error Exponents for Backhaul-Constrained Parallel Relay Networks**", *in the pro-*

ceedings of IEEE International Symposium Personal, Indoor and Mobile Radio Communications (PIMRC), September 2010, Istanbul, Turkey.

et sera présenté comme une partie de

- Erhan Yilmaz, Raymond Knopp and David Gesbert, "**Coding strategies and Error exponents for multi-source Parallel Relay Networks**", under preparation.

Dans le Chapitre 4, nous considérons des communications cellulaires en liaison montante avec relais. En considérant des fréquences orthogonales pour les liens des couples mobile-relais et relais-base, le débit moyen réalisable sont analysés pour les relais en mode AF, DF, CF et QF. Les performances sont comparés à celles de deux systèmes cellulaires bien connus à savoir le système cellulaire classique et le système idéal d'antennes distribuées (DAS). Les effets du positionnement et du choix de la structure des antennes des RSs sont examinés. Les résultats ont été publiés dans

- Erhan Yilmaz, Raymond Knopp and David Gesbert, "**Some System Aspects Regarding Compressive Relaying with Wireless Infrastructure Links**", *in the proceedings of IEEE Global Communications Conference (GLOBECOM)*, New Orleans, USA, 2008.
- Erhan Yilmaz, Raymond Knopp and David Gesbert, "**Relaying with Wireless Infrastructure Links in Cellular Networks**", *in the proceedings of the IEEE Winter School on Information Theory*, Loen, Norway, à March 29 Ú April 3, 2009.
- Erhan Yilmaz, Raymond Knopp and David Gesbert, "**On the gains of fixed relays in cellular networks with intercell interference**", *in the proceedings of IEEE International Workshop on Signal Processing Advances in Wireless Communications (SPAWC)*, Perugia, Italy, June 21–24, 2009.

et sera présenté comme

- Erhan Yilmaz, Raymond Knopp and David Gesbert, "**On the gains of fixed relays in cellular uplink communications with intercell interference**", under preparation.

Dans le Chapitre 5, nous proposons un algorithme d'ordonnement distribué pour les transmissions DL des systèmes cellulaires avec relais, où un utilisateur mobile donné peut soit être desservi par la station de base ou par un relais, d'une manière opportuniste. Nous montrons qu'une telle approche distribuée permet de *réduire* les messages de retours comparé au cas centralisé, surtout quand un retour scalaire simple n'est pas suffisant pour estimer la qualité du canal. En raison des exigences d'évaluation réduites le système devient plus *évolutif*, puisque de nouveaux relais peuvent être déployés en cas de besoin sans avoir besoin de réaliser une planification avancée du réseau. Les résultats ont été publiés dans

- Erhan Yilmaz, Federico Boccardi and Angeliki Alexiou, "**Distributed and Centralized Architectures for Relay-Aided Cellular Systems**", *in the proceedings of IEEE Vehicular Technology Conference (VTC Spring)*, 2009, Barcelona, Spain (*invited paper*).

Dans le Chapitre 6, nous analysons différentes stratégies de codage pour les canaux de relais bidirectionnels. En particulier, nous étudions le décodage pariel basé sur les lattices ainsi que les stratégies de compression. Nous montrons que les relais en mode CF, fondée sur l'ncapsulation au niveau du RS, peut presque atteindre des performances optimales lorsque la puissance de transmission du relais augmente. Les résultats ont été publiés dans

- Erhan Yilmaz and Raymond Knopp, "**Coding Strategies for Two-Way Relay Channels**", under preparation.

Dans le Chapitre 7, nous considérons un canal de relais bidirectionnel (TWRC) multi-paire où des paires de MSs avec une seule antenne chacun chercher à communiquer via une interface RS avec des antennes multiples. Dans la TWRC multi-paires, le principal facteur limitant du système est l'interférence perçue par chacun des mobiles en raison des autres paires en communications. Nous proposons différents schémas d'émetteurs/récepteurs appliqués au niveau des RSs, en mode AF et QF, afin de résoudre ce problème dans le domaine *spatial* en exploitant les antennes multiples présentes sur les RS. Ce travail a été réalisé en collaboration avec la doctorante Randa Zakhour, et les résultats ont été publiés dans

- Erhan Yilmaz, Randa Zakhour, David Gesbert and Raymond Knopp, "**Multi-pair Two-way Relay Channel with Multiple Antenna Relay Station**", *in the proceedings of IEEE International Conference on Communications (ICC)*, June 2010, Cape Town, South Africa.

9.3 Résumé du Chapitre 2

Dans ce chapitre, nous nous proposons d'examiner une version générale des réseaux Gaussiens parallèles de relais (PRNs) avec atténuation de phase, précédemment proposés et étudiés dans [23, 55]. Un PRN général avec atténuation de phase consiste en plusieurs sources et noeuds relais et un seul noeud destination et où les noeuds sources veulent communiquer avec la destination par l'intermédiaire des stations relais (RSs). Il n'y a donc pas de lien direct reliant la source à la destination. En ce qui concerne les liens entre les stations relais (RSs) et la destination, nous considérons deux modèles de canaux:

- un canal à accès multiples (MAC) ordinaire avec des gains de canal constants et des déplacements de phase aléatoires (i.e., un MAC partagé sans fil)

- une liaison orthogonale sans erreurs à capacité limitée (e.g., des liens micro-ondes ou un câble de fibre optique) entre les RSs et la destination (MAC orthogonal).

Nous remarquons que, si faisable, chaque n-uplet de débits des liaisons orthogonales sans erreur des RSs à la destination (cas du MAC orthogonal) pourrait correspondre à un point de fonctionnement dans une région de MAC sans fil partagé. Ainsi, nous pouvons avoir la même performance que dans le cas du MAC partagé sans fil en sélectionnant plusieurs n-uplets de débits pour le cas du MAC orthogonal.

Motivation

Le PRN étudié dans ce chapitre, dans lequel nous supposons l'existence d'une connexion sans erreurs à capacité limitée et d'une connexion MAC ordinaire entre les RSs et la destination, pourrait trouver ses *applications* dans les réseaux cellulaires des liens de communication ascendants (UL).

Dans les systèmes cellulaires futurs, l'usage du MCP s'annonce prometteur pour l'augmentation de l'efficacité spectrale et de la fiabilité. Ceci pourrait être réalisé (i) en réduisant l'interférence inter-cellulaire à travers un traitement joint des signaux des BSs reçus par une unité centrale distante (remote central unit RCU) pour les communications UL, ce qui va constituer l'une des stations de bases coopérante et (ii) en procurant une diversité spatiale (et/ou une diversité par effets de masque) [29, 56, 57]. En outre, permettre un traitement joint limiterait la puissance d'émission nécessaire au niveau des MSs. Dans la plupart des évaluations du MCP réalisées jusqu'à présent, il est supposé que les BSs sont connectées à la RCU via une liaison fiable et à capacité limitée, ce qui constitue une hypothèse irréaliste lorsque l'on considère un système à forte charge. Donc, dans ce chapitre, nous considérons un modèle de système plus réaliste où les BSs (dans notre configuration RSs) sont connectées à travers des liens sans perte à capacité limitée.

Le modèle de PRN considéré pourrait également trouver ses applications dans les réseaux de capteurs à portée étendue où les RSs seraient des satellites à espace lointain des stations terrestres. De plus, les réseaux à infrastructure rapidement déployable (pour les applications civiles ou militaires) pourraient également constituer une catégorie d'applications visées par les PRNs étudiés dans ce chapitre. Dans ce genre de réseaux (à infrastructure rapidement déployable), quelques RSs nomadiques sont placées à différents emplacements, sont connectées à une RCU à travers des liens fiables mais à capacité limitée, et fournissent une couverture pour les MSs (en fonction de l'application, ceux-ci pourraient constituer des utilisateurs finaux voulant accéder au coeur du réseau ou des capteurs émettant des données environnementales vers une centrale chargée de la collecte des données).

Comme mentionné précédemment, les antennes à réception multiples pourraient être imitées en supposant des liens à capacité infinie entre les RSs et le noeud destination. Cette hypothèse représente également une limite extrême

pour les débits réalisables. Cependant, étant donné que cette hypothèse n'est pas pratique, nous nous proposons d'étudier une configuration de PRN plus simple et plus pratique où une capacité limitée est considérée pour les liens. A noter que les performances du système dépendent fortement des capacités de traitement des RSs. Dans ce chapitre, nous examinons s'il est possible d'atteindre les performances d'un système MIMO à utilisateurs multiples en utilisant des RSs simples et pas chères avec une liaison à capacité limitée.

Travaux antérieurs

Le PRN consistant en une seule source, deux relais et une seule destination a été introduit pour la première fois par Schein et Gallager dans [23, 55] où les capacités extrêmes, qui est toujours un problème ouvert, sont dérivées et où plusieurs stratégies de codage sont proposées supposant des modèles de canaux Gaussiens, discrets et sans mémoire. Pour le cas Gaussien scalaire, ils proposent Amplify-and-Forward (AF), Decode-and-Forward (DF) et aussi une autre stratégie de relayage basée sur le partage du temps de ces stratégies. Pour le cas discret, où les liens entre les relais et la destination sont supposés à débit limité sans perte et orthogonaux, ils proposent une stratégie de relayage originale fondée sur la stratégie de compression de Wyner-Ziv [32] suivie d'une stratégie de "binning" de Slepian-Wolf [58]. Ils appellent leur stratégie de relayage *block-quantization and random binning* (BQRB). Pour les canaux Gaussiens, ils spéculent que les schémas de relayage basés sur la compression ne peuvent pas aboutir à de meilleures performances que la technique AF à cause de l'effet *coherent combining* (combinaison cohérente) du canal Gaussien.

Dans [25, 59], il est démontré que pour un PRN Gaussien opérant en régime large-bande, il n'y a aucun intérêt gagné de l'usage de la stratégie AF étant donné qu'une partie de la puissance de la station relais est gaspillée en amplifiant le bruit du récepteur ce qui aboutit à un faible gain AF.

Dans [24, 60], il est démontré qu'avec des transmissions non codées à la source, la stratégie de relayage AF à deux-sauts réalise une capacité tant que le nombre de relais augmente. Récemment, dans [26], une stratégie de relayage Rematch-and-Forward (RF), basée sur l'usage de décodage à base lattice, a été proposée pour un type de PRN où il y a une disparité entre la bande passante des canaux source-relais et relais-destination. Un modèle similaire avec des relais semi-duplex est étudié dans [30]. Utilisant une approche déterministe, voir [61], les auteurs de [62] montrent que leur nouveau débit réalisable pour un réseau général scalaire Gaussien est dans la tranche supérieure de la capacité. Un nouveau débit réalisable pour le travail d'origine du réseau de Schein est dérivé dans [27] en utilisant un schéma combinant AF et DF (AF-DF). Récemment, le modèle vectoriel Gaussien du PRN, impliquant une source à antennes multiples et une destination est considéré dans [31] où plusieurs résultats intéressants sont dérivés.

Contributions

Les contributions de ce chapitre sont:

- Plusieurs limites extrêmes et débits réalisables sont examinés par Shein dans [23, 55] pour un simple PRN Gaussien impliquant une seule source et deux noeuds relais. Ici, nous dérivons une nouvelle limite qui est la généralisation multi-source du schéma de Shein et comparons ceci à la tranche supérieure consistant uniquement en des "cuts" broadcast et à accès multiples. Ensuite, nous examinons à quel point les débits réalisables correspondant aux stratégies de relayage AF, DF, BQRB et QF sont loin des débits extrêmes.
- Schein dans sa thèse montre que si la qualité du canal broadcast (BC) est inférieure à celle du canal à accès multiples, alors le relayage DF est presque optimal. Cependant, le relayage AF réalise une capacité réseau à la limite d'une capacité illimitée au niveau des composants MAC et ce dû à l'effet *coherent combining* à la destination. Pour ce scénario, l'usage du fameux codage à la source (reproduire l'observation de la RS avec une certaine fidélité) n'aboutit pas à de meilleures performances [23]. In [23], pour les PRNs discrets où les relais sont connectés à la destination à travers des liens orthogonaux, sans bruit, et à capacité limitée, il est démontré que si les liens ont suffisamment de capacité pour reproduire les observations de la RS au noeud destination, alors l'usage de la technique BQRB peut atteindre la capacité réseau. Nous notons cependant que pour les PRNs Gaussiens à atténuation de phase (*phase fading*), l'effet de combinaison cohérente (*coherent combining*) n'est plus valide et que la transmission *indépendante* des signaux est le moyen optimal pour les communications MACs à atténuation de phase [17,18]. Nous pouvons donc appliquer les outils de quantification et de "binning" aléatoire [32, 58] aux observations de la RS et obtenir ainsi des débits réalisables plus importants que ceux proposés dans [23]. A noter que, bien que les observations de la RS sont des variables aléatoires dépendantes (RVs), ainsi que leurs versions quantifiées, l'usage du "binning" aléatoire (indépendamment du signal émis par la source) résulte en des indices de "bin" indépendants. C'est précisément cet aspect qui nous permet d'atteindre de meilleurs débits réalisables comparés à ceux obtenus par les stratégies de relayage AF et DF.
- Avec une qualité du canal plus faible dans la partie BC que dans la partie MAC, la région de débit réalisable du BQEB est montrée comme ayant de meilleures performances que les schémas de relayage AF et DF et comme étendant la région de débit réalisable par un MAC avec une destination à antennes multiples au cas de sources multiples.
- Dans la plupart des papiers traitant la stratégie de relayage CF (ou QF), l'usage des codebooks Gaussiens à la sources et le mapping Gaussien aux RSs sont supposés, sans prétendre l'optimalité, afin d'analyser des schémas

de relayage plus simples [17, 18]. Dernièrement, dans [28, Section VI-B], il est montré que pour un transmetteur nomadique où une source communique avec la destination à travers deux stations relais chacune ayant un lien sans perte à capacité 1 [bit/transmission] vers la destination, le débit réalisé en utilisant la signalisation BPSK à la source avec un détecteur dur à deux niveaux à chaque RS réalise de meilleures performances que la signalisation Gaussienne à la source et le mapping Gaussien aux RSs. Des conclusions parallèles sont également constatées dans [63, 64] pour la configuration de canaux relais Gaussiens avec modulation codée (CM) à la source et un lien relais-à-destination orthogonal où le schéma EF est étudié avec différents mappings RSs. Ils ont conclu que, pour le scénario CM à *faible* SNR source-relais, EF avec mapping Gaussien à la RS est le meilleur, que à *fort* SNR source-relais, DF est meilleur et que à SNR *moyen*, EF avec *hard-decision per symbol* à la RS est bien meilleur que les deux premières techniques. Motivés par ces observations, nous avons étudié les schémas de relayage BQRB et QF en supposant des codebooks à constellation limitée (i.e., M-ary Quadratic Amplitude Modulation (M-QAM)) à la source et un mapping non-Gaussien (une simple quantification scalaire uniform (uSQ)) aux RSs.

- Les aptitudes de traitement des RSs affectent d'une manière significative les performances du système. Ainsi, dans ce chapitre, nous examinons la possibilité d'avoir de bonnes performances en utilisant des RSs simples et pas chères avec des connexions à capacité limitée vers la destination. Plus particulièrement, nous nous intéressons à une technique de quantification plus *simple* et plus *pratique* au niveau des RSs qui se repose sur une uSQ symbole par symbole puisque dans le régime à haute résolution la perte de performance comparée à la quantification vectorielle (VQ) devient négligeable [65–67].
- Dans le régime à *faible* SNR, où le relayage CF ou QF donne de meilleurs gains [18], il est possible d'approcher les limites du système en utilisant CM à la source. De plus, avec CM à la source, il est possible d'exploiter la *structure* des codewords en utilisant un mapping non-Gaussien aux RSs. A travers des simulations numériques, nous constatons que du régime à faible SNR à celui à SNR moyen, avec des aptitudes de lien de retour suffisantes pour transmettre les bits décodés d'une manière efficace à la destination, le débit total réalisable en utilisant QF avec CM à la source et uSQ aux RSs est bien meilleur que celui obtenu en utilisant une signalisation Gaussienne à la source. En outre, nous observons que ce débit total réalisable est directement proportionnel à la taille de l'alphabet de modulation.

9.4 Modèle du canal

Nous étudions le modèle du PRN général illustré par la Figure 9.2 où un ensemble de $\mathcal{T} = \{1, 2, \dots, T\}$ sources voudraient communiquer avec la destination

avec l'assistance d'un ensemble $\mathcal{K} = \{1, 2, \dots, K\}$ de RSs. Nous ne supposons l'existence d'un lien direct ni entre les sources et la destination ni entre les RSs. Tous les canaux sont modélisés comme des canaux sans mémoire à bruit blanc Gaussien additif (AWGN) et à gain constant (ce qui correspond à un affaiblissement de trajet entre chaque émetteur et récepteur) et une atténuation de phase ergodique.

Les RSs opèrent en mode *full-duplex* (FD). Chaque noeud source encode son message $W_t \in \mathcal{W}_t$, où $\mathcal{W}_t = \{1, 2, \dots, 2^{nR_t}\}$ et R_t est le débit d'émission de la t -ème source, dans le codeword $X_t^n(W_t)$. Toutes les données su canal sont indépendantes entre elles. Le signal reçu à la k -ème RS après l'usage du i -ème canal, pour $i \in [1, n]$, est

$$Y_{R_k,i} = \sum_{t=1}^T h_{kt} e^{j\Phi_{kt,i}} X_{t,i} + Z_{k,i}, \quad \forall k \in \mathcal{K}, \quad (9.1)$$

où $h_{kt} \in \mathbb{R}^+$ pour tout $k \in \mathcal{K}$ et $t \in \mathcal{T}$, est le gain fixe du canal de la t -ème source à la k -ème RS. $\Phi_{kt,i}$, $\forall \{k, t\}$ désigne l'ensemble des phases aléatoires causées par les canaux de la t -ème source à la k -ème RS. Nous supposons une contrainte de puissance moyenne pour chaque codeword $X_t^n(W_t)$ transmis par les sources et dont la limite $n \rightarrow \infty$ pourrait être exprimée comme suit

$$\frac{1}{n} \sum_{i=1}^n |X_{t,i}(W_t)|^2 \leq P_s \quad (9.2)$$

pour tout $t \in \mathcal{T}$ et $W_t \in \mathcal{W}_t$.

La k -ème RS transmet X_{R_k} en se basant sur les signaux précédemment reçus (encodage causal) [10]

$$X_{R_k,i} = f_{R_k,i}(Y_{R_k,1}, Y_{R_k,2}, \dots, Y_{R_k,i-1}) \quad (9.3)$$

où $i \in [1, n]$ est l'indice temps. Pour lcanal d'accès des RSs à la destination, nous considérons deux différents modèles de canal: 1) un AWGN MAC ordinaire avec gain de canal constant et une atténuation de phase aléatoire et 2) des liens orthogonaux sans perte à capacité limitée entre chaque RS et la destination.

Un MAC partagé entre les RSs et la destination

Dans ce cas, nous considérons une AWGN MAC des RSs à la destination consistant en un gain de canal constant et une atténuation de phase aléatoire uniforme tel que le montre la Figure 9.2. Nous supposons une contrainte de puissance moyenne pour chaque RS dont la limite $n \rightarrow \infty$ pourrait être exprimée comme suit

$$\frac{1}{n} \sum_{i=1}^n |X_{R_k,i}|^2 \leq P_r, \quad \forall k \in \mathcal{K}. \quad (9.4)$$

Avec ce modèle, le signal reçu à la destination après l'utilisation du i -ème canal, pour $i \in [1, n]$, est donné par

$$Y_i = \sum_{k=1}^K g_k e^{j\Phi_{Dk,i}} X_{Rk,i} + Z_i \quad (9.5)$$

où $g_k \in \mathbb{R}^+$, $\forall k \in \mathcal{K}$, est le gain fixe du canal de la k -ème RS à la destination, et $Z_i \sim \mathcal{CN}(0, \sigma^2)$ est un complex AWGN circulairement symétrique à la destination. $\Phi_{Dk,i}$, $\forall k \in \mathcal{K}$ désigne l'ensemble des phases aléatoires causées par le canal de la k -ème RS à la destination à l'usage du i -ème canal. A noter que nous supposons l'utilisation d'une atténuation de phase ergodique où chaque $\Phi_{kt,i}$ et $\Phi_{Dk,i}$ est une variable aléatoire uniformément distribuée sur $[-\pi; \pi]$. Les phases aléatoires sont parfaitement connues aux récepteurs concernés et inconnues aux transmetteurs.

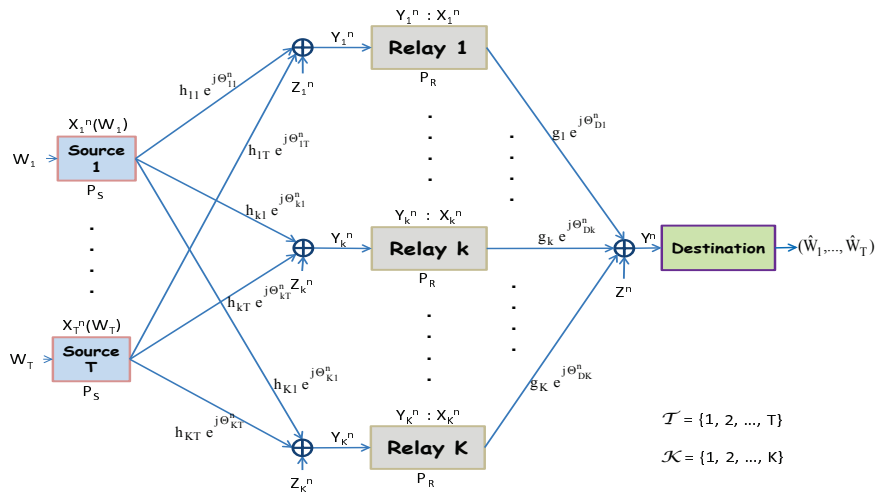


Figure 9.2: Un PRN général avec M -sources, k -relais et une seule destination avec atténuation de phase.

Des liens orthogonaux à capacité limitée entre les RSs et la destination

Considérant les systèmes de téléphonie cellulaire, il est possible que certaines BSs se connectent à une unité centrale de contrôle soit à travers les liens en fibre optique soit via des liens à micro-ondes. Afin de rajouter ces scénarios d'application à l'étendue de ce chapitre, nous considérons également un modèle de canal entre les RSs et la destination avec des liens orthogonaux sans erreur et à capacité limitée. C_i in [bits/channel use] désigne la capacité entre la i -ème RS et la destination. Ce schéma est illustré par la Figure 9.3.

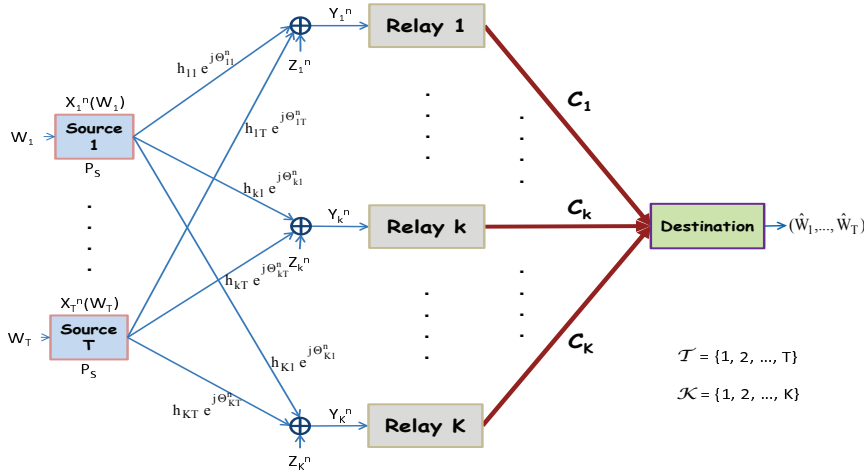


Figure 9.3: Un PRN général avec M -sources, k -relais et une seule destination avec des liens orthogonaux sans erreur à capacité limitée entre les RSs et la destination, où C_i in [bits/usage du canal] est la capacité du lien entre la i -ème RS et la destination, pour $i = 1, 2, \dots, K$.

9.5 Résumé du Chapitre 3

La connaissance de la capacité d'un système est insuffisante pour une caractérisation approfondie de sa performance. C'est pourquoi dans ce chapitre la mesure de performance considérée est l'exposant d'erreur de codage aléatoire (random coding error exponent (EE)) [69] : ce dernier définit une fonction de la fiabilité du canal qui représente un taux de probabilité d'erreur de décodage décroissant en fonction de la longueur du mot de code. En particulier, on évalue les EEs de codage aléatoire correspondant aux stratégies de relayage DF, CF et QF pour les scenarios PRN ayant une source ou deux. Pour la stratégie de DF, on suppose des codes Gaussiens aux sources et un décodage par maximum de vraisemblance (maximum likelihood - ML) aux relais où chaque relai transmet à la destination sa propre décision ainsi qu'une *fonction de fiabilité* correspondante : la destination utilise ces derniers pour prendre la décision finale concernant les mots d'information transmis par la source et ceci sans avoir besoin de CSI. Pour la stratégie BQRB (ou CF), on suppose des codes Gaussiens aux sources, VQ aux relais et un décodage ML à la destination. Pour la stratégie QF, on suppose une modulation codée (M-QAM) aux sources et uSQ aux relais. Nous montrons, grâce à une analyse numérique, que, quand le système est dans le régime de faible SNR et que la capacité du backhaul est suffisante, l'utilisation d'une constellation à alphabet fini (c'est-à-dire M-QAM) aux sources ainsi qu'un traitement simple aux RSs (c'est-à-dire uSQ symbole par symbole) peut résulter en de meilleurs EEs que des stratégies plus complexes (telles les stratégies de

relayages DF et CF pour lesquelles une signalisation Gaussienne aux sources et des mappings Gaussiens au RS sont adoptés). Ceci est du à la structure inhérente aux alphabets de modulation considérés, qu'une signalisation Gaussienne ne possède pas.

9.5.1 Directions Futures

Vu le potentiel de stratégies pratiques de relayage, il serait intéressant d'analyser les taux d'erreur de bloc (block error rate - BLER) pour des techniques pratiques de codage de canal, par exemple celles du standard LTE consistant d'un codeur turbo, d'un entrelaceur et utilisation une modulation M-QAM pourraient être utilisées, pour les stratégies de relayage étudiées dans cette thèse.

Dans ce chapitre, pour le cas de relayage DF, nous avons supposé que chaque RS transmet gratuitement à la destination son information sur la fiabilité de sa décision. Cependant, en pratique, chaque RS ferait un contrôle de redondance cyclique (CRC) juste après l'étape de décodage et, selon le résultat, utiliserait le backhaul pour renvoyer les bits décodés à la destination (ou une demande de répétition automatique (ARQ) à la (aux) source(s)). Les ressources de backhaul ne sont donc pas *toujours* exploitées par les RSs dans le cas de relayage DF, ce qui n'est pas le cas pour les stratégies de relayage BQRB et QF. Il serait donc intéressant d'examiner la relation entre les stratégies de relayage et l'utilisation du backhaul correspondante.

Un autre travail futur pourrait considérer le cas où l'ingénieur système voudrait simplifier les RSs autant que possible et laisser l'étape de décodage à la destination. Dans ce cas, les RSs pourraient générer des rapports de log-vraisemblance (log-likelihood ratios - LLRs) et en envoyer des versions quantifiées à la destination qui combinerait toutes ces informations *souples* et exécuterait le décodage final. La question serait si c'est la quantification du signal reçu (relayage BQRB) ou celle de l'information souple (relayage DF partiel) qui résulterait en une meilleure performance.

9.6 Résumé du Chapitre 4

Dans ce chapitre, nous considérons un réseau cellulaire aidé par des RSs fixes, qui sont utilisés par les MSs pour accéder à la station de base (BS) via une stratégie de relayage, en particulier Amplify-and-forward (AF), DF, Compress-and-forward (CF) et Quantize-and-forward (QF). Nous analysons la somme des taux réalisable pour des communications en voie ascendante. Nous comparons les stratégies de relayage avec deux systèmes cellulaires connus: dans le premier, les antennes de la BS sont supposées co-localisées (système cellulaire conventionnel) et dans le second cas elles sont supposées distribuées dans la cellule et liées à la BS via des liens filaires à capacité très élevée, c.à.d. un système d'antennes distribuées (DAS) parfait. On suppose que les signaux des MS et RS sont émis sur des bandes fréquence *orthogonales*, avec la possibilité d'avoir une bande passante plus grande dédiée aux liens entre les RS et BS. Les contributions de ce

chapitre sont les suivantes:

- Le modèle du canal relais orthogonal généralisé (Generalized orthogonal relay channel - GORC) est introduit. Des bornes supérieures et des taux réalisables sont obtenus pour différentes stratégies de relayage.
- Nous proposons une analyse théorique des gains obtenus grâce aux relais fixes dans un scénario multicellulaire, le point-clé étant la capacité de l'ingénieur système à exploiter des liens presque directs (line-of-sight - LOS) entre les relais et la station de base lors du déploiement.
- Nous tenons explicitement compte de l'effet de l'interférence intercellulaire sur la performance des relais et comparons les formes principales de relayage, à savoir AF, DF et QF. Nous observons que la stratégie QF surpasse les autres.
- Nous évaluons les gains obtenus grâce aux RSs fixes comparés aux systèmes cellulaires conventionnels.
- Nous montrons qu'avec un choix judicieux des paramètres du système, tels que la bande passante, la puissance de transmission et le mécanisme de relayage, le relayage à plusieurs sauts (multi-hop) a une performance pas trop éloignée de celle d'un DAS parfait.

Nous considérons une communication en voie ascendante (des MSs vers la BS) dans un réseau multicellulaire comportant des RSs en infrastructure, pour lequel les canaux des MSs vers les RSs et BSs sont orthogonaux aux canaux des RSs vers les BSs. Ce modèle du canal est appelé *GORC*. Nous supposons $B + 1$ cellules chacune contenant M MSs désirant communiquer avec la BS située au centre de la cellule via K RSs placée de manière arbitraire dans la cellule.

La communication en voie ascendante se fait en deux étapes (sauts): les MSs accèdent aux RSs et à la BS en une première étape de communication alors que les RSs renvoient les données des MSs vers la BS via le canal sans fil lors de la deuxième étape, l'accès aux canaux de backhaul ayant des bandes de fréquences orthogonales: un relayage duplexage de division de fréquence (frequency division duplex - FDD) est adopté. La communication entre RS n'est pas permise puisqu'elle nécessite des protocoles de routage plus intelligents aux couches supérieures. Nous supposons que la bande passante allouée au premier saut (deuxième saut) est W_1 (W_2) avec une bande passante totale de $W_{tot} = W_1 + W_2$. Le rapport de bande passante F est égal à $W_2/W_1 \in \mathcal{R}^+$, voir la Figure 9.4. Comme le montrent nos résultats numériques ci-dessous, l'allocation des ressources, c.à.d. le choix de F , a un impact direct sur la performance du système.

Vu qu'on suppose un facteur de réutilisation de fréquence égal à 1, les communications dans une certaine cellule sont soumises à de l'interférence intercellulaire. Supposant une connaissance statistique de l'état des canaux interférents à chaque récepteur, nous modelons les signaux d'interférence intercellulaire comme du bruit Gaussien de moyenne zéro et variance spécifiée par le gain du canal

entre l'émetteur interférent et le récepteur considéré. A noter cependant qu'une connaissance parfaite des canaux interférents pourrait résulter en une meilleure performance.

Les BSs sont équipées de N antennes directionnelles chacune dirigée vers l'une des RSs l'entourant et chaque MS possède une seule antenne omnidirectionnelle. Pour les RSs, nous considérons les deux possibilités. Chaque cas correspond à un scenario de déploiement différent.

Nous analysons la performance du système en obtenant les *sommes de taux réalisables*.

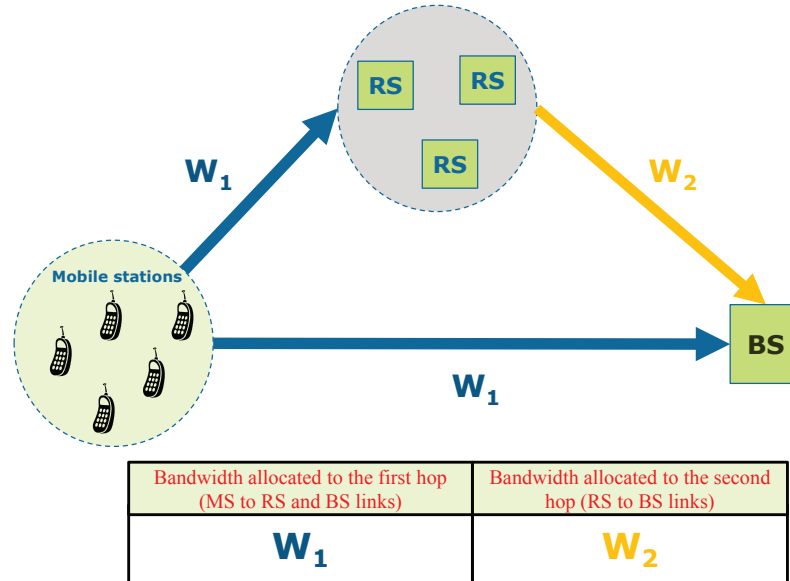


Figure 9.4: L'allocation de la bande passante pour les première et deuxième étapes.

9.6.1 Conclusions

Dans ce chapitre, nous avons considéré la voie ascendante d'un système cellulaire utilisant des relais en présence d'interférence intercellulaire. Supposant des bandes fréquences orthogonales allouées aux transmissions MS-vers-RS et RS-vers-BS, les sommes de taux réalisables sont analysées pour des stratégies de relayage AF, DF, CF et QF et comparées à deux systèmes cellulaires connus, à savoir un système cellulaire conventionnel et un système d'antennes distribuées parfait.

Nous observons que le choix des paramètres du système, tels que les positions des stations relais et les motifs des antennes qu'elles utilisent, influe significativement les taux réalisables. L'allocation des ressources aux liens d'accès et de backhaul joue un rôle crucial dans la performance du système. La stratégie de relayage de CF surpasse les autres stratégies considérées.

Bien qu'on ait fourni une certaine analyse, une étude plus approfondie du positionnement des relais dans les systèmes cellulaires doit également être entreprise. On pourrait également considérer la question d'équité puisque l'une des raisons d'introduire des relais est de stabiliser la charge du système. La procédure que nous proposons dans [84], basée sur l'annulation successive de l'interférence (successive interference cancellation - SIC), pourrait être améliorée pour en tenir compte.

9.7 Résumé du Chapitre 5

Dans ce chapitre, nous étudions un problème de déploiement RS dans les réseaux cellulaires pour les communications DL où l'on tient compte de manière réaliste les caractéristiques du réseau cellulaire afin de combler certaines lacunes dans les programmes proposés dans [2, 4, 33–36]. Plus précisément, nous nous concentrons notre attention sur un système distribué de relais pour les transmissions DL, où une donnée MS peut être desservi par la BS ou par une RS (jusqu'à deux sauts sont pris en compte). Ce régime, comme il sera détaillé dans les sections suivantes, nécessite une quantité réduite de commentaires en ce qui concerne le cas centralisé, en particulier lorsque plusieurs antennes sont déployées dans chaque nœud et un retour simple scalaire n'est pas suffisant. En raison des exigences d'évaluation réduit le système est plus évolutive, en tant que RSS nouvelles peuvent être déployées en cas de besoin. En outre, en déplaçant la transformation vers le côté RS, la coopération locale entre RSs devient possible. Comme dans le cas centralisé pris en compte dans [4] (et différente de [33] où la notion de taux commun est utilisé au maximum), nous garantissons l'utilisateur équité en prenant des décisions de planification basées sur l'état des files d'attente des MSs et sur l'estimation du signal instantané à des ratios des interférences plus bruit (SINRs). Aussi, à la différence de [33], nous ne supposons pas une séparation orthogonale des ressources entre les BS-à-RS liens et BS/RS-à-MS liens.

La technique proposée fonctionne en deux phases. Dans la première phase, la BS prend ses décisions de programmation pour ce créneau horaire en tenant compte des conditions du canal et des états file d'attente des RSs et MSs. La destination choisie pourrait être soit une RS ou d'une sclérose en plaques. Dans la deuxième phase, chaque RS, si elle n'avait pas été prévue par la BS dans la première phase, prévoit une MS considérer conditions canal et les états file d'attente. Nous étudions les performances de la proposition par le biais d'un simulateur de multicellulaire.

9.7.1 Modèle de système

Nous considérons un système cellulaires de relais déployés pour la communication DL où plusieurs RSs fixes sont présents dans chaque cellule et la réutilisation des fréquences de l'un est utilisé. Considérant wrap-around cellule hexagonale de mise en page, nous nous concentrons sur la cellule dans le centre d'évaluation des performances. Les paquets de données correspondant à chaque MS dans la cellule arriver à la BS correspondante, puis sont placés dans les files d'attente appropriée. Les RSs ont aussi des files d'attente correspondant à chaque MS qui leur sont assignées, où ils reçoivent les données de la BS via une liaison sans fil (il n'ya pas de connexions entre backhaul BSs et RSs). Nous considérons au plus de communication à double-hop des BSs à l'MS où cela est approvisionnée pour les futurs systèmes cellulaires composé des RSs. Cette hypothèse a les conséquences suivantes: il n'existe aucun lien (ou de la communication) entre les RSs et les MSs, soit directement, recevoir des données de la BS ou via une RS. Chaque MS est affecté à un émetteur, c'est à dire, la BS ou l'un des RSs. Les affectations des MSs peut être fait de différentes manières.

Pour le relais, DF est adopté, qui est la meilleure stratégie de relais lorsque les BS-à-RS liens sont mieux que les autres liens [18]. Décoder le signal qu'ils reçoivent, ils retransmettent les mêmes données à l'un des MSs qui leur sont assignées. Comme on le verra ci-dessous, les RSs peut aussi faire la planification des décisions dans notre système. Au début de chaque période, pour la planification centralisée à la BS est supposé avoir la connaissance du taux de transmission instantanée sur tous les liens au cours de cette trame, et également une connaissance de la taille des files d'attente correspondant à chaque RS à tous les émetteurs (BS et RSs) dans la cellule. Pour algorithme d'ordonnancement décentralisée, nous supposons que le BS ne reçoit que les informations d'état de chaque file d'attente de RS. En outre, il ne nécessite pas de taux de transmission instantanée sur les liens entre les RSs et les MSs qui désigne un grande réduction de la rétroaction de RSs de la BS.

9.7.2 Conclusion et Perspectives

Nous avons proposé un système distribué de relais pour les transmissions DL, où une donnée MS peut être desservi par la BS ou par une RS, d'une manière opportuniste. Cette approche distribuée, permettre une réduite commentaires à l'égard du cas centralisé, surtout quand un retour simple scalaire n'est pas suffisant pour évaluer la qualité de canal. En raison des exigences d'évaluation réduit, le système devient plus évolutive, et donc nouveau RSs peut être déployé sans la nécessité d'une planification du réseau prudent.

9.8 Résumé du Chapitre 6

Dans ce chapitre, nous considérons un réseau de communication comprenant des nœuds de communication bidirectionnelle avec l'aide d'une RS commun. Les nœuds sont supposés ne pas avoir de liens de communication directs. Une

coupe-ensemble externe à destination de l'ensemble des taux dans le cadre de cette topologie du réseau est donnée pour deux cas particuliers en supposant FD (full-duplex) capacités de transmission. Nous étudions d'abord un canal additionneur binaire avec bruit additif au niveau des noeuds et la RS, puis généraliser à un canal additif blanc gaussien multi-utilisateurs à la RS et un bruit gaussien additif au niveau des noeuds où nous améliorons les résultats des dernières faisabilité pour les codes en treillis et le décodage partiel à la RS. Nous montrons aussi que la limite externe est pratiquement réalisable par de la couche physique de réseau de codage, en utilisant les codes de groupe et le décodage partiel à la RS dans les deux modèles de canaux. Nous comparons ensuite ces systèmes de codage à binning (hachage et de compression avec le côté de l'information) où la RS ne pas tenter de partiellement décoder le signal somme et amplifient-and-forward (AF) relayer des stratégies à la RS. Il est démontré que les stratégies de solides liens RS-à-noeud de compression peuvent fournir près des performances optimales sans la nécessité d'une pleine CSI à la fin de transmission.

9.8.1 Le modèle de canal

Considérons le réseau général sans fil avec une RS seule Figure 9.5, où les noeuds sont supposés à échanger toutes les informations via une RS car aucun liens de communication directs sont disponibles. Il faut noter d'emblée que dans le problème considéré ici la RS n'est pas un point d'accès à un autre réseau comme c'est principalement le cas pour un BS cellulaire ou un accès WiFi-point. Dans ces exemples, le lien à double sens, le volume du trafic échangé entre les utilisateurs dans la même cellule est généralement négligeable par rapport au montant relayé par le point d'accès par le réseau de l'opérateur à l'autre cellule ou à l'Internet.

Pour les multi-stratégies de codage nous considérons dans ce travail, l'aspect le plus important pratiques de loin, est la capacité du système de contrôle des phases des signaux entrants au RS. Dans un système de communication sans fil réel de cette varieront rapidement en raison de facteurs autres que le milieu de propagation, surtout la dérive d'horloge, la fréquence porteuse-bruit de phase et de décalages. La capacité de suivre la phase du signal reçu par la RS à la émetteurs est donc une question de grande importance pratique concernant les résultats présentés ici, mais au-delà de la portée de cette étude préliminaire.

Si l'on considère un canal varie lentement, le modèle de communication allait changer de façon significative à intégrer une utilisation plus sophistiquée de la CSI à l'émission qui comprennent le pouvoir de contrôle et compliquerait beaucoup les choses. Nous avons également laisser ce type de modèle de canal pour les travaux futurs.

Dans ce chapitre, nous avons comparé les différentes stratégies de codage pour les canaux TWR. Pour la stratégie de décodage partiel basé sur Lattice, l'aspect le plus important pratiques de loin, est la capacité du système de contrôle des phases des signaux entrants au RS. Dans un système de communication sans fil réels, cela varie rapidement en raison de facteurs autres que le milieu

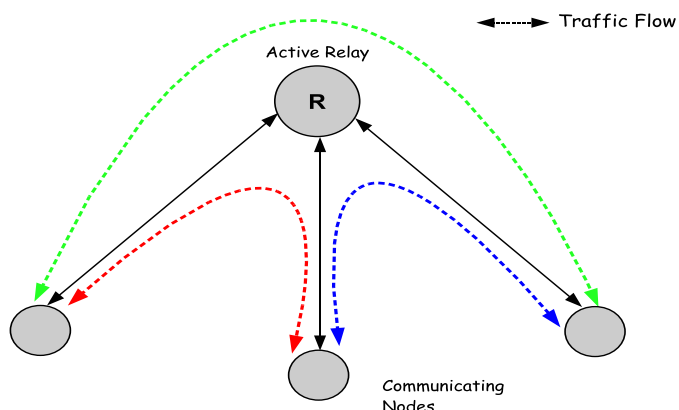


Figure 9.5: Réseau de relais à double sens

de propagation, principalement la dérive d'horloge, la fréquence porteuse, les compensations et le bruit de phase. En conséquence, l'utilisation de stratégies de mise en cellule de type peut être une approche plus pratique, malgré la perte d'efficacité spectrale, car la cohérence de phase des signaux à la RS n'est pas nécessaire. Notre travail actuel porte sur l'utilisation des informations dans la stratégie de codage au niveau des bornes, une question qui a été négligé ici.

9.9 Résumé du Chapitre 7

Dans ce chapitre, nous considérons un canal de relais avec multi-paire dans les deux sens (TWRC) où sur chaque paire une antenne MS essaye de communiquer. Cette communication est faisable via une antenne commune multiple RS. Dans la multi-paire TWRC, la performance du système est limitée par l'interférence vue par chaque MS et qui est provoquée par tous les autres paires MS. Nous allons essayer d'aborder cette problématique dans le domaine spatiale en utilisant des antennes multiples dans la RS. Récemment, des travaux de recherche ont été élaboré multi-paire TWRC [94–96]. [94] et [96] ont traité le cas multi-paire multi-antenne RS TWRC avec un relai DF suivie par un codage réseau numérique (XOR par bit). Dans [94], un algorithme d'optimisation de précodage de matrice est développé pour maximiser le débit total du système, tandis que [96] propose une méthode basée sur un multi-groupe multi-cast avec du beamforming pour la transmission dans la seconde phase. Dans ces deux travaux, les MSs sont séparés spatialement en utilisant des multi-antennes RS. Par ailleurs, dans [95], un TWRC multi-paire est étudié où une seule antenne RS essaye d'orthogonaliser les utilisateurs dans les multi-paire TWRC en utilisant

un Code Division Multiple Access (CDMA). Toutefois, dans [94, 96], les MSs sont séparés spatialement par une multi-antenne RS.

Dans ce chapitre, nous nous sommes concentrés sur les deux stratégies de relais AF et QF. Ces dernières sont intéressantes dans le cas où il y a une contrainte de complexité dans le noeud relais ou lorsque la liste de codage des MSs est inconnue, auquel cas la stratégie DF n'est pas applicable. En outre, comme nous constaterons dans les résultats de simulation, pour certaines régions du SNR, les deux stratégies AF et QF donnent des résultats meilleurs comparés à la stratégie DF. Nous proposerons alors dans ce travail des schémas spécifiques pour les deux types de relais et nous analyserons leurs performances en termes de débit total du système. En particulier, deux méthodes basées sur le beamforming sont développées pour le relais AF: une simple méthode Tx-Rx zéro forçage (ZF) et une deuxième méthode Tx-Rx bloc-diagonalisation (BD), adaptée à notre contexte. Nous montrons que la méthode BD donne de meilleures performances en termes de débit totale du système comparé à la méthode ZF. En effet, pour la méthode BD, contrairement au cas du ZF, le relais n'a pas besoin d'inverser la totalité du canal, et par conséquent une économie de l'énergie du système. Pour le relais basé sur le QF, c'est à la RS de séparer les signaux correspondant aux MSs dans chaque paire et de quantifier les signaux reçus pour s'approcher le plus possible du débit adéquat pour la deuxième phase de communication. En tenant compte des informations pour chaque MS, nous réalisons une quantification scalaire qui est une combinaison linéaire convenablement choisie du signal reçu RS sous forme de vecteur, évitant ainsi une quantification vectorielle. Cette approche peut être considérée comme une forme analogique du codage facilitant l'auto annulation d'interférence à chaque MS.

9.10 Conclusions

L'objectif majeur de cette thèse est de développer une antenne RS de scénarios potentiels de RS de communication sans fil avec des taux réalisables et de fiabilité de nos principales figures de mérite. L'insuffisance du courant classique des systèmes cellulaires de répondre aux demandes de croissance des applications sans fil constitue la motivation pour cette étude. Afin de fournir omniprésente, fiable, un taux élevé de services de données sans fil nécessite une puce et complexe des dessins d'architecture réseau, l'intégration des interfaces radio différentes pour former de grands réseaux. Il est donc important de rechercher des approches rentables et les technologies qui permettront d'améliorer l'efficacité spectrale et la fiabilité. Bien que l'intégration a récemment développé des techniques de transmission de pointe, telles que MIMO, OFDM et techniques d'annulation d'interférence, dans les systèmes sans fil offre un meilleur débit, fiabilité et les performances de couverture, ces techniques ne suffisent pas à répondre aux besoins futurs des systèmes sans fil, sans poursuivre le déploiement de dispositifs d'infrastructure. Il est donc nécessaire de changer la façon dont les systèmes sans fil sont conçus et déployés. À cette fin, l'intégration de multi-sauts (ou relais) dans les réseaux sans fil conventionnels a été considérée comme une so-

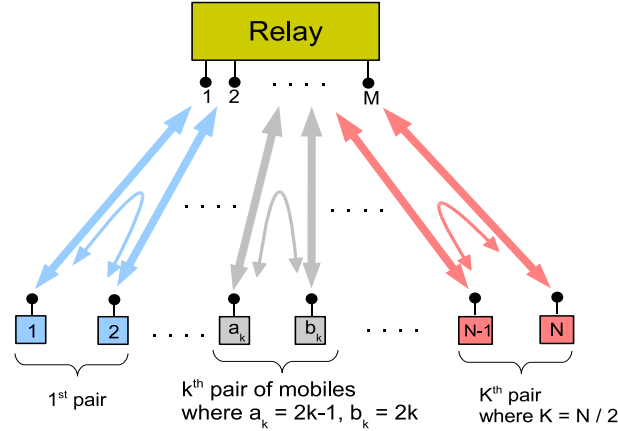


Figure 9.6: K -pair ($N = 2K$ MSs) TWRC avec M antennes RS.

lution prometteuse. Ainsi, nous avons donné notre attention à l'utilisation des RSs dans les différents systèmes de communication sans fil, où le relais différents et des stratégies de codage ont été examinés.

Les approches suivantes ont été étudiées dans cette thèse.

Nous avons d'abord concentré sur les réseaux de relais en parallèle, qui pourrait trouver un large éventail de applications sans fil, et a examiné la possibilité d'avoir de bonnes performances pouvant être atteintes en utilisant simple et à bas prix RSs. Nous avons fourni une enveloppe extérieure plancher reposant sur des travers-bancs, et l'analyse des taux de diverses stratégies réalisables pour le relais. Considérant modèles phase canal à évanouissements, nous avons montré que la quantification s'opposer à un projet et binning aléatoire (BQRB) relayer la stratégie joue très bien en raison de l'antenne mise en commun d'effet sur le côté du récepteur. Nous avons également montré la possibilité de réaliser des performances relativement bonnes avec les hypothèses simplifiées à la source et de flux RSs. Plus précisément, nous avons montré que dans certains régimes les taux atteints par de simples stratégies de relais (dans laquelle la modulation finie alphabet et simple uSQ symbole par symbole sont utilisés à des sources et des flux RSs, respectivement), sont meilleurs que les taux obtenus par plus complexe relais stratégies (listes de codage dans lequel gaussien, VQ et le décodage ML sont utilisés à des sources, de relais et de destination, respectivement). Cela montre donc que le fichier structure inhérente à l'alphabet de modulation finis utilisés par les sources peuvent être utiles dans le mouvement de précession de quantification à les RSs.

Afin d'avoir une caractérisation approfondie des performances des réseaux à

relais parallèle, nous avons également étudié l'erreur du codage aléatoire correspondant aux stratégies DF, BQRB et QF. Nous avons proposé des stratégies de relai DF et nous avons dérivé l'erreur correspondante. Dans le même but que d'analyser le débit total du système, nous pouvons remarquer qu'en utilisant un alphabet fini, par exemple M-QAM, au niveau des nœuds source avec une quantification scalaire uniforme au niveau des RSs, pourrait fournir une erreur meilleure qu'en utilisant des stratégies de relai plus complexe et non applicable. Ceci est grâce, encore une fois, à la structure inhérente dans le schéma modulation considéré.

Ensuite, nous allons nous concentrer au réseau cellulaire de relai assisté et analyser la somme du débit totale pour les communications de liaison montante (uplink) en supposant que les signaux MS et RS sont émis sur des bandes de fréquences orthogonales. En particulier, prenant en compte l'impact des interférences inter-cellulaires sur la performance du relais, nous avons dérivé les expressions du débit du système pouvant être atteintes par les stratégies AF, DF, CF et QF. Nous avons montré que la FC donne la meilleure performance en termes de débit. En outre, l'importance de l'allocation des ressources en systèmes cellulaires à relai-assisté a été évaluée.

Poursuivant avec les communications DL pour les systèmes cellulaires a relais déployé, nous avons proposé un algorithme d'ordonnement distribué dans laquelle une MS peut être desservi par la BS ou par une RS, d'une façon opportuniste. Avec cet algorithme d'ordonnement distribué, nous avons essayé de répondre à certaines des inconvénients qui surviennent avec le déploiement RS: la perte lors du multiplexage en raison de multi-sauts, l'effet de l'interférence qui augmente avec le nombre des RSs déployée, et les frais généraux d'évaluation. Il a été montré qu'une telle approche distribuée exploite pleinement la réutilisation spatiale dans le système et permet de réduire le retour en ce qui concerne le cas centralisé, surtout dans le cas où le simple retour scalaire n'est pas suffisant pour estimer la qualité du canal. En raison des exigences d'évaluation réduit, le système devient plus évolutif, tant que les nouvelles RSs peuvent être déployées en cas de besoin, sans avoir besoin d'une planification du réseau prudent. En outre, en déplaçant la transformation vers le côté RS, la coopération locale entre RSs devient possible.

Dans cette thèse, nous avons poursuivi l'analyse des différentes stratégies de codage pour TWRCs. En supposant que les capacités de transmission est full-duplex, une borne extérieure limite est développée. Nous avons remarqué que cette borne extérieure est pratiquement réalisable par le codage réseau de la couche physique, en utilisant les codes de groupe et le décodage partiel à la station de relais pour les deux modèles additionneur binaire et canal Gaussien. Nous avons ensuite proposé des schémas de codage basé sur binning (hachage et compression avec information), où le relais n'est pas tenté de décoder partiellement la somme du signal. Il a été montré que pour les stratégies basées sur le fort relais pour les liens de noeud de compression peuvent fournir des performances optimales sans la nécessité d'une connaissance totale du canal à la fin de la transmission.

Enfin, nous avons étendu le modèle TWRC à un modèle multi-pair. Dans

le multi-pair TWRC, le problème majeur sur la performance du système est l'interférence perçue par chaque MS des autres paires MS. Nous avons proposé des nouvelles méthodes de transmission/réception basées sur le beamforming au niveau du RS en vue de résoudre ce problème dans le domaine spatial en utilisant plusieurs antennes au niveau du RS.

9.10.1 Futures travaux

Même si nous avons essayé de résoudre certains problèmes qui se posent du déploiement RS dans plusieurs systèmes de communication sans fil, un certain nombre de questions doivent encore examiner de plus près. La plus notable d'entre eux est de voir les performances des mécanismes de relai proposés appliquée pour un simulateur. Par exemple, en examinant les potentiels des méthodes de relais proposées pour les réseaux de relais en parallèle, il est intéressant de déployer des codes de canal pratique en utilisant les blocs émetteur/récepteur du standard LTE, et d'analyser les taux d'erreur par bloc (BLER) correspondant. La recherche de mécanisme de contrôle d'erreur dans les stations de relais et de leurs conséquences sur l'utilisation des blocs serait également un sujet de recherche intéressant.

Dans le cadre de l'UL cellulaire à relais-assisté, plusieurs problématiques restent encore à être étudiées. La problématique la plus notable est l'équité, puisque l'un des potentialités offertes par le relai est de stabiliser le poids du système. Nous avons montré que dans le cas du DL cellulaire, l'approche que nous avons proposée d'ordonnancement distribué donne des résultats similaires comparée à l'approche centralisée lorsque le capteur de la cellule n'est pas trop élevé. Une étude complémentaire pourrait améliorer les performances du système dans la région d'interférence limitée à l'aide du traitement d'antennes multiples et de coopération locales entre les RSs. Dans les systèmes de communication classiques, par exemple quand il n'y a pas de RS, la communication entre deux nœuds est composée de deux étapes. Dans la première étape, un nœud transmet et l'autre nœud reçoit. Dans la seconde étape, les deux nœuds inversent les rôles de transmission et de réception. Notant que même si ce système de communication semble être simple par rapport aux systèmes de communication modernes, dans les réseaux cellulaires (ou WLAN), il pourrait être nécessaire pour une MS d'avoir une puissance de transmission élevée pour accéder à la BS (ou au point d'accès). Cependant, en utilisant une RS intermédiaire, les problèmes de la puissance de transmission MS pourrait être résolu, et par un multiplexage avant (DL) et arrière (UL) de communications via un relai dans les deux sens et une meilleure efficacité spectrale pourrait être atteinte.

Bibliography

- [1] T. M. Cover and J. A. Thomas, *Elements of Information Theory*. United States: John Wiley & Sons, 1991.
- [2] R. Pabst, B. H. Walke, D. C. Schultz, P. Herhold, H. Yanikomeroglu, S. Mukherjee, H. Viswanathan, M. Lott, W. Zirwas, M. Dohler, H. Aghvami, D. D. Falconer, and G. P. Fettweis, "Relay-based deployment concepts for wireless and mobile broadband radio," *IEEE Communications Magazine*, vol. 42, pp. 80–89, September 2004.
- [3] H. Wu, C. Qiao, S. De, and O. Tonguz, "Integrated cellular and Ad-hoc relaying systems: iCAR," *IEEE Journal on Selected Areas in Communications*, vol. 19, pp. 2105–2115, October 2001.
- [4] H. Viswanathan and S. Mukherjee, "Performance of cellular networks with relays and centralized scheduling," *IEEE Transactions on Wireless Communications*, vol. 4, pp. 2318–2328, 2005.
- [5] Y. D. J. Lin and Y. C. Hsu, "Multihop cellular: A new architecture for wireless communications," in *Proc. IEEE Conf. on Compute Communication*, 2000, pp. 1273–1282.
- [6] A. Zemlianov and G. de Veciano, "Capacity of ad hoc wireless networks with infrastructure support," *IEEE Journal on Selected Areas in Communications*, vol. 23, pp. 657–667, March 2005.
- [7] *IEEE 802.16: Air Interface for Fixed and Mobile Broadband Wireless Access Systems: Multihop Relay Specification*, IEEE 802.16j Task Group Std.
- [8] O. Oyman, J. N. Laneman, and S. Sandhu, "Multihop relaying for broadband wireless mesh networks: From theory to practice," *IEEE Communications Magazine*, vol. 45, pp. 116 – 122, November 2007.
- [9] E. C. van der Meulen, "Three-terminal communication channels," *Adv. Appl. Probab.*, vol. 3, pp. 120–154, 1971.
- [10] T. M. Cover and A. A. E. Gamal, "Capacity theorems for the Relay Channel," *IEEE Transactions on Information Theory*, vol. 25, pp. 572–584, September 1979.

-
- [11] A. B. Carleial, "Multiple-access channels with different generalized feedback signals," *IEEE Transactions on Information Theory*, vol. 28, pp. 841–850, November 1982.
- [12] J. N. Laneman, D. N. C. Tse, and G. W. Wornell, "Distributed Space-Time-Coded protocols for exploiting cooperative diversity in wireless networks," *IEEE Transactions on Information Theory*, vol. 49, pp. 2415–2425, October 2003.
- [13] A. Sendonaris, E. Erkip, and B. Aazhang, "User cooperation diversity Part-I: System description," *IEEE Transactions on Communications*, vol. 51, pp. 1927–1938, November 2003.
- [14] —, "User cooperation diversity Part-II: Implementation aspects and performance analysis," *IEEE Transactions on Communications*, vol. 51, pp. 1939–1948, November 2003.
- [15] J. N. Laneman, D. N. C. Tse, and G. W. Wornell, "Cooperative diversity in wireless networks: Efficient protocols and outage behavior," *IEEE Transactions on Information Theory*, vol. 50, pp. 3062–3080, December 2004.
- [16] A. Nosratinia, T. E. Hunter, and A. Hedayat, "Cooperative communication in wireless networks," *IEEE Communications Magazine*, pp. 74–80, October 2004.
- [17] A. Host-Madsen and J. Zhang, "Capacity bounds and power allocation for wireless relay channel," *IEEE Transactions on Information Theory*, vol. 51, pp. 2020–2040, June 2005.
- [18] G. Kramer, M. Gastpar, and P. Gupta, "Cooperative strategies and capacity theorems for relay networks," *IEEE Transactions on Information Theory*, February 2004.
- [19] R. U. Nabar, H. Bölcskei, and F. W. Kneubühler, "Fading relay channels: Performance limits and Space-Time signal design," *IEEE Journal on Selected Areas in Communications*, vol. 22, pp. 1099–1109, August 2004.
- [20] A. H.-M. B. Wang, J. Zhang, "On the capacity of MIMO relay channels," *IEEE Transactions on Information Theory*, vol. 51, pp. 29–43, January 2005.
- [21] H. Bölcskei, R. U. Nabar, O. Oyman, and A. J. Paulraj, "Capacity scaling laws in MIMO relay networks," *IEEE Transactions on Wireless Communications*, June 2006.
- [22] X. Tang and Y. Hua, "Optimal waveform design for MIMO relaying," in *Proc. IEEE Workshop on Signal Processing Advances in Wireless Communications*, 2005.

- [23] B. E. Schein, "Distributed coordination in network information theory," Ph.D. dissertation, MIT, Cambridge, MA, October 2001.
- [24] M. Gastpar and M. Vetterli, "On the capacity of large gaussian relay networks," *IEEE Transactions on Information Theory*, vol. 51, pp. 765–779, March 2005.
- [25] I. Maric and R. D. Yates, "Bandwidth and power allocation for cooperative strategies in gaussian relay networks," *IEEE Transactions on Information Theory*, vol. 56, pp. 1880–1889, April 2010.
- [26] Y. Kochman, A. Khina, U. Erez, and R. Zamir, "Rematch and forward for parallel relay networks," in *Proc. IEEE Int. Symp. on Information Theory*, Toronto, Canada, July 2008.
- [27] S. S. C. Rezaei, S. O. Gharan, and A. K. Khandani, "A new achievable rate for the gaussian parallel relay channel," in *Proc. IEEE Int. Symp. on Information Theory*, Seoul, Korea, June-July 2009.
- [28] A. Sanderovich, S. S. (Shitz), Y. Steinberg, and G. Kramer, "Communication via decentralized processing," *IEEE Transactions on Information Theory*, vol. 54, pp. 3008–3023, July 2008.
- [29] A. Sanderovich, O. Somekh, H. V. Poor, and S. S. (Shitz), "Uplink macro diversity of limited backhaul cellular network," *IEEE Transactions on Information Theory*, vol. 55, pp. 3457–3478, August 2009.
- [30] F. Xue and S. Sandhu, "Cooperation in a half-duplex gaussian diamond relay channel," *IEEE Transactions on Information Theory*, vol. 53, pp. 3806–3814, October 2007.
- [31] M. Kim and S.-Y. Chung, "Cooperative transmission for a vector gaussian parallel relay network," in *revision for IEEE Transactions on Information Theory*, September 2009.
- [32] A. D. Wyner and J. Ziv, "The rate-distortion function for source coding with side information at the decoder," *IEEE Transactions on Information Theory*, vol. 22, pp. 1–10, January 1976.
- [33] K. Balachandran, J. Kang, K. Karakayali, and J. Singh, "Capacity benefits of relays with in-band backhauling in cellular networks," in *Proc. IEEE Int. Conf. on Communication*, Beijing, China, June 2008.
- [34] A. Maltsev, V. S. Sergeyev, and A. V. Pudneyev, "Backhaul network based on WiMAX with relays - System level performance analysis," in *ISWPC*, Greece, 2008.
- [35] C. Raman, G. J. Foschini, and R. A. Valenzuela, "Power savings from half-duplex relaying in downlink cellular systems," in *Proc. Conf. on Communication, Control, and Computing*, IL, USA, Sept 30 - Oct 2 2009.

- [36] —, “Resource partitioning in downlink cellular systems with half-duplex relays,” in *to be submitted*, 2008.
- [37] D. Soldani and S. Dixit, “Wireless relays for broadband access,” *IEEE Communications Magazine*, vol. 46, pp. 58–66, March 2008.
- [38] B. Rankov and A. Wittneben, “Spectral efficient signaling for half-duplex relay channels,” in *Proc. Conf. on Signals, Systems, and Computers*, Pacific Grove, CA, Nov. 2005.
- [39] R. Knopp, “Two-way radio network with a star topology,” in *Int. Zurich Seminar on Communications*, February 2006.
- [40] T. J. Oechtering and H. Boche, “Optimal resource allocation for a bidirectional regenerative half-duplex relaying,” in *ISITA*, Seoul, Korea, 2006.
- [41] P. Popovski and H. Yomo, “The anti-packets can increase the achievable throughput of a wireless multi-hop network,” in *Proc. IEEE Int. Conf. on Communication*, Istanbul, Turkey, June 2006.
- [42] P. Larsson, N. Johansson, and K. E. Sunell, “Coded bi-directional relaying,” May 2006.
- [43] R. Knopp, “Two-way wireless communication via a relay station,” in *GDRISIS meeting*, March 2007.
- [44] S. Katti, S. Gollakota, and D. Katabi, “Embracing wireless interference: Analog Network Coding,” in *ACM SIGCOMM*, 2007.
- [45] D. Gündüz, E. Tuncel, and J. Nayak, “Rate regions for the separated two-way relay channel,” in *Proc. Conf. on Communication, Control, and Computing*, Monticello, IL, September 2008.
- [46] R. Ahlswede, N. Cai, S. Y. R. Li, and R. W. Yeung, “Network information flow,” *IEEE Transactions on Information Theory*, vol. 46, pp. 1204–1216, 2000.
- [47] Y. Wu, P. A. Chou, and S. Kung, “Information exchange in wireless networks with network coding and physical-layer broadcast,” in *Proc. IEEE Conference of Information Sciences and Systems*, March 2005.
- [48] B. Rankov and A. Wittneben, “Spectral efficient protocols for half-duplex fading relay channels,” *IEEE Journal on Selected Areas in Communications*, vol. 45, pp. 379–389, February 2007.
- [49] P. Popovski and H. Yomo, “Bi-directional amplification of throughput in a wireless multi-hop network,” in *in proc. of the IEEE VTC-Spring*, 2006, pp. 588–593.

- [50] T. J. Oechtering, C. Schnurr, I. Bjelakovic, and H. Boche, "Achievable rate region of a two phase bidirectional relay channel," in *Proc. IEEE Conference of Information Sciences and Systems*, March 2007.
- [51] S. Katti, I. Maric, A. Goldsmith, D. Katabi, and M. Medard, "Joint relaying and network coding in wireless networks," in *Proc. IEEE Int. Symp. on Information Theory*, June 2007.
- [52] S. Zhang, S. C. Liew, and P. P. Lam, "Physical-layer network coding," in *Proc. Annual International Conference on Mobile computing and Networking (MOBIHOC)*, 2006.
- [53] S. J. Kim, P. Mitran, and V. Tarokh, "Performance bounds for bidirectional coded cooperation protocols," in *in proc. of the 27th Int'l conf. on Distributed Computing Systems Workshops, ICDCSW*, June 2007.
- [54] B. Rankov and A. Wittneben, "Achievable rate region for the two-way relay channel," in *Proc. IEEE Int. Symp. on Information Theory*, July 2006.
- [55] B. E. Schein and R. G. Gallager, "The gaussian parallel relay network," in *Proc. IEEE Int. Symp. on Information Theory*, Sorrento, Italy, June 2000, p. 22.
- [56] S. S. (Shitz), O. Somekh, O. Simeone, A. Sanderovich, B. M. Zaidel, and H. V. Poor, "Cooperative multi-cell networks: impact of limited-capacity backhaul and inter-users links," in *in the Proc. of Joint Workshop on Coding and Communications*, Dürnstein, Austria, October 2007.
- [57] S. S. (Shitz), O. Simeone, O. Somekh, and H. V. Poor, "Joint multi-cell processing for downlink with limited-capacity backhaul," in *Proc. Information Theory and Applications Workshop*, San Diego, CA, Jan. 27- Feb. 1 2008.
- [58] D. Slepian and J. Wolf, "Noiseless coding of correlated information sources," *IEEE Transactions on Information Theory*, vol. IT-19, pp. 471–480, 1973.
- [59] I. Maric and R. D. Yates, "Forwarding strategies for gaussian parallel-relay networks," in *Proc. IEEE Conference of Information Sciences and Systems*, Princeton, NJ, March 2004.
- [60] M. Gastpar and M. Vetterli, "On The Capacity of wireless networks: The Relay Case," in *Proc. IEEE Conf. on Compute Communication*, New York, June 2002.
- [61] A. S. Avestimehr, S. N. Diggavi, and D. N. C. Tse, "A deterministic approach to wireless relay networks," in *Proc. Conf. on Communication, Control, and Computing*, Illinois, September 2007.
- [62] —, "Approximate capacity of gaussian relay networks," in *Proc. IEEE Int. Symp. on Information Theory*, Toronto, Canada, July 2008.

- [63] R. Dabora and S. Servetto, "Estimate-and-Forward relaying for the Gaussian relay channel with coded modulation," Nice, France, June 2007.
- [64] —, "On the role of Estimate-and-Forward with time-sharing in cooperative communication," *IEEE Transactions on Information Theory*, October 2008.
- [65] A. Gersho and R. M. Gray, *Vector Quantization and Signal Compression*. Norwell, MA: Kluwer Academics, 1992.
- [66] A. Orłitsky, "Scalar versus Vector quantization: Worst case analysis," *IEEE Transactions on Information Theory*, vol. 48, pp. 1393–1409, June 2002.
- [67] A. Chakrabarti, E. Erkip, A. Sabharwal, and B. Aazhang, "Code designs for cooperative communication," *IEEE Signal Processing Magazine*, vol. 24, pp. 16–26, September 2007.
- [68] Y. Oohama, "The rate-distortion function for the Quadratic Gaussian CEO problem," *IEEE Transactions on Information Theory*, vol. IT-44, pp. 1057–1070, May 1998.
- [69] R. G. Gallager, *Information theory and reliable communication*. John Wiley & Sons, 1968.
- [70] I. E. Telatar, "Capacity of multi-antenna gaussian channels," *European Trans. on Telecommunications*, vol. 10, pp. 585–596, Nov. 1999.
- [71] R. G. Gallager, "A perspective on multi-access channels," *IEEE Transactions on Information Theory*, vol. 31, pp. 124–142, March 1985.
- [72] O. Simeone, O. Somekh, G. Kramer, S. S. (Shitz), and H. V. Poor, "Cellular systems with multicell processing and conferencing links between mobile stations," in *Proc. Information Theory and Applications Workshop*, San Diego, CA, Jan. 27- Feb. 1 2008.
- [73] O. Simeone, O. Somekh, H. V. Poor, and S. S. (Shitz), "Distributed mimo in multi-cell wireless systems via finite-capacity links," in *in the Proc. of IEEE 3rd International Symposium on Communications, Control and Signal Processing*, March 2008.
- [74] V. Sreng, H. Yanikomeroglu, and D. Falconer, "Coverage enhancement through two-hop relaying in cellular radio systems," in *Proc. IEEE Wireless Communication and Networking Conf.*, March 2002.
- [75] R. Irmer and F. Diehm, "On coverage and capacity of relaying in LTE-advanced in example deployments," in *Proc. IEEE Int. Symp. on Personal, Indoor and Mobile Radio Communications*, September 2008.

- [76] S. W. Peters, A. Y. Panah, K. T. Truong, and R. W. Heath, "Relay architectures for 3GPP LTE-Advanced," *EURASIP Journal on Wireless Communications and Networking*, vol. 2009, Article ID 618787, 14 pages, 2009. doi:10.1155/2009/618787.
- [77] A. A. E. Gamal and S. Zahedi, "Capacity of a class of relay channels with orthogonal components," *IEEE Transactions on Information Theory*, vol. 51, pp. 1815–1817, May 2005.
- [78] Y. Liang and V. V. Veeravalli, "Gaussian orthogonal relay channels: Optimal resource allocation and capacity," *IEEE Transactions on Information Theory*, vol. 51, pp. 3284–3289, Sep. 2005.
- [79] L. Sankaranarayanan, G. Kramer, and N. B. Mandayam, "Capacity theorems for the multiple-access relay channel," in *Proc. Conf. on Communication, Control, and Computing*, IL, USA, Sep./Oct. 2004, pp. 1782–1791.
- [80] E. Yilmaz, R. Knopp, and D. Gesbert, "Some system aspects regarding compressive relaying with wireless infrastructure links," in *Proc. IEEE Global Communications Conf.*, New Orleans, USA, November 2008.
- [81] E. Yilmaz, D. Gesbert, and R. Knopp, "Parallel relay networks with phase fading," in *Proc. IEEE Global Communications Conf.*, New Orleans, USA, November 2008.
- [82] A. Ozgur, O. Leveque, and D. Tse, "Hierarchical cooperation achieves optimal capacity scaling in ad hoc networks," *IEEE Transactions on Information Theory*, vol. 53, pp. 3549–3572, October 2007.
- [83] C. A. 231, "Digital mobile radio toward future generation systems, final report," in *European Communities, EUR 18957, Tech. Report*, 1999.
- [84] E. Yilmaz, R. Knopp, and D. Gesbert, "On the gains of fixed relays in cellular networks with intercell interference," in *Proc. IEEE Workshop on Signal Processing Advances in Wireless Communications*, Perugia, Italy, June 21-24 2009.
- [85] C. Schnurr, S. Stanczak, and T. J. Oechtering, "Coding theorems for the restricted half-duplex two-way relay channel with joint decoding," in *Proc. IEEE Int. Symp. on Information Theory*, Canada, July 2008.
- [86] A. D. Wyner, J. K. Wolf, and F. M. J. Willems, "Communicating via a processing broadcast satellite," *IEEE Transactions on Information Theory*, vol. 48, June 2002.
- [87] C. E. Shannon, "Two-way communication channels," in *Proc. 4th Berkeley Symp. Math. Stat. Prob.*, University of California Press, Berkeley, 1961, pp. 611–644.

- [88] A. P. Hekstra and F. M. J. Willems, "Dependence balance bounds for single-output two-way channels," *IEEE Transactions on Information Theory*, vol. 35, pp. 44–53, 1989.
- [89] K. Narayanan, M. P. Wilson, and A. Sprintson, "Joint physical layer coding and network coding for bi-directional relaying," in *Proc. Conf. on Communication, Control, and Computing*, September 2007.
- [90] R. Urbanke and B. Rimoldi, "Lattice codes can achieve capacity on the awgn channel," *IEEE Transactions on Information Theory*, vol. 44, pp. 273–278, 1998.
- [91] W. Nam, S. Y. Chung, and Y. H. Lee, "Capacity bounds for two-way relay channels," in *Int. Zurich Seminar on Communications (IZS)*, March 2008, pp. 144–147.
- [92] T. Unger and A. Klein, "Duplex schemes in multiple-antenna two-hop relaying," *EURASIP JASP, (special issue: "Multihop-Based Cellular Networks")*, vol. 8, pp. 1–14, January 2008.
- [93] R. Zhang, Y. C. Liang, C. C. Chai, and S. Cui, "Optimal beamforming for two-way multi-antenna relay channel with analogue network coding," <http://arxiv.org/abs/0808.0075v2>.
- [94] C. Esli and A. Wittneben, "One- and two-way decode-and-forward relaying for wireless multi-user MIMO networks," in *Proc. IEEE Global Communications Conf.*, November 2008.
- [95] M. Chen and A. Yener, "Multi-user two-way relaying for interference limited systems," in *Proc. IEEE Int. Conf. on Communication*, May 2008.
- [96] A. U. T. Amah, A. Klein, Y. C. B. Silva, and A. Fernekess, "Multi-group multicast beamforming for multi-user two-way relaying," in *Int'l ITG Workshop on Smart Antennas-WSA*, February 2009.
- [97] Q. H. Spencer and M. H. A. L. Swindlehurst, "Zero-Forcing methods for downlink spatial multiplexing in multiuser MIMO channels," *IEEE Transactions on Signal Processing*, vol. 52, pp. 461–471, February 2004.